Targeted nanomedicines for the treatment of inflammatory disorders and cancer

The printing of this thesis was financially supported by:

MediTrans

Utrecht Institute for Pharmaceutical Sciences

J.E. Jurriaanse Stichting

Enceladus, Amsterdam, The Netherlands

Cristal Delivery, Utrecht, The Netherlands

Lipoid GmbH, Ludwigshafen, Germany

ISBN: 978-90-39357460

Printed by Ipskamp Drukkers B.V., Enschede, The Netherlands

TARGETED NANOMEDICINES FOR THE TREATMENT OF INFLAMMATORY DISORDERS AND CANCER

Gerichte nanomedicijnen voor de behandeling van ontstekingsziekten en kanker

(met een samenvatting in het Nederlands)

Proefschrift

ter verkrijging van de graad van doctor aan de Universiteit Utrecht op gezag van de rector magnificus, prof.dr. G.J. van der Zwaan, ingevolge het besluit van het college voor promoties in het openbaar te verdedigen op maandag 5 maart 2012 des middags te 2.30 uur

door

Bart Johan Crielaard

geboren op 17 juni 1980 te Emmen

Promotoren:	Prof.dr. G. Storm
	Prof.dr. W.E. Hennink
Co-promotoren:	Dr. R.M. Schiffelers
	Dr. T. Lammers

This work was supported by MediTrans, an Integrated Project funded by the European Commission under the “nanotechnologies and nano-sciences, knowledge-based multifunctional materials and new production processes and devices” (NMP), thematic priority of the Sixth Framework Program.

Voor Pa

Table of Contents

1

General introduction

B.J. Crielaard

1. General introduction

Targeted drug delivery, a strategy using drug delivery systems for changing the pharmacological properties of conventional drugs, as well as biotherapeutics such as proteins and nucleic acids, to improve their therapeutic outcome, is a rapidly advancing field in pharmaceutical research. By (1) improving the concentration of the associated drug at the target site (i.e. improving efficacy), by (2) reducing the concentration of the drug at non-target tissues (i.e. reducing toxicity), allowing for higher doses, or by (3) directing the therapeutic agent to its target cells (i.e. improving cell localization and/or uptake), drug targeting has shown to be a highly efficacious approach for the treatment a number of diseases. Already more than a century ago, Thomas Huxley and Paul Ehrlich envisaged a future where doctors could employ a 'very cunningly contrived torpedo' [1] or 'Zauberkugeln' ('magic bullets') [2] to attack a specific diseased area in the body, while leaving the other, healthy, tissues unharmed. Only in the last decades, with the development of colloidal systems such as liposomes and polymeric micelles, this vision has slowly started to come into reality [3, 4]. Not by magic, but enabled by pathophysiological changes in the microenvironment in diseased tissues, these nanoparticulates with a typical size of 50-200 nm extravasate preferentially in these pathological areas upon systemic administration, making them disease-specific targeted drug delivery vehicles [5]. As schematically shown for breast cancer in Figure 1, the increased vascular permeability and reduced lymphatic drainage in tumors and inflamed tissues, which is commonly referred to as the Enhanced Permeability and Retention (EPR) effect, results in passive target tissue-accumulation of drugs associated with long-circulating nanocarriers and macromolecules [6].

Another example of a drug targeting strategy exploiting the specific pathophysiological characteristics of the diseased target tissue is the interference with newly formed vasculature. As a result of low levels of oxygen and nutrients within pathological areas, such as tumors, there is a physiological response stimulating the growth of new blood vessels, known as angiogenesis, to increase the supply of these essential resources [7]. These new capillaries that sprouted from the existing vasculature are structurally and functionally different from normal blood vessels, making them excellent targets for angiogenesis-specific therapies [8, 9]. For example, vascular disrupting agents (VDAs) interfere with the different structural stability of endothelial cells in angiogenic vasculature. By affecting the integrity of the vascular endothelial lining, this leads to massive hemostasis and subsequent deprivation of

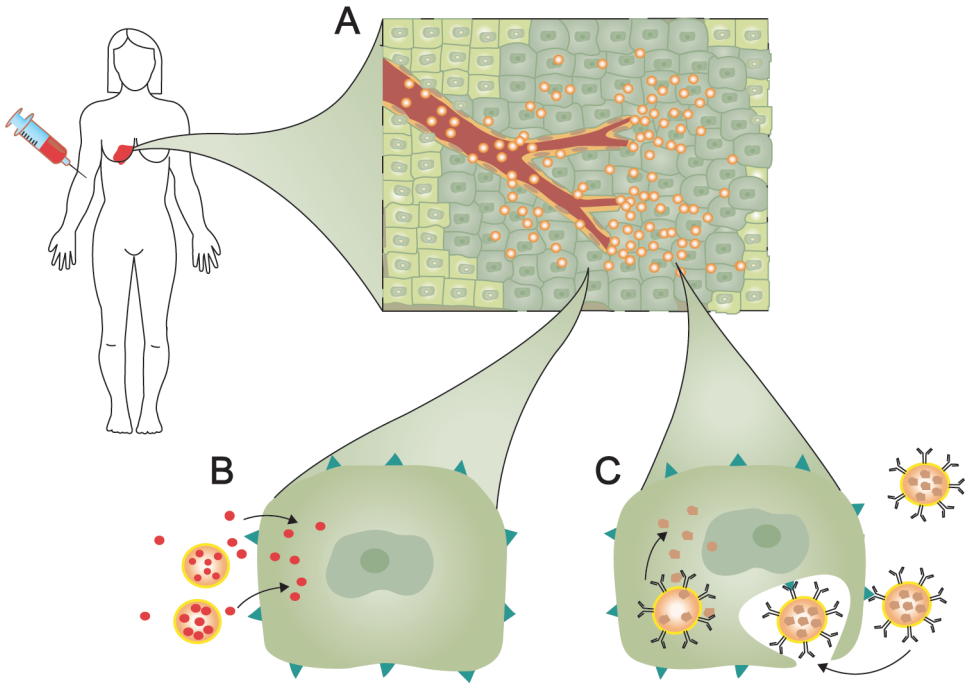

Figure 1. Schematic representation of EPR-mediated drug targeting to breast cancer. Systemically administered drugs encapsulated in a nanosized carrier system are confined to the circulatory tract due to their relatively large size. However, because of the presence of increased vascular permeability and reduced lymphatic drainage (Enhanced Permeability and Retention, EPR) in diseased tissues, in this case a mammary tumor, the nanomedicines will extravasate and localize in these tissues (A). Then, upon localization of the carrier system, the associated drug may translocate passively (B), or actively (C) into the target cells. From [5]. Reprinted with permission from AAAS.

neighboring cells from oxygen and nutrients, ultimately resulting in tissue necrosis (Figure 2) [10].

From a drug targeting-perspective, there are many similarities between cancer and chronic inflammatory disorders, such as rheumatoid arthritis (RA), multiple sclerosis (MS) and inflammatory bowel disease (IBD). First of all, the EPR effect, the phenomenon most commonly known for its responsibility for the tumoritropic localization of systemically circulating macromolecules in cancer, has also been observed in arthritic joints in RA [11], in demyelinating plaques in MS [12], and in inflamed intestinal mucosa in IBD [13]. Secondly, angiogenesis, the formation of new blood vessels from preexisting vasculature, is generally considered one of the hallmarks of cancer, but is also shown to be one of the key components in chronic inflammatory diseases. For example, vascular

endothelial growth factor (VEGF), a family of proteins with strong angiogenic activity [14], has been demonstrated to be involved in the pathogenesis of RA [15], MS [16], as well as IBD [17]. Consequently, (VEGF-mediated) anti-angiogenic therapy has shown to be a promising approach in the treatment of autoimmune disorders [18-21]. Finally, during the last decades it has been increasingly acknowledged that cancer is in fact a chronic inflammatory disease itself, and therefore can respond favorably to (targeted) anti-inflammatory therapies [22-24].

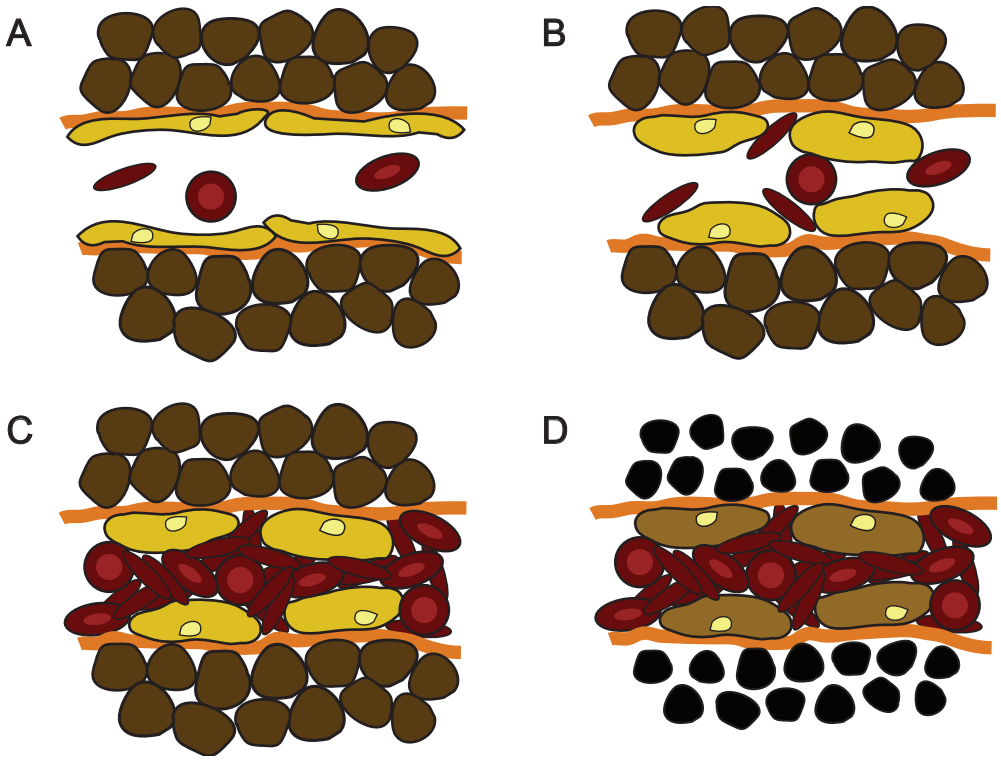

Figure 2. Schematic representation of vascular disruption. **A.** Angiogenic blood vessel lined with endothelial cells (yellow) and basement membrane (orange). **B.** By interfering with the structural stability of the (abnormal) endothelial cells, these cells loose their elongated shape and the basement membrane is exposed. **C.** The blood flowing in the damaged blood vessel starts to coagulate and eventually the blood flow is arrested. **D.** Due to a lack of oxygen and nutrients, the pathological tissue in the vicinity of the disrupted vessel will become necrotic.

Many different types of drug-loaded nanocarrier systems, or nanomedicines, have been under investigation [25]. Liposomes [26], polymer-drug conjugates [27], protein-drug conjugates [28], polymer-protein conjugates [29], nanogels [30], and polymeric micelles [31], have all shown their value as a drug carrier system in several preclinical models of various disorders. As schematically depicted in Figure 3, each of these nanomedicines possesses particular physiochemical properties, and therefore may have its own 'identity' as a drug carrier. For example, liposomes (often additionally coated with poly(ethylene glycol) (PEG) to render them 'stealth'-like and give them long-circulating properties) are vesicles with a size of around 100 nm, composed of a (phospho-)lipid bilayer surrounding an aqueous core, in which various hydrophilic and hydrophobic therapeutic agents can be encapsulated.

The drug release from liposomes is in most cases not adjustable and, even for triggered release-capable liposomal systems, with an 'all-or-nothing' profile. Polymer-drug conjugates, however, have completely different characteristics. Depending on the molecular weight of the polymer, the size of these conjugates generally does not exceed 10 nm, and typically the therapeutic agents are (bio)reversibly conjugated to the nanocarrier, making the drug

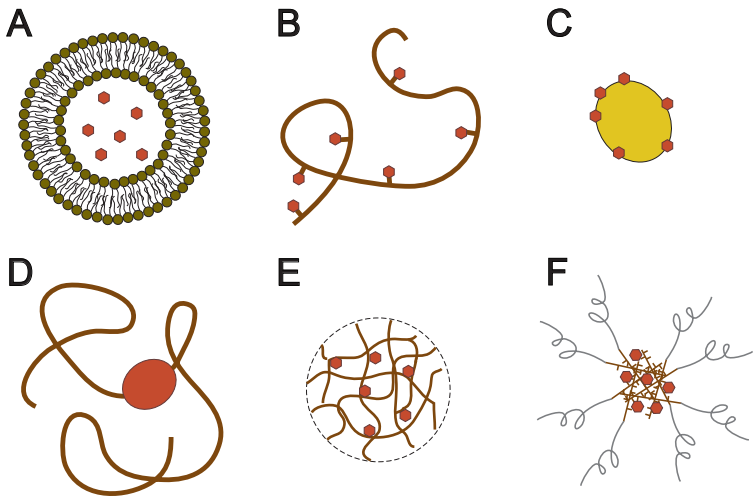

Figure 3. Schematic representation of various nanomedicines. **A.** Drugs encapsulated in the aqueous core of a liposome. Size: varies from 50-200 nm. **B.** Drugs conjugated to a high-molecular weight polymer. Size: 5-10 nm. **C.** Drugs conjugated to a (physiological) protein. Size: 5-25 nm **D.** (High-molecular weight) polymers coupled to a therapeutic protein. Size: 5-25 nm. **E.** Drugs entrapped inside a nanogel. **F.** drugs entrapped inside a core-crosslinked micelle. Size: 50-100 nm.

release kinetics from the polymer an important and tunable parameter.

The extensive choice of different carrier systems for drug targeting may be considered a luxury, for it provides future flexibility to select the appropriate system depending on the drug and its target, as well as the disease. However, since a true comparison regarding the characteristics and therapeutic efficacy of several drug-carriers has never been performed, it is nearly impossible to make such selection. Therefore, disease-oriented studies evaluating and comparing several nanosized delivery systems for a given application are required to answer such questions, to allow targeted nanomedicines to become an essential part of clinical therapies.

1.1. Aims and outline

The aim of this thesis is to investigate the therapeutic value of various targeted nanomedicines in several inflammatory disorders, including cancer, and to explore which nanocarrier may be most suitable for a specific therapeutic application. Following the current introductory chapter, **Chapter 2** provides an overview of drug targeting systems presently available for anti-inflammatory therapy and addresses the type of comparative ('all for one') research that is needed besides technology-oriented ('one for all') research, for selecting the optimal targeted nanomedicine for future clinical applications. Then, the thesis falls apart in three sections: two sections diverging the therapeutic scope of several novel and established targeted nanomedicines to various inflammatory diseases and cancer, and a final section to bring these and other efforts together in the quest for the 'optimal' nanomedicine for a given application.

The first section deals with the preclinical evaluation of targeted dexamethasone-containing carriers in three different models of inflammatory disease. In **Chapter 3**, the therapeutic activity of dexamethasone encapsulated into the aqueous core of long-circulating liposomes is studied in mice with experimental autoimmune encephalomyelitis (EAE), a model for multiple sclerosis (MS), as well as in mice with dextran sodium sulfate (DSS)-induced colitis, a model for inflammatory bowel disease (IBD). Then, **Chapter 4** reports on the synthesis and evaluation of a dexamethasone-delivery system based on core-crosslinked polymeric micelles, which demonstrated strong therapeutic efficacy in two preclinical models of rheumatoid arthritis (RA).

The second section is focused on the development of new nanomedicines derived from colchicine with vascular disrupting activity. **Chapter 5** describes the synthesis, liposomal

encapsulation and *in vitro* characterization of two polymeric prodrugs of colchicine. In **Chapter 6**, one of the prodrugs is selected for preclinical evaluation in tumor-bearing mice, to demonstrate the *in vivo* vascular activity of this new type of colchicine-derivatives. As part of the third and last section, which addresses the application-oriented search for an optimal nanocarrier system for drug targeting, **Chapter 7** describes the evaluation of three different nanocarriers of dexamethasone in a comparative study to assess their therapeutic efficacy in two animal models of RA. Then, to allow for the screening of different nanomedicines without requiring extensive usage of laboratory animals, an *in vitro* assay for predicting the *in vivo* circulation kinetics of liposomes is presented in **Chapter 8**. Finally, **Chapter 9** concludes with a summarizing discussion regarding the findings presented in this thesis.

2. References

[1] T.H. Huxley, The connection of the biological sciences with medicine, Science 2(63) (1881) 426-429.

[2] P. Ehrlich, Experimental researches on specific therapy. On immunity with special relationship between distribution and action of antigens. Harben Lecture, Royal Institute of Public Health, London, 1908, p. 107.

[3] G. Gregoriadis, C.P. Swain, E.J. Wills, A.S. Tavill, Drug-carrier potential of liposomes in cancer chemotherapy, The Lancet 303(7870) (1974) 1313-1316.

[4] M. Yokoyama, T. Okano, Y. Sakurai, H. Ekimoto, C. Shibazaki, K. Kataoka, Toxicity and Antitumor activity against solid tumors of micelle-forming polymeric anticancer drug and its extremely long circulation in blood, Cancer Res. 51(12) (1991) 3229-3236.

[5] T.M. Allen, P.R. Cullis, Drug delivery systems: entering the mainstream, Science 303(5665) (2004) 1818-1822.

[6] Y. Matsumura, H. Maeda, A New Concept for Macromolecular Therapeutics in Cancer Chemotherapy: Mechanism of Tumoritropic Accumulation of Proteins and the Antitumor Agent Smancs, Cancer Res. 46(12 Part 1) (1986) 6387-6392.

[7] P. Carmeliet, Angiogenesis in health and disease, Nat. Med. 9(6) (2003) 653-660.

[8] D. Neri, R. Bicknell, Tumour vascular targeting, Nat Rev Cancer 5(6) (2005) 436-446.

[9] D.M. McDonald, P.L. Choyke, Imaging of angiogenesis: from microscope to clinic, Nat. Med. 9(6) (2003) 713-725.

[10] P.E. Thorpe, Vascular targeting agents as cancer therapeutics, Clin. Cancer Res. 10(2) (2004) 415-427.

[11] I. Kushner, J.A. Somerville, Permeability of human synovial membrane to plasma proteins. Relationship to molecular size and inflammation, Arthritis Rheum. 14(5) (1971) 560-570.

[12] K. Kristensson, H.M. Wiśniewski, Chronic relapsing experimental allergic encephalomyelitis, Acta Neuropathol. (Berl). 39(3) (1977) 189-194.

[13] T. Aychek, K. Vandoorne, O. Brenner, S. Jung, M. Neeman, Quantitative analysis of intravenously administered contrast media reveals changes in vascular barrier functions in a murine colitis model, Magn. Reson. Med. 66(1) (2011) 235-243.

[14] G.D. Yancopoulos, S. Davis, N.W. Gale, J.S. Rudge, S.J. Wiegand, J. Holash, Vascular-specific growth factors and blood vessel formation, Nature 407(6801) (2000) 242-248.

[15] Z. Szekanecz, T. Besenyei, Á. Szentpétery, A.E. Koch, Angiogenesis and vasculogenesis in rheumatoid arthritis, Curr. Opin. Rheumatol. 22(3) (2010) 299-306.

[16] M.A. Proescholdt, S. Jacobson, N. Tresser, E.H. Oldfield, M.J. Merrill, Vascular endothelial growth factor is expressed in multiple sclerosis plaques and can induce inflammatory lesions in experimental allergic encephalomyelitis rats, J. Neuropathol. Exp. Neurol. 61(10) (2002) 914-925.

[17] S. Danese, M. Sans, C. de la Motte, C. Graziani, G. West, M.H. Phillips, R. Pola, S. Rutella, J. Willis, A. Gasbarrini, C. Fiocchi, Angiogenesis as a Novel Component of Inflammatory Bowel Disease Pathogenesis, Gastroenterology 130(7) (2006) 2060-2073.

[18] C.-S. Zhu, X.-Q. Hu, Z.-J. Xiong, Z.-Q. Lu, G.-Y. Zhou, D.-J. Wang, Adenoviral delivery of soluble VEGF receptor 1 (sFlt-1) inhibits experimental autoimmune encephalomyelitis in dark Agouti (DA) rats, Life Sciences 83(11-12) (2008) 404-412.

[19] N. Schoettler, E. Brahn, Angiogenesis inhibitors for the treatment of chronic autoimmune inflammatory arthritis, Current Opinion in Investigational Drugs 10(5) (2009) 425-433.

[20] J. Miotla, R. Maciewicz, J. Kendrew, M. Feldmann, E. Paleolog, Treatment with soluble VEGF receptor reduces disease severity in murine collagen-induced arthritis, Laboratory Investigation 80(8) (2000) 1195-1205.

[21] O.A. Hatoum, J.A.N. Heidemann, D.G. Binion, The intestinal microvasculature as a therapeutic target in inflammatory bowel disease, Ann. N. Y. Acad. Sci. 1072(1) (2006) 78-97.

[22] L.M. Coussens, Z. Werb, Inflammation and cancer, Nature 420(6917) (2002) 860-867.

[23] K.E. de Visser, A. Eichten, L.M. Coussens, Paradoxical roles of the immune system during cancer development, Nat Rev Cancer 6(1) (2006) 24-37.

[24] M. Coimbra, S.A. Kuijpers, S.P. van Seters, G. Storm, R.M. Schiffelers, Targeted delivery of anti-inflammatory agents to tumors, Curr. Pharm. Des. 15(16) (2009) 1825-1843.

[25] R. Duncan, R. Gaspar, Nanomedicine(s) under the microscope, Mol. Pharm. 8(6) (2011) 2101-41.

[26] D.B. Fenske, P.R. Cullis, Liposomal nanomedicines, Expert. Opin. Drug. Deliv. 5(1) (2008) 25-44.

[27] T. Lammers, Improving the efficacy of combined modality anticancer therapy using HPMA copolymer-based nanomedicine formulations, Adv. Drug Deliv. Rev. 62(2) (2010) 203-230.

[28] E. Neumann, E. Frei, D. Funk, M.D. Becker, H.H. Schrenk, U. Muller-Ladner, C. Fiehn, Native albumin for targeted drug delivery, Expert Opin Drug Deliv 7(8) (2010) 915-925.

[29] M.J. Joralemon, S. McRae, T. Emrick, PEGylated polymers for medicine: from conjugation to self-assembled systems, Chem. Commun. 46(9) (2010) 1377-1393.

[30] A.V. Kabanov, S.V. Vinogradov, Nanogels as pharmaceutical carriers: finite networks of infinite capabilities, Angew. Chem. Int. Ed. 48(30) (2009) 5418-5429.

[31] M. Talelli, C.J.F. Rijcken, C.F. van Nostrum, G. Storm, W.E. Hennink, Micelles based on HPMA copolymers, Adv. Drug Deliv. Rev. 62(2) (2010) 231-239.

2

Drug targeting systems for inflammatory disease: one for all, all for one

B.J. Crielaard [1], T. Lammers [2], R.M. Schiffelers [1,3] and G. Storm [1]

1. Department of Pharmaceutics, Utrecht Institute for Pharmaceutical Sciences (UIPS), Utrecht University, Utrecht, The Netherlands
2. Department of Experimental Molecular Imaging, RWTH – Aachen University, Aachen, Germany
3. Department of Clinical Chemistry and Haematology, University Medical Center Utrecht, Utrecht, The Netherlands

J. Control. Release 2011, doi:10.1016/j.jconrel.2011.12.014

Abstract

In various systemic disorders, structural changes in the microenvironment of diseased tissues enable both passive and active targeting of therapeutic agents to these tissues. This has led to a number of targeting approaches that enhance the accumulation of drugs in the target tissues, making drug targeting an attractive strategy for the treatment of various diseases. Remarkably, the strategic principles that form the basis of drug targeting are often employed for tumor targeting, while chronic inflammatory diseases appear to draw much less attention. To provide the reader with a general overview of the current status of drug targeting to inflammatory diseases, the passive and active targeting strategies that have been used for the treatment of rheumatoid arthritis (RA) and multiple sclerosis (MS) are discussed. The last part of this review addresses the dualism of platform technology-oriented ("one for all") and disease-oriented drug targeting research ("all for one"), both of which are key elements of effective drug targeting research.

1. Introduction

In the last decades, targeted drug delivery has become an established field in pharmaceutical research. By using a targeting system that assists in directing a drug to the site in the body where it needs to exert its effect, target tissue specificity of the therapeutic agent can be increased while the off target effects can be limited [1, 2]. Although a drug targeting strategy can potentially improve the clinical efficacy of therapeutic interventions in many, if not all, diseases, most drug targeting research has been focused on cancer (Figure 1) [3-5]. The high morbidity and mortality among cancer patients evidently justifies this focus working on tumor-targeted drug delivery systems. At the same time, the large socio-economical impact of chronic inflammatory disorders, such as rheumatoid arthritis and multiple sclerosis, on both patient and society appears not to be fully appreciated in drug targeting research [6-8].

It is remarkable that there is only limited attention for these diseases, since in principle many strategies employed for targeted drug delivery to tumors would seem applicable for drug targeting to sites of inflammation. In fact, cancer is strongly linked to inflammation and is often designated as a chronic inflammatory disease itself, illustrating the overlap of cancer and inflammation in the context of drug delivery [9-11]. This contribution aims to provide the reader with an update of the current status of the field with respect to drug

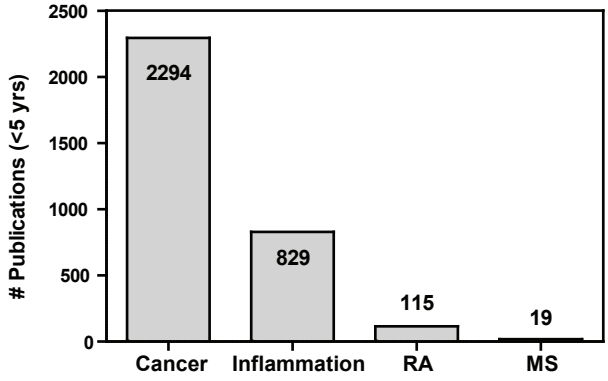

Figure 1. Number of research publications over the last 5 years related to drug targeting to diseases. Results represent the number of hits of MEDLINE searches (query "drug delivery" OR "drug targeting" OR "nanomedicine"), specified to malignant diseases (using "cancer"), inflammatory diseases (using "inflamm*"), rheumatoid arthritis (RA, using "rheum*" OR "arthritis"), and multiple sclerosis (MS, using "multiple sclerosis" OR "encephalomyelitis").

targeting in inflammatory disorders. In addition, we will give our perspective on how drug targeting can be approached to improve its clinical impact.

2. Drug Targeting to Inflammatory Disease

2.1. Passive Drug Targeting

A quarter of a century ago, Maeda and coworkers demonstrated for the first time the tumoritropic accumulation of proteins and macromolecules [12]. By coupling poly(styrene-co-maleic acid) to a protein (neocarzinostatin) that has anti-tumor activity, a conjugate (SMANCS) with increased molecular weight was formed which showed an improved *in vivo* half-life compared to the unmodified protein [13]. To relate the efficacy of SMANCS to its target tissue concentration, the plasma clearance and tumor accumulation of neocarzinostatin, SMANCS and several other plasma proteins including albumin, were determined. A clear positive correlation between plasma half-life, molecular size and tumor-specific accumulation was observed, which was attributed to a 'highly enhanced leakiness' of the tumor vasculature for macromolecules [12]. Moreover, upon intratumoral injection of Evans blue-albumin complexes, there was a remarkable reduction of clearance of the complexes in the tumor compared to healthy tissues, indicating a tumor-specific deficit in lymphatic drainage. This phenomenon of enhanced vascular leakiness and impaired lymphatic drainage, now known as the 'enhanced permeability and retention (EPR) effect', has since been used extensively for passive tumor-specific drug delivery, also described as passive targeting, using macromolecular and particulate drug targeting systems [2, 14-18].

However, the EPR effect has not been observed exclusively in tumors. In fact, in 1971, 15 years before the landmark study of Matsumara and Maeda, Kushner and Somerville described a similar relationship between the molecular size of proteins and their localization in arthritic joints of patients with rheumatoid arthritis (RA) and other arthritic diseases [19]. Although the precise mechanism remained unclear, one of the suggested mechanisms was an inflammation-induced 6- to 40-fold increase of blood-joint barrier permeability for high molecular weight molecules [20]. Consequently, a complication frequently observed in patients with RA is hypoalbuminemia, which may be attributed to an increased albumin extravasation and metabolism within the inflamed joint [21, 22]. Similarly, an increase in blood brain barrier (BBB) permeability for serum proteins, such as fibrinogen, has directly

been correlated to areas of (active) demyelinization (i.e. plaques) in multiple sclerosis (MS) [23-25]. Therefore, passively targeted drug delivery strategies utilizing the EPR effect have also been applied successfully to models of inflammatory diseases such as RA and MS [26-30].

It is important to emphasize that the size and the pharmacokinetic profile of the drug carrier are key characteristics of passively targeted drug delivery systems [31, 32]. A lower size limit of ~50 kDa and an upper size limit in the range of ~200 nm enhance targeting of the carrier-associated drug by means of the EPR effect while preventing glomerular filtration [33, 34]. The long circulation time of these carriers increases the statistical probability for sufficient target accumulation of the drug to take place. Indeed, significantly higher drug concentrations may be obtained in the target tissue by employing such passively targeted drug delivery systems, but the term 'targeted' may appear somewhat deceptive in this context [35, 36]. Macromolecules and nanoparticulate carrier systems that are too large to be cleared renally from the body are taken up by phagocytic cells of the reticuloendothelial system (RES), mainly in liver and spleen [37]. As a result, by far the largest part of the injected dose is 'targeted' to these organs, while on average only a much smaller fraction (less than 10%) of the injected dose will end up in the tissue where the drug needs to exert its effect. Nevertheless, the therapeutic consequences of passive targeting (of macrophages) are likely more complex than the mere target tissue accumulation: there is, for example, evidence that the anti-tumor effect of liposomal glucocorticoids may be related to a decrease in white blood cells, rather than the accumulation in the target tissue [38].

2.2. Active Drug Targeting

While local drug concentrations in the diseased tissue can be increased by employing a passive targeting strategy, directing the drug delivery system to a specific cell type by means of a targeting ligand (i.e. active targeting) may help to further improve the efficacy of the targeted drug. Generally, such strategies do not increase the overall concentration in the target tissue, but rather change the distribution within the tissue. A notable exception in this case is targeting within the blood stream for which extravasation is not required and therefore not the rate-limiting step. In chronic inflammatory diseases such as RA and MS, a shortage of oxygen and nutrients induces the formation of new blood vessels, a process known as angiogenesis, which contributes to the pathogenesis and development of these diseases [39-44]. By interfering with the angiogenic process in preclinical models of

RA and MS, it has been shown that the disease intensity can be alleviated [45-48]. Both vascular endothelial cells and monocyte-derived cells, including macrophages, are closely involved in the angiogenic process in chronic inflammatory diseases, which makes them attractive targets for an active drug targeting approach [49-53]. As a result of the pro-inflammatory microenvironment, membrane receptors that are involved in angiogenesis signaling are upregulated, marking the cells expressing them 'inflammation-specific', and designating them as possible targets for drug delivery [54].

Although several receptors are recognized as being suitable targets, primarily the folate receptor (FR) and the $\alpha_v\beta_3$ integrin have been used for active drug targeting purposes [55-57]. In 1991, Laemon and Low were the first to show that macromolecules, such as proteins, when conjugated to folate or folic acid were internalized *in vitro* by a number of different types of cells [58]. Later studies reported that the receptor mediating the uptake, i.e. the folate receptor, is overexpressed by several epithelial tumor cells and activated macrophages [59, 60]. Since the tissue specific expression of FR makes it an attractive target, FR-directed drug targeting has developed into a mature strategy for active drug targeting [61-64]. FR-expressing cancer cells and activated macrophages express distinct FR isoforms, FR-α and FR-β, respectively [65, 66], and much research has been focused on tumor-targeting via FR-α [67, 68]. However, the potential of folate-functionalized drug delivery systems in the treatment of chronic inflammatory diseases by targeting FR-β expressed by activated macrophages should not be underestimated. In fact, there is evidence that the anti-tumor efficacy of FR-targeted drug delivery systems for cancer therapy is, at least partly, macrophage-mediated [69].

The $\alpha_v\beta_3$ integrin, a heterodimeric surface receptor expressed by several cells including endothelial cells and macrophages, enhances cell adhesion and migration of infiltrating cells during tissue inflammation [54]. Having a key role in angiogenesis, the $\alpha_v\beta_3$ integrin is only expressed on the luminal surface of endothelial cells that are associated with the neovascularization process, making these cells a specific target for anti-angiogenic therapy [70]. $\alpha_v\beta_3$-targeted therapies that directly interfere with the binding of ligands to the receptor have shown efficacious angiogenesis inhibition and suppressing effects on disease development in models of both neoplastic and inflammatory diseases [71-73]. The strategies exploiting this integrin to target drugs to angiogenic tissues in tumors, as well as inflammatory diseases, often by using the cyclic Arg-Gly-Asp (RGD) peptide as a ligand, have been quite successful [57, 74, 75]. The strong similarities between active drug

targeting approaches in cancer and those in chronic inflammatory diseases, as illustrated by the examples given above, emphasizes the importance of not focusing merely on a single disease but keeping a broad horizon regarding applications of a drug targeting system. In the following sections, several drug targeting strategies for the treatment of RA and MS are discussed in more detail.

2.3. Drug targeting in Rheumatoid Arthritis

RA is a systemic disorder characterized by a chronic inflammation in the synovium of one or several joints, initiated by an immunological response against a currently unknown endogenous or cross-reactive exogenous antigen [76]. Mediated by the release of pro-inflammatory cytokines and matrix metalloproteinases (MMPs) by various infiltrating immune cells, including macrophages, B cells, T cells, fibrocytes and synoviocytes (synovial fibroblasts), joint inflammation progresses into joint destruction [49, 50, 76, 77]. In RA, activated synoviocytes exhibit invasive growth into the joint cartilage, and stimulate the differentiation and proliferation of osteoclasts responsible for joint destruction [77-79]. The activated synoviocytes are also considered to be responsible for the progression of the disease from one arthritic joint to other, unaffected joints, a role which bears resemblance to that of metastatic tumor cells in cancer [80]. Similarly, the activation of the vascular endothelium and its proliferation is comparable to the angiogenesis that occurs during tumor growth [39, 41]. The enzymatic and osteoclastic destruction of the arthritic joint leads to joint deformation and loss of function, and to pain and morbidity for patients suffering from RA [76]. Moreover, although not regarded as a lethal disease, RA reduces the mean life expectancy of patients with 5-10 years, depending on disease severity [81, 82].

There are several therapeutic strategies available in the clinical management of RA, aiming at the reduction of joint inflammation and the prevention of joint destruction [76, 83]. To improve the efficacy of conventional therapies, a number of systemic drug targeting strategies taking advantage of the functional and cellular changes in the synovial inflammatory environment have shown to be promising. The role of phagocytic cells in the clearance of systemically injected macromolecular and nanoparticulate drug delivery systems, as well as their importance in the development and progression of chronic inflammatory diseases, likely make macrophages and synoviocytes residing in the joint tissue important mediators in the therapeutic effect of targeted nanomedicines.

In fact, several studies have investigated the effect of macrophage depletion on synovial inflammation using liposomes loaded with bisphosphonates, such as clodronate disodium, which induce cellular apoptosis when endocytosed [84-87]. Indeed, upon macrophage depletion joint inflammation was effectively suppressed. These studies confirmed that (activated) synovial macrophages and synoviocytes fulfill a key pro-inflammatory role in rheumatoid arthritis, and that these cells can be efficiently targeted by passively targeted drug delivery systems [84]. Over the years, a number of drug targeting systems containing several types of antirheumatic drugs have been prepared and evaluated in animal models for RA, as will be discussed further below.

2.3.1. Glucocorticoids

The therapeutic efficacy of glucocorticoids, which are frequently used in RA for suppressing

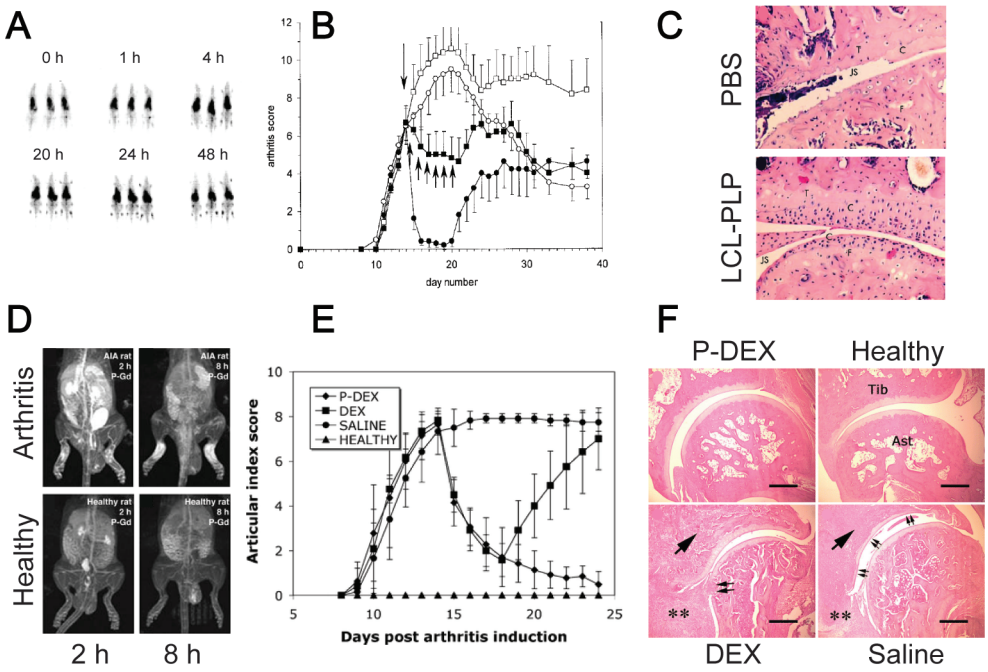

Figure 2. Targeted glucocorticoids in RA. Glucocorticoids targeted to arthritic joints in rats using PEGylated liposomes (**A**-**C**) or pHPMA-conjugates (**D**-**F**). **A**. Whole body scintigraphic images showing the accumulation of ^{111}In-labeled PEGylated liposomes in the inflamed joints of rats with adjuvant-induced arthritis (AIA) up to 48 hours post-injection [30]. **B**. Therapeutic activity of a single dose of PEGylated liposomes loaded with PLP (10 mg/kg, circles) on day 14, compared to

exacerbations of joint inflammation, has been greatly enhanced upon encapsulation into long-circulating PEGylated liposomes [30, 88-92]. For example, a single i.v. injection of 10 mg/mL prednisolone phosphate (PLP) encapsulated in liposomes almost completely resolved joint inflammation in rats with adjuvant-induced (AIA) arthritis, while 7 daily i.v. injections of free drug at the same dose only resulted in a mild reduction of the inflammation (Figure 2B and C) [30]. Similar effects have been observed for the more potent corticosteroid dexamethasone phosphate (DXP) at lower doses in the same model [88], as well as in another, murine collagen-induced (CIA), model of RA [89]. By active targeting of DXP liposomes to the angiogenic endothelial cells in the inflamed synovium using RGD-functionalized PEG-lipids, their therapeutic efficacy could be further enhanced, even at early inflammatory stages , illustrating the versatility of this liposomal system [57]. In a study comparing the therapeutic index of liposomes encapsulating PLP,

7 daily injections of free PLP (10 mg/kg, closed squares) on the clinical arthritis score. Rats treated with either saline (open squares) or PBS containing PEG-liposomes (open circles) presented with an increase in disease intensity during the days after injection. Upon daily treatment with free PLP, a stabilization of disease intensity was obtained, while a single injection of liposomal targeted PLP resulted in a nearly complete abolishment of paw inflammation, clearly illustrating the strong effect of targeting [30]. **C**. Histological staining of arthritic knees of rats with collagen-induced arthritis, 1 week after treatment with PBS or PEGylated liposomes loaded with PLP (LCL-PLP, 10 mg/kg). In the joints of rats treated with PBS, severe damage of the cartilage was observed (upper panel), while the joint cartilage of rats treated with PLP-liposomes appeared to be hardly affected (lower panel). T, tibia; F, femur, JS, joint space; C, cartilage layer. [93]. **D**. MR imaging of pHPMA-DOTA-Gadolinium conjugates in the inflamed joints of rats with AIA (upper panels) and the joints of healthy rats (lower panels). A clear accumulation of the pHPMA conjugates was observed 2h (upper left) and 8h (upper right) after i.v. injection, whereas no pHPMA conjugate accumulation could be observed in the joints of healthy rats after 2h (lower left) or 8h (lower right) [94]. **E**. Therapeutic activity of a single dose of pHPMA-dexamethasone conjugates (P-DEX, 10 mg/kg) on day 14, compared to 4 daily doses of free dexamethasone (DEX, 2.5 mg/kg) on the clinical arthritis score of rats with AIA. The i.v. injection of 4 × 2.5 mg/kg free DEX or 1 × 10 mg/kg P-DEX resulted in a similar strong reduction in joint inflammation. The therapeutic effect of free DEX, however, lasted only until the last injection, whereas P-DEX continued to reduce the signs of inflammation until a level similar to healthy controls [96]. **F**. Histological staining (H&E) of arthritic joints of rats with AIA, 10 days after treatment with P-DEX (single dose 10 mg/kg, upper-left), DEX (4 doses of 2.5 mg/kg, lower-left), saline (4 doses, lower-right), compared to healthy control (upper-right). The joints of rats treated with saline or DEX presented with clear bone destruction (single arrow) and damage of the cartilage (double arrow), and moderate synovial cell lining and villous hyperplasia (two asterisks). In the case of P-DEX treatment there was in most cases no bone and cartilage damage observed, resulting in a similar appearance as the joints of healthy rats [96].

DXP and budesonide phosphate (BUP), in arthritic (AIA) rats, it was observed that BUP-liposomes possess the highest therapeutic efficacy, while showing the least systemic side-effects [90]. The beneficial effect of the glucocorticoid-loaded liposomes on joint inflammation is explained by the passive accumulation of the liposomes in the synovium of arthritic joints, which is not observed in healthy joints (Figure 2A) [30, 93].

This arthrotropic accumulation is not only seen for liposomes, but also for other nanomedicines. Both high-molecular-weight (>55 kDa) polymeric drug-conjugates, such as poly(N-(hydroxypropyl)methacrylamide) (pHPMA), and plasma albumin exhibited a comparable passive accumulation in arthritic joints, indicating that many types of macromolecules could serve as effective drug delivery systems for glucocorticoids and other agents for RA therapy (Figure 2D) [94]. Indeed, joint inflammation, as well as arthritic bone resorption and joint destruction, could be strongly reduced in a number of arthritic rat models by systemic application of a pHPMA-conjugate carrying dexamethasone via a pH-responsive hydrazone linker (Figure 2C and D) [29, 95-97].

Using the same strategy, two poly(ethylene glycol) (PEG)-conjugated hydrazone-linked prodrugs of dexamethasone were synthesized using another moiety of dexamethasone [98]. Although the authors conclude that the relatively fast hydrolysis rate of the prodrug should provide it with therapeutic properties for RA treatment, appropriate *in vivo* evaluation has not (yet) been performed. An interesting glucocorticoid-polymer construct consisting of α-methyl prednisolone (MP) coupled via ester-linkage to a linear cyclodextrin polymer, self-assembled into nanoparticles of around 30 nm, showed a significantly enhanced reduction of joint inflammation compared to free MP [99].

Another promising systemic approach for passive glucocorticoid delivery to arthritic joints in RA is the use of solid polymeric nanoparticles prepared from poly(D,L-lactic/glycolic acid) (PLGA), poly(D,L-lactic acid) (PLA) and PEG-PLGA/PLA copolymers entrapping betamethasone disodium 21-phosphate, which is slowly released over time upon polymer hydrolysis [100-102]. Due to the sustained release kinetics of the glucocorticoid from the nanoparticles, drug concentrations could be measured in the joint up to 14 days after single intravenous administration [102]. This resulted in a long-term suppression of joint inflammation in rats with AIA, as well as in mice with collagen antibody-induced arthritis (CAIA), which in both cases was superior to a 3 times higher dose of the free drug [101].

2.3.2. Non-steroidal anti-inflammatory drugs

Due to the high risk of gastrointestinal complications, the use of non-steroidal anti-inflammatory drugs (NSAIDs) in RA therapy is currently limited [103]. However, several attempts have been made to benefit from the strong anti-inflammatory properties of NSAIDs by using a systemic drug targeting strategy. For example, indomethacin (IND), a lipophilic NSAID, has been entrapped in and conjugated to several types of nanoparticulate systems and macromolecules. IND entrapped in the bilayer of nanosized liposomes (100 nm) effectively reduced joint inflammation in adjuvant-arthritic rats, whereas a 2 times higher dose of free IND showed only a limited effect [104]. Similarly, IND encapsulated in the oily core of PEGylated long-circulating lipid nanospheres (150 nm) showed higher accumulation in joints of rats with AIA compared to free IND [105]. Although this indicates the ability of the lipid nanospheres to passively target the joint inflammation, unfortunately no therapeutic activity studies were performed. Several studies have described the application of (modified) poly(amidoamine) (PAMAM) dendrimers for the hydrophobic complexation of IND [106-108]. When complexed with 4th generation PAMAM dendrimers, 2 to 3 times higher concentrations of IND could be recovered from the joints of arthritic rats as compared to free drug administration [106]. Subsequent modifications of the PAMAM dendrimer with PEG and folate targeting ligands were performed to further improve joint accumulation [107, 108]. Surprisingly, whereas the *in vivo* anti-inflammatory efficacy of PAMAM dendrimer-IND complexes was improved compared to free IND, it was not higher than that of PAMAM dendrimers without IND, which the authors explained by an immunomodulating effect of the dendrimers themselves [109].

A polymeric methacrylamide derivative containing a 4-aminophenoxy spacer has been used to create a cleavable macromolecular delivery system for ibuprofen [110]. The hydrolytic release of ibuprofen and the 4-aminophenoxy spacer residue, which is a natural metabolite of acetaminophen (paracetamol), upon systemic injection and subsequent joint localization of the polymer-drug conjugate, resulted in an anti-inflammatory and analgesic effect *in vivo*. The selective cyclooxygenase 2 (COX-2) inhibitor celecoxib has been successfully encapsulated into albumin microspheres [111]. Although due to their relatively large size (5μm) the celecoxib albumin microspheres mainly accumulated in the lungs, a 2.5 fold higher concentration of celecoxib was detected in the inflamed paw compared to the healthy paw of rats with mono-articular arthritis. A possible explanation

might lie in the uptake of the microspheres by peripheral macrophages that subsequently traveled to the site of inflammation, taking along the microsphere-encapsulated cargo. In any case, it is evident that the targeting of NSAIDs by means of a drug targeting system is a valuable way to improve its therapeutic efficacy in the treatment of RA.

2.3.3. Methotrexate

Both liposomes and human serum albumin (HSA) have been used as carriers for arthritic joint delivery of methotrexate (MTX), a disease-modifying antirheumatic drug (DMARD) often used in RA therapy to prevent joint inflammation and disease progression [28, 112-115]. Phospholipid-conjugated MTX incorporated into the lipid bilayer of conventional liposomes and PEG-coated long-circulating liposomes exhibited a modest *in vivo* antirheumatic activity in rats with CIA [112, 113]. Although the activity was lower than that of free MTX, the MTX liposomes were better tolerated, as indicated by a reduced haematological toxicity. In this case, the role of the liposomes probably lies more in site-specific evasion, e.g. the bone marrow, than site-specific delivery. Encouraging results for MTX delivery with respect to RA therapy were obtained with albumin-based delivery systems. When covalently coupled to HSA, 4 to 5 times lower doses of MTX were equally effective as free MTX in inhibiting the onset of arthritis in mice with CIA [28]. Interestingly, when a combination of the MTX-HSA conjugate and MTX was administered, the anti-inflammatory effect was stronger than each of them at a double dose, which indicates that MTX and MTX-HSA may act synergistically through different mechanisms [114]. Since albumin conjugates were effectively endocytosed by synovial fibroblasts and mononuclear blood cells, including monocytes, granulocytes, B cells and T cells, it is plausible that a change in cellular distribution is a main contributing factor explaining these synergistic effects [28, 114]. More recently, in order to circumvent the need for exogenous albumin isolated from blood donors, a methotrexate prodrug that specifically binds albumin *in vivo* has been developed [115]. Similar to MTX-HSA, an improved therapeutic outcome of this MTX-albumin system, compared to free MTX, was observed in arthritic mice (CIA), confirming the potential of albumin-based drug targeting systems for RA therapy.

2.4. Drug Targeting in Multiple Sclerosis

Multiple sclerosis (MS) is a chronic inflammatory disease of the central nervous system (CNS), which is characterized by progressive inflammation and damage of the myelin sheet of neuronal axons in different locations within the CNS (plaques) [116]. Although initially the axon itself is preserved, the loss of myelin (demyelinization) hinders axonal conduction and will eventually lead to axonal degeneration [117-119]. As a result, MS often manifests with various neurological symptoms, including fatigue, loss of vision, diplopia, paresis and bladder dysfunction. In spite of a clear genetic predisposition and the fact that several infectious agents have been associated with the pathogenesis of MS, the underlying etiology remains unclear [116]. Since the primary target of the inflammatory response in MS is myelin, several myelin-associated proteins have been under investigation in search of the responsible antigen. Although some of these proteins, such as myelin basic protein (MBP), proteolipid protein (PLP) and myelin oligodendrocyte glycoprotein (MOG), are being employed to induce experimental autoimmune (or allergic) encephalomyelitis (EAE) in rodents – a condition that shows strong similarities with MS in humans and is extensively used as a preclinical model for MS – no definite antigen for MS has been identified yet [120]. During active demyelinating inflammation, activated T cells, macrophages and macrophage-like microglia infiltrate the focal plaques, attacking the myelin sheet and releasing pro-inflammatory cytokines [117, 118, 121]. Besides leading to axonal injury and neuronal dysfunction, the inflammatory process also disrupts the integrity of the blood brain barrier, which normally limits the accessibility to the CNS for drugs and drug delivery systems [122]. As a consequence, drug targeting strategies employing the 'EPR-like leakiness' of the blood brain barrier have shown promising effects in preclinical models for MS.

Glucocorticoids are commonly used in high doses to reduce disease activity in MS, like in RA, making them a good candidate for drug targeting, as targeting may help increasing the efficacy and limiting the side effects [123]. Long-circulating PEGylated liposomes containing methylprednisolone, prednisolone phosphate or dexamethasone phosphate have shown, compared to the free drug, an improved therapeutic efficacy in several studies using rat and mouse EAE models (Figure 3D and E) [27, 124-126]. In addition, liposomes encapsulating other anti-inflammatory compounds have been studied for their potency in MS. For example, minocycline, a tetracycline derivative which reduces matrix metalloproteinase 9 activity (Figure 3C) [127], tempamine, a piperidine nitroxide which

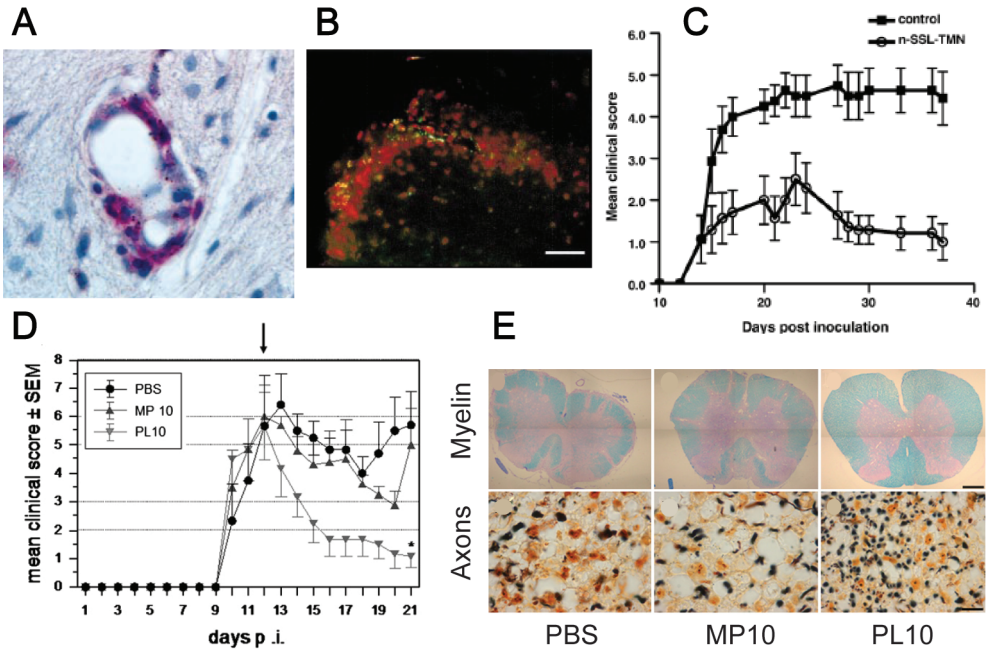

Figure 3. Drug targeting in MS. **A**. Histological staining of the spinal cord of a rat with EAE showing the accumulation of gold-labeled liposomes (black dots) in relation to macrophages (ED1 mAb, red) 5 days after treatment. The liposomes were mostly located in the macrophages around the vasculature in the inflamed sites of the CNS [27]. **B**. Fluorescence microscopy images of transverse sections of the spinal cord of a rat with EAE illustrating the accumulation of fluorescently labeled PEGylated polycyanoacrylate nanoparticles (green) in relation to macrophages (ED1 mAb, red) 24 h after treatment. Significant amounts of fluorescent nanoparticles accumulated in the inflamed areas in the white matter of the brain and spinal cord, which colocalized mainly in the macrophage infiltrations [26]. **C**. Therapeutic efficacy of tempamine-loaded PEGylated liposomes (n-SSL-TMN), upon daily i.v. injections of 8.5 mg/kg from day 10 post inoculation (p.i.), compared to saline on the clinical EAE score of mice with chronic EAE. Daily injections of liposomal tempamine, when compared to control, resulted in a significant reduction in several parameters of disease activity, such as disease duration, mean clinical score and histological score. Daily injections of free tempamine (8.5 mg/kg) did not result in significant differences compared to the control (not shown in plot) [128]. **D**. Therapeutic efficacy of 10 mg/kg prednisolone phosphate-loaded PEGylated liposomes (PL10), after a single injection on day 12 p.i. (arrow), compared to PBS and 3 daily injections of 10 mg/kg methylprednisolone (MP10) on the clinical EAE score of rats with acute relapsing EAE. PL10 treatment resulted in a significant alleviation of clinical systems of EAE, and protected against a relapse of disease activity. Three subsequent MP10 injections did not lead to an improvement in disease activity, and could not prevent the relapse occurring around day 20 [125]. **E**. Histological staining of spinal cords of rats with acute EAE, 9 days after treatment with PBS (left), MP10 (middle) or PL10 (right), illustrating the reduced demyelinization (blue, upper row) and the preservation of axons (black, lower row) upon treatment with glucocorticoid-loaded liposomes [125].

possesses anti-oxidant activity [128], and leupeptin, a tripeptide protease inhibitor [129], all have shown EAE suppressing activity upon their encapsulation into liposomes. Like in RA, there is strong evidence that the favorable therapeutic effects of targeted drug delivery systems in MS may be – at least in part – mediated by their uptake by macrophages and macrophage-like microglia, since their depletion, by using either clodronate liposomes or silica quartz microparticles, led to an alleviation of the clinical symptoms in EAE [130, 131].

Interestingly, most of the work concerning drug targeting to MS has been done using liposomes [27, 124-129, 132-135], although there is no reason to assume that other types of drug delivery systems would be unsuitable for this purpose. Whereas there are several studies demonstrating the accumulation of liposomes in sites of active inflammation within the CNS [125, 132, 133], there is in fact only one report that shows the *in vivo* accumulation of a non-liposomal system, i.e. PEGylated polycyanoacrylate nanoparticles, in rats with EAE (Figure 3A and B) [26]. However, since in the latter study only nanoparticles without a drug were used, their effectiveness in MS therapy has yet to be demonstrated.

2.5. Drug Targeting in Inflammatory Bowel Disease

Similar to RA and MS, IBD commonly presents with an intermittent course of disease, including regular exacerbations and remissions of active intestinal inflammation, and is frequently treated with glucocorticoids and other anti-inflammatory therapies [136]. Also, due to an inflammation-specific increase in intestinal vascular permeability (i.e. the EPR effect), IBD may be targeted systemically: studies using intravenously injected radiolabelled liposomes or biotinylated albumin-GdDTPA conjugates observed a 10- to 37-fold increase in accumulation of nanocarriers in inflamed colons compared to colons of healthy animals [137-139]. Whereas the EPR effect in IBD certainly enables the systemic application of passively targeted drug delivery systems, most research has focused on an oral delivery approach targeting the inflamed intestinal mucosa using e.g. polymeric micro- and nanoparticles [140-143]. For intestinal inflammatory diseases such as IBD, an oral strategy is a logical and straightforward choice, and consequently, studies employing a systemic drug delivery strategy for IBD therapy are few, and with limited success [126]. Nevertheless, the systemic nature of IBD does make systemic drug delivery a promising approach, and merits a more thorough evaluation of this strategy, especially in view of the

current clinical management of IBD, for which no drug targeting system is available yet.

3. Perspectives

The research done in the context of drug delivery in inflammatory bowel disease (IBD), as described previously in section 2.5, may be considered a good example of how drug targeting research might benefit from a more structured approach to improve its outcome. In the authors' opinion, a systematic exploration of a specific targeting technology in several preclinical models of (inflammatory) diseases on the one hand, or several targeting systems in a specific disease model on the other hand, often seems to be lacking. As discussed in this review, many inflammatory diseases, including cancer, may be targeted using the same strategic principles, e.g. using the EPR effect and upregulation of target-specific receptors, and drugs, such as anti-inflammatory and anti-angiogenic drugs. With this in mind, one could pose that it is a suboptimal use of knowledge and resources to focus all efforts on merely a single technology for targeted delivery to a single disease. Nevertheless, all too often research groups have restricted their research in this manner, focusing on the development of one technology for a specific application – in many cases a single type of cancer. As a result, there are many specialists in the field that gained extensive knowledge and experience concerning a specific delivery technology, in a specific disease, using a specific model, while in fact the role of drug targeting systems in the clinical management of these diseases remains limited. From this point of view, we wish to elaborate on a dualistic approach as schematically depicted in Figure 4, which represents an attractive strategy for drug targeting research in order to enhance its clinical applicability.

3.1. One for all – Platform technology-oriented Drug Targeting Research

The most commonly adopted strategy in drug targeting research concerns the 'one for all' approach. In this approach the emphasis is placed on a specific drug targeting technology, which is developed and optimized for drug targeting to several diseases. At a certain point in the development, the targeting system is evaluated in preclinical models, typically cancer models. Subsequent efforts are primarily focused on improving the system – often by making it more complex – and expanding the knowledge with respect to the technology. The 'one for all' drug targeting forms a sensible and necessary element in drug delivery research: it contributes to a deeper understanding of the platform technology in question

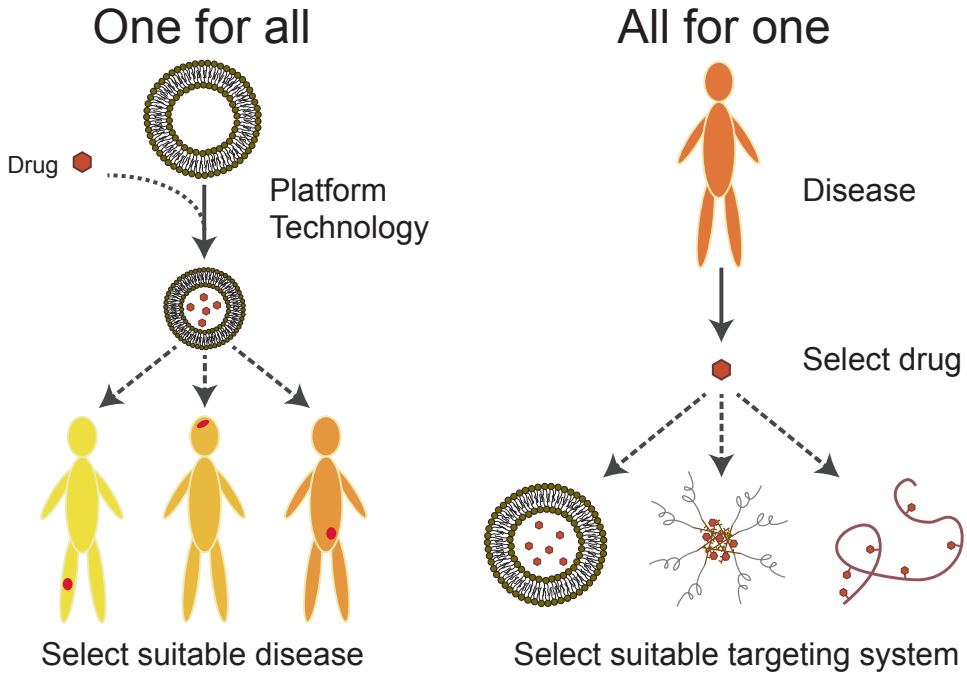

Figure 4. Schematic representation of the dualistic approach for drug targeting research. The 'one for all' strategy focuses on a single platform technology, which may consist of a carrier system with or without a specific drug. This drug targeting system is then evaluated in various (preclinical) models of inflammatory disease, e.g. RA, MS and IBD. In contrast, the 'all for one' strategy is focused on a specific disease for which a drug is selected that could benefit of a targeted approach, e.g. due to its intrinsic low activity and/or high toxicity. For the targeted delivery of the drug, several candidate targeting systems, e.g. liposomes, micelles and polymer-drug conjugates, are then selected and evaluated in a (preclinical) model of the disease in question.

and the principles by which it works, it allows for structured patenting, and it strengthens the expertise of the research groups involved.

3.2. All for one – Disease-oriented Drug Targeting Research

In our opinion, the 'all for one' approach is advantageous in stimulating the translation of drug targeting research into clinical applications. In contrast to the technology-oriented 'one for all' perspective, i.e. taking a technology and searching for suitable applications, the disease-oriented 'all for one' perspective, which focuses on the pursuit of an optimal drug targeting system for the therapy for a specific disease, appears to be much less adopted. Based on basic knowledge concerning the underlying pathological processes, proven therapeutic efficacy *in vitro* and/or *in vivo* and current clinical treatment strategies,

drug candidates which are expected to interfere with the disease are elected and applied in 'aspirant' drug targeting systems. To enable the selection of the most promising targeted carrier systems for the drug in question, there are several critical questions that should be answered. These, sometimes obvious, questions include: what are the physicochemical properties of the compound? (Is it hydrophobic or hydrophilic? What is its pKa?) What type of release kinetics is required? (Burst release? Slow release?) Which cells are the target cells? How do we reach these cells? Could a targeting ligand improve the carrier localization at these cells?

After the selection of targeted carrier candidates and their proper *in vitro* characterization, these drug targeting systems require a thorough evaluation in reliable, well-accepted clinically relevant models for the disease. Evidently, for each model the pathological pathways in which the targeted drug will be interfering should resemble the human pathology as close as possible.

The 'all for one' approach, by evaluating several drug delivery strategies utilizing the same drug in the same models, provides a better insight in which system may be optimal for that specific clinical application, which, without a doubt, improves the chances of a drug targeting system reaching clinical practice. Another important advantage of 'all for one' research is its multidisciplinary character, since only a few research groups possess sufficient expertise and experience concerning all involved targeting system technologies, *in vitro* characterization methods, and *in vivo* models for therapeutic evaluation, to successfully perform this research. Therefore, a stronger collaboration between groups, each with their own specialties regarding e.g. a drug targeting technology, *in vitro* characterization, preclinical modeling, tissue analysis, or clinical translation, is imperative. Such collaborations improve the creativity and, most likely, stimulate the generation of drug targeting systems with strong clinical potential.

4. Conclusions

Despite the evident focus on cancer therapy in drug targeting research, a large number of drug targeting systems have shown good therapeutic efficacy in various preclinical models of inflammatory diseases. Nevertheless, although many inflammatory diseases show strong similarities and may be targeted using the same principles, a thorough evaluation of one delivery system in several diseases (one for all), or reversely, several delivery systems in one

disease (all for one), is often lacking. In our view, in order to stimulate the development of clinically applicable drug targeting systems, the employment of the more systematic 'one for all' and 'all for one' approaches as proposed in this review, might prove to be highly beneficial.

5. Acknowledgements

This work was supported by MediTrans, an Integrated Project funded by the European Commission under the "nanotechnologies and nano-sciences, knowledge-based multifunctional materials and new production processes and devices" (NMP), thematic priority of the Sixth Framework Program.

6. References

[1] R. Duncan, Polymer therapeutics as nanomedicines: new perspectives, Curr. Opin. Biotechnol. 22(4) (2011) 492-501.

[2] V.P. Torchilin, Drug Deliv., Vol. 197, Springer Berlin Heidelberg, 2010, pp. 3-53.

[3] R. Duncan, Polymer conjugates as anticancer nanomedicines, Nat. Rev. Cancer 6(9) (2006) 688-701.

[4] T. Lammers, W.E. Hennink, G. Storm, Tumour-targeted nanomedicines: principles and practice, Br. J. Cancer 99(3) (2008) 392-397.

[5] F. Danhier, O. Feron, V. Préat, To exploit the tumor microenvironment: Passive and active tumor targeting of nanocarriers for anti-cancer drug delivery, J. Control. Release 148(2) (2010) 135-146.

[6] E. Yelin, L. Murphy, M.G. Cisternas, A.J. Foreman, D.J. Pasta, C.G. Helmick, Medical care expenditures and earnings losses among persons with arthritis and other rheumatic conditions in 2003, and comparisons with 1997, Arthritis Rheum. 56(5) (2007) 1397-1407.

[7] T. Kirchhoff, J. Ruof, T. Mittendorf, M. Rihl, M. Bernateck, W. Mau, H. Zeidler, R.E. Schmidt, S. Merkesdal, Cost of illness in rheumatoid arthritis in Germany in 1997-98 and 2002: cost drivers and cost savings, Rheumatology 50(4) (2011) 756-761.

[8] P. Rieckmann, Socio-economic aspects of neuroimmunological diseases, J. Neurol. 253(Suppl. 5) (2006) V87-90.

[9] M. Coimbra, S.A. Kuijpers, S.P. van Seters, G. Storm, R.M. Schiffelers, Targeted delivery of anti-inflammatory agents to tumors, Curr. Pharm. Des. 15(16) (2009) 1825-1843.

[10] K.J. O'Byrne, A.G. Dalgleish, Chronic immune activation and inflammation as the cause of malignancy, Br. J. Cancer 85(4) (2001) 473-483.

[11] R.M. Schiffelers, M. Banciu, J.M. Metselaar, G. Storm, Therapeutic application of long-circulating liposomal glucocorticoids in auto-immune diseases and cancer, J. Liposome Res. 16(3) (2006) 185-194.

[12] Y. Matsumura, H. Maeda, A new concept for macromolecular therapeutics in cancer chemotherapy: Mechanism of tumoritropic accumulation of proteins and the antitumor agent smancs, Cancer Res. 46(12 I) (1986) 6387-6392.

[13] H. Maeda, M. Ueda, T. Morinaga, T. Matsumoto, Conjugation of poly(styrene-co-maleic acid) derivatives to the antitumor protein neocarzinostatin: pronounced improvements in pharmacological properties, J. Med. Chem. 28(4) (1985) 455-461.

[14] J. Fang, H. Nakamura, H. Maeda, The EPR effect: Unique features of tumor blood vessels for drug delivery, factors involved, and limitations and augmentation of the effect, Adv. Drug Deliv. Rev. 63(3) (2011) 136-151.

[15] H. Maeda, Y. Matsumura, EPR effect based drug design and clinical outlook for enhanced cancer chemotherapy, Adv. Drug Deliv. Rev. 63(3) (2011) 129-130.

[16] H. Maeda, J. Wu, T. Sawa, Y. Matsumura, K. Hori, Tumor vascular permeability and the EPR effect in macromolecular therapeutics: A review, J. Control. Release 65(1-2) (2000) 271-284.

[17] M. Talelli, C.J.F. Rijcken, C.F. van Nostrum, G. Storm, W.E. Hennink, Micelles based on HPMA copolymers, Adv. Drug Deliv. Rev. 62(2) (2010) 231-239.
[18] T. Lammers, Improving the efficacy of combined modality anticancer therapy using HPMA copolymer-based nanomedicine formulations, Adv. Drug Deliv. Rev. 62(2) (2010) 203-230.
[19] I. Kushner, J.A. Somerville, Permeability of human synovial membrane to plasma proteins. Relationship to molecular size and inflammation, Arthritis Rheum. 14(5) (1971) 560-570.
[20] J.R. Levick, Permeability of rheumatoid and normal human synovium to specific plasma proteins, Arthritis Rheum. 24(12) (1981) 1550-1560.
[21] C. Gómez-Vaquero, J.M. Nolla, J. Fiter, J.M. Ramon, R. Concustell, J. Valverde, D. Roig-Escofet, Nutritional status in patients with rheumatoid arthritis, Joint Bone Spine 68(5) (2001) 403-409.
[22] F.C. Ballantyne, A. Fleck, W.C. Dick, Albumin metabolism in rheumatoid arthritis., Ann. Rheum. Dis. 30(3) (1971) 265–270.
[23] J. Bennett, J. Basivireddy, A. Kollar, K.E. Biron, P. Reickmann, W.A. Jefferies, S. McQuaid, Blood-brain barrier disruption and enhanced vascular permeability in the multiple sclerosis model EAE, J. Neuroimmunol. 229(1-2) (2010) 180-191.
[24] J. Kirk, J. Plumb, M. Mirakhur, S. McQuaid, Tight junctional abnormality in multiple sclerosis white matter affects all calibres of vessel and is associated with blood-brain barrier leakage and active demyelination, J. Pathol. 201(2) (2003) 319-327.
[25] E.E. Kwon, J.W. Prineas, Blood-brain barrier abnormalities in longstanding multiple sclerosis lesions. An immunohistochemical study, J. Neuropathol. Exp. Neurol. 53(6) (1994) 625-636.
[26] P. Calvo, B. Gouritin, H. Villarroya, F. Eclancher, C. Giannavola, C. Klein, J.P. Andreux, P. Couvreur, Quantification and localization of PEGylated polycyanoacrylate nanoparticles in brain and spinal cord during experimental allergic encephalomyelitis in the rat, Eur. J. Neurosci. 15(8) (2002) 1317-1326.
[27] J. Schmidt, J.M. Metselaar, M.H.M. Wauben, K.V. Toyka, G. Storm, R. Gold, Drug targeting by long-circulating liposomal glucocorticosteroids increases therapeutic efficacy in a model of multiple sclerosis, Brain 126(8) (2003) 1895-1904.
[28] A. Wunder, U. Müller-Ladner, E.H.K. Stelzer, J. Funk, E. Neumann, G. Stehle, T. Pap, H. Sinn, S. Gay, C. Fiehn, Albumin-based drug delivery as novel therapeutic approach for rheumatoid arthritis, J. Immunol. 170(9) (2003) 4793-4801.
[29] D. Wang, S. Miller, X.-M. Liu, B. Anderson, X.S. Wang, S. Goldring, Novel dexamethasone-HPMA copolymer conjugate and its potential application in treatment of rheumatoid arthritis, Arthrit. Res. Ther. 9(1) (2007) R2.
[30] J.M. Metselaar, M.H.M. Wauben, J.P.A. Wagenaar-Hilbers, O.C. Boerman, G. Storm, Complete remission of experimental arthritis by joint targeting of glucocorticoids with long-circulating liposomes, Arthritis Rheum. 48(7) (2003) 2059-2066.
[31] S.M. Grayson, W.T. Godbey, The role of macromolecular architecture in passively targeted polymeric carriers for drug and gene delivery, J. Drug Target. 16(5) (2008) 329-356.
[32] E.A. Simone, T.D. Dziubla, V.R. Muzykantov, Polymeric carriers: role of geometry in drug delivery, Expert. Opin. Drug. Deliv. 5(12) (2008) 1283-1300.

[33] E.R. Gillies, E. Dy, J.M.J. Fréchet, F.C. Szoka, Biological evaluation of polyester dendrimer: poly(ethylene oxide) "bow-tie" hybrids with tunable molecular weight and architecture, Mol. Pharm. 2(2) (2005) 129-138.

[34] T. Yamaoka, Y. Tabata, Y. Ikada, Distribution and tissue uptake of poly(ethylene glycol) with different molecular weights after intravenous administration to mice, J. Pharm. Sci. 83(4) (1994) 601-606.

[35] Y.H. Bae, K. Park, Targeted drug delivery to tumors: myths, reality and possibility, J. Control. Release 153(3) (2011) 198-205.

[36] P. Ruenraroengsak, J.M. Cook, A.T. Florence, Nanosystem drug targeting: facing up to complex realities, J. Control. Release 141(3) (2010) 265-276.

[37] T.M. Allen, L. Murray, S. MacKeigan, M. Shah, Chronic liposome administration in mice: effects on reticuloendothelial function and tissue distribution, J. Pharmacol. Exp. Ther. 229(1) (1984) 267-275.

[38] E. Kluza, S.Y. Yeo, S. Schmid, D.W. van der Schaft, R.W. Boekhoven, R.M. Schiffelers, G. Storm, G.J. Strijkers, K. Nicolay, Anti-tumor activity of liposomal glucocorticoids: The relevance of liposome-mediated drug delivery, intratumoral localization and systemic activity, J. Control. Release 151(1) (2011) 10-17.

[39] C. Costa, J. Incio, R. Soares, Angiogenesis and chronic inflammation: cause or consequence?, Angiogenesis 10(3) (2007) 149-166.

[40] Z. Szekanecz, T. Besenyei, Á. Szentpétery, A.E. Koch, Angiogenesis and vasculogenesis in rheumatoid arthritis, Curr. Opin. Rheumatol. 22(3) (2010) 299-306.

[41] A. Koch, O. Distler, Vasculopathy and disordered angiogenesis in selected rheumatic diseases: rheumatoid arthritis and systemic sclerosis, Arthrit. Res. Ther. 9(Suppl 2) (2007) S3.

[42] A. Luttun, M. Tjwa, L. Moons, Y. Wu, A. Angelillo-Scherrer, F. Liao, J.A. Nagy, A. Hooper, J. Priller, B. De Klerck, V. Compernolle, E. Daci, P. Bohlen, M. Dewerchin, J.-M. Herbert, R. Fava, P. Matthys, G. Carmeliet, D. Collen, H.F. Dvorak, D.J. Hicklin, P. Carmeliet, Revascularization of ischemic tissues by PlGF treatment, and inhibition of tumor angiogenesis, arthritis and atherosclerosis by anti-Flt1, Nat. Med. 8(8) (2002) 831-840.

[43] T.J. Seabrook, A. Littlewood-Evans, V. Brinkmann, B. Pöllinger, C. Schnell, P.C. Hiestand, Angiogenesis is present in experimental autoimmune encephalomyelitis and pro-angiogenic factors are increased in multiple sclerosis lesions, J. Neuroinflamm. 7 (2010) 95.

[44] J.E. Holley, J. Newcombe, J.L. Whatmore, N.J. Gutowski, Increased blood vessel density and endothelial cell proliferation in multiple sclerosis cerebral white matter, Neurosci. Lett. 470(1) (2010) 65-70.

[45] D.J. Veale, U. Fearon, Inhibition of angiogenic pathways in rheumatoid arthritis: potential for therapeutic targeting, Best Pract. Res. Clin. Rheumatol. 20(5) (2006) 941-947.

[46] Z. Szekanecz, A.E. Koch, Angiogenesis and its targeting in rheumatoid arthritis, Vascul. Pharmacol. 51(1) (2009) 1-7.

[47] S.A. Yoo, S.K. Kwok, W.U. Kim, Proinflammatory role of vascular endothelial growth factor in the pathogenesis of rheumatoid arthritis: prospects for therapeutic intervention, Mediators Inflamm. 2008 (2008) 129873.

[48] C.-S. Zhu, X.-Q. Hu, Z.-J. Xiong, Z.-Q. Lu, G.-Y. Zhou, D.-J. Wang, Adenoviral delivery of soluble VEGF receptor 1 (sFlt-1) inhibits experimental autoimmune encephalomyelitis in dark Agouti (DA) rats, Life Sci. 83(11-12) (2008) 404-412.

[49] R.W. Kinne, B. Stuhlmüller, G.R. Burmester, Cells of the synovium in rheumatoid arthritis. Macrophages, Arthritis Research and Therapy 9(6) (2007).

[50] R.A. Reilkoff, R. Bucala, E.L. Herzog, Fibrocytes: Emerging effector cells in chronic inflammation, Nat. Rev. Immunol. 11(6) (2011) 427-435.

[51] H. Li, M.L. Cuzner, J. Newcombe, Microglia-derived macrophages in early multiple sclerosis plaques, Neuropathol. Appl. Neurobiol. 22(3) (1996) 207-215.

[52] M.A. Proescholdt, S. Jacobson, N. Tresser, E.H. Oldfield, M.J. Merrill, Vascular endothelial growth factor is expressed in multiple sclerosis plaques and can induce inflammatory lesions in experimental allergic encephalomyelitis rats, J. Neuropathol. Exp. Neurol. 61(10) (2002) 914-925.

[53] R.A. Fava, N.J. Olsen, G. Spencer-Green, K.T. Yeo, T.K. Yeo, B. Berse, R.W. Jackman, D.R. Senger, H.F. Dvorak, L.F. Brown, Vascular permeability factor/endothelial growth factor (VPF/VEGF): Accumulation and expression in human synovial fluids and rheumatoid synovial tissue, J. Exp. Med. 180(1) (1994) 341-346.

[54] D. Cox, M. Brennan, N. Moran, Integrins as therapeutic targets: lessons and opportunities, Nat. Rev. Drug Discov. 9(10) (2010) 804-820.

[55] D. Gerlag, E. Borges, P. Tak, H.M. Ellerby, D. Bredesen, R. Pasqualini, E. Ruoslahti, G. Firestein, Suppression of murine collagen-induced arthritis by targeted apoptosis of synovial neovasculature, Arthritis Res. 3(6) (2001) 357 - 361.

[56] P.S. Low, W.A. Henne, D.D. Doorneweerd, Discovery and development of folic-acid-based receptor targeting for imaging and therapy of cancer and inflammatory diseases, Acc. Chem. Res. 41(1) (2008) 120-129.

[57] G.A. Koning, R.M. Schiffelers, M.H.M. Wauben, R.J. Kok, E. Mastrobattista, G. Molema, T.L.M. ten Hagen, G. Storm, Targeting of angiogenic endothelial cells at sites of inflammation by dexamethasone phosphate–containing RGD peptide liposomes inhibits experimental arthritis, Arthritis Rheum. 54(4) (2006) 1198-1208.

[58] C.P. Leamon, P.S. Low, Delivery of macromolecules into living cells: A method that exploits folate receptor endocytosis, Proc. Natl. Acad. Sci. U. S. A. 88(13) (1991) 5572-5576.

[59] S.D. Weitman, R.H. Lark, L.R. Coney, D.W. Fort, V. Frasca, V.R. Zurawski Jr, B.A. Kamen, Distribution of the folate receptor GP38 in normal and malignant cell lines and tissues, Cancer Res. 52(12) (1992) 3396-3401.

[60] N. Nakashima-Matsushita, T. Homma, S. Yu, T. Matsuda, N. Sunahara, T. Nakamura, M. Tsukano, M. Ratnam, T. Matsuyama, Selective expression of folate receptor Î² and its possible role in methotrexate transport in synovial macrophages from patients with rheumatoid arthritis, Arthritis Rheum. 42(8) (1999) 1609-1616.

[61] M.J. Turk, G.J. Breur, W.R. Widmer, C.M. Paulos, L.C. Xu, L.A. Grote, P.S. Low, Folate-targeted imaging of activated macrophages in rats with adjuvant-induced arthritis, Arthritis Rheum. 46(7) (2002) 1947-1955.

[62] P.S. Low, A.C. Antony, Folate receptor-targeted drugs for cancer and inflammatory diseases, Adv. Drug Deliv. Rev. 56(8) (2004) 1055-1058.

[63] W. Xia, A.R. Hilgenbrink, E.L. Matteson, M.B. Lockwood, J.X. Cheng, P.S. Low, A functional folate receptor is induced during macrophage activation and can be used to target drugs to activated macrophages, Blood 113(2) (2009) 438-446.

[64] M.D. Salazar, M. Ratnam, The folate receptor: What does it promise in tissue-targeted therapeutics?, Cancer Metastasis Rev. 26(1) (2007) 141-152.

[65] X. Wang, F. Shen, J.H. Freisheim, L.E. Gentry, M. Ratnam, Differential stereospecificities and affinities of folate receptor isoforms for folate compounds and antifolates, Biochem. Pharmacol. 44(9) (1992) 1898-1901.

[66] H. Elnakat, M. Ratnam, Distribution, functionality and gene regulation of folate receptor isoforms: implications in targeted therapy, Adv. Drug Deliv. Rev. 56(8) (2004) 1067-1084.

[67] J.F. Kukowska-Latallo, K.A. Candido, Z. Cao, S.S. Nigavekar, I.J. Majoros, T.P. Thomas, L.P. Balogh, M.K. Khan, J.R. Baker Jr, Nanoparticle targeting of anticancer drug improves therapeutic response in animal model of human epithelial cancer, Cancer Res. 65(12) (2005) 5317-5324.

[68] X. Zhao, H. Li, R.J. Lee, Targeted drug delivery via folate receptors, Expert. Opin. Drug. Deliv. 5(3) (2008) 309-319.

[69] M.J. Turk, D.J. Waters, P.S. Low, Folate-conjugated liposomes preferentially target macrophages associated with ovarian carcinoma, Cancer Lett. 213(2) (2004) 165-172.

[70] P.C. Brooks, R.A.F. Clark, D.A. Cheresh, Requirement of vascular integrin avb3 for angiogenesis, Science 264(5158) (1994) 569-571.

[71] C.M. Storgard, D.G. Stupack, A. Jonczyk, S.L. Goodman, R.I. Fox, D.A. Cheresh, Decreased angiogenesis and arthritic disease in rabbits treated with an avb3 antagonist, J. Clin. Invest. 103(1) (1999) 47-54.

[72] P.C. Brooks, A.M.P. Montgomery, M. Rosenfeld, R.A. Reisfeld, T. Hu, G. Klier, D.A. Cheresh, Integrin avb3 antagonists promote tumor regression by inducing apoptosis of angiogenic blood vessels, Cell 79(7) (1994) 1157-1164.

[73] Y. Takada, Y. Ono, J. Sagusa, C. Mitsiades, N. Mitsiades, J. Tsai, Y. He, E. Maningding, A. Coleman, D. Ramirez-Maverakis, R. Rodriquez, E. Maverakis, A T cell-binding fragment of fibrinogen can prevent autoimmunity, J. Autoimmun. 34(4) (2010) 453-459.

[74] H.F. Zhou, H.W. Chan, S.A. Wickline, G.M. Lanza, C.T.N. Pham, avb3-Targeted nanotherapy suppresses inflammatory arthritis in mice, FASEB J. 23(9) (2009) 2978-2985.

[75] N. Nasongkla, X. Shuai, H. Ai, B.D. Weinberg, J. Pink, D.A. Boothman, J. Gao, cRGD-functionalized polymer micelles for targeted doxorubicin delivery, Angew. Chem. 43(46) (2004) 6323-6327.

[76] L. Klareskog, A.I. Catrina, S. Paget, Rheumatoid arthritis, The Lancet 373(9664) (2009) 659-672.

[77] E. Karouzakis, M. Neidhart, R.E. Gay, S. Gay, Molecular and cellular basis of rheumatoid joint destruction, Immunol. Lett. 106(1) (2006) 8-13.

[78] H. Takayanagi, H. Iizuka, T. Juji, T. Nakagawa, A. Yamamoto, T. Miyazaki, Y. Koshihara, H. Oda, K. Nakamura, S. Tanaka, Involvement of receptor activator of nuclear factor ϰB ligand/osteoclast differentiation factor in osteoclastogenesis from synoviocytes in rheumatoid arthritis, Arthritis Rheum. 43(2) (2000) 259-269.

[79] G.S. Firestein, Invasive fibroblast-like synoviocytes in rheumatoid arthritis. Passive responders or transformed aggressors?, Arthritis Rheum. 39(11) (1996) 1781-1790.

[80] S. Lefèvre, A. Knedla, C. Tennie, A. Kampmann, C. Wunrau, R. Dinser, A. Korb, E.M. Schnäker, I.H. Tarner, P.D. Robbins, C.H. Evans, H. Stürz, J. Steinmeyer, S. Gay, J. Schölmerich, T. Pap, U. Müller-Ladner, E. Neumann, Synovial fibroblasts spread rheumatoid arthritis to unaffected joints, Nat. Med. 15(12) (2009) 1414-1420.

[81] T.K. Kvien, Epidemiology and burden of illness of rheumatoid arthritis, Pharmacoeconomics 22(2 Suppl.) (2004) 1-12.

[82] F. Wolfe, D.M. Mitchell, J.T. Sibley, J.F. Fries, D.A. Bloch, C.A. Williams, P.W. Spitz, M. Haga, S.M. Kleinheksel, M.A. Cathey, The mortality of rheumatoid arthritis, Arthritis Rheum. 37(4) (1994) 481-494.

[83] M.E. Weinblatt, J.M. Kremer, A.D. Bankhurst, K.J. Bulpitt, R.M. Fleischmann, R.I. Fox, C.G. Jackson, M. Lange, D.J. Burge, A trial of etanercept, a recombinant tumor necrosis factor receptor:Fc fusion protein, in patients with rheumatoid arthritis receiving methotrexate, N. Engl. J. Med. 340(4) (1999) 253-259.

[84] P. Barrera, A. Blom, P.L.E.M. van Lent, L. van Bloois, J.H. Beijnen, N. van Rooijen, M.C. de Waal Malefijt, L.B.A. van de Putte, G. Storm, W.B. van den Berg, Synovial macrophage depletion with clodronate-containing liposomes in rheumatoid arthritis, Arthritis Rheum. 43(9) (2000) 1951-1959.

[85] N. van Rooijen, E. van Kesteren-Hendrikx, Clodronate liposomes: perspectives in research and therapeutics, J. Liposome Res. 12(1-2) (2002) 81-94.

[86] P.L. van Lent, A.E. Holthuysen, N. van Rooijen, L.B. van de Putte, W.B. van den Berg, Local removal of phagocytic synovial lining cells by clodronate-liposomes decreases cartilage destruction during collagen type II arthritis, Ann. Rheum. Dis. 57(7) (1998) 408-413.

[87] P.J. Richards, A.S. Williams, R.M. Goodfellow, B.D. Williams, Liposomal clodronate eliminates synovial macrophages, reduces inflammation and ameliorates joint destruction in antigen-induced arthritis, Rheumatology 38(9) (1999) 818-825.

[88] R. Anderson, A. Franch, M. Castell, F.J. Perez-Cano, R. Bräuer, D. Pohlers, M. Gajda, A.P. Siskos, T. Katsila, C. Tamvakopoulos, U. Rauchhaus, S. Panzner, R.W. Kinne, Liposomal encapsulation enhances and prolongs the anti-inflammatory effects of water-soluble dexamethasone phosphate in experimental adjuvant arthritis, Arthrit. Res. Ther. 12(4) (2010).

[89] U. Rauchhaus, F.W. Schwaiger, S. Panzner, Separating therapeutic efficacy from glucocorticoid side-effects in rodent arthritis using novel, liposomal delivery of dexamethasone phosphate: long-term suppression of arthritis facilitates interval treatment, Arthritis Research and Therapy 11(6) (2009).

[90] J.M. van den Hoven, W. Hofkens, M.H.M. Wauben, J.P.A. Wagenaar-Hilbers, J.H. Beijnen, B. Nuijen, J.M. Metselaar, G. Storm, Optimizing the therapeutic index of liposomal glucocorticoids in experimental arthritis, Int. J. Pharm. 416(2) (2011) 471-7.

[91] Y. Avnir, R. Ulmansky, V. Wasserman, S. Even-Chen, M. Broyer, Y. Barenholz, Y. Naparstek, Amphipathic weak acid glucocorticoid prodrugs remote-loaded into sterically stabilized nanoliposomes evaluated in arthritic rats and in a Beagle dog: A novel approach to treating autoimmune arthritis, Arthritis Rheum. 58(1) (2008) 119-129.

[92] T. Harigai, H. Hagiwara, Y. Ogawa, T. Ishizuka, S. Kaneda, J. Kimura, Prednisolone phosphate-containing TRX-20 liposomes inhibit cytokine and chemokine production in human fibroblast-like synovial cells: a novel approach to rheumatoid arthritis therapy, J. Pharm. Pharmacol. 59(1) (2007) 137-143.

[93] J.M. Metselaar, W.B. van den Berg, A.E.M. Holthuysen, M.H.M. Wauben, G. Storm, P.L.E.M. van Lent, Liposomal targeting of glucocorticoids to synovial lining cells strongly increases therapeutic benefit in collagen type II arthritis, Ann. Rheum. Dis. 63(4) (2004) 348-353.

[94] D. Wang, S.C. Miller, M. Sima, D. Parker, H. Buswell, K.C. Goodrich, P. Kopečková, J. Kopeček, The arthrotropism of macromolecules in adjuvant-induced arthritis rat model: a preliminary study, Pharm. Res. 21(10) (2004) 1741-1749.

[95] X.-M. Liu, L.-d. Quan, J. Tian, F.C. Laquer, P. Ciborowski, D. Wang, Syntheses of click PEG-dexamethasone conjugates for the treatment of rheumatoid arthritis, Biomacromolecules 11(10) (2010) 2621-2628.

[96] X.-M. Liu, L.-D. Quan, J. Tian, Y. Alnouti, K. Fu, G. Thiele, D. Wang, Synthesis and evaluation of a well-defined HPMA copolymer–dexamethasone conjugate for effective treatment of rheumatoid arthritis, Pharm. Res. 25(12) (2008) 2910-2919.

[97] L.-D. Quan, P.E. Purdue, X.-M. Liu, M. Boska, S. Lele, G. Thiele, T. Mikuls, H. Dou, S. Goldring, D. Wang, Development of a macromolecular prodrug for the treatment of inflammatory arthritis: mechanisms involved in arthrotropism and sustained therapeutic efficacy, Arthrit. Res. Ther. 12(5) (2010) R170.

[98] D. Funk, H.H. Schrenk, E. Frei, Development of a novel polyethylene glycol-corticosteroid-conjugate with an acid-cleavable linker, J. Drug Target. 19(6) (2011) 434-445.

[99] J. Hwang, K. Rodgers, J.C. Oliver, T. Schluep, α-Methylprednisolone conjugated cyclodextrin polymer-based nanoparticles for rheumatoid arthritis therapy, Int. J. Nanomedicine 3(3) (2008) 359 - 371.

[100] M. Higaki, T. Ishihara, N. Izumo, M. Takatsu, Y. Mizushima, Treatment of experimental arthritis with poly(d,l-lactic/glycolic acid) nanoparticles encapsulating betamethasone sodium phosphate, Ann. Rheum. Dis. 64(8) (2005) 1132-1136.

[101] T. Ishihara, T. Kubota, T. Choi, M. Higaki, Treatment of experimental arthritis with stealth-type polymeric nanoparticles encapsulating betamethasone phosphate, J. Pharmacol. Exp. Ther. 329(2) (2009) 412-417.

[102] T. Ishihara, M. Takahashi, M. Higaki, Y. Mizushima, T. Mizushima, Preparation and characterization of a nanoparticulate formulation composed of PEG-PLA and PLA as anti-inflammatory agents, Int. J. Pharm. 385(1-2) (2010) 170-175.

[103] M.M. Tielemans, T. Eikendal, J.B.M.J. Jansen, M.G.H. van Oijen, Identification of NSAID users at risk for gastrointestinal complications: a systematic review of current guidelines and consensus agreements, Drug Saf. 33(6) (2010) 443-453.

[104] P. Srinath, S.P. Vyas, P.V. Diwan, Preparation and pharmacodynamic evaluation of liposomes of indomethacin, Drug Dev. Ind. Pharm. 26(3) (2000) 313-321.

[105] S. Palakurthi, S.P. Vyas, P.V. Diwan, Biodisposition of PEG-coated lipid microspheres of indomethacin in arthritic rats, Int. J. Pharm. 290(1-2) (2005) 55-62.

[106] A.S. Chauhan, N.K. Jain, P.V. Diwan, A.J. Khopade, Solubility enhancement of indomethacin with poly(amidoamine) dendrimers and targeting to inflammatory regions of arthritic rats, J. Drug Target. 12(9-10) (2004) 575-583.
[107] D. Chandrasekar, R. Sistla, F.J. Ahmad, R.K. Khar, P.V. Diwan, Folate coupled poly(ethyleneglycol) conjugates of anionic poly(amidoamine) dendrimer for inflammatory tissue specific drug delivery, J. Biomed. Mater. Res. A 82A(1) (2007) 92-103.
[108] D. Chandrasekar, R. Sistla, F.J. Ahmad, R.K. Khar, P.V. Diwan, The development of folate-PAMAM dendrimer conjugates for targeted delivery of anti-arthritic drugs and their pharmacokinetics and biodistribution in arthritic rats, Biomaterials 28(3) (2007) 504-512.
[109] A.S. Chauhan, P.V. Diwan, N.K. Jain, D.A. Tomalia, Unexpected in vivo anti-inflammatory activity observed for simple, surface functionalized poly(amidoamine) dendrimers, Biomacromolecules 10(5) (2009) 1195-1202.
[110] P.A. Liso, M. Rebuelta, J.S. Román, A. Gallardo, A.M. Villar, Polymeric drugs derived from Ibuprofen with improved antiinflammatory profile, J. Biomed. Mater. Res. 32(4) (1996) 553-560.
[111] H. Thakkar, R.K. Sharma, A.K. Mishra, K. Chuttani, R.R. Murthy, Albumin microspheres as carriers for the antiarthritic drug celecoxib, AAPS PharmSciTech 6(1) (2004) E65–E73.
[112] A. Williams, R. Goodfellow, N. Topley, N. Amos, B. Williams, The suppression of rat collagen-induced arthritis and inhibition of macrophage derived mediator release by liposomal methotrexate formulations, Inflamm. Res. 49(4) (2000) 155-161.
[113] A.S. Williams, S.G. Jones, R.M. Goodfellow, N. Amos, B.D. Williams, Interleukin-1beta (IL-1beta) inhibition: a possible mechanism for the anti-inflammatory potency of liposomally conjugated methotrexate formulations in arthritis, Br. J. Pharmacol. 128(1) (1999) 234-240.
[114] C. Fiehn, U. Müller-Ladner, S. Gay, S. Krienke, S. Freudenberg-Konrad, J. Funk, A.D. Ho, H. Sinn, A. Wunder, Albumin-coupled methotrexate (MTX-HSA) is a new anti-arthritic drug which acts synergistically to MTX, Rheumatology 43(9) (2004) 1097-1105.
[115] C. Fiehn, F. Kratz, G. Sass, U. Müller-Ladner, E. Neumann, Targeted drug delivery by in vivo coupling to endogenous albumin: an albumin-binding prodrug of methotrexate (MTX) is better than MTX in the treatment of murine collagen-induced arthritis, Ann. Rheum. Dis. 67(8) (2008) 1188-1191.
[116] B.M. Keegan, J.H. Noseworthy, Multiple sclerosis, Annu. Rev. Med. 53(1) (2002) 285-302.
[117] C. Stadelmann, Multiple sclerosis as a neurodegenerative disease: pathology, mechanisms and therapeutic implications, Curr. Opin. Neurol. 24(3) (2011) 224-229.
[118] A. Bitsch, J. Schuchardt, S. Bunkowski, T. Kuhlmann, W. Brück, Acute axonal injury in multiple sclerosis. Correlation with demyelination and inflammation, Brain 123(6) (2000) 1174-1183.
[119] R. Dutta, B.D. Trapp, Pathogenesis of axonal and neuronal damage in multiple sclerosis, Neurology 68(22 Suppl. 3) (2007) S22-S31.
[120] C. Stadelmann, C. Wegner, W. Brück, Inflammation, demyelination, and degeneration -- Recent insights from MS pathology, BBA-Mol. Basis Dis. 1812(2) (2011) 275-282.

[121] L.M. Schönrock, G. Gawlowski, W. Brück, Interleukin-6 expression in human multiple sclerosis lesions, Neurosci. Lett. 294(1) (2000) 45-48.
[122] A.R. Calabria, E.V. Shusta, Blood-brain barrier genomics and proteomics: elucidating phenotype, identifying disease targets and enabling brain drug delivery, Drug Discov. Today 11(17-18) (2006) 792-799.
[123] F. Brusaferri, L. Candelise, Steriods for multiple sclerosis and optic neuritis: a meta-analysis of randomized controlled clinical trials, J. Neurol. 247(6) (2000) 435-442.
[124] J. Schmidt, J.M. Metselaar, R. Gold, Intravenous liposomal prednisolone downregulates in situ TNF-a production by T-cells in experimental autoimmune encephalomyelitis, J. Histochem. Cytochem. 51(9) (2003) 1241-1244.
[125] R.A. Linker, C. Weller, F. Lühder, A. Mohr, J. Schmidt, M. Knauth, J.M. Metselaar, R. Gold, Liposomal glucocorticosteroids in treatment of chronic autoimmune demyelination: Long-term protective effects and enhanced efficacy of methylprednisolone formulations, Exp. Neurol. 211(2) (2008) 397-406.
[126] B.J. Crielaard, T. Lammers, M.E. Morgan, L. Chaabane, S. Carboni, B. Greco, P. Zaratin, A.D. Kraneveld, G. Storm, Macrophages and liposomes in inflammatory disease: friends or foes?, Int. J. Pharm. 416(2) (2011) 499-506.
[127] W. Hu, J.M. Metselaar, L.-H. Ben, P.D. Cravens, M.P. Singh, E.M. Frohman, T.N. Eagar, M.K. Racke, B.C. Kieseier, O. Stüve, PEG minocycline-liposomes ameliorate CNS autoimmune disease, PLoS ONE 4(1) (2009) e4151.
[128] P. Kizelsztein, H. Ovadia, O. Garbuzenko, A. Sigal, Y. Barenholz, Pegylated nanoliposomes remote-loaded with the antioxidant tempamine ameliorate experimental autoimmune encephalomyelitis, J. Neuroimmunol. 213(1-2) (2009) 20-25.
[129] T. Osanai, Y. Nagai, Suppression of experimental allergic encephalomyelitis (EAE) with liposome-encapsulated protease inhibitor: therapy through the blood-brain barrier, Neurochem. Res. 9(10) (1984) 1407-1416.
[130] I. Huitinga, N. van Rooijen, C. de Groot, B. Uitdehaag, C. Dijkstra, Suppression of experimental allergic encephalomyelitis in Lewis rats after elimination of macrophages, J. Exp. Med. 172(4) (1990) 1025-1033.
[131] C.F. Brosnan, M.B. Bornstein, B.R. Bloom, The effects of macrophage depletion on the clinical and pathologic expression of experimental allergic encephalomyelitis, J. Immunol. 126(2) (1981) 614-620.
[132] G. Cavaletti, A. Cassetti, A. Canta, S. Galbiati, A. Gilardini, N. Oggioni, V. Rodriguez-Menendez, A. Fasano, G.M. Liuzzi, U. Fattler, S. Ries, J. Nieland, P. Riccio, H. Haas, Cationic liposomes target sites of acute neuroinflammation in experimental autoimmune encephalomyelitis, Mol. Pharm. 6(5) (2009) 1363-1370.
[133] V. Rousseau, B. Denizot, J.J. Le Jeune, P. Jallet, Early detection of liposome brain localization in rat experimental allergic encephalomyelitis, Exp. Brain Res. 125(3) (1999) 255-264.
[134] J.M. Boggs, A. Goundalkar, F. Doganoglu, N. Samji, J. Kurantsin-Mills, K.M. Koshy, Antigen-targeted liposome-encapsulated methotrexate specifically kills lymphocytes sensitized to the nonapeptide of myelin basic protein, J. Neuroimmunol. 17(1) (1987) 35-48.

[135] K. Avrilionis, J.M. Boggs, Suppression of experimental allergic encephalomyelitis by the encephalitogenic peptide, in solution or bound to liposomes, J. Neuroimmunol. 35(1-3) (1991) 201-210.
[136] J.R.F. Cummings, S. Keshav, S.P.L. Travis, Medical management of Crohn's disease, BMJ 336(7652) (2008) 1062-1066.
[137] V. Awasthi, B. Goins, L. McManus, R. Klipper, W.T. Phillips, [99mTc] liposomes for localizing experimental colitis in arabbit model, Nucl. Med. Biol. 30(2) (2003) 159-168.
[138] V.D. Awasthi, B. Goins, R. Klipper, W.T. Phillips, Accumulation of PEG-liposomes in the inflamed colon of rats: potential for therapeutic and diagnostic targeting of inflammatory bowel diseases, J. Drug Target. 10(5) (2002) 419-427.
[139] T. Aychek, K. Vandoorne, O. Brenner, S. Jung, M. Neeman, Quantitative analysis of intravenously administered contrast media reveals changes in vascular barrier functions in a murine colitis model, Magn. Reson. Med. 66(1) (2011) 235-243.
[140] B. Moulari, D. Pertuit, Y. Pellequer, A. Lamprecht, The targeting of surface modified silica nanoparticles to inflamed tissue in experimental colitis, Biomaterials 29(34) (2008) 4554-4560.
[141] A. Makhlof, Y. Tozuka, H. Takeuchi, pH-Sensitive nanospheres for colon-specific drug delivery in experimentally induced colitis rat model, Eur. J. Pharm. Biopharm. 72(1) (2009) 1-8.
[142] A. Lamprecht, U. Schäfer, C.-M. Lehr, Size-dependent bioadhesion of micro- and nanoparticulate carriers to the inflamed colonic mucosa, Pharm. Res. 18(6) (2001) 788-793.
[143] A. Lamprecht, N. Ubrich, H. Yamamoto, U. Schäfer, H. Takeuchi, P. Maincent, Y. Kawashima, C.-M. Lehr, Biodegradable nanoparticles for targeted drug delivery in treatment of inflammatory bowel disease, J. Pharmacol. Exp. Ther. 299(2) (2001) 775-781

3

Macrophages and liposomes in inflammatory disease: friends or foes?

B.J. Crielaard [1], T. Lammers [1,2], M.E. Morgan [3], L. Chaabane [4], S. Carboni [4], B. Greco [4], P. Zaratin [5], A.D. Kraneveld [3] and G. Storm [1]

1. Department of Pharmaceutics, Utrecht Institute for Pharmaceutical Sciences (UIPS), Utrecht University, Utrecht, The Netherlands
2. Department of Experimental Molecular Imaging, RWTH – Aachen University, Aachen, Germany
3. Department of Pharmacology, UIPS, Utrecht University, Utrecht, The Netherlands
4. Department of Scientific Innovation and Partnerships and Autoimmune Diseases, Merck Serono, Geneva, Switzerland
5. Italian Foundation of Multiple Sclerosis, FISM Onlus – AISM, Genoa, Italy

Int. J. Pharm. 2011 416(2):499-506

Abstract

Liposome-encapsulated corticosteroids have shown to exert strong beneficial effects in inflammatory diseases, such as arthritis and cancer. To extend the clinical applicability of these potent nanomedicines, the therapeutic effect of dexamethasone phosphate loaded long-circulating liposomes (LCL-DXP) was evaluated in animal models of Multiple Sclerosis (MS) and Crohn's Disease (CD).

In mice with Experimental Autoimmune Encephalitis (EAE), a model for MS, treatment with LCL-DXP, but not free DXP, resulted in a decrease in disease activity when compared to PBS treated mice. In contrast, in mice with chronic DSS-induced colitis, a model for CD, treatment with LCL-DXP did not induce an improvement, but in fact worsened the fecal blood loss after treatment, indicating an aggravation of the disease. It is hypothesized that modulation of macrophage polarization towards a M2 phenotype underlies the efficacy of corticosteroid-based drug delivery systems, which is supported by the presented data. On the one hand, M1 polarized macrophages are part of the pathogenesis of MS; the modulation to M2-polarization by LCL-DXP is therefore beneficial. On the other hand, M1-polarized intestinal macrophages fulfill a protective and inflammation-suppressing role in intestinal homeostasis; changing their phenotype to M2 causes reduced protection to invading microorganisms, leading to a more severe intestinal inflammation. These findings therefore indicate that the interplay between the specific phenotype of macrophages and the specific inflammatory context of the inflammatory disease in question may be an important determining factor in the therapeutic applicability of liposomal corticosteroids in inflammatory disease.

1. Introduction

In the last decade, targeting strategies using liposome-encapsulated corticosteroids have shown to have a distinct therapeutic effect in several animal models of inflammatory diseases, such as rheumatoid arthritis (RA), multiple sclerosis (MS) and cancer [1-3]. The increased leakiness of blood vessels and the reduced lymphatic drainage occurring in inflamed tissues and tumors, referred to as the Enhanced Permeability and Retention (EPR) effect [4], enables enhanced accumulation of long-circulating nanosized carrier systems in these target tissues [5]. In this regard, liposomes with a poly(ethylene glycol) (PEG) coating are most advanced, with a long circulation time and favorable biodistribution, and therefore frequently used as drug carriers [6]. Although the administration of such long-circulating liposomes leads to higher concentrations of the encapsulated drug at the inflamed site, the precise mechanism of how these encapsulated drugs interact with the target inflammatory tissue is still quite unclear.

There is compelling evidence that macrophages play a crucial role in this mechanism. Macrophages and other phagocytic cells of the reticuloendothelial system (RES) are essential in the elimination of liposomes from the circulation [7, 8]. Although these cells are mainly residing in the liver and spleen, they are also responsible for the phagocytosis of liposomes in other (target) tissues [9]. After degradation of the liposomal carrier by these target tissue macrophages, the drug that had been encapsulated can have various fates: 1) the liberated drug molecules are degraded within the lysosomal vesicles, 2) liposome-phagocytosing macrophages act as a 'reservoir' for the liberated drugs and can slowly release the drug in time [10], or 3) the liberated drug has an effect on the macrophage itself and inhibits macrophage activity [11]. In the case of liposomal glucocorticoids, there is strong evidence that the latter mechanism is the most important; in similar models for inflammatory diseases, therapy with bisphosphonate clodronate liposomes, which induce apoptosis of phagocytosing macrophages, leads to equivalent therapeutic results as therapy with liposomal corticosteroids [11, 12]. Macrophages, like other cells of the immune system, show a strong intracellular expression of the glucocorticoid receptor (GR), which, after activation by the liberated corticosteroids, leads to suppression of NF-κB activity, downregulation of macrophage activity, and thus reduction of secretion of pro-inflammatory cytokines, such as TNF-α, IFN-γ, IL-2 and IL-12 [13-15].

Even though therapy with liposomal corticosteroids proved successful in a number of

preclinical models of inflammatory disease, additional research is still ongoing. In some cases more evidence is needed to confirm previously obtained preclinical results, to justify a next step to clinical assessment. For example, both liposomal prednisolone phosphate and liposomal 6α-methylprednisolone phosphate have successfully been employed to attenuate the inflammatory response in experimental autoimmune encephalitis (EAE) induced in rats [3, 16]. The rat EAE model is a well-accepted model for MS, however, there are several methods in use to induce this condition in species other than the rat, each with its own similarities to the human pathophysiology [17]. For this reason, SJL mice with myelin proteolipid protein-induced EAE, which have a disease profile similar to human MS, were used in the present study [18].

The therapeutic indication of liposome-encapsulated corticosteroids could be expanded to other inflammatory diseases, including Crohn's Disease (CD). CD is a chronic inflammatory disease of the gastrointestinal tract, which together with Colitis Ulcerosa is commonly referred to as inflammatory bowel disease (IBD). The disease activity in CD is characterized by an intermittent course with exacerbations and remissions; the latter most commonly being induced by corticosteroid treatment [19, 20]. In light of this intermittent disease activity, which shows resemblance with that of MS and RA, it can be envisaged that liposomal corticosteroids will be beneficial in the treatment of CD, as indicated already in preclinical models of RA and MS.

In the current study, the therapeutic efficacy of liposomal dexamethasone phosphate (DXP) was assessed in mouse models of MS and CD. DXP is a phosphate derivative of dexamethasone, which is a corticosteroid with strong anti-inflammatory potency. Dexamethasone is found to be 6-10 times more potent than prednisolone and 5 times more potent than 6α-methylprednisolone with respect to their glucocorticoid activities [21, 22]. It was anticipated that the employment of long-circulating DXP-liposomes would reduce the disease activity in both models of inflammatory disease, which would aid in the development of liposomal corticosteroid formulations for clinical anti-inflammatory therapy.

2. Materials and Methods

2.1. Materials

1,2-Distearoyl-*sn*-glycero-3-phosphoethanolamine-*N*-[methoxy(polyethylene glycol)-2000] (DSPE-PEG_{2000}) and dipalmitoylphosphatidylcholine (DPPC) were provided by Lipoid (Germany). Cholesterol was purchased from Sigma-Aldrich (Germany). Dexamethasone phosphate (DXP) was obtained from BUFA (The Netherlands). Posphate Buffered Saline (PBS) with pH 7.4 was purchased from B. Braun (The Netherlands). Dextran sodium sulfate (DSS) with molecular weight of 36-50 kDa was supplied by MP Biomedicals (France). Beckman Coulter Hemoccult® SENSA® tests were obtained from Bipharma Diagnostics B.V. (The Netherlands).

2.2. Preparation of long-circulating liposomes

DPPC, DSPE-PEG_{2000} and cholesterol were dissolved in a 1.85:0.15:1 molar ratio in a roundbottom flask in 5-10 mL ethanol. A lipid film was formed by rotary evaporation (Buchi, Switzerland), which was dried further under a nitrogen flow. The lipid film was hydrated with a 100 mg/mL solution of DXP in reversed osmosis water to form liposomes. The size and polydispersity of the liposomes were decreased by extruding the dispersion through two polycarbonate filters (Whatman, USA) mounted in an LIPEX extruder (Northern Lipids Inc, Canada). Starting with two extrusions through a double 200 nm filter and two extrusions through a 200 and 100 nm filter, the liposomes were extruded ten times through two 100 nm filters. DXP not encapsulated into the liposomes was removed by means of dialysis in PBS at 4 °C for 48 hours, while replacing the PBS regularly in order to remove all free corticosteroid. Particle size and polydispersity of extruded dispersions was determined by dynamic light scattering (DLS) using a Malvern ALV CGS-3 (Malvern Instruments). DLS results are given as a z-average particle size diameter and a polydispersity index (PDI), which is expressed on a scale of 0 to 1; 0 meaning complete monodispersity and 1 meaning complete polydispersity. All used liposomes had an average diameter of around 100 nm and a PDI smaller than 0.1. The DXP concentration in the liposomal dispersion was measured using Ultra Performance Liquid Chromatography (UPLC) (Waters) equipped with a Acquity UPLC BEH C18 column, using 1:3 acetonitrile in water (pH 2) as eluent. Prior to analysis the DXP was recovered from the liposomes after extraction of the aqueous phase [23].

2.3. Animal experiments

Mice were housed in groups of 8-10 per cage and supplied *ad libitum* with water and standard diet pellets for rodents (801730 CRM (E) Expanded, Special Diets Services, England). All animal experiments were conducted in agreement with local law.

2.4. EAE model

Female SJL mice (Charles River) were immunized by subcutaneous injection in each flank of proteolipid protein in Complete Freund's Adjuvant containing Mycobacterium tuberculosis. Immediately after, animals received a solution of pertussis toxin by intraperitoneal injection. Starting from day 7 post-immunization, clinical disease activity was assessed daily and scored on a range from 0 to 5: 0 = normal, 0.5 = partial tail paralysis, 1 = tail paralysis, 1.5 = tail paralysis and partial unilateral hindlimb paralysis, 2 = tail paralysis and hindlimb weakness or partial hindlimb paralysis, 2.5 = tail paralysis and unilateral hindlimb paralysis or severe hindlimb paresis (lowered pelvis), 3 = tail paralysis and complete hindlimb paralysis, 3.5 = tail paralysis and complete hindlimb paralysis and incontinence, 4 = tail paralysis and hindlimb paralysis and weakness or partial paralysis of forelimbs, 5 = moribund or dead. Clinical signs were monitored daily in each group of treatment in a blind fashion. At the onset of disease (score ≥ 1, day 0), each animal was randomly assigned to one of four experimental groups. Groups of 9-10 mice were treated intravenously with a single dose of PBS, DXP (10 mg/kg), or long-circulating DXP-liposomes (LCL-DXP, 10 mg/kg). All animals were sacrificed 7 weeks after immunization. All statistical analyses were performed using the PBS treated mice as reference.

2.5. DSS-induced colitis model

Murine chronic colitis was induced using a protocol for dextran sodium sulfate (DSS) induced colitis [24, 25]. Female, 12-week old C57BL/6 mice (Charles River) were given 1.5% DSS in their drinking water during 5 consecutive days, followed by 10 days of normal drinking water. This cycle was repeated two more times to induce a chronic inflammatory response. Before each DSS interval, a fresh DSS solution was prepared by dissolving 1.5% w/v in standard tap water. Bottles were wrapped in foil to protect the solution from light, and were washed after each interval.

All mice were assessed 4 times a week for clinical signs of colitis, i.e. stool consistency and fecal blood loss. Fresh droppings of each animal, which were collected by temporarily

separating mice in individual cages, were smeared on the detection window of a Hemoccult® SENSA® test card to determine the consistency of the stool and the presence of any visible blood. The stool consistency was recorded using a stool score ranging from 0 to 4: 0 = normal stool, 1 = smearable stool, 2 = loose stool, 3 = very loose / shapeless stool and or slime, 4 = diarrhea. Within one week after stool collection, the tests cards were developed and the animals were scored for the degree of fecal blood loss: 0 = no fecal blood loss, 2 = occult fecal blood loss (no visible blood, positive test), 4 = macroscopic fecal blood loss. Test cards were stored for at least 48 hours at room temperature before development, to reduce the chance on false positive results due to dietary peroxidases, as specified in the product instructions.

Mice were randomly assigned to an experimental group, and evenly distributed among the cages to exclude any cage related effects. Mice were treated after the third interval of DSS administration (day 36). Three groups of 8 mice were treated intravenously with a single dose of DXP (5 mg/kg), long-circulating liposomes containing PBS (LCL-PBS) or LCL-DXP (5 mg/kg). Two groups of 4 mice received LCL-DXP at doses 10 mg/kg or 20 mg/kg. Three groups of 5 mice, which did not receive DSS in their drinking water, served as healthy controls and were injected with DXP (5 mg/kg), LCL-PBS or LCL-DXP (5 mg/kg). After treatment, all mice were assessed on a daily basis and scored for stool consistency and hematochezia by an experimenter who was blinded for the treatment they received. All animals were sacrificed 9 days after treatment. All statistical analyses were performed using the LCL-PBS treated mice as reference.

3. Results

3.1. EAE model

To assess the effect of long-circulating DXP-liposomes in a chronic relapsing murine EAE, female SJL mice were immunized with proteolipid protein and scored on a daily basis until 7 weeks (49 days) after immunization [18]. Between 11 to 16 days after immunization all mice developed clinical EAE (score≥1), at which time they were treated with a single

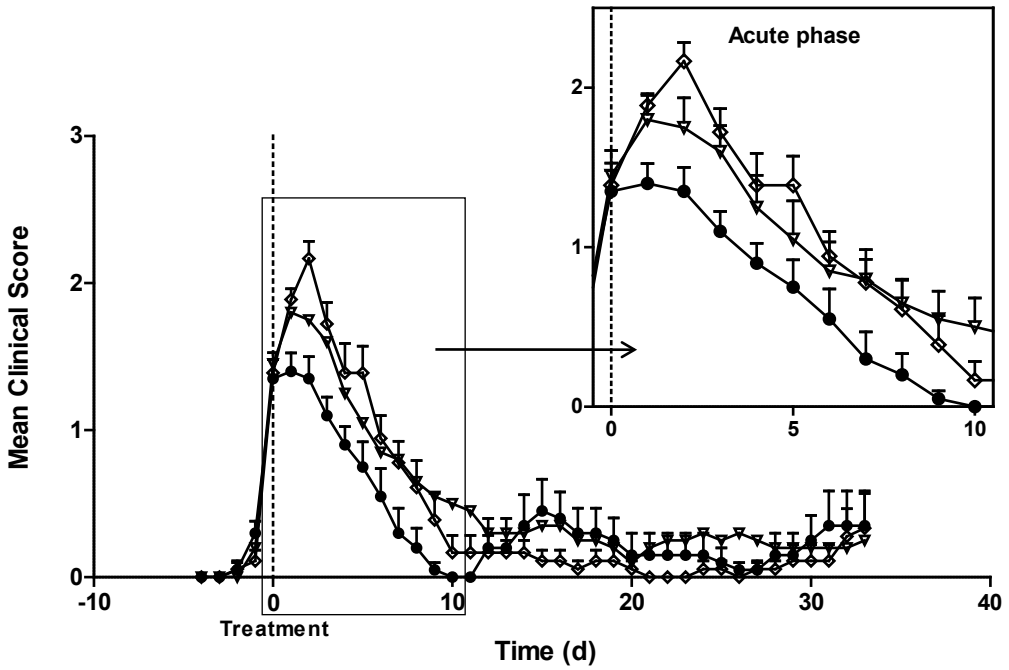

Figure 1. Clinical EAE score of mice with EAE after treatment with (liposomal) DXP. Experimental autoimmune encephalomyelitis (EAE) was induced in female SJL mice by immunization with proteolipid protein in Complete Freund's Adjuvant containing mycobacterium tuberculosis, followed by a boost of pertussis toxin. The clinical score was monitored daily. At the onset of disease (clinical score ≥ 1, day 0) mice were treated with PBS (◇), 10 mg/kg DXP (▽) or 10 mg/kg long-circulating DXP-liposomes (LCL-DXP, ●). Depicted are the mean clinical score and SEM of each experimental group (n=9-10) until 49 days post-immunization. Clinical score: 0 = normal, 0.5 = partial tail paralysis, 1 = tail paralysis, 1.5 = tail paralysis and partial unilateral hindlimb paralysis, 2 = tail paralysis and hindlimb weakness or partial hindlimb paralysis, 2.5 = tail paralysis and unilateral hindlimb paralysis or severe hindlimb paresis (lowered pelvis), 3 = tail paralysis and complete hindlimb paralysis, 3.5 = tail paralysis and complete hindlimb paralysis and incontinence, 4 = tail paralysis and hindlimb paralysis and weakness or partial paralysis of forelimbs, 5 = moribund or dead.

dose of 10 mg/kg DXP, 10 mg/kg LCL-DXP or PBS (day 0). After onset, the clinical course of the disease could be separated into a severe acute phase from day 0 to day 10, and a much more moderate disease activity in the following chronic phase (Figure 1). Treatment with free DXP or PBS, did not show an effect on the disease activity in the acute or chronic phase. Lack of effect was also the case with LCL-DXP treatment in the chronic phase of EAE (data not shown). In the acute phase, however, the maximal clinical score that LCL-DXP treated mice received throughout the experiment was significantly lower than that of mice treated with PBS ($p<0.01$, nonparametric one-way ANOVA) (Figure 2). Finally, the total disease load, as represented by the area-under-the-curve (AUC), was in the acute phase significantly lower for animals treated with LCL-DXP compared to the animals that received PBS ($p<0.05$, one-way ANOVA) (Figure 3).

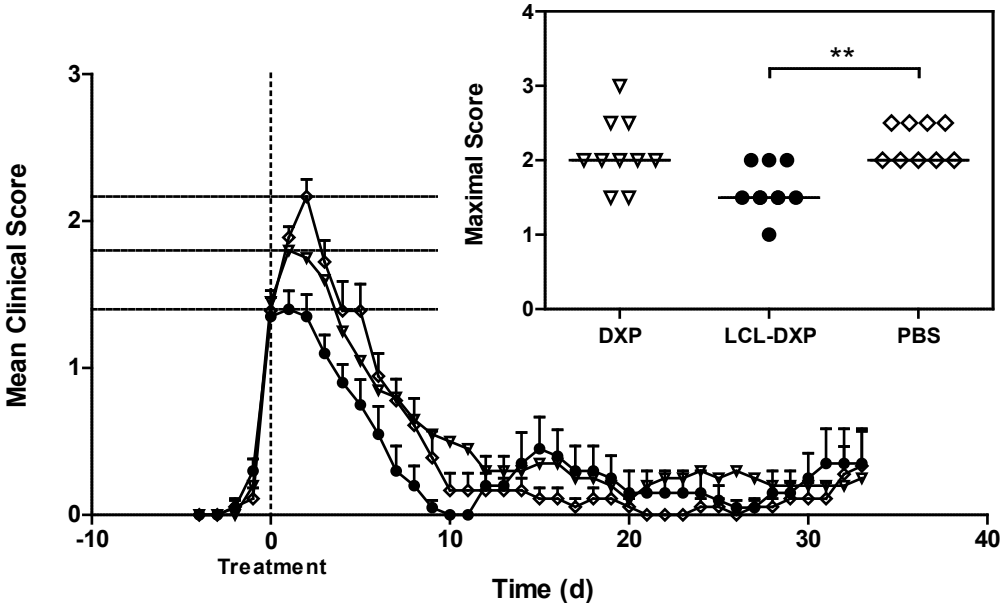

Figure 2. Maximal clinical score of mice with EAE after treatment with (liposomal) DXP. The maximal clinical score of each animal was determined by the largest clinical score they received throughout the experiment, which in all cases corresponded to the height of the peak on day 1, 2 or 3. Depicted is the averaged clinical score curve of each experimental group with the maximal mean clinical score (dotted lines) of the group (main graph), and the maximal score of each individual mouse treated with PBS (◇), DXP (▽) or LCL-DXP (●) and the median of the maximal scores within the group (insert). There was a significant reduction of median maximal score after treatment with LCL-DXP (**, $p<0.01$), but not after treatment with DXP (compared with PBS, one-way ANOVA (nonparametric Kruskal-Willis test, followed by Dunn's multiple comparison test).

Treatment	Mean disease load
PBS	12.7
DXP	11.8
LCL-DXP	8.0

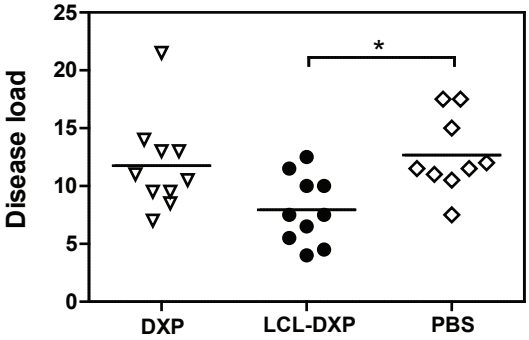

Figure 3. Disease load during acute phase of mice with EAE after treatment with (liposomal) DXP. The disease load of each animal during the acute phase was defined as the area under the clinical score curve during the first 10 days after treatment. Depicted is the mean disease load of each experimental group (table), and the disease load of each individual mouse treated with PBS, DXP or LCL-DXP, with the average of the experimental group as a straight line (graph). There was a significant reduction of mean disease load after treatment with LCL-DXP (*), but not after treatment with DXP ($p<0.05$ compared with PBS, one-way ANOVA followed by Bonferroni's multiple comparison test).

3.2. DSS-induced colitis model

To assess the effect of long-circulating DXP-liposomes in a chronic colitis model of CD, DSS-induced colitis was established in female C57BL/6 mice [24]. By periodically giving 1.5% DSS in their drinking water, in three cycles of 5 days of DSS followed by 10 days of tap water, a chronic inflammation of the large intestine was induced. On the day the mice switched for the third time to standard tap water (day 36), they were treated with a single i.v. injection of DXP (5 mg/kg), 'empty' long-circulating liposomes (LCL-PBS), or LCL-DXP (5 mg/kg, 10 mg/kg or 20 mg/kg). Before treatment, all mice were scored 4 times a week for stool consistency and fecal blood loss. After treatment, scoring was done on a daily basis until the end of the study, nine days after treatment (day 44). The control groups of mice, that did not receive DSS but only the treatments, did not show any signs of colitis throughout the study (data not shown). In the groups with DSS-induced colitis, all mice developed an acute colitis immediately after starting the first cycle of DSS, as indicated by their stool consistency (Figure 4) and fecal blood loss (Figure 5). The disease severity dropped in intensity after returning to normal tap water, and subsequently increased, although less severe, during the second and third cycle of DSS. Treatment of the mice with DXP, LCL-PBS or LCL-DXP after the third interval of DSS administration did not lead to any significant differences in their stool consistency score (Figure 4).

Interestingly, there was a clear effect of treatment on the fecal blood loss of the mice which received LCL-DXP in any dosage. However, unexpectedly, LCL-DXP treatment did not result in an improvement but in a worsening of the disease (Figure 5). Moreover, the total

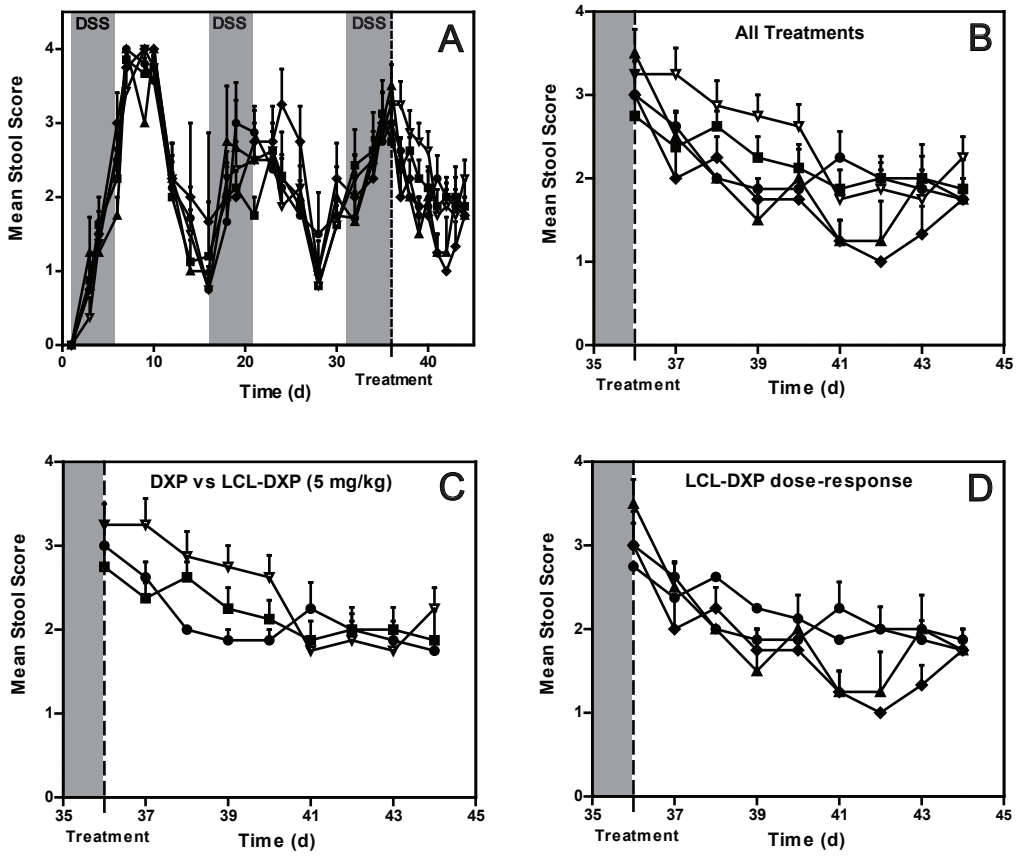

Figure 4. Stool consistency of mice with DSS-induced colitis after treatment with (liposomal) DXP. Chronic colitis was induced in female C57BL/6 mice by changing their drinking water during three cycles of 5 days of 1.5% DSS and 10 days of normal tap water. After the last interval of DSS (day 36), all mice were treated with 'empty' long-circulating liposomes (LCL-PBS, ■), DXP (5 mg/kg, ▽), or liposomal DXP (LCL-DXP, 5 mg/kg ●, 10 mg/kg ▲, or 20 mg/kg ◆).
A. The average stool score and SEM of all groups from disease induction (day 1) until 9 days after treatment (day 44). **B**. Stool score of all groups after treatment. **C**. Stool score after treatment of mice treated with DXP (5 mg/kg) or liposomal DXP (5 mg/kg). **D**. Stool score after treatment of mice treated with different dose of LCL-DXP (5, 10 and 20 mg/kg). Depicted are mean of stool score and SEM of the experimental group (n=8). No significant differences in stool score after treatment was observed (versus LCL-PBS, two-way ANOVA).
Stool score for consistency: 0 = normal stool, 1 = smearable stool, 2 = loose stool, 3 = very loose / shapeless stool and or slime, 4 = diarrhea

fecal blood score after treatment was significantly larger for the mice treated with 5, 10 or 20 mg/kg LCL-DXP compared with LCL-PBS treated mice ($p<0.05$, $p<0.01$, $p<0.001$ respectively, one-way ANOVA) (Figure 6). Although a higher average total blood score

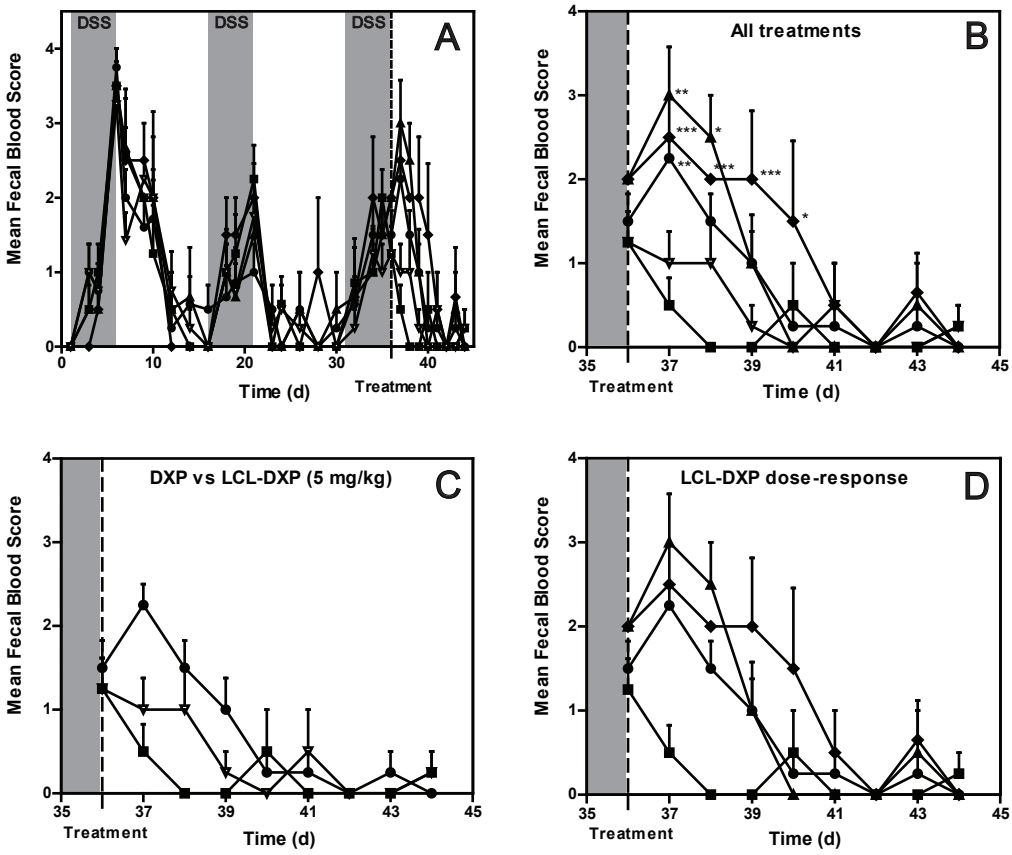

Figure 5. Fecal blood score of mice with DSS-induced colitis after treatment with (liposomal) DXP. Chronic colitis was induced in female C57BL/6 mice by changing their drinking water during three cycles of 5 days of 1.5% DSS and 10 days of normal tap water. After the last interval of DSS (day 36), all mice were treated with 'empty' long-circulating liposomes (LCL-PBS, ■), DXP (5 mg/kg, ▽), or liposomal DXP (LCL-DXP, 5 mg/kg ●, 10 mg/kg ▲, or 20 mg/kg ◆) **A**. The average fecal blood score and SEM of all groups from disease induction (day 1) until 9 days after treatment (day 44). **B**. Fecal blood score of all groups after treatment. **C**. Fecal blood score after treatment of mice treated with DXP (5 mg/kg) or liposomal DXP (5 mg/kg). **D**. Fecal blood score after treatment of mice treated with different doses of LCL-DXP (5, 10 and 20 mg/kg). Depicted are the average fecal blood score and SEM of the experimental group (n=8). Treatment was a significant parameter in the observed variance in fecal blood loss ($p<0.0001$, two-way ANOVA). * $p<0.05$; ** $p<0.01$; and *** $p<0.001$ compared to LCL-PBS (two-way ANOVA, followed by Bonferroni's post-test). Fecal blood score: 0 = no fecal blood loss, 2 = occult fecal blood loss (no visible blood, positive test), 4 = macroscopic fecal blood loss.

Treatment	Mean TFB score
LCL-PBS	2.5
DXP (5 mg/kg)	4.0
LCL-DXP (5 mg/kg)	7.0
LCL-DXP (10mg/kg)	9.0
LCL-DXP (20 mg/kg)	11.0

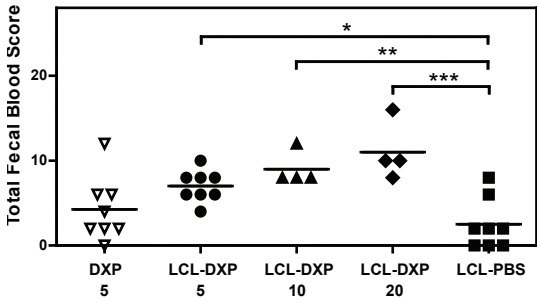

Figure 6. Total fecal blood score of mice with DSS-induced colitis after treatment with (liposomal) DXP. The total fecal blood score of each mouse was defined by the sum of fecal blood scores after treatment, corresponding to the area under the fecal blood score curve. Depicted is the mean total fecal blood (TFB) score of each experimental group (table), and the total fecal blood score of each individual mouse treated with LCL-PBS, DXP or LCL-DXP (5, 10 or 20 mg/kg), with the average of the experimental group as a straight line (graph). There was a significant increase of total fecal blood score of mice treated with LCL-DXP at all doses (* $p<0.05$; ** $p<0.01$; and *** $p<0.001$), but not of mice treated with DXP (compared with LCL-PBS, one-way ANOVA followed by Bonferroni's multiple comparison test).

was found in mice receiving a higher dose of LCL-DXP, this relation was not significant.

4. Discussion

So far, long-circulating liposome-encapsulated prednisolone and 6α-methylprednisolone have been studied for their efficacy in models of RA (rat), MS (rat) and cancer (mouse) [1-3]. This study aimed to broaden the applicability of liposome-encapsulated corticosteroids by evaluating another corticosteroid in mouse models for MS and CD. Both liposomal prednisolone phosphate and liposomal 6α-methylprednisolone phosphate have shown therapeutic efficacy in rat models for MS [3, 16], but to date this has never been confirmed in other species. CD forms a completely new indication in the research on the therapeutic applicability of liposomal corticosteroids. In both preclinical models it was expected that treatment with liposome-encapsulated DXP, which has a higher glucocorticoid potency than prednisolone, would lead to a clinical improvement. In the EAE model there was indeed a significant improvement after single-dose treatment with 10 mg/kg LCL-DXP, with a reduced disease intensity and disease load. However, surprisingly, in the DSS-induced IBD model, there was a worsening of the disease after treatment with 5, 10 or 20 mg/kg LCL-DXP, indicated by a significant increase in fecal blood loss. The question

arises why long-circulating DXP-liposomes are favorable in case of EAE and not in DSS-induced colitis. Since previous data showed that the effect of liposomal glucocorticoids is - at least partly - mediated by local tissue macrophages [10-12], these results suggest a contrasting role of these macrophages in MS and CD. Our hypothesis is that the dissimilar effects of LCL-DXP relate to differences in the polarization status of the target tissue macrophages in both diseases.

The concept that macrophage phenotype and function is dependent on the environment where it resides, is not new [26]. Populations of macrophages have previously been classified as M1- versus M2-polarized, making a distinction between a cytotoxic and a regulatory macrophage activity, respectively. This is similar to the Th1 and Th2 T-helper cell classification [27, 28]. This classification has been developed further into a model where macrophages are categorized into 'classical activated', 'wound-healing', and 'regulatory' macrophages [29, 30]. Classical activated macrophages are generally formed in response to TNF-α and IFN-γ, and are strongly associated with Th1- and Th17-mediated cellular immunity. When stimulated, they release pro-inflammatory cytokines such as IL-1, IL-6 and IL-23. Wound-healing macrophages arise after exposure to IL-4 and IL-13, which are important regulatory cytokines in Th2-associated humoral immunity. As the name implies, this type of macrophage is involved in the process of tissue regeneration, by producing collagen for the extracellular matrix and releasing tissue-repair promoting factors [28]. Finally, regulatory macrophages are formed following exposure to IL-10 produced by regulatory T-cells. Regulatory macrophages, together with regulatory T-cells, dampen the inflammatory response and stimulate tissue repair by inducing Th2- and M2-polarization, which result in high levels of IL-4 and consequently formation of wound-healing macrophages [29]. The polarization of macrophages is not definite: macrophages retain the capability to change their phenotype according to the local environment [31, 32]. In particular, glucocorticoids have been shown to interfere with the macrophage phenotype: they drive the macrophage population towards a more anti-inflammatory, regulatory M2-polarization [33]. This means that, in light of the natural tropism of liposomes for macrophages, DXP encapsulated in liposomes is even more potent in doing so. This is supported by the observed results in the EAE model, and previously in RA, which are primarily M1 macrophage-mediated diseases [34, 35]. In EAE, shifting the macrophage polarization towards a M2-/Th2-polarization, results in amelioration of the clinical disease activity [36, 37]. The finding that liposomal dexamethasone reduces

the clinical score in mice with EAE, can therefore be explained by a similar modulation of the macrophages in the nervous system. Intestinal macrophages, however, respond differently to their surroundings than other tissue macrophages; a property that can be related to the constant threat of commensal microorganisms from the intestinal lumen [38]. Intestinal macrophages therefore possess the capability to phagocytose and eradicate microorganisms and act in a M1-polarized manner, without showing a pro-inflammatory phenotype. In fact, there is strong evidence that intestinal macrophages are key regulators in maintaining an immunological tolerance towards these invading microorganisms [39]. In the absence of such control mechanism for intestinal homeostasis, a permanent inflammation of the whole gastrointestinal tract would occur. Also in CD, several reports indicate that M1-activated macrophages indeed are essential in the preservation of mucosal integrity and defense, and fulfill a protective role in the development of the disease. First of all, DSS-induced colitis in intestinal macrophage-depleted mice has a more severe course compared to mice with an intact intestinal macrophage function [40]. Secondly, therapy with granulocyte macrophage colony-stimulating factor (GM-CSF), which stimulates innate immunity by inducing a shift in macrophage polarization towards M1, leads to improvement of DSS colitis [41, 42]. In fact, Sargramostim, a recombinant GM-CSF, shows beneficial effects in CD patients, and is currently in phase II clinical trials [43]. Therefore, changing the phenotype of intestinal macrophages from M1 to M2 by treatment with DXP-liposomes may indeed lead to a worsening of clinical symptoms in colitis, making CD a notable exception in the field of inflammatory diseases, which does not respond favorably to liposomal corticosteroid treatment.

In conclusion, the current study shows contrasting disease outcomes after treatment with liposomal DXP in models of CD and MS. In EAE, a model for MS, treatment with liposomal DXP leads to a clinical improvement of the disease, resulting in a reduction of maximal disease intensity and disease load. In contrast, in the DSS-induced colitis model for CD treatment with liposomal DXP leads to a clinical worsening, marked by an increase in fecal blood loss. This remarkable difference could be due to the different inflammatory context of both diseases, which makes that modulation of macrophage polarization to M2 in each of these diseases leads to these opposing effects.

Since most, if not all, nanomedicines generally accumulate in cells of the RES, including those at inflammatory sites, this could prove to be a valuable lesson for future efforts in the development of anti-inflammatory targeted drug formulations.

5. Acknowledgements

This work was supported by MediTrans, an Integrated Project funded by the European Commission under the "nanotechnologies and nano-sciences, knowledge-based multifunctional materials and new production processes and devices" (NMP), thematic priority of the Sixth Framework Program.

6. References

[1] J.M. Metselaar, M.H.M. Wauben, J.P.A. Wagenaar-Hilbers, O.C. Boerman, G. Storm, Complete remission of experimental arthritis by joint targeting of glucocorticoids with long-circulating liposomes, Arthritis Rheum. 48(7) (2003) 2059-2066.

[2] R.M. Schiffelers, J.M. Metselaar, M.H.A.M. Fens, A.P.C.A. Janssen, G. Molema, G. Storm, Liposome-encapsulated prednisolone phosphate inhibits growth of established tumors in mice, Neoplasia 7 (2005) 118-127.

[3] J. Schmidt, J.M. Metselaar, M.H.M. Wauben, K.V. Toyka, G. Storm, R. Gold, Drug targeting by long-circulating liposomal glucocorticosteroids increases therapeutic efficacy in a model of multiple sclerosis, Brain 126(8) (2003) 1895-1904.

[4] Y. Matsumura, H. Maeda, A new concept for macromolecular therapeutics in cancer chemotherapy: mechanism of tumoritropic accumulation of proteins and the antitumor agent Smancs, Cancer Res. 46(12 Part 1) (1986) 6387-6392.

[5] B.S. Sandanaraj, H.-U. Gremlich, R. Kneuer, J. Dawson, S. Wacha, Fluorescent nanoprobes as a biomarker for increased vascular permeability: implications in diagnosis and treatment of cancer and inflammation, Bioconj. Chem. 21(1) (2010) 93-101.

[6] D.B. Fenske, P.R. Cullis, Liposomal nanomedicines, Expert. Opin. Drug. Deliv. 5(1) (2008) 25-44.

[7] M.J. Hsu, R.L. Juliano, Interactions of liposomes with the reticuloendothelial system : II. Nonspecific and receptor-mediated uptake of liposomes by mouse peritoneal macrophages, BBA-Mol. Cell. Res. 720(4) (1982) 411.

[8] T.M. Allen, C.B. Hansen, D.E.L. de Menezes, Pharmacokinetics of long-circulating liposomes, Adv. Drug Deliv. Rev. 16(2-3) (1995) 267.

[9] S.K. Huang, K.D. Lee, K. Hong, D.S. Friend, D. Papahadjopoulos, Microscopic localization of sterically stabilized liposomes in colon carcinoma-bearing mice, Cancer Res. 52(19) (1992) 5135-5143.

[10] G. Storm, P.A. Steerenberg, F. Emmen, M. van Borssum Waalkes, D.J.A. Crommelin, Release of doxorubicin from peritoneal macrophages exposed in vivo to doxorubicin-containing liposomes, BBA-Gen. Subjects 965(2-3) (1988) 136.

[11] M. Banciu, J.M. Metselaar, R.M. Schiffelers, G. Storm, Antitumor activity of liposomal prednisolone phosphate depends on the presence of functional tumor-associated macrophages in tumor tissue, Neoplasia 10(2) (2008) 108-117.

[12] N. van Rooijen, E. van Kesteren-Hendrikx, Clodronate liposomes: perspectives in research and therapeutics, J. Liposome Res. 12(1-2) (2002) 81-94.

[13] N. Auphan, J.A. DiDonato, C. Rosette, A. Helmberg, M. Karin, Immunosuppression by glucocorticoids: inhibition of NF-kB activity through induction of IkB synthesis, Science 270(5234) (1995) 286-290.

[14] C.K. Glass, K. Saijo, Nuclear receptor transrepression pathways that regulate inflammation in macrophages and T cells, Nat. Rev. Immunol. 10(5) (2010) 365-376.

[15] I.J. Elenkov, Glucocorticoids and the Th1/Th2 Balance, Ann. N. Y. Acad. Sci. 1024 (2004) 138-146.

[16] R.A. Linker, C. Weller, F. Lühder, A. Mohr, J. Schmidt, M. Knauth, J.M. Metselaar, R. Gold, Liposomal glucocorticosteroids in treatment of chronic autoimmune demyelination: long-term protective effects and enhanced efficacy of methylprednisolone formulations, Exp. Neurol. 211(2) (2008) 397.

[17] R. Gold, C. Linington, H. Lassmann, Understanding pathogenesis and therapy of multiple sclerosis via animal models: 70 years of merits and culprits in experimental autoimmune encephalomyelitis research, Brain 129(8) (2006) 1953-1971.

[18] V.K. Tuohy, R.A. Sobel, M.B. Lees, Myelin proteolipid protein-induced experimental allergic encephalomyelitis. Variations of disease expression in different strains of mice, J. Immunol. 140(6) (1988) 1868-1873.

[19] E. Benchimol, C. Seow, A. Steinhart, A. Griffiths, Traditional corticosteroids for induction of remission in Crohn's disease, Cochrane Database Syst. Rev.(2) (2008) Art. No.: CD006792.

[20] J.R.F. Cummings, S. Keshav, S.P.L. Travis, Medical management of Crohn's disease, BMJ 336(7652) (2008) 1062-1066.

[21] A. Gilman, L. Goodman, Goodman & Gilman's The Pharmacological Basis of Therapeutics, The McGraw-Hill Companies Inc, New York, 2006.

[22] C. Grossmann, T. Scholz, M. Rochel, C. Bumke-Vogt, W. Oelkers, A.F. Pfeiffer, S. Diederich, V. Bahr, Transactivation via the human glucocorticoid and mineralocorticoid receptor by therapeutically used steroids in CV-1 cells: a comparison of their glucocorticoid and mineralocorticoid properties, Eur. J. Endocrinol. 151(3) (2004) 397-406.

[23] E. Bligh, W. Dyer, A rapid method of total lipid extraction and purification, Can. J. Biochem. Physiol. 37(8) (1959) 911-917.

[24] I. Okayasu, S. Hatakeyama, Y. Masahiro, O. Toshifumi, Y. Inagaki, R. Nakaya, A novel method in the induction of reliable experimental acute and chronic ulcerative colitis in mice, Gastroenterology 98(3) (1990) 694-702.

[25] S. Wirtz, C. Neufert, B. Weigmann, M.F. Neurath, Chemically induced mouse models of intestinal inflammation, Nat. Protoc. 2(3) (2007) 541.

[26] S. Gordon, P.R. Taylor, Monocyte and macrophage heterogeneity, Nat. Rev. Immunol. 5(12) (2005) 953-964.

[27] A. Mantovani, A. Sica, S. Sozzani, P. Allavena, A. Vecchi, M. Locati, The chemokine system in diverse forms of macrophage activation and polarization, Trends Immunol. 25(12) (2004) 677-686.

[28] F.O. Martinez, L. Helming, S. Gordon, Alternative activation of macrophages: an immunologic functional perspective, Annu. Rev. Immunol. 27(1) (2009) 451-483.

[29] D.M. Mosser, J.P. Edwards, Exploring the full spectrum of macrophage activation, Nat. Rev. Immunol. 8(12) (2008) 958-969.

[30] J.P. Edwards, X. Zhang, K.A. Frauwirth, D.M. Mosser, Biochemical and functional characterization of three activated macrophage populations, J. Leukoc.Biol. 80(6) (2006) 1298-1307.

[31] R.D. Stout, C. Jiang, B. Matta, I. Tietzel, S.K. Watkins, J. Suttles, Macrophages sequentially change their functional phenotype in response to changes in microenvironmental influences, J. Immunol. 175(1) (2005) 342-349.

[32] R.D. Stout, J. Suttles, Functional plasticity of macrophages: reversible adaptation to changing microenvironments, J. Leukoc. Biol. 76(3) (2004) 509-513.

[33] J. Ehrchen, L. Steinmuller, K. Barczyk, K. Tenbrock, W. Nacken, M. Eisenacher, U. Nordhues, C. Sorg, C. Sunderkotter, J. Roth, Glucocorticoids induce differentiation of a specifically activated, anti-inflammatory subtype of human monocytes, Blood 109(3) (2007) 1265-1274.

[34] F. Brennan, R. Maini, M. Feldmann, Role of pro-inflammatory cytokines in rheumatoid arthritis, Springer Semin. Immunopathol. 20(1) (1998) 133-147.

[35] L.M. Schönrock, G. Gawlowski, W. Brück, Interleukin-6 expression in human multiple sclerosis lesions, Neurosci. Lett. 294(1) (2000) 45-48.

[36] T.J. Imler Jr, T.M. Petro, Decreased severity of experimental autoimmune encephalomyelitis during resveratrol administration is associated with increased IL-17+IL-10+ T cells, CD4-IFN-[gamma]+ cells, and decreased macrophage IL-6 expression, Int. Immunopharmacol. 9(1) (2009) 134-143.

[37] J. Mikita, N.g. Dubourdieu-Cassagno, M.S.A. Deloire, A. Vekris, M. Biran, G.r. Raffard, B. Brochet, M.-H.l.n. Canron, J.-M. Franconi, C. Boiziau, K.G. Petry, Altered M1/M2 activation patterns of monocytes in severe relapsing experimental rat model of Multiple Sclerosis. Amelioration of clinical status by M2 activated monocyte administration, Mult. Scler. (2010).

[38] S.E.M. Heinsbroek, S. Gordon, The role of macrophages in inflammatory bowel diseases, Expert Rev. Mol. Med. 11 (2009) e14.

[39] A.M. Platt, A.M. Mowat, Mucosal macrophages and the regulation of immune responses in the intestine, Immunol. Lett. 119(1-2) (2008) 22-31.

[40] J.E. Qualls, A.M. Kaplan, N. van Rooijen, D.A. Cohen, Suppression of experimental colitis by intestinal mononuclear phagocytes, J. Leukoc. Biol. 80(4) (2006) 802-815.

[41] E. Bernasconi, L. Favre, M.H. Maillard, D. Bachmann, C. Pythoud, H. Bouzourene, E. Croze, S. Velichko, J. Parkinson, P. Michetti, D. Velin, Granulocyte-macrophage colony-stimulating factor elicits bone marrow-derived cells that promote efficient colonic mucosal healing, Inflamm. Bowel Dis. 16(3) (2010) 428-441.

[42] S.K. Sainathan, E.M. Hanna, Q. Gong, K.S. Bishnupuri, Q. Luo, M. Colonna, F.V. White, E. Croze, C. Houchen, S. Anant, B.K. Dieckgraefe, Granulocyte macrophage colony-stimulating factor ameliorates DSS-induced experimental colitis, Inflamm. Bowel Dis. 14(1) (2008) 88-99.

[43] J.F. Valentine, R.N. Fedorak, B. Feagan, P. Fredlund, R. Schmitt, P. Ni, T.J. Humphries, Steroid-sparing properties of sargramostim in patients with corticosteroid-dependent Crohn's disease: a randomised, double-blind, placebo-controlled, phase 2 study, Gut 58(10) (2009) 1354-1362.

4

Glucocorticoid-loaded core-crosslinked polymeric micelles with tailorable release kinetics for targeted rheumatoid arthritis therapy

B.J. Crielaard [1], C.J.F. Rijcken [1,2], L.D. Quan [3], M. van der Pot [1], I. Altintas [1], S. van der Wal [4], R.M.J. Liskamp [4], R.M. Schiffelers [1,5], C.F. van Nostrum [1], W.E. Hennink [1], D. Wang [3], T. Lammers [1,6], G. Storm [1]

1. Department of Pharmaceutics, Utrecht Institute for Pharmaceutical Sciences, Utrecht University, Utrecht, The Netherlands
2. Cristal Delivery B.V., Utrecht, The Netherlands
3. Department of Pharmaceutical Sciences, University of Nebraska Medical Center, Omaha, Nebraska, U.S.A.
4. Department of Medicinal Chemistry, Utrecht Institute for Pharmaceutical Sciences, Utrecht University, Utrecht, The Netherlands
5. Department of Clinical Chemistry and Haematology, University Medical Center Utrecht, Utrecht, The Netherlands
6. Department of Experimental Molecular Imaging, RWTH – Aachen University, Aachen, Germany

Submitted for publication

Abstract

In the current study, a novel drug carrier system for the targeted delivery of corticosteroids in rheumatoid arthritis (RA) is presented. Core-crosslinked polymeric micelles based on degradable poly(ethylene glycol)-b-poly(*N*-(2-hydroxypropyl)-methacrylamide-lactate) (mPEG-b-pHPMAmLac$_n$) block copolymers, which have recently shown promising results for the targeted delivery of anti-cancer agents to tumors, were loaded with dexamethasone (DEX). DEX was derivatized with novel polymerizable, hydrolytically cleavable linkers, thereby obtaining DEX prodrugs, which enabled its transiently stable entrapment upon crosslinking of the micellar core. Due to the different degrees of oxidation of the thioether of each linker, its ester cleavage rate – and thus the release rate from the polymeric micelle – could be tightly controlled, with a half-life ranging from 10 to 170 days. Upon intravenous administration of the fastest releasing DEX-loaded polymeric micellar formulation, highly efficient disease treatment was achieved in two different animal models, with clinical signs of RA dropping to levels observed for healthy controls. In conclusion, our findings convincingly show that core-crosslinked polymeric micelles with covalently linked corticosteroids possess significant potential for the treatment of rheumatoid arthritis and possibly other inflammatory diseases.

1. Introduction

Glucocorticoids play a prominent role in the therapeutic management of rheumatoid arthritis (RA) and other chronic inflammatory diseases [1-3]. However, the occurrence of significant adverse effects, such as peptic ulcers, Cushing syndrome, and opportunistic infections due to immune suppression, especially when high doses are required, forms an important limitation with respect to the clinical application of glucocorticoids [2]. Targeted delivery strategies for improving the target tissue accumulation of glucocorticoids have therefore attracted considerable attention in recent years, especially for RA therapy [4, 5]. In RA, such strategies commonly exploit the up to 40-fold increase in blood-joint barrier permeability of the inflamed synovium for macromolecules and nanoparticulates, which has been observed initially for large plasma proteins that localized strongly in the arthritic joints of patients with rheumatoid arthritis [6]. This preferred distribution of systemically applied drug-loaded nanosized carrier systems to arthritic joints, by exploiting this increase in synovial permeability, enables the inflammation-specific targeting of glucocorticoids, improving the therapeutic index of these agents [4, 7, 8].

In the last decades, many types of delivery systems for drug targeting to pathological sites have been developed, including liposomes, polymeric drug-derivatives, protein-drug conjugates and micelles [9-13]. Their specific properties, such as size, circulation time, (bio)degradability, cellular distribution and internalization, and drug release kinetics, are important factors determining the efficacy of a system for a given therapeutic application. Core-crosslinked polymeric micelles (PMs) based on poly(ethylene glycol)-b-poly(*N*-(2-hydroxypropyl)methacrylamide-lactate) (mPEG-b-pHPMAmLac$_n$) have attracted considerable attention because of their favorable characteristics in this regard: (1) degradability under physiological conditions, (2) a 50-100 nm size range (which is very suitable for drug targeting purposes), (3) prolonged circulation kinetics, and (4) a tunable drug release profile, make them a highly versatile system for the targeted delivery of hydrophobic drugs [12, 14-16].

Following promising preclinical results obtained with PMs for tumor-targeting of doxorubicin using a pH-sensitive linker [17], the current study evaluates the potential of PMs for glucocorticoid targeting in RA. To this end, dexamethasone (DEX), a potent glucocorticoid, was derivatized with 3 different methacrylated linkers via ester linkages, thereby creating polymerizable DEX prodrugs. By employing linkers containing thioethers

with different degrees of oxidation, the hydrolysis rate of the ester bond, and therefore the drug release rate upon entrapment into the micellar core, should be controllable. To confirm this hypothesis, the drug release kinetics for core-crosslinked PM prepared with each type of DEX prodrug were determined *in vitro*. Finally, DEX-loaded micelles with the most optimal drug release kinetics were selected for evaluation in two different animal models of rheumatoid arthritis.

2. Materials and Methods

2.1. Materials

tert-Butyl bromoacetate, trifluoroacetic acid (TFA), 2-mercaptoethanol, 4-(dimethylamino) pyridine (DMAP), methacryloyl chloride, *N,N'*-dicyclohexylcarbodiimide (DCC), hydroquinone monomethyl ether (MEHQ), magnesium sulfate ($MgSO_4$) *N,N,N',N'*-tetramethylethylenediamine (TEMED), deuterated water (D_2O), deuterated chloroform ($CDCl_3$), deuterated DMSO, and dexamethasone (DEX) were purchased from Sigma Aldrich (Germany). Sodium periodate ($NaIO_4$), silicagel for column chromatography (0.035-0.070 mm, 60Å), carbon tetrachloride (CCl_4), periodic acid, ruthenium (III) chloride hydrate ($RuCl_3$) were obtained from Acros Organics (Belgium). Triethylamine (TEA), hydrogen peroxide, potassium persulphate (KPS), sodium hydrogen carbonate ($NaHCO_3$), hydrochloric acid 32% (HCl), anhydrous acetic acid and silica gel 60Å F_{254} plates for thin layer chromatography (TLC) were provided by Merck (USA). Dichloromethane (CH_2Cl_2), tetrahydrofuran (THF), methanol, ethyl acetate (EtOAc), hexane (Hex), acetonitrile (ACN) and chloroform were purchased from BioSolve (The Netherlands).

All buffers were filtered through 0.2 μm filters (Schleicher & Schuell MicroScience GmbH, Germany) prior to use. Arthritogenic monoclonal antibodies (Arthrogen-CIA, 5 clone cocktail kit) were obtained from Chondrex (USA).

2.2. DLS and NMR analysis

The mean particle size (Z_{ave}) and polydispersity index (PDI) of the polymeric micelles was determined with dynamic light scattering (DLS) using a Malvern ALV/CGS-3 Goniometer. DLS results are given as a z-average particle size diameter and a polydispersity index (PDI), which is expressed on a scale of 0 to 1; 0 meaning complete monodispersity

and 1 meaning complete polydispersity. ^{1}H- and ^{13}C-NMR spectra were recorded with a Gemini 300 MHz spectrometer (Varian Associates Inc., NMR Instruments, USA). ESI mass analysis was performed on a Shimadzu LCMS-QP8000 single quadrupole spectrometer.

2.3. Polymer synthesis

Block copolymers containing a hydrophilic monomethoxy-PEG (M_n of 5000 g/mol) block and a thermosensitive block composed of the monolactate (36%) and dilactate (64%) of *N*-2-hydroxypropyl methacrylamide (HPMAm) were prepared as described previously [16, 18]. Subsequently, a fraction (10-15%) of the lactate side chains was methacrylated upon reaction with methacrylic anhydride as reported by Rijcken et al. [16]. The molecular weight (M_w) of the block copolymers and the critical micelle temperature (CMT) was in all cases ~ 25 kDa and 8 to 12 °C, respectively.

2.4. Synthesis of DEX prodrugs

The DEX prodrugs DMSL1, DMSL2 and DMSL3 were synthesized and fully characterized as described in the Supporting Information.

2.5. Preparation of DEX-loaded and unloaded core-crosslinked polymeric micelles

Core-crosslinked polymeric micelles (PMs) were formed by the heat shock method according to Rijcken et al [18]. An ice-cold ammonium acetate buffered (pH 5.0, 150 mM) solution of PEG-pHPMAm copolymers with 14% methacrylation (8.3 volumes, dissolved overnight at 4 °C) was mixed with KPS (0.45 volumes, dissolved in ammonium acetate buffer) and TEMED (0.25 volumes, dissolved in ammonium acetate buffer). Subsequently, DEX-prodrugs in ethanol (1 volume) were added, followed by rapid heating to 50 °C while stirring vigorously during 1 minute to form polymeric micelles. The final concentration of polymer, KPS, TEMED and DEX prodrug (DEX equivalents) was 20, 1.35, 3 and 2 mg/mL, respectively. After letting the dispersion cool down to room temperature, the micelles were covalently stabilized by core-crosslinking the methacrylated polymers in a N_2-atmosphere for 1 h at RT, to obtain DEX-loaded core-crosslinked polymeric micelles (DEX-PMs) [16]. The polymeric micelles were filtered using a 0.2 μm filter, to remove any aggregated unencapsulated drug. The same procedure, only without the addition of DEX-prodrugs, was used to prepare unloaded polymeric micelles. The

amount of dexamethasone entrapped in the PM was determined upon hydrolysis of the ester bonds in a buffer of pH 9.4 at 37 °C, which was considered complete when a plateau in the dexamethasone concentration was reached. The concentration of DEX was measured by UPLC, using the method described in the following section.

2.6. In vitro DEX release from DEX-loaded core-crosslinked polymeric micelles

DEX-PMs were diluted in phosphate buffer (pH 7.4, 150 mM) and borate buffers (pH 8.4, 150 mM and pH 9.4, 150 mM). In addition, all buffers contained 1% Tween to solubilize the released drug. The release of DEX was monitored at 37 °C using an UPLC system (Waters, USA) equipped with an Acquity BEH C18 column 1.7 µm column (2.1×50 mm) (Waters) and a tuneable ultraviolet/visible light detector (TUV, Waters) set at 246 nm. The mobile phase consisted of ACN/H_2O (23/77, *v*/*v*) with a flow rate of 1 mL/min. The dexamethasone calibration curve was linear between 0.2 and 60 µg/mL.

2.7. In vivo therapeutic efficacy in mice with collagen-induced arthritis

All animal experiments were conducted in compliance with the local applicable Dutch law, 'Wet op de dierproeven' (art. 9) (1977), and were approved by the ethical committee for animal experimentation. Six month old male DBA/1 mice were obtained from Janvier (France). The mice were housed in groups of 7, exposed to a 12 h light/dark cycle, with *ad libitum* access to standard dietary pellets for rodents (801730 CRM (E) Expanded, Special Diets Services, England) and water.

Collagen antibody-induced arthritis (CAIA) was induced using a protocol as suggested by the supplier of the antibody cocktail (Chondrex). On day 0, the mice were injected intravenously (i.v.) with 150 µL of 10 mg/mL antibody cocktail. Subsequently, 100

Table 1. Scoring system for clinical symptoms of arthritis in mice with CAIA [19]

Clinical symptoms	Score
Normal	0
Mild redness, slight swelling of ankle or wrist	1
Moderate swelling of ankle or wrist	2
Severe swelling, including some digits, ankle or foot	3
Maximally inflamed	4

μL of 0.5 mg/mL of lipopolysaccharide from *E. coli* 0111:B4 was administered on day 3 by intraperitoneal (i.p.) injection. On day 5, the mice were treated i.v. with PBS, unloaded micelles, free dexamethasone (DEX) at different doses (1, 5 or 10 mg/kg) or dexamethasone-loaded core-crosslinked micelles (DEX-PM) at different doses (1, 5 or 10 mg/kg, dexamethasone equivalents). Each treatment group consisted of 6-7 mice, and 5 untreated mice without CAIA served as healthy controls.

All mice were monitored daily for clinical signs of arthritis from day 4, using a scoring system described by Khachigian [19]. Each limb received a score from 0-4 based on the severity of the inflammation using the scoring system depicted in Table 1, which were summed to obtain the arthritis score.

Additionally, to assess the inflammatory swelling of the joints, the ankle diameters of the mice were measured daily using a digital caliper.

2.8. In vivo therapeutic efficacy in rats with adjuvant-induced arthritis

All animal experiments were performed using a protocol approved by the University of Nebraska Medical Center Institutional Care and Use Committee in accordance with Principles of Laboratory Animal Care [20]. Arthritis was induced by subcutaneous injection of 1 mg *Mycobacterium tuberculosis* H37Ra and 5 mg *N,N*-dioctadecyl-*N',N'*-bis(2-hydroxyethyl)-1,3-propanediamine (LA, prepared as described in [21]) mixed in paraffin oil (100 μL). On day 15, rats with established AIA were treated with 10 mg/kg DEX or DEX-PM (n=7). One group of 7 rats was treated with PBS and 6 rats without AIA served as healthy controls. Clinical symptoms of joint inflammation were assessed

Table 2. Scoring system for clinical symptoms of arthritis in rats with AIA [8]

Clinical symptoms	Score
Normal	0
Slight swelling and/or erythema	1
Low-to-moderate edema and signs involving the tarsals	2
Pronounced edema with limited use of the joint and signs extending to the metatarsals	3
Excessive edema with joint rigidity and severe signs involving the entire hind paw	4

and scored for both hind paws of each rat, using the scoring system presented in Table 2, which were summed to obtain the arthritis score. From day 8, the arthritis score of all rats was measured on a daily basis, as well as the medial to lateral ankle diameter, using a digital caliper, as a measure of inflammatory swelling.

2.9. Statistical analysis

Statistical analyses were performed using GraphPad Prism software v5.03. Two-way ANOVA analysis (Repeated measures (mixed model) ANOVA) followed by Bonferroni post-testing was used to evaluate the differences between treatments in time. One-way ANOVA in combination with Bonferroni post-testing was used to determine statistical differences in disease loads between treatment groups.

3. Results and Discussion

3.1. Synthesis of DEX-loaded core-crosslinked polymeric micelles

In the current study, a novel strategy for the targeted delivery of dexamethasone (DEX) using polymeric micelles (PMs) is presented. The PMs were prepared from block copolymers consisting of a hydrophilic poly(ethylene glycol) (PEG) block and a thermosensitive poly(*N*-(2-hydroxypropyl)methacrylamide lactate) (pHPMAmLac$_n$) block, which is either hydrophilic or hydrophobic depending on the temperature (Figure 1A) [18]. At a temperature below the lower critical solution temperature (LCST) the pHPMAmLac$_n$ block is hydrophilic, and therefore, in aqueous conditions, will be completely dissolved. However, when the temperature is raised above the LCST, the pHPMAmLac$_n$ block will become hydrophobic, rendering the block copolymer amphiphilic, which in aqueous media results in the formation of micellar nanostructures.

The lactate side chains of the pHPMA backbone, responsible for the LCST behavior of the polymer block, play an essential role in the stability and degradability of the micelle. Crosslinking of the micellar core by polymerization of the methacrylated mono- and dilactates ensures particle stability below the critical micelle concentration (CMC), thereby preventing rapid dissociation upon systemic administration. Over time, however, the ester bonds linking the lactate groups to the backbone will undergo hydrolysis in aqueous conditions, which eventually results in destabilization of the crosslinked core. Moreover, the loss of the lactate chains due to hydrolysis increases the LCST of the pHPMAm

derivative, which eventually causes the micelle to dissociate and the polymers to dissolve at physiological temperature, allowing their renal excretion. The outer shell of the PM is composed of hydrophilic PEG blocks, which forms a 'steric barrier' hindering the recognition and uptake of the nanoparticles by the cells of the reticuloendothelial system (RES) upon systemic administration, and is therefore a key component for providing these nanoparticles with stealth-like properties, resulting in prolonged circulation times and efficient EPR-mediated drug targeting to tumors and sites of inflammation [15, 17, 22-24].

To allow transiently stable entrapment of DEX in the PM, methacrylate-functionalized linkers that are susceptible to hydrolysis were synthesized as depicted in Scheme 1. In a final single step, these polymerizable linkers were coupled with high efficiency to dexamethasone, thereby generating polymerizable DEX prodrugs. An important advantage of this strategy lies in its versatility towards other therapeutic applications, for the same linkers may be

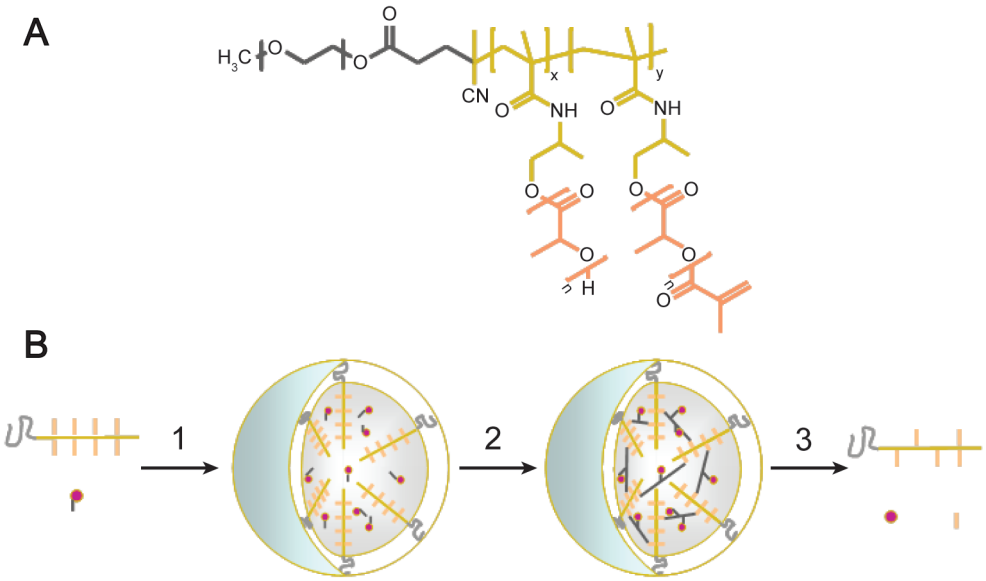

Figure 1. Schematic representation of dexamethasone-loaded core-crosslinked polymeric micelles (DEX-PM). **A**. Chemical structure of thermosensitive poly(ethylene glycol)-b-poly(*N*-(2hydroxypropyl)-methacrylamide-lactate) (mPEG-b-pHPMAmLacn). **B**. Preparation and degradation of DEX-PM. (1) micelle formation and encapsulation of hydrophobic DEX prodrugs by rapid heating, (2) copolymerization of methacrylated lactate side chains and DEX prodrugs in the micelle core, (3) hydrolytic cleavage of lactate moieties, drugs and drug linkers, leading to micellar degradation and drug release .

used to couple different therapeutic agents. To prepare DEX-loaded polymeric micelles, the hydrophobic DEX prodrugs were first loaded in the micellar core during micelle formation, and subsequently covalently entrapped in the particle core upon free radical polymerization of the methacrylate moieties (Figure 1B). A highly efficient encapsulation

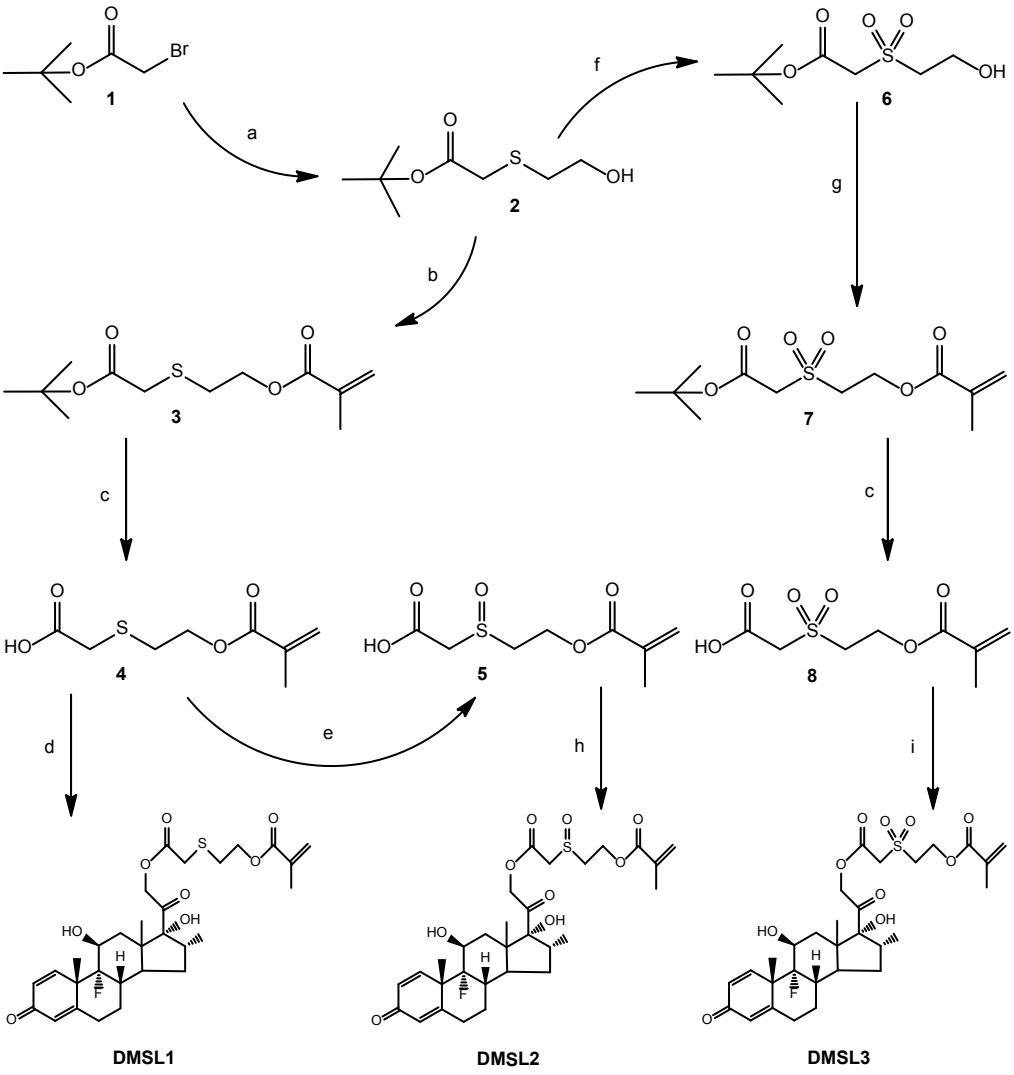

Scheme 1. Synthesis of polymerizable dexamethasone prodrugs.
a) 2-mercaptoethanol, TEA, CH_2Cl_2; b) methacryloyl chloride, TEA, CH_2Cl_2; c) MEHQ, TFA; e) $NaIO_4$, ACN, H_2O; f) $NaIO_4$, $RuCl_3$, H_2O, ACN, CCl_4; g) methacryloyl chloride, TEA, DCM; d) dexamethasone, DMAP, DCC, CH_2Cl_2, THF; h) dexamethasone, DMAP, DCC, THF; i) dexamethasone, DMAP, DCC, DCM, THF.

of the prodrugs (>80%) was obtained at drug/polymer feed of 10% (w/w). Consequently, the ratio of polymer methacrylate units versus number of prodrug molecules was calculated to be 1.8. Importantly, it was shown that quantitative methacrylate conversion took place, as determined using a previously described method [25]. The resulting (DEX-loaded) core-crosslinked polymeric micelles were rather monodisperse with a size of approximately 70 nm and a polydispersity index of around 0.1.

3.2. In vitro dexamethasone release from core-crosslinked polymeric micelles

In this study, hydroxyethylmethacrylate was conjugated to dexamethasone via a sulfide (DMSL1), a sulfoxide (DMSL2) and a sulfone (DMSL3) ester. A higher degree of oxidation of the sulfur atom was expected to increase its electron withdrawing properties, thereby reducing the electron density of the neighboring ester bond, which in turn is expected to accelerate the hydroxyl ion-driven hydrolysis of this bond, and thus releasing the drug more quickly. These linkers with different hydrolysis kinetics ensure proper release of DEX over time, while allowing the rate of release from the core-crosslinked PM to be tailored. Indeed, under physiological conditions (37 °C, pH 7.4), when compared to the relatively slow drug release from PMs containing sulfide ester-linked DEX (DMSL1, < 5% in 7 days, estimated $t_{1/2}$ 170 d), the drug release rates from PMs containing the sulfoxide ester-linked DEX (DMSL2, $t_{1/2}$ 18.4 ±0.41 d), or the sulfone ester-linked DEX (DMSL3, $t_{1/2}$ 8.9 ±0.14 d) were much faster (Figure 2A). For the further assessment of the drug release

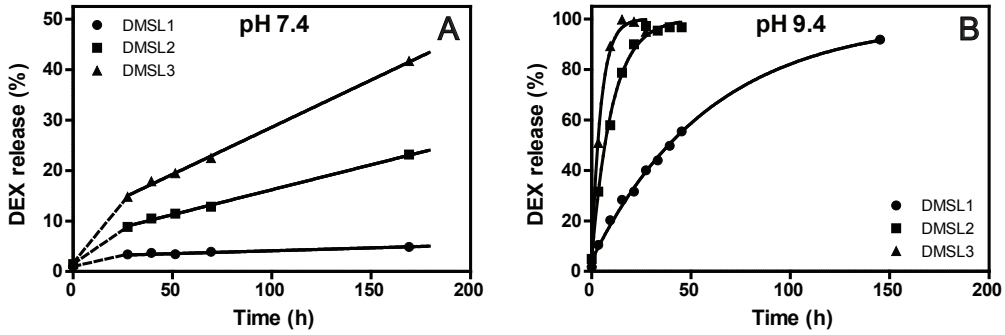

Figure 2. The release of DEX from core-crosslinked polymeric micelles loaded with different DEX prodrugs at 37°C and pH 7.4 (A) or pH 9.4 (B). DEX is covalently linked to the hydrophobic core of the micelle via hydrolysable linkers based on a sulfide ester (DMSL1), a sulfoxide ester (DMSL2) or a sulfone ester (DMSL3) (Scheme 1). The release rate from the PM was dependent on the degree of oxidation of the sulfur atom in the DEX-linker, with the order in release rate: DMSL3 > DMSL2 > DMSL1.

kinetics of the DEX-loaded PM, the OH^--driven ester hydrolysis was accelerated by incubating the PMs at a higher pH [26]. As expected, at pH 9.4, drug release from the DEX-loaded PM followed first-order kinetics and, in line with the results obtained at pH 7.4, DSML3 ($t_{1/2}$ 3.2 ±0.3 h) was cleaved faster than DMSL2 $t_{1/2}$ 7.1 ±0.4 h), which in turn was cleaved considerably faster than DMSL1 ($t_{1/2}$ 41.3 ±1.5 h) (Figure 2B). The release kinetics at pH 9.4 were approximately a factor 100 faster than at pH 7.4, which demonstrated that the hydrolysis reaction is indeed driven by OH^- and that experiments at high pH can be used to predict the drug release under physiological conditions. These data demonstrate that the release kinetics of DEX from core-crosslinked polymeric micelles can be modulated by employing DEX prodrugs containing a thioether with different degrees of oxidation.

3.3. Anti-rheumatic efficacy of DEX-loaded core-crosslinked polymeric micelles in mice with CAIA

Due to the acute inflammatory character of both arthritis models, DEX-PMs prepared using DMSL3, having the highest DEX release rate, were selected for *in vivo* evaluation. Mice with collagen antibody-induced arthritis (CAIA), an acute and reproducible arthritis

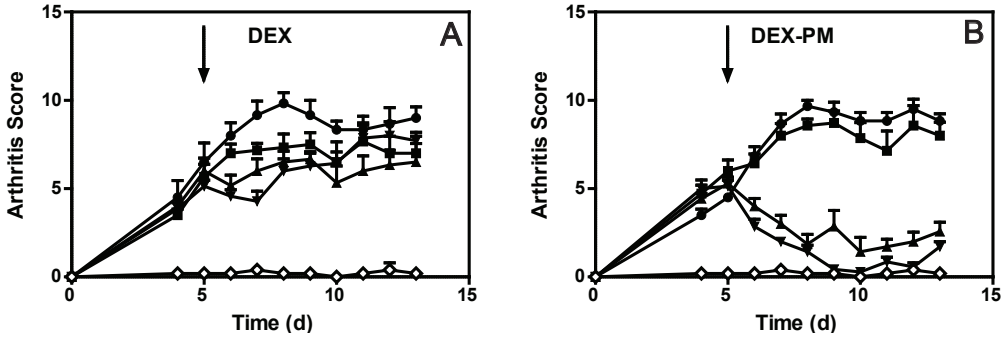

Figure 3. Arthritis score of mice with collagen antibody-induced arthritis (CAIA) upon treatment with free dexamethasone phosphate (A, DEX) or dexamethasone polymeric micelles (B, DEX-PM). Polyarthritis was induced by i.v. injection of a collagen antibody cocktail on day 0, followed by an i.p. administration of LPS on day 3. The arthritis score was determined daily using the scoring system presented in Table 1. On day 5 (arrow), when all CAIA-induced animals presented with clear signs of inflammation, these mice received an i.v. injection of DEX or DEX-PM dosed at 1 mg/kg (■), 5 mg/kg (▲), or 10 mg/kg (▼). Control mice (●) received PBS or unloaded micelles. One group of mice without CAIA served as healthy control (◇). The data is presented as the mean score with SEM of each group.

model [19], were treated intravenously with a single administration of PBS, unloaded micelles, free DEX or DEX-PM. By using different doses of free DEX and DEX-PM, i.e. 1 mg/kg, 5 mg/kg and 10 mg/kg, the dose-dependent efficacy of DEX-PM in relation to that of the free drug was assessed. As compared to PBS-treated controls, treatment with free DEX merely resulted in a very moderate, dose-dependent, reduction in clinical signs of arthritis, which was only significant on day 7, 8 and 10 for 5 mg/kg ($p<0.05$, two-way ANOVA), and on day 6 to 9 ($p<0.05$) for 10 mg/kg (Figure 3A).

In contrast, mice with CAIA treated with DEX-PM at 5 mg/kg or 10 mg/kg showed a strong and long-lasting reduction in arthritic symptoms as compared to controls ($p<0.01$ from day 6 until end of study, in case of 5 mg/kg; $p<0.001$ from day 6 until end of study, in case of 10 mg/kg) (Figure 3B). In fact, mice receiving DEX-PM dosed at 10 mg/kg, showed no or very little signs of arthritis from day 10 onwards (i.e. 5 days after treatment), as illustrated by arthritis scores that were comparable to those of healthy mice.

The pronounced improvement in therapeutic efficacy of DEX upon encapsulation in polymeric micelles is clearly illustrated when comparing the total disease load (defined as the area under the arthritis score curve) of DEX-PM-treated mice with that of free DEX-treated mice at equal doses (Figure 4). Mice receiving PBS or unloaded micelles endured

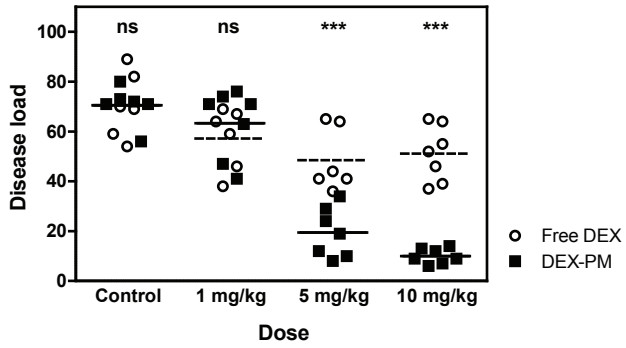

Figure 4. The disease load of mice with CAIA upon treatment. The disease load was defined as the area under the arthritis score curve from treatment (day 5) until the end of the study (day 13). Depicted is the disease load of each mouse treated with free DEX (○) or DEX-PM (■) at the specified dose, with the mean of the experimental group presented as a straight line (dashed - free DEX, solid - DEX-PM). Control animals were injected with PBS (free DEX group) or unloaded micelles (DEX-PM group). At a dose of 5 mg/kg or 10 mg/kg, but not at 1 mg/kg, there was a significant reduction of mean disease load after treatment DEX-PM when compared to free DEX (one-way ANOVA followed by Bonferroni's multiple comparison test). ***, $p<0.001$; ns, not significant.

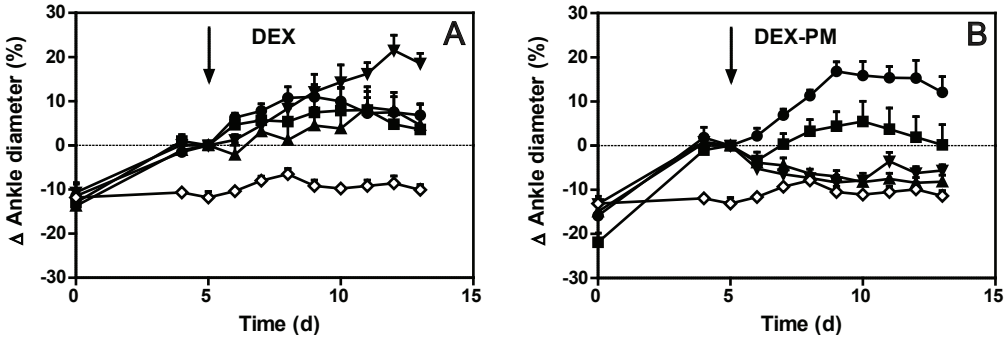

Figure 5. The change in ankle diameter of mice with collagen antibody-induced arthritis (CAIA) upon treatment with free dexamethasone phosphate (DEX) or dexamethasone polymeric micelles (DEX-PM). Polyarthritis was induced by i.v. injection of a collagen antibody cocktail on day 0, followed by an i.p. administration of LPS on day 3. The medial to lateral ankle width was determined daily using a digital caliper. On day 5 (arrow), when all CAIA-induced animals presented with clear signs of inflammation, these mice received an i.v. injection of DEX or DEX-PM dosed at 1 mg/kg (■), 5 mg/kg (▲), or 10 mg/kg (▼). Control mice (●) received PBS or unloaded micelles. One group of mice without CAIA served as healthy control (◇).To evaluate the change in ankle swelling upon treatment, the width on day 5 of mice with CAIA was used as reference measurement (0%). The data is presented as the mean change (%) with SEM of each group.

a very similar disease load, indicating that, as expected, the carrier system has no inherent anti-arthritic efficacy.

The change in ankle diameter, as a measure of the effect of free DEX or DEX-PM treatment on inflammation-related joint swelling, yielded similar results (Figure 5). DEX-PM dosed at 1 mg/kg only limited the increase in swelling, rather than actually reducing it ($p<0.05$, day 9 until end of study, two-way ANOVA). Higher doses of DEX-PM, i.e. 5 mg/kg or 10 mg/kg, strongly reduced ankle swelling to a width close to normal, which lasted until the end of the study ($p<0.01$, day 7 until end of study, both doses). In contrast, free DEX, administered at any of the tested doses, did not influence the joint swelling significantly.

3.4. Anti-rheumatic efficacy of DEX-loaded core-crosslinked polymeric micelles in rats with AIA

The corticosteroid delivery system based on PM was also evaluated in rats with adjuvant-induced arthritis (AIA), a widely used arthritis model displaying a T lymphocyte-mediated inflammatory response against cartilage proteoglycan, which is in many respects similar to human RA [27, 28]. Rats with established AIA-induced polyarthrits were treated intravenously with a single administration of 10 mg/kg free DEX, 10 mg/kg DEX-PM,

unloaded PM or PBS (Figure 6). Although the administration of free DEX resulted in a significant alleviation of the clinical signs of arthritis, as indicated by the arthritis score (Figure 6A) ($p<0.001$ on day 17 till 21, compared to PBS, two-way ANOVA) and ankle swelling (Figure 6B) ($p<0.001$ on day 17 until 23; $p<0.05$ on day 25), this effect was only transient and started to weaken from 5 days after treatment.

In contrast, upon treatment with DEX-PM at the same dose, an immediate and prolonged

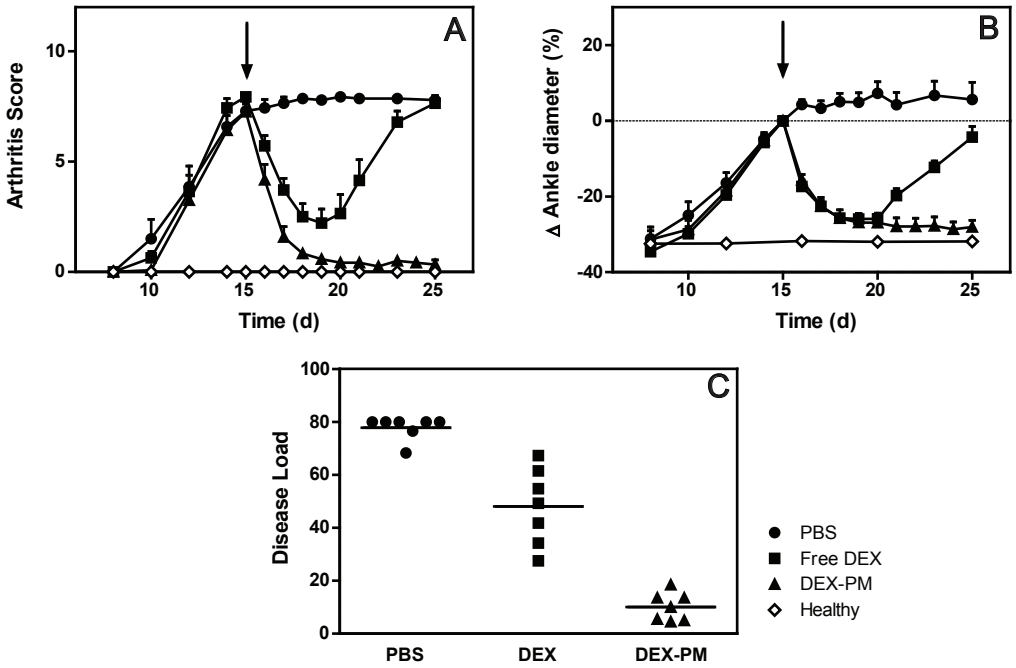

Figure 6. The therapeutic effects of free dexamethasone phosphate (DEX) or dexamethasone polymeric micelles (DEX-PM) in rats with adjuvant-induced arthritis (AIA). Arthritis was induced on day 0 by subcutaneous administration of Mycobacterium tuberculosis H37Ra in the base of the tail. On day 15 (arrow), the rats (n=7, all groups) with established arthritis were treated with a single administration 10 mg/kg of free DEX or DEX-PM. Control rats received PBS, and one group of rats without AIA served as healthy controls. A. The arthritis score of all rats (shown as mean with SEM of each group), determined daily using the scoring system presented in Table 2. B. The medial to lateral ankle diameter of all rats (shown as mean with SEM), measured daily using a digital caliper. To evaluate the change in ankle swelling upon treatment, the diameter on day 15 of rats with AIA was used as reference measurement (0%). C. The disease load, defined as the area under the arthritis score curve from treatment (day 15) until the end of the study (day 25), of each individual rat, presented with the mean of the treatment group as a straight line. The disease load of animals in each treatment group was significantly different from those in the other groups ($p<0.001$, one-way ANOVA followed by Bonferroni's multiple comparison test).

anti-arthritic effect was achieved ($p<0.001$ from day 16 until end of study, compared to PBS, for arthritis score and ankle diameter). When compared to free DEX at the same dose, DEX-PM was significantly more effective in terms of reducing the arthritis score ($p<0.05$ on day 16 and 20; $p<0.001$ from day 21 until the end of the study), as well as minimizing the ankle swelling ($p<0.001$ on day 23 and 25). Finally, while there was a disease load-limiting effect of 10 mg/kg free DEX ($p<0.01$, one-way ANOVA vs PBS), the total disease load of arthritic rats treated with DEX-PM was consistently lower than the disease load of rats treated with either PBS ($p<0.001$, one-way ANOVA) or free DEX ($p<0.001$).

The high therapeutic potential of nanocarrier-mediated targeting of dexamethasone(-prodrugs) in RA therapy, has been established previously using PEGylated liposomes (currently in clinical trials) [29-31] and macromolecular poly(*N*-(hydroxypropyl) methacrylamide)-drug conjugates [5, 8, 32, 33]. Although both of these carrier systems were shown to effectively accumulate in the synovium of inflamed joints, the exact mechanism by which they convey their therapeutic effect has not yet been completely clarified [31]. Since nanoparticulate systems with a size above the renal threshold are primarily eliminated from the circulation by phagocytic cells such as macrophages and joint synoviocytes, which, in addition, have a key role in the pathogenic processes underlying rheumatoid arthritis, it can be anticipated that these cells are important mediators in the anti-arthritic efficacy of these targeted drug delivery systems [5, 34-39]. Upon uptake of the drug carrier by these RES-associated cells, the subsequent release of its payload is likely depending on the type of delivery system used. Whereas the release of drugs encapsulated in the aqueous core of liposomes may be occurring relatively rapidly once the liposomal bilayers are being degraded, the drug release from polymeric prodrugs depends on the cleavage rate of the bonds that link the drug to the polymeric carrier system, which in case of DEX-PM is relatively slow. It is, however, currently not clear what would be the optimal release profile (i.e. fast or slow release), for the therapy of RA or other chronic inflammatory diseases.

An important advantage of the PM system for corticosteroids targeting, is the tailorability of the release rate of dexamethasone from the carrier system, which allows future optimization of drug release kinetics for the treatment of RA, as well as other diseases. Although in this study only the fastest releasing PM were tested in the arthritis models, it can be expected that slower DEX releasing micelles have more long-lasting effects in these and

other chronic inflammatory disease models. By incorporating a combination of prodrugs with different conversion rates within a single micellar formulation, it is possible to fine-tune the DEX release profile even further, e.g. with a rapid-release and with a slow-release component. Additionally, when compared to polymer-drug conjugates, this PM system does not require the employment of non-degradable high molecular weight polymers that may give rise to concerns regarding biocompatibility. Also, since the therapeutic agent is entrapped in the hydrophobic core of the PM, any unwanted exposure of the therapeutic agent to its environment is limited. Finally, since the synthesis procedure for preparing polymerizable dexamethasone prodrugs only requires the drug to be present in the final step of the process, the linker technology presented here is broadly applicable for preparing core-crosslinked polymeric micelles entrapping a range of compounds with therapeutic activity, making this system enormously versatile and promising, not only for targeted RA therapy but also for many other disorders.

4. Conclusions

In this study, a novel delivery system for the targeted delivery of dexamethasone to RA is presented. Three different polymerizable prodrugs of dexamethasone based on a sulfide, sulfoxide, and sulfone ester were prepared, incorporated into to the core of core-crosslinked mPEG-b-pHPMAmLac$_n$ micelles, and evaluated for their release kinetics *in vitro*. Polymeric micelles prepared from the DEX-prodrug containing the thioether with the highest degree of oxidation (sulfone) showed, as expected, the fasted release kinetics, and were therefore assessed *in vivo* for their therapeutic activity in mice with collagen antibody-induced arthritis and rats with adjuvant-induced arthritis. When compared with free dexamethasone, dexamethasone-loaded core-crosslinked polymeric micelles showed strong therapeutic effects on disease activity, total disease load and joint swelling, thereby convincingly demonstrating their large potential for the treatment of RA, and possibly also other chronic inflammatory diseases.

5. Acknowledgements

This work was supported by MediTrans, an Integrated Project funded by the European Commission under the "nanotechnologies and nano-sciences, knowledge-based multifunctional materials and new production processes and devices" (NMP), thematic priority of the Sixth Framework Program, NWO-CW/STW (grants 790.36.110 and 10154), and NIH grant R01 AR053325.

6. References

[1] D. Tischner, H.M. Reichardt, Glucocorticoids in the control of neuroinflammation, Mol. Cell. Endocrinol. 275(1-2) (2007) 62-70.

[2] J.N. Hoes, J.W.G. Jacobs, F. Buttgereit, J.W.J. Bijlsma, Current view of glucocorticoid co-therapy with DMARDs in rheumatoid arthritis, Nat. Rev. Rheumatol. 6(12) (2010) 693-702.

[3] A.C. Ford, C.N. Bernstein, K.J. Khan, M.T. Abreu, J.K. Marshall, N.J. Talley, P. Moayyedi, Glucocorticosteroid therapy in inflammatory bowel disease: systematic review and meta-analysis, Am. J. Gastroenterol. 106(4) (2011) 590-599.

[4] J.M. Metselaar, M.H.M. Wauben, J.P.A. Wagenaar-Hilbers, O.C. Boerman, G. Storm, Complete remission of experimental arthritis by joint targeting of glucocorticoids with long-circulating liposomes, Arthritis Rheum. 48(7) (2003) 2059-2066.

[5] L.-d. Quan, P.E. Purdue, X.-m. Liu, M. Boska, S. Lele, G. Thiele, T. Mikuls, H. Dou, S. Goldring, D. Wang, Development of a macromolecular prodrug for the treatment of inflammatory arthritis: mechanisms involved in arthrotropism and sustained therapeutic efficacy, Arthrit. Res. Ther. 12(5) (2010) R170.

[6] I. Kushner, J.A. Somerville, Permeability of human synovial membrane to plasma proteins. Relationship to molecular size and inflammation, Arthritis Rheum. 14(5) (1971) 560-570.

[7] D. Wang, S.C. Miller, M. Sima, D. Parker, H. Buswell, K.C. Goodrich, P. Kopečková, J. Kopeček, The arthrotropism of macromolecules in adjuvant-induced arthritis rat model: a preliminary study, Pharm. Res. 21(10) (2004) 1741-1749.

[8] X.-M. Liu, L.-D. Quan, J. Tian, Y. Alnouti, K. Fu, G. Thiele, D. Wang, Synthesis and evaluation of a well-defined HPMA copolymer–dexamethasone conjugate for effective treatment of rheumatoid arthritis, Pharm. Res. 25(12) (2008) 2910-2919.

[9] V.P. Torchilin, Recent advances with liposomes as pharmaceutical carriers, Nat. Rev. Drug Discov. 4(2) (2005) 145.

[10] J. Sanchis, F. Canal, R. Lucas, M.J. Vicent, Polymer-drug conjugates for novel molecular targets, Nanomedicine 5(6) (2011) 915-935.

[11] E. Neumann, E. Frei, D. Funk, M.D. Becker, H.H. Schrenk, U. Muller-Ladner, C. Fiehn, Native albumin for targeted drug delivery, Expert. Opin. Drug. Deliv. 7(8) (2010) 915-925.

[12] M. Talelli, C.J.F. Rijcken, C.F. van Nostrum, G. Storm, W.E. Hennink, Micelles based on HPMA copolymers, Adv. Drug Deliv. Rev. 62(2) (2010) 231-239.

[13] T. Lammers, V. Subr, P. Peschke, R. Kühnlein, W.E. Hennink, K. Ulbrich, F. Kiessling, M. Heilmann, J. Debus, P.E. Huber, G. Storm, Image-guided and passively tumour-targeted polymeric nanomedicines for radiochemotherapy, Br. J. Cancer 99(6) (2008) 900-910.

[14] C.J.F. Rijcken, O. Soga, W.E. Hennink, C.F.v. Nostrum, Triggered destabilisation of polymeric micelles and vesicles by changing polymers polarity: An attractive tool for drug delivery, J. Control. Release 120(3) (2007) 131-148.

[15] C.J. Rijcken, M. Talelli, C.F. van Nostrum, G. Storm, W.E. Hennink, Crosslinked micelles with transiently linked drugs – a versatile drug delivery system, European Journal of Nanomedicine 3(1) (2010) 19-24.

[16] C.J.F. Rijcken, C.J. Snel, R.M. Schiffelers, C.F. van Nostrum, W.E. Hennink, Hydrolysable core-crosslinked thermosensitive polymeric micelles: synthesis, characterisation and in vivo studies, Biomaterials 28(36) (2007) 5581-5593.

[17] M. Talelli, M. Iman, A.K. Varkouhi, C.J.F. Rijcken, R.M. Schiffelers, T. Etrych, K. Ulbrich, C.F. van Nostrum, T. Lammers, G. Storm, W.E. Hennink, Core-crosslinked polymeric micelles with controlled release of covalently entrapped doxorubicin, Biomaterials 31(30) (2010) 7797-7804.

[18] C.J.F. Rijcken, T.F.J. Veldhuis, A. Ramzi, J.D. Meeldijk, C.F. van Nostrum, W.E. Hennink, Novel fast degradable thermosensitive polymeric micelles based on PEG-block-poly(N-(2-hydroxyethyl)methacrylamide-oligolactates), Biomacromolecules 6(4) (2005) 2343-2351.

[19] L.M. Khachigian, Collagen antibody-induced arthritis, Nat. Protoc. 1(5) (2006) 2512-2516.

[20] Guide for the care and use of laboratory animals. NIH Publication No. 85-23. Revised 1985.

[21] T. Cronin, H. Faubl, W. Hoffman, J. Korst, Xylenediamines as antiviral agents. US patent 4,034,040. 1977.

[22] A. Vonarbourg, C. Passirani, P. Saulnier, J.-P. Benoit, Parameters influencing the stealthiness of colloidal drug delivery systems, Biomaterials 27(24) (2006) 4356.

[23] F. Alexis, E. Pridgen, L.K. Molnar, O.C. Farokhzad, Factors affecting the clearance and biodistribution of polymeric nanoparticles, Mol. Pharm. 5(4) (2008) 505-515.

[24] C.J. Rijcken, C.J. Snel, R.M. Schiffelers, C.F. van Nostrum, W.E. Hennink, Hydrolysable core-crosslinked thermosensitive polymeric micelles: synthesis, characterisation and in vivo studies, Biomaterials 28(36) (2007) 5581-5593.

[25] R.J.H. Stenekes, W.E. Hennink, Polymerization kinetics of dextran-bound methacrylate in an aqueous two phase system, Polymer 41(15) (2000) 5563-5569.

[26] W.N.E. van Dijk-Wolthuis, M.J. van Steenbergen, W.J.M. Underberg, W.E. Hennink, Degradation kinetics of methacrylated dextrans in aqueous solution, J. Pharm. Sci. 86(4) (1997) 413-417.

[27] W. van Eden, B.H. Waksman, Immune regulation in adjuvant-induced arthritis: possible implications for innovative therapeutic strategies in arthritis, Arthritis Rheum. 48(7) (2003) 1788-1796.

[28] W. van Eden, J.E.R. Tholet, R. van der Zee, A. Noordzij, J.D.A. van Embden, E.J. Hensen, I.R. Cohen, Cloning of the mycobacterial epitope recognized by T lymphocytes in adjuvant arthritis, Nature 331(6152) (1988) 171-173.

[29] R. Anderson, A. Franch, M. Castell, F.J. Perez-Cano, R. Bräuer, D. Pohlers, M. Gajda, A.P. Siskos, T. Katsila, C. Tamvakopoulos, U. Rauchhaus, S. Panzner, R.W. Kinne, Liposomal encapsulation enhances and prolongs the anti-inflammatory effects of water-soluble dexamethasone phosphate in experimental adjuvant arthritis, Arthrit. Res. Ther. 12(4) (2010).

[30] J.M. van den Hoven, W. Hofkens, M.H.M. Wauben, J.P.A. Wagenaar-Hilbers, J.H. Beijnen, B. Nuijen, J.M. Metselaar, G. Storm, Optimizing the therapeutic index of liposomal glucocorticoids in experimental arthritis, Int. J. Pharm. 16(2) (2011) 471-477.

[31] U. Rauchhaus, F. Schwaiger, S. Panzner, Separating therapeutic efficacy from glucocorticoid side-effects in rodent arthritis using novel, liposomal delivery of dexamethasone phosphate: long-term suppression of arthritis facilitates interval treatment, Arthrit. Res. Ther. 11(6) (2009) R190.

[32] L.-d. Quan, F. Yuan, X.-m. Liu, J.-g. Huang, Y. Alnouti, D. Wang, Pharmacokinetic and biodistribution studies of N-(2-Hydroxypropyl)methacrylamide copolymer-dexamethasone conjugates in adjuvant-induced arthritis rat model, Mol. Pharm. 7(4) (2010) 1041-1049.

[33] D. Wang, S. Miller, X.-M. Liu, B. Anderson, X.S. Wang, S. Goldring, Novel dexamethasone-HPMA copolymer conjugate and its potential application in treatment of rheumatoid arthritis, Arthrit. Res. Ther. 9(1) (2007) R2.

[34] D. Wang, S.R. Goldring, The bone, the joints and the Balm of Gilead, Mol. Pharm. 8(4) (2011) 991-993.

[35] S.K. Huang, K.D. Lee, K. Hong, D.S. Friend, D. Papahadjopoulos, Microscopic localization of sterically stabilized liposomes in colon carcinoma-bearing mice, Cancer Res. 52(19) (1992) 5135-5143.

[36] T.M. Allen, L. Murray, S. MacKeigan, M. Shah, Chronic liposome administration in mice: effects on reticuloendothelial function and tissue distribution, J. Pharmacol. Exp. Ther. 229(1) (1984) 267-275.

[37] U. Rauchhaus, R.W. Kinne, D. Pohlers, S. Wiegand, A. Wölfert, M. Gajda, R. Bräuer, S. Panzner, Targeted delivery of liposomal dexamethasone phosphate to the spleen provides a persistent therapeutic effect in rat antigen-induced arthritis, Ann. Rheum. Dis. 68(12) (2009) 1933-1934.

[38] P. Barrera, A. Blom, P.L.E.M. van Lent, L. van Bloois, J.H. Beijnen, N. van Rooijen, M.C. de Waal Malefijt, L.B.A. van de Putte, G. Storm, W.B. van den Berg, Synovial macrophage depletion with clodronate-containing liposomes in rheumatoid arthritis, Arthritis Rheum. 43(9) (2000) 1951-1959.

[39] S. Lefèvre, A. Knedla, C. Tennie, A. Kampmann, C. Wunrau, R. Dinser, A. Korb, E.M. Schnäker, I.H. Tarner, P.D. Robbins, C.H. Evans, H. Stürz, J. Steinmeyer, S. Gay, J. Schölmerich, T. Pap, U. Müller-Ladner, E. Neumann, Synovial fibroblasts spread rheumatoid arthritis to unaffected joints, Nat. Med. 15(12) (2009) 1414-1420.

[40] K. Sato, M. Hyodo, M. Aoki, X.-Q. Zheng, R. Noyori, Oxidation of sulfides to sulfoxides and sulfones with 30% hydrogen peroxide under organic solvent- and halogen-free conditions, Tetrahedron 57(13) (2001) 2469-2476.

[41] C.M. Rodríguez, J.M. Ode, J.M. Palazón, V.S. Martín, Simple and efficient oxidation of sulfides to sulfones using catalytic ruthenium tetroxide, Tetrahedron 48(17) (1992) 3571-3576.

Supporting Information

Synthesis of tert-butyl 2-(2-hydroxyethylthio)acetate (2)

tert-Butyl bromoacetate **1** (15 g, 0.077 mol) and triethylamine (16 g, 0.16 mol) were dissolved in CH_2Cl_2 (100 mL) under nitrogen and cooled to 0 °C. Next, 2-mercaptoethanol (6.3 g, 0.081 mol) was slowly added to the mixture and the reaction mixture was warmed to room temperature while stirring. Completion of the reaction was monitored by TLC (EtOAc/Hex, 1:1, R_f 0.88). Base and acid extractions were carried out with KCO_3 (1M, pH 10) and NaOAc (1M, pH 3.5), twice, respectively. The combined organic layers were washed with brine, dried with $MgSO_4$ and filtered through Ø 185 mm whatman filter papers. The filtrate was concentrated *in vacuo* to obtain **2** (9.2 g, 62% yield) as a colourless oil.

^{1}H-NMR ($CDCl_3$): δ (ppm) 3.7 (q, 2H), 3.18 (s, 2H), 2.8 (d, 2H), 1.47 (s, 9H)
^{1}H-NMR (DMSO): δ (ppm) 4.77 (s, OH), 3.52 (s, 2H), 3.19 (s, 2H), 2.62 (t, 2H), 1.39 (s, 9H)

Synthesis of 2-(2-tert-butoxy-2-oxoethylthio)ethyl methacrylate (3)

Compound **2** (8.6 g, 0.045 mol) and triethylamine (9.05 g, 0.089 mol) were dissolved in CH_2Cl_2 (20 mL) on ice under nitrogen. Methacryloyl chloride (5.6 g, 0.054 mol) was added slowly to the mixture. The reaction mixture was warmed to room temperature and stirred for 2 h. Completion of the reaction was confirmed by TLC (EtOAc/Hex, 1:1, R_f 0.86). Excess of methacryloyl chloride was removed by methanol to form methyl methacrylate. 3 was extracted twice with a saturated $NaHCO_3$ solution of pH 8. The combined organic layers were washed with brine and dried with $MgSO_4$ and filtered through Ø 185 mm whatman filter papers. The filtrate was concentrated *in vacuo*. Co-solvent evaporation with EtOAc, Hex and CH_2Cl_2, respectively, was performed to remove volatile impurities. **3** (10.5 g, 90% yield) was obtained as a yellow oil.

^{1}H-NMR ($CDCl_3$): δ (ppm) 6.12 (s, H), 5.58 (s, H), 4.34 (t, 2H), 3.18 (s, 2H), 2.93 (t, 2H), 1.94 (s, 3H), 1.47 (s, 9H)
^{13}C-NMR ($CDCl_3$): δ (ppm) 18.5 (CH_3), 28.2 (CH_3), 31.0 (CH_2), 35.1 (CH_2), 63.5 (CH_2), 81.9 (CH_2), 126. 1 (C), 136.3 (C), 167.3 (C), 169.6 (C)

Synthesis of 2-(2-(methacryloyloxy)ethylthio)acetic acid (4)

Compound **3** (2 g, 7.7 mmol) was slowly dissolved in TFA (10 mL) on ice under nitrogen. A trace amount of MEHQ was added to the reaction mixture to prevent polymerization. The reaction mixture was allowed to warm to room temperature and the reaction mixture was stirred for 2 h at 55 °C. Completion of the reaction was monitored by TLC ($CHCl_3$ /MeOH/HOAc, 9:1:0.1, R_f 0.17). Excess of TFA was removed by evaporation and coevaporation with CH_2Cl_2 and the residue was purified on a silica gel column (Hex/EtOAc, 4:1). **4** was dried with $MgSO_4$ and filtered through Ø 185 mm whatman filter papers. The filtrate was concentrated *in vacuo*. **4** (1 g, 63% yield) was obtained as a light yellow oil.

^{1}H-NMR ($CDCl_3$): δ (ppm) 6.13 (s, 1H), 5.59 (s, 1H), 3.65 (t, 2H), 3.34 (s, 2H), 2.96 (t, 2H), 1.95 (s, 3H)
^{1}H-NMR (DMSO): δ (ppm) 6.02 (s, 1H), 5.67 (s, 1H), 4.24 (t, 2H), 3.3 (s, 2H), 2.85 (t, 2H), 1.86 (s, 3H)
^{13}C-NMR (DMSO): δ (ppm) 23.36 (CH_3), 35.69 (CH_2), 38.73 (CH_2), 68.68 (CH_2), 131.3 (CH_2), 141.1 (C), 171.9 (C), 176.8 (C)

Synthesis of 2-(2-(2-((8S,9R,10S,11S,16R,17R)-9-fluoro-11,17-dihydroxy-10,13,16-trimethyl-3-oxo-6,7,8,9,10,11,12,13,14,15,16,17-dodecahydro-3H-cyclopenta[α]phenanthren-17-yl)-2-oxoethoxy)-2-oxoethylthio)ethyl methacrylate (DMSL1)

Compound **4** (0.25 g, 1.2 mmol) and DMAP (0.077 g, 0.63 mmol) were dissolved in dry CH_2Cl_2 (20 mL) under nitrogen. The reaction mixture was cooled on ice and DCC (0.29 g, 1.4 mmol) was then added to the mixture together with dexamethasone (0.5 g, 1.3 mmol) dissolved in dry THF (20 mL). The reaction was cooled to room temperature and stirred overnight. The completion of the reaction was confirmed by TLC (EtOAc/Hex, 3:2, R_f 0.76). Most of the solvent was evaporated and the remaining mixture was purified on a 15 cm silica gel column (EtOAc/Hex, 3:2, R_f: 0.44). DMSL1 (0.5 g, 70% yield) was obtained as a white fluffy solid.

ESI-MS $[M+H]^+$ = 578.85. calculated = 579.69
$[2M+H]^+$ = 1157.25, calculated = 1158.38

^{1}H-NMR (DMSO): δ (ppm) 7.26 (d, 1H), 6.22 (d, 1H), 6.02 (s, 1H), 5.98 (s, 1H*), 5.68 (s, 1H*), 5.39 (s, 1H), 5.19 (s, 1H), 5.18 (d, 1H), 4.82 (d, 1H), 4.27 (t, 2H*), 3.51 (s, 2H*), 2.91 (t, 2H*), 1.87 (s, 3H*), 1.46 (s, 3H), 0.86 (s, 3H), 0.78 (d, 3H)
^{13}C-NMR (DMSO): δ (ppm) 20.54 (CH_3), 21.66 (CH_3), 23.42 (CH_3*), 28.44 (CH_3), 32.73 (CH_2), 35.61 (CH_2*), 35.7 (CH_2), 37.35 (CH_2), 38.02 (CH^{2*}), 39.19 (CH), 40.87 (CH_2), 41.09 (CH), 48.73 (CH), 53.42 (CH_2), 68.55 (CH_2*), 74.11 (CH), 75.68 (C), 76.16 (C), 95.93 (CH2), 105.54 (CH), 107.85 (C), 129.52 (C), 131.43 (CH_2*), 134.41 (CH), 141.14 (C*), 158.15 (CH), 171.77 (C*), 172.46 (CH), 174.93 (C*), 190.68 (C)

Synthesis of 2-(2-(methacryloyloxy)ethylsulfinyl)acetic acid (5)

Compound **4** (1 g, 4.9 mmol) in ACN (10 mL) was mixed with a solution of sodium periodate (1.1 g, 4.9 mmol) dissolved in H_2O (10 mL). The reaction mixture was stirred at RT overnight. The completion of the reaction was confirmed by TLC (CHCl3/MeOH/TFA, 75:25:0.1, R_f 0.23). The reaction mixture was filtered by vacuum filtration to remove sodium iodate salts by EtOAc, dried with $MgSO_4$, and filtered through Ø 185 mm whatman filter papers. The filtrate was concentrated *in vacuo* and co-evaporated with CH_2Cl_2. **5** (0.87 g, 81% yield) was obtained as a white solid.

^{1}H-NMR ($CDCl_3$): δ (ppm) 6.15 (s, 1H), 5.64 (s, 1H), 4.58 (m, 2H), 3.9 (d, 1H), 3.7 (d, 1H), 3.39 (m, 2H), 1.94 (s, 3H)
^{1}H-NMR (DMSO): δ (ppm) 6.04 (s, 1H), 5.70 (s, 1H), 4.4 (m, 2H), 3.95 (d, 1H), 3.74 (d, H), 3.17 (m, 2H), 1.87 (s, 3H)
^{13}C -NMR (DMSO): δ (ppm) 23.34 (CH_3), 55.38 (CH_2), 61.67 (CH_2), 62.83 (CH_2), 131.78 (CH_2), 140.96 (C), 171.64 (C), 172.93 (C)

Synthesis of 2-(2-(2-((8S,9R,10S,11S,16R,17R)-9-fluoro-11,17-dihydroxy-10,13,16-trimethyl-3-oxo-6,7,8,9,10,11,12,13,14,15,16,17-dodecahydro-3H-cyclopenta[α]phenanthren-17-yl)-2-oxoethoxy)-2-oxoethylsulfinyl)ethyl methacrylate (DMSL2)

Compound **5** (0.54 g, 2.4 mmol) was dissolved in dry THF (5 mL) and DMAP (0.14 g, 1.2 mmol) was added to the solution under nitrogen. After cooling on ice, a dexamethasone solution (0.91 g, 2.3 mmol) in dry THF (25 mL) and DCC (0.525 g, 2.5 mmol) were added to the mixture. The reaction mixture was slowly warmed to room temperature and stirred overnight at RT. The completion of the reaction was confirmed by TLC (EtOAc/Hex, 20:1, R_f 0.24). Excessive solvent was evaporated and the remaining solution was purified on a 20 cm silica gel column (EtOAc/Hex, 20:1). DMSL2 (1 g, 73% yield) was

obtained as a yellow fluffy solid.

ESI-MS $[M+H]^+$ = 595.10, calculated = 595.69
$[2M+H]^+$ = 1189.65, calculated = 1190.38
^{1}H-NMR (DMSO): δ (ppm) 7.29 (d, 1H), 6.22 (d, 1H), 6.05 (s, 1H), 5.99 (s, 1H), 5.71 (s, 1H), 5.40 (d, 1H), 5.19 (s, OH), 5.18 (d, 1H), 4.88 (d, 1H), 4.5 (t, 2H), 4.18 (s, 1H), 4.15 (d, 1H), 4.00 (d, 1H), 2.86 (s, 1H), 1.88 (s, 3H), 1.47 (s, 3H), 0.87 (s, 3H), 0.78 (d, 3H)
^{13}C-NMR (DMSO): δ (ppm) 20.51 (CH_3), 21.62 (CH_3), 23.32 (CH_3*), 28.34 (CH_3), 32.69 (CH_2), 35.68 (CH_2*), 35.84 (CH_2), 37.32 (CH_2), 39.80 (CH), 41.07 (CH), 48.72 (CH), 53.66 (CH_2), 55.53 (CH2), 61.67 (CH_2), 62.72 (CH_2), 74.11 (CH), 75.66 (C), 76.14 (C), 95.92 (CH_2), 105.54 (CH), 107.85 (C), 129.53 (C), 131.78 (CH), 134.42 (CH), 140.94 (C), 158.17 (CH), 170.98 (C), 171.60 (CH), 172.48 (C), 190.71 (C)

Synthesis of tert-butyl 2-(2-hydroxyethylsulfonyl)acetate (6)

Compound **2** (2.0 g, 10.4 mmol) was dissolved in ACN (20 mL) and CCl_4 (20 mL). A solution of $NaIO_4$ (6.7 g, 31 mmol) in 30 mL water was added to reaction mixture with vigorous stirring. $RuCl_3$ (43 mg, 0.21 mmol) was added, once the two phases were mixed into an emulsion. The reaction mixture was then heated to 35 °C and stirred overnight [40, 41]. The reaction was monitored via TLC (EtOAc/Hex, 3:2, R_f **6**: 0.16, **2**: 0.53). Once the reaction was complete, the reaction mixture was diluted with ether (100 mL), stirred vigorously for 15 minutes, dried with $MgSO_4$ and filtered through Ø 185 mm whatman filter papers. The residue was washed with ether (3x30 mL) and the filtrate concentrated *in vacuo* in a fume hood. This was later purified on a silica gel column (EtOAc/Hex, 3:2). **6** (1.15 g, 50% yield) was obtained as a yellow oil.

^{1}H-NMR (DMSO): δ (ppm) 5.17 (s, OH), 4.22 (s, 2H), 3.80 (t, 2H), 3.37 (t, 2H), 1.42 (s, 9H)

Synthesis of 2-(2-tert-butoxy-2-oxoethylsulfonyl)ethyl methacrylate (7)

Compound **6** (1 g, 4.6 mmol) was dissolved in dry CH_2Cl_2 (10 mL) under nitrogen. Triethylamine (0.93 g, 9.2 mmol) and subsequently methacryloyl chloride (0.57 g, 5.5 mmol) were added on ice to the reaction mixture. The mixture was allowed to warm to room temperature and was stirred for 3 h. The completion of the reaction was confirmed by TLC (EtOAc/Hex, 3:2), R_f **7**: 0.69, **6**: 0.27). Excess of methacryloyl chloride was removed with methanol to form methyl methacrylate. Base extraction ($NaHCO_3$, pH 8)

was carried out twice. The reaction mixture was dried with $MgSO_4$, filtered through Ø 185 mm whatman filter papers, and concentrated *in vacuo*. The filtrate was purified on a silica gel column (100% EtOAc). **7** (1.15 g, 86% yield) was obtained as an orange oil.

^{1}H-NMR (DMSO): δ (ppm) 6.06 (s, 1H), 5.71 (s, 1H), 4.48 (t, 2H), 4.29 (s, 2H), 3.69 (t, 2H), 1.87 (s, 3H), 1.42 (s, 9H)

Synthesis of 2-(2-(methacryloyloxy)ethylsulfonyl)acetic acid (8)

Compound **7** (1.2 g, 3.9 mmol) was dissolved in TFA (15 mL) under nitrogen. A trace amount of MEHQ was added to the mixture and the reaction was stirred for 3 h at 55 °C. Completion of the reaction was confirmed by TLC (EtOAc/Hex/TFA, 60:40:0.1, R_f 0.38). The reaction mixture was purified on a silica gel column (EtOAc/Hex, 3:2). **8** (0.6 g, 65% yield) was obtained as yellow oil.

1H-NMR (DMSO): δ (ppm) 6.05 (s, 1H), 5.71 (s, 1H), 4.48 (t, 2H), 4.29 (s, 2H), 3.67 (t, 2H), 1.86 (s, 3H)

Synthesis of 2-(2-(2-((8S,9R,10S,11S,16R,17R)-9-fluoro-11,17-dihydroxy-10,13,16-trimethyl-3-oxo-6,7,8,9,10,11,12,13,14,15,16,17-dodecahydro-3H-cyclopenta[α]phenanthren-17-yl)-2-oxoethoxy)-2-oxoethylsulfonyl)ethyl methacrylate (DMSL3)

Compound **8** (67 mg, 0.28 mmol) was dissolved in dry DCM (10 mL) and DMAP (0.017 g, 0.14 mmol) was added to the reaction mixture under nitrogen. Dexamethasone was dissolved (0.11 g, 0.27 mmol) in dry THF (10 mL). After cooling the mixture on ice, DCC (0.21 g, 0.46 mmol) and the dexamethasone solution were added to the mixture. The reaction was stirred overnight at RT and the completion was confirmed by TLC (EtOAc/Hex, 7:3, R_f 0.47). Excessive solvent was evaporated and the remaining solution was purified on a 20 cm silica gel column (EtOAc/Hex, 7:3). DMSL3 (0.1 g, 60% yield) was obtained as a white solid.

ESI-MS $[M+H]^+$ = 611.05, calculated = 611.69
$[2M+H]^+$ = 1221.20, calculated = 1222.38

^{1}H-NMR (DMSO): δ (ppm) 7.29 (d, 1H), 6.22 (d, 1H), 6.05 (s, 1H), 5.99 (s, 1H), 5.71 (s, 1H), 5.40 (d, 1H), 5.19 (s, OH), 5.18 (d, 1H), 4.88 (d, 1H), 4.59 (s,2H), 4.51 (t, 2H), 3.78 (t, 2H), 1.87 (s, 3H), 1.47 (s, 3H), 0.87 (s, 3H), 0.77 (d, 3H)

^{13}C-NMR (DMSO): δ (ppm) (CH_3), (CH_3), 15.79 (CH_3), 16.93 (CH_3), 18.55 (CH_2), 23.63 (CH_2), 25.16 (CH_2), 27.98 (CH_2) 30.96 (CH), 32.59 (CH), 34.04 (CH), 36.36 (CH_2), 44.00 (CH_2), 48.75 (CH_2), 52.77 (CH_2), 58.24 (CH), 70.09 (C), 71.40 (C), 91.18 (CH_2), 124.80 (C), 127.25 (C), 129.69 (CH), 136.05 (CH), 153.42 (C), 163.23 (CH), 166.74 (C), 167.73 (CH), 185.96 (C), 204.66 (C)

5

Liposomes as carriers for colchicine-derived prodrugs: vascular disrupting nanomedicines with tailorable drug release kinetics

B.J. Crielaard, S. van der Wal, H.T. Le, A.T.L. Bode, T. Lammers, W.E. Hennink, R.M. Schiffelers, M.H.A.M. Fens and G. Storm

Department of Pharmaceutics, Utrecht Institute for Pharmaceutical Sciences (UIPS), Utrecht University, Utrecht, The Netherlands

Eur. J. Pharm. Sci. 2012 45(4):429-435

Abstract

Newly formed tumor vasculature has proven to be an effective target for tumor therapy. A strategy to attack this angiogenic tumor vasculature is to initiate local blood vessel congestion and consequently induce massive tumor cell necrosis. Vascular disrupting agents (VDAs) typically bind to tubulin and consequently disrupt microtubule dynamics. Colchicine and its derivatives (colchicinoids) are very potent tubulin-binding compounds but have a narrow therapeutic index, which may be improved by employing a liposomal targeting strategy. However, as a result of their physicochemical properties, colchicinoids are problematic to retain in liposomes, as they are released relatively rapidly upon encapsulation. To overcome this limitation, two hydrolysable PEGylated derivatives of colchicine were developed for encapsulation into the aqueous core of long-circulating liposomes: a moderately rapid hydrolyzing PEGylated colchicinoid containing a glycolic acid linker (prodrug I), and a slower hydrolyzing PEGylated colchicinoid with a lactic acid linker (prodrug II). Hydrolysis studies at 37°C and pH 7.4 showed that prodrug I possessed relatively rapid conversion characteristics ($t_{1/2}$ = 5.4 h) whereas prodrug II hydrolyzed much slower ($t_{1/2}$ = 217 h). Upon encapsulation into liposomes, colchicine was released rapidly, whereas both PEGylated colchicine derivatives were efficiently retained and appeared to be released only after cleavage of the PEG-linker. This study therefore demonstrates that, in contrast to colchicine, these novel PEGylated colchicine-derived prodrugs are retained within the aqueous interior after encapsulation into liposomes, and that the release of the active parent can be controlled by using different biodegradable linkers.

1. Introduction

Newly formed angiogenic endothelium has become an important target for the design of anticancer agents [1]. As tumor vasculature develops relatively fast during early tumor growth, blood vessels appear immature, disorganized and imperfect, which makes them a vulnerable target for cancer therapy [2, 3]. Vascular disrupting agents (VDAs) initiate local disruption of tumor endothelium by interfering with the immature vasculature, causing site-specific blood vessel congestion. As a consequence, tumor cells are deprived from nutrients and oxygen, leading to rapid and massive tumor cell necrosis [4-6]. Tubulin binding agents (TBAs), such as colchicine and the structurally and pharmacologically similar colchicinoids, display vascular disrupting activity by binding irreversibly to tubulin at its colchicine domain, thereby inhibiting tubulin dynamics and microtubule formation [7, 8]. Because endothelial cells in the tumor vasculature rely more on tubulin than actin to maintain their cell shape, the binding of TBAs to tubulin leads to rapid rounding of these cells, resulting in loss of vascular integrity and, ultimately, to hemostasis [3, 9]. TBAs are considered to be useful in cancer therapy not only because of their ability to disrupt existing angiogenic tumor vasculature, but also because of their capabilities to induce mitotic arrest of tumor cells and inhibition of angiogenesis [5, 9-11].

Colchicine is currently used clinically in low doses for the treatment of acute gout [12, 13], familial Mediterranean fever (FMF) [14], and dermatologic [15] and auto-inflammatory diseases [16]. However, the utility of colchicine for cancer therapy is currently limited, as only doses close to the maximal tolerated dose (MTD) can induce reduction in tumor blood perfusion leading to a high risk for toxicity [17, 18].

A potential strategy for improving the therapeutic index of colchicine, i.e. limiting the side effects and improving the efficacy, may be the employment of a colloidal drug delivery system, such as long-circulating liposomes [19, 20]. Advantages associated with the use of long-circulating liposomes include their prolonged circulation kinetics, their passive targeting properties, as well as the possibility to encapsulate both hydrophobic and hydrophilic drugs [21]. However, it remains a challenge to formulate long-circulating liposomes that allow the retention of drugs with moderate lipophilicity, such as colchicinoids, while enabling appropriate release kinetics once accumulated in the target site [22]. Colchicinoids localize mainly in the lipid bilayer and leak out readily, which makes it troublesome to control their retention and release rate [23, 24]. A

potential way to overcome this challenge is to make use of prodrugs, which are (inactive) bioreversible derivatives of the active drug but often possess different physicochemical properties than the parent compound [22]. After enzymatic and/or chemical conversion of the prodrug, the parent molecule with its original pharmacological activity is recovered [25]. If the prodrug is designed to be very hydrophilic, it may be encapsulated solely in the aqueous core of liposomes, thereby limiting its diffusion over the lipid bilayer. Only upon conversion of the prodrug in the aqueous interior, the parent drug molecule, in this case the colchicinoid, may be released from the liposome by its ability to diffuse over the lipid bilayer. A useful method for developing hydrophilic prodrugs of small molecular weight drugs is the conjugation with poly(ethylene glycol) (PEG). PEG has high aqueous solubility, it is non-toxic, non-immunogenic and non-antigenic [26, 27]. In addition, by utilizing a PEG-linker that is susceptible to hydrolysis, PEGylated prodrugs that can be cleaved in the liposomal interior are created. The molecular structure of the linker can influence the rate of hydrolysis, and therefore, by employing different linkers, the rate of conversion to the active drug can be controlled [28].

In the current study, two PEGylated colchicinoid prodrugs were synthesized and encapsulated into long-circulating liposomes. The presented strategy allows retention of the colchicinoids - in their prodrug form - in the aqueous core of the liposomes, and at the

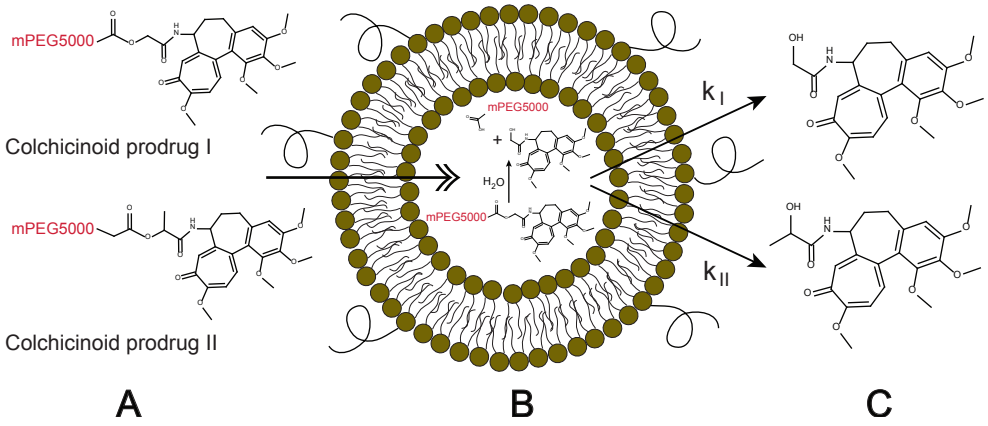

Figure 1. Schematic outline of the liposomal colchicine-derived prodrug strategy. PEGylated colchicine-derived prodrugs with different hydrolysis kinetics are synthesized by using different biodegradable PEG-linkers (A). These colchicinoid prodrugs are encapsulated into long-circulating liposomes (B). Upon hydrolysis of prodrug I or II in the aqueous core of the liposomes, the pharmacologically active parent is released from the liposomes with rate k_I and k_{II} ($k_I > k_{II}$), respectively (C).

same time enables release of the cleaved prodrug from the liposome, at a rate that can be tailored by adjustment of the hydrolysis kinetics (Figure 1). The hydrolysis rate is controlled by using a hydrolysable PEG-linker based on a primary alcohol, which is more prone hydrolysis, or a linker based on a secondary alcohol, which is more resistant to hydrolysis. Since colchicinoids are able to pass the lipid bilayer, the release rate of colchicinoid from the liposome is directly related to the cleavage rate of the colchicinoid prodrug. Obviously, the release kinetics of colchicinoids from the liposomes, once they have accumulated in the tumor, is a critical determinant for therapeutic activity. Therefore, a tailorable drug delivery system for colchicine derivates may prove of great value for improving the therapeutic index of colchicinoids in the therapy of solid tumors.

2. Materials and Methods

2.1. Materials

1,2-Distearoyl-*sn*-glycero-3-phosphoethanolamine-*N*-[methoxy(polyethylene glycol)-2000] (DSPE-PEG_{2000}) and dipalmitoylphosphatidylcholine (DPPC) were provided by Lipoid (Germany). All other chemicals were ordered from Sigma-Aldrich (Germany) and used without further purification. Phosphate buffered saline (PBS) with pH 7.4 was purchased from B. Braun (The Netherlands). Solvents were obtained from Biosolve (The Netherlands) and used without distillation. Acetonitrile and dichloromethane were stored on molecular sieves prior to use (3 and 4 Å, respectively). All reactions were performed without direct lighting and with flasks covered in aluminum foil to prevent degradation of colchicine. Flash chromatography was performed using silica gel of 0.035-0.070 mm 60 Å mesh (Acros Organics, Belgium). TLC analysis was performed using plastic backed silica 60 F_{254} plates (Merck, Germany) and NMR spectra were recorded on a Varian Gemini 300 MHz spectrometer. ESI mass analysis was performed on a Shimadzu LCMS-QP8000 single quadrupole spectrometer in positive ionization mode.

2.2. Synthesis of N-Boc-colchicine (2)

Colchicine (**1**, 4.9 g, 12.3 mmol) and DMAP (1.5 g, 12.5 mmol) were dissolved in acetonitrile (50 mL). Subsequently Boc_2O (17.4 g, 79.7 mmol), dissolved in acetonitrile (50 mL), and dry Et_3N (3 mL, 21.5 mmol) were added. The reaction mixture was refluxed for 1.5 h after which additional Boc_2O was added (1.6 g, 7.3 mmol) and stirred at RT for

an additional 2 h.

The reaction mixture was concentrated *in vacuo* and re-dissolved in chloroform. The chloroform was extracted three times with saturated aqueous citric acid (pH 2), and the aqueous fractions extracted again with chloroform. The combined organic extracts were washed with brine and dried over $MgSO_4$. After flash chromatography in ethylacetate/acetone 4:1, **2** was obtained as a brownish yellow solid (3.52 g, 57%).

TLC: R_f = 0.35 in EtOAc/acetone 4:1

^{1}H NMR (300 MHz, $CDCl_3$) δ 1.58 (s, 9 H), 1.90-2.16 (m, 2 H), 2.28 (s, 3H), 2.44-2.70 (m, 2 H), 3.65 (s, 3 H), 3.89, 3.93, 3.97 (3 x s, 3 x 3 H), 5.14 (dd, 1 H), 6.52 (s, 1 H), 6.77 (d, 1 H, *J* = 10.7 Hz), 7.21 (d, 1 H, *J* = 10.7 Hz), 7.60 (s, 1 H) ppm.

2.3. Synthesis of N-(Boc-deacetyl)-colchicine (3)

N-Boc-colchicine (**2**, 3.52 g, 7.0 mmol) was dissolved in methanol (40 mL). Sodium methoxide in methanol (9 mL 25% *w*/*v*, ~40 mmol) was added at 4 °C and stirred for 45 min. The reaction was stopped by addition of saturated NH_4Cl solution (40 mL). Excess brine was added and the now cloudy suspension was extracted with Et_2O. After drying over $MgSO_4$ and concentration *in vacuo* a light brown solid was obtained.

The progress of the reaction was followed by NMR (R_f was also 0.35 in EtOAc/acetone 4:1), which showed complete removal of the acetyl group. The product was deemed pure enough and was used directly without further purification.

^{1}H NMR (300 MHz, $CDCl_3$) δ 1.37 (s, 9 H), 1.63-1.70 (m, 1 H), 2.22-2.51 ppm (m, 3 H), 3.65 (s, 3H), 3.89, 3.93, 3.99 (3x s, 9 H), 4.36-4.41 (m, 1 H), 4.95 (d, 1 H, *J* = 7.4 Hz), 6.52 (s, 1 H), 6.81 (d, 1 H, *J* = 10.7 Hz), 7.26 (d, 1 H, *J* = 10.7 Hz), 7.51 (s, 1 H) ppm

2.4. Synthesis of N-deacetyl-colchicine (4)

N-(Boc-deacetyl)-colchicine (**3**) was dissolved in CH_2Cl_2 (40 mL) after which TFA (9 mL) was added. The reaction mixture was stirred for 2 h after which a saturated sodium carbonate solution (pH ~10) was carefully added to quench the reaction. This was extracted twice with CH_2Cl_2 and once with EtOAc. After pooling the organic fractions, drying over $MgSO_4$ and concentration *in vacuo*, a thick brown oil was obtained. After flash chromatography with CH_2Cl_2/MeOH/Et_3N (90:10:0.1 R_f 0.38) and concentration,

4 was obtained as a slightly yellow solid (1.98 g, 79% in two steps).

ESI-MS $[M+Na]^+$ = 380.05, calculated 380.15
$[M+Na+CH3CN]^+$ = 420.90, calculated 421.17
^{1}H NMR (300 MHz, $CDCl_3$) δ 1.56-1.62 (m, 1H + broad S, -NH2, disappeared on D2O addition), 2.26-2.47 (m, 3 H), 3.64 (s, 3 H), 3.64-3.72 (m, 1 H), 3.89 (s, 6 H), 3.98 (s, 3 H), 6.52 (s, 1 H), 6.78 (d, 1 H, *J* = 10.7 Hz), 7.17 (d, 1 H, *J* = 10.7 Hz), 7.73 (s, 1 H) ppm.

2.5. Synthesis of N-(2-hydroxyacetyl)-deacetylcolchicine (5)

N-deacetyl-colchicine (**4**, 250 mg 0.67 mmol), glycolic acid (50 mg, 0.66 mmol), Et_3N (0.3 mL, 2 mmol) and *N*-hydroxysuccinimide (60 mg, 0.5 mmol) were dissolved in CH_2Cl_2 (10 mL). DIC (150 μL, 0.95 mmol) was added and stirred for 16 h. After concentration in vacuo, flash column chromatography was performed using CH_2Cl_2/MeOH (90:10). After filtration in water followed by lyophilization, **5** was obtained as a slightly yellow solid (75 mg, 27%).

TLC: R_f = 0.40 in $CHCl_3$/MeOH/AcOH 90:10:0.1
ESI-MS $[M+Na]^+$ = 438.20, calculated 438.15
^{1}H NMR (300 MHz, $CDCl_3$) δ 1.96-2.58 (4x m, 5 H), 3.64 (s, 3 H), 3.90, 3.93, 3.98 (3x s, 9 H), 4.04-4.20 (m, 2 H), 4.63-4.75 (m, 1 H), 6.54 (s, 1 H), 6.86 (d, 1 H, *J* = 10.7 Hz), 7.33 (d, 1 H, *J* = 10.7 Hz), 7.60 (s + broad s, 2 H) ppm.
^{13}C NMR (300 MHz, $CDCl_3$) δ 30.1, 37.0, 52.0, 56.3, 56.5, 61.6, 61.7, 62.5, 107.6, 113.0, 125.9, 131.3, 134.4, 135.7, 137.1, 141.9, 151.4, 152.0, 153.8, 164.2, 172.8, 179.9 ppm.

2.6. Synthesis of mPEG-acetyl-N-(2-hydroxyacetyl)-deacetylcolchicine ester (prodrug I, 6)

N-(2-hydroxyacetyl)-deacetylcolchicine (**5**, 20 mg, 0.048 mmol), DMAP (15 mg, 0.12 mmol) and $mPEG_{5000}$-acetic acid (210 mg, 0.041 mmol) were dissolved in 5 mL CH_2Cl_2. DIC (15 μL, 0.095 mmol) was added and the reaction mixture was stirred for 16 h at room temp. Next, the reaction mixture was concentrated in vacuo and dissolved in ammonium acetate buffer (3 mL, pH 5.5, 20 mM). This was filtered and separated on a PD-10 column (GE Healthcare, Belgium) equilibrated with the same buffer. After two gel filtrations, no low molecular weight starting material could be detected on TLC ($CHCl_3$/MeOH/AcOH, 90:10:0.1). The PEG-conjugate was precipitated in diethyl ether, collected by centrifugation, and after drying in vacuo, prodrug I (**6**) was obtained as a slightly yellow

solid (120 mg, 52%, composed of a mixture of unreacted mPEG-acetic acid and **6**). The amount of colchicine derivate conjugated to PEG was determined with an UPLC system (Waters) equipped with an Acquity BEH C18 1.7 µm column (2.1×50mm) (Waters) and photodiode array detector (Acquity PDA, Waters) set at 350 nm, using a gradient mobile phase from 5 to 95% acetonitrile in water with trifluoroacetic acid (TFA) as modifier.

2.7. Synthesis of N-(2-hydroxypropionyl)-deacetylcochicine (7)

N-deacetyl-colchicine (**4**, 15 mg, 0.04 mmol), *N*-hydroxysuccinimide (7 mg, 0.06 mmol), DL-lactic acid (5.4 mg, 0.06 mmol) and 10 µL of Et_3N were dissolved in CH_2Cl_2 (3 mL). DCC (12.4 mg, 0.06 mmol) in CH_2Cl_2 (3 mL) was subsequently added and stirred for 16 h. After concentration *in vacuo* the product was purified using flash chromatography in CH_2Cl_2/MeOH 9:1. Further purification with flash chromatography using chloroform/MeOH/Et_3N 91:9:0.2 (R_f = 0.4) yielded **7** as a yellow solid (14 mg, 82%).

ESI-MS $[M]^+$ = 428.10, calculated 428.46
^{1}H NMR (300 MHz, $CDCl_3$) δ = 1.35 (d, 3 H), 1.88-2.59 (4x m, 5 H), 3.62 (s, 3 H), 3.89, 3.93, 3.98 (3 x s, 9 H), 4.22 (q, 1 H), 4.64 (m, 1 H), 6.54 (s, 1H), 6.87 (d, 1 H, *J* = 11.0), 7.32 (d, 1 H, *J* = 10.7), 7.45 (s, 2 x 1H) ppm.
^{13}C NMR (300 MHz, $CDCl_3$) δ 20.8, 30.1, 36.8, 51.8, 56.3, 56.5, 61.4, 61.7, 68.4, 107.6, 113.1, 125.8, 131.2, 134.5, 135.7, 137.0, 141.8, 151.4, 151.9, 153.7, 164.1, 175.6, 179.8 ppm.

2.8. Synthesis of mPEG-propionyl-N-(2-hydroxypropionyl-)-deacetylcolchicine ester (prodrug II, 8)

N-(2-hydroxypropionyl)-deacetylcochicine (**7**, 14 mg, 0.033 mmol), DMAP (15 mg, 0.12 mmol) and $mPEG_{5000}$-propionic acid (210 mg, 0.041 mmol) were dissolved in CH_2Cl_2 (5 mL). DIC (15 µL, 0.095 mmol) was added and stirred for 16 h. The reaction mixture was concentrated *in vacuo*, dissolved in ammonium acetate buffer (pH 5.5, 20 mM), filtered and finally separated on a PD-10 column (GE Healthcare, Belgium) equilibrated with the same buffer. No low molecular weight starting material could be detected by TLC ($CHCl_3$/MeOH/AcOH, 90:10:0.1). After lyophilization, prodrug II (**8**) was obtained as a stringy offwhite solid (153 mg, 67%, composed of a mixture of unreacted mPEG-propionic acid and **8**). The amount of colchicine derivate conjugated to PEG was determined by UPLC, as described in section 2.6.

2.9. In vitro degradation kinetics

The hydrolysis kinetics of the prodrugs were studied at 4 °C and 37 °C in phosphate buffer (20 mM, pH 7.4) for both prodrug I (**6**) and prodrug II (**8**), and at 37 °C in sodium hydrogen carbonate buffer (20 mM, pH 9.0) for prodrug II (**8**). Samples were taken at several time points during 72 h, and stored at -20 °C before analysis. The concentration of both PEGylated and hydrolyzed colchicine-derivatives was determined by UPLC, as described in section 2.6.

2.10. Encapsulation in liposomes

DPPC, DPSE-PEG_{2000} and cholesterol were dissolved in ethanol in a molar ratio of 1.85:0.15:1. Lipid films were formed by rotary evaporation, which were dried further under a nitrogen flow for 30 min. The lipid films were hydrated with solutions of colchicine (40 mg/mL), prodrug I (90 mg/mL) or prodrug II (60 mg/mL) in PBS to form liposomes. The size and polydispersity of the liposomes were decreased by repeated extrusions using an extruder (LIPEX, Northern Lipids Inc, Canada) equipped with polycarbonate filters with pore sizes of 200 nm and 100 nm (Whatman, USA). Colchicine and prodrugs not encapsulated into the liposomes was removed by ultracentrifugation (Beckman Coulter, The Netherlands) for 45 min at 250.000 g. After resuspending the liposome pellet in PBS, the particle size and size distribution were measured by dynamic light scattering using a Malvern ALV CGS-3 (Malvern Instruments, UK). The concentration of colchicine and colchicine derived prodrugs in the liposome dispersions was determined by UPLC, as described in section 2.6.

2.11. In vitro release kinetics

The *in vitro* release kinetics of colchicine and colchicine derived (pro)drugs from long-circulating liposomes were determined by dialysis of the liposome formulations against PBS at 4 °C and 37 °C. 1 mL of liposome dispersion was added to a Slide-A-Lyzer Cassette (Thermo Scientific, USA) with a molecular weight cut-off of 10 kDa, which was dialyzed against 200 mL of PBS. Samples were taken from the dialysate at several time points during 72 h, and stored at -20 °C before measurement by UPLC, as described in section 2.6.

2.12. Data analysis

The hydrolysis and liposomal release data were analysed using Graphpad Prism v5.03 (Graphpad Software Inc, USA). LogP calculations were performed with MarvinSketch 5.3.2 (ChemAxon Ltd, Hungary).

3. Results and Discussion

3.1. Synthesis of colchicine-derived prodrugs

Two novel types of PEGylated colchicine-derived prodrugs were synthesized following the scheme depicted in Figure 2. Since colchicine lacks functional groups suitable for conjugating PEG, derivatives were synthesized and modified at the acetamide moiety at the B-ring of colchicine, which is not part of the pharmacophore and not essential for its tubulin binding activity [7, 29]. Earlier studies have shown that modification at this site indeed does not result in a loss of activity, provided that the modification does not cause too much steric hindrance [30-32]. The *N*-acetyl moiety of colchicine was substituted with an *N*-2-hydroxyacetyl- or *N*-2-hydroxypropionyl moiety, which are both suitable for esterification (Figure 2). These colchicinoids (**5** and **7**) were synthesized in two steps, monitored by ESI-MS and NMR. First, the acetamide moiety of colchicine (1) was protected (2), deacetylated (3) and deprotected (4), with a final yield of 40%, using a strategy based on earlier reported methodology (Figure 2, phase I) [30, 32].

Then, the obtained deacetylcolchicine was re-acylated with glycolic acid (**5**, yield 27%) and lactic acid (**7**, yield 82%), respectively, allowing for conjugation with an acid-functionalized methoxy PEG (Figure 2, phase II). The glycolic acid derivative, also known as colchifoline, has similar tubulin binding properties and toxicity as its parent compound colchicine [33]. Although the synthesis of colchifoline has been described in the literature [34], a more straightforward method for the synthesis of both colchifoline and the related compound 7 is presented here. By using of *N*,*N*'-dicyclohexylcarbodiimide (DCC) instead of acid chlorides in the modification of colchicine, a higher yield of colchicine derivatives could be achieved [35]. Finally, the conjugation of PEG_{5000} by esterification was performed using methoxy PEG-acetic acid to obtain prodrug I (**6**) and methoxy PEG-propionic acid to obtain prodrug II (**8**) (Figure 2, phase III). After conjugation, the product consisted of a mixture of unreacted PEG and colchicine-derived prodrug. The amount of colchicinoid prodrug present in each synthesized product was quantified by UPLC, which was 34%

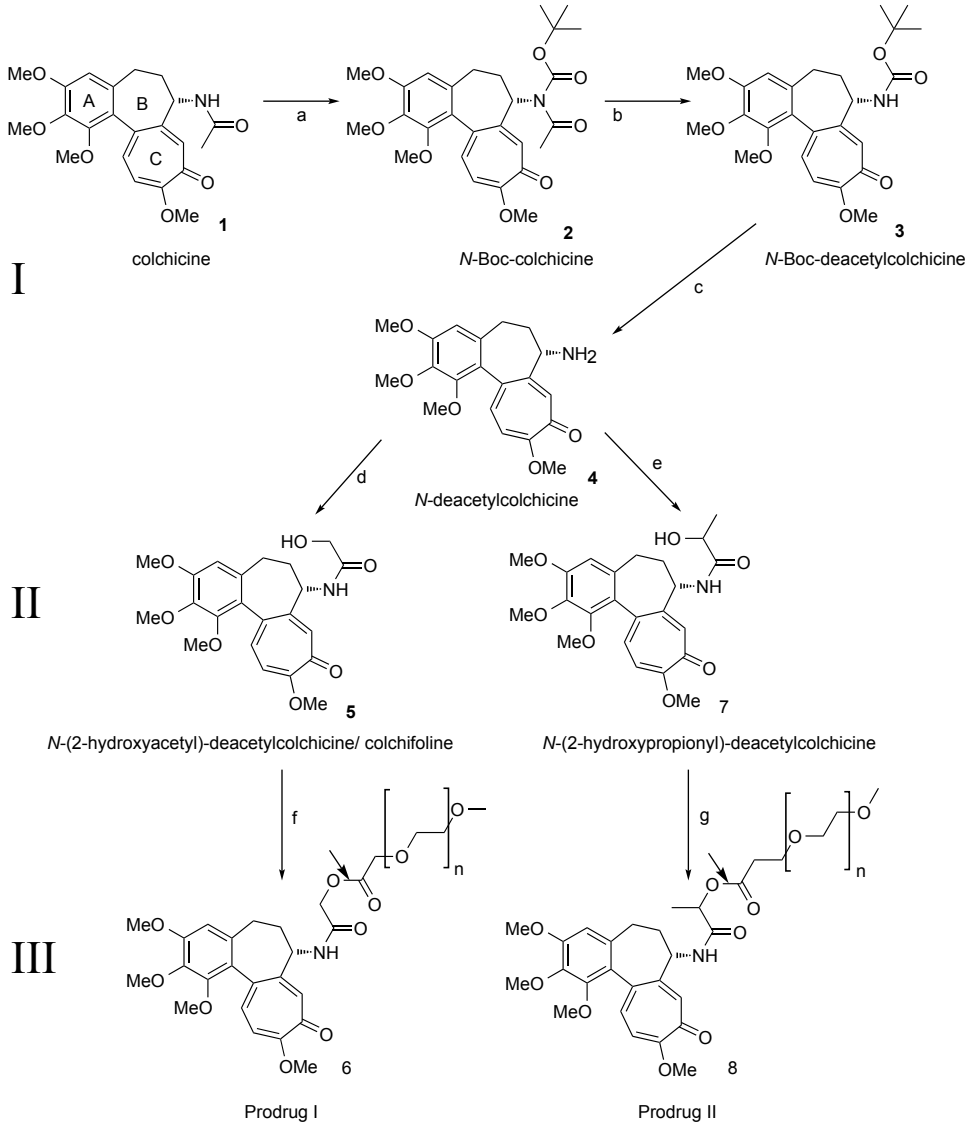

Figure 2. Synthesis of PEGylated colchicine-derived prodrugs. Prodrug I and II are synthesized in three phases. In phase I, colchicine is deacetyled in three steps. First, the acetamide is Bocylated; second, the acetyl group is removed using methoxide; third, the Boc group is removed using TFA, yielding intermediate **4**. In phase II, the deacetylcolchicine is reacted with glycolic acid or lactic acid by carbodiimide coupling to give the hydroxyl-functionalized colchicine derivatives **5** and **7**, respectively. In phase III, the hydroxyl group is conjugated via a hydrolysable ester bond to PEG bearing a carboxyl moiety (indicated by an arrow).

Reagents: a) Boc_2O, DMAP, Et_3N, Acetonitrile; b) NaOMe, MeOH; c) TFA, DCM; d) glycolic acid, DIC, *N*-hydroxysuccinimide, Et_3N, CH_2Cl_2; e) lactic acid, DCC, N-hydroxysuccinimide, Et_3N, CH_2Cl_2; f) $mPEG_{5000}$-CH_2COOH, DIC, DMAP, CH_2Cl_2; g) $mPEG_{5000}$-$(CH_2)_2COOH$, DIC, DMAP, CH_2Cl_2

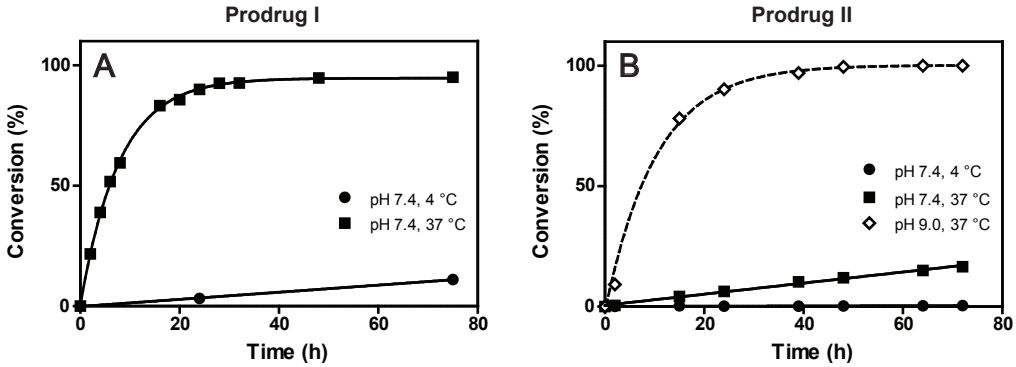

Figure 3. Hydrolysis of PEGylated colchicine-derived prodrugs. The hydrolysis in phosphate buffer of pH 7.4 at 4 °C (●) and 37 °C (■) was measured for both prodrug I (A) and prodrug II (B). For prodrug I, the calculated hydrolysis half-life ($t_{1/2}$) at 4 °C was 14 d (zero-order kinetics, r^2 0.64) and at 37 °C 5.4 h (first-order kinetics, r^2 1.00). For prodrug II in phosphate buffer of pH 7.4 at 4 °C (●), the calculated hydrolysis half-life ($t_{1/2}$) was 500 d (zero-order kinetics, r^2 0.69) and at pH 7.4 at 37 °C (■) it was 9 d (zero-order kinetics, r^2 0.87) . In order to demonstrate the liability of prodrug II to hydrolysis, the hydrolysis was also determined in carbonate buffer of pH 9 at 37 °C (◇), resulting in a calculated hydrolysis half-life of 7.1 h (first-order kinetics, r^2 = 0.99).

(*w/w*) for prodrug I and 74% (*w/w*) for prodrug II.

3.2. In vitro hydrolysis kinetics

It was anticipated that the synthesized PEG-colchicinoids are hydrolyzed at different rates under physiological conditions. The main difference between prodrug I and prodrug II is that prodrug I is an ester of a primary alcohol, which is more prone to hydrolysis than esters of secondary alcohols, such as prodrug II. Additionally, the closer proximity of the ether moiety to the carboxylic end group of the mPEG in prodrug I further influences the degradation rate due to electronic destabilization of the ester bond [28]. Incubation of prodrug I in 20 mM phosphate buffer with pH 7.4 at 37 °C resulted in first-order hydrolysis kinetics with a calculated half-life ($t_{1/2}$) of 5.4 h and degradation of approximately 90% of the total amount after 24 h incubation (Figure 3A). Furthermore, the hydrolysis in PBS at 4 °C appeared to be slow (zero-order kinetics, calculated hydrolysis $t_{1/2}$ = 14 d). Prodrug II was found to be more resistant to hydrolysis at pH 7.4, with a calculated half-life of approximately 9 d at 37 °C and a virtually absent degradation at 4 °C (0.4% after 72 h) (Figure 3B). When the pH was increased to pH 9, to assess the susceptibility of prodrug II to hydrolysis, the calculated half-life at 37 °C dropped to 7.1 h.

3.3. Liposomal encapsulation and release

3.3.1. Liposomes containing colchicine

Colchicine was encapsulated in long-circulating liposomes with a mean particle size of around 100 nm and low polydispersity, using the well-known lipid film hydration method. As expected, due to its physicochemical properties, colchicine was released readily (Figure 4A). This has been observed before [23]. Colchicine has moderate water solubility with a partition coefficient (logP) of around 1.0 [36, 37], and localizes in the lipid bilayer [24]. The rapid release, i.e. 100% within 24h, indicates that colchicine will also leak out of the

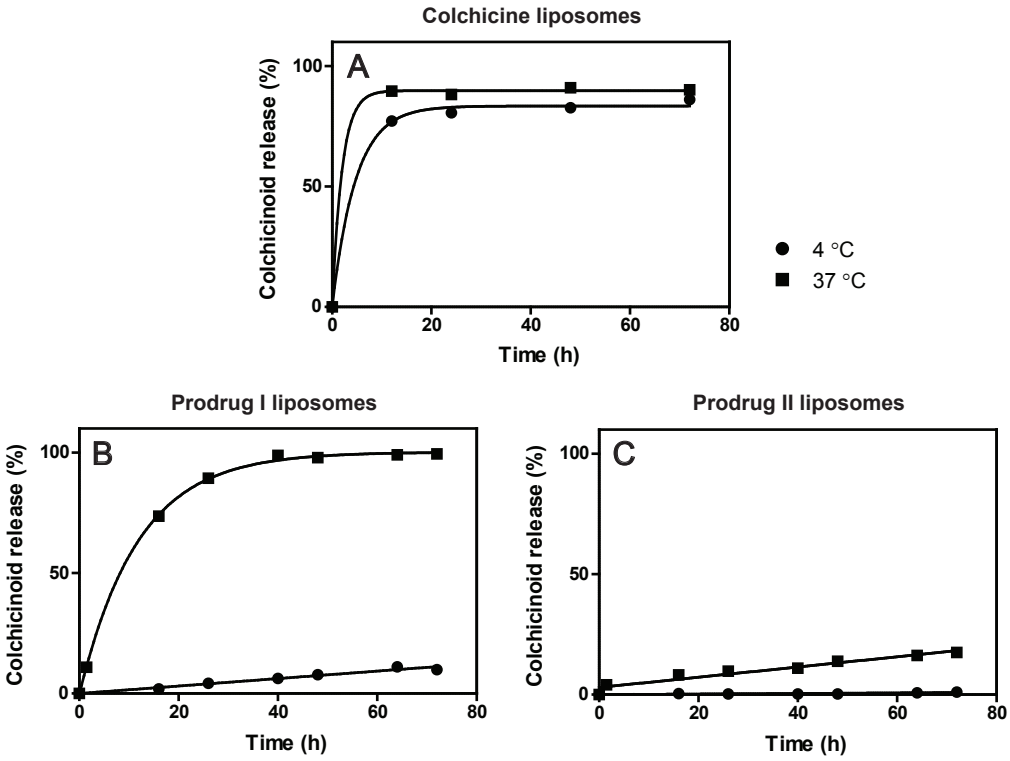

Figure 4. Release of colchicine and colchicine derivatives from long-circulating liposomes. Colchicine and colchicine-derived prodrugs were encapsulated into long-circulating liposomes. Upon dialysis against PBS at 4 °C (●) and 37 °C (■), unmodified colchicine leaked out very rapidly (A). The release kinetics of colchicinoid from liposomes encapsulating prodrug I (B) was more controlled, with slow release at 4 °C (zero-order kinetics, r^2 0.96, release $t_{1/2}$ = 13 d) and faster release at 37 °C (first-order kinetics, r^2 1.00, release $t_{1/2}$ = 8.2 h). The colchicinoid release from liposomes encapsulating prodrug II (C) was much slower: at 4 °C the release was negligible (zero-order kinetics, r^2 0.73, release $t_{1/2}$ = 181 d), while at 37 °C the release was higher (zero-order kinetics, r^2 0.94, release $t_{1/2}$ = 10 d), but still slow as compared to prodrug I.

liposomes when they are circulating in the bloodstream before they reach the target site, making this formulation unsuitable for therapeutic applications.

3.3.2. Liposomes containing colchicine-derived prodrugs

By conjugating colchicine to PEG_{5000} using a biodegradable linker, prodrugs with large molecular weight and high aqueous solubility (calculated logP: -4.44 (prodrug I) and -3.64 (prodrug II)) were obtained. The improved solubility allows encapsulation into the aqueous core of long-circulating liposomes. Both prodrug I and II were entrapped into long-circulating liposomes with a mean diameter of around 100 nm and low polydispersity. At pH 7.4, the two liposomal prodrug formulations showed a release profile of colchicinoid that strongly resembled the hydrolysis kinetics of each prodrug. At 37°C, long-circulating liposomes loaded with prodrug I showed a rapid release of colchicinoid (first-order kinetics, release $t_{1/2}$ = 8.2 h) (Figure 4B), whereas liposomes containing prodrug II released the colchicinoid much slower (zero-order kinetics, release $t_{1/2}$ = 10 d) (Figure 4C). At 4 °C, the release of colchicinoid from liposomes loaded with prodrug I was slow (zero-order kinetics, release $t_{1/2}$ = 13 d), whereas almost no release was observed from liposomes loaded with prodrug II (zero-order kinetics, release $t_{1/2}$ = 181 d). These data demonstrate that the release of colchicinoid is mainly determined by the hydrolysis rate of the prodrug, as both prodrugs have similar physicochemical characteristics as such. The partitioning coefficients of the colchicinoids used for the synthesis of prodrug I and II are similar to that of colchicine (calculated logP: 0.6 and 1.2 respectively), which indicates that these colchicinoids, like colchicine, will be rapidly released from the long-circulating liposomes. Both prodrugs, however, are retained within the aqueous core of the liposomes, and only after cleavage of the PEG chain by hydrolysis of the ester bond, the formed colchicinoid can diffuse over the lipid bilayer. These results demonstrate that by adjusting the PEG-linker, and thus modifying the hydrolysis rate of the colchicine-derived prodrugs, the release rate of colchicinoid from liposomes can be tailored. After i.v. administration, targeted nanomedicines such as liposomes need time to localize passively in the target tissue, and during this period the drug should not be released. On the other hand, there should be efficient drug release after localization in the target area to induce a therapeutic effect. Although the optimal release profile at the target site needs to be established experimentally, the presented prodrug strategy shows that premature leakage in the circulation is prevented.

4. Conclusions

This work demonstrates that the release kinetics of colchicinoids from long-circulating liposomes can be tailored by encapsulating rationally designed PEGylated colchicinoid prodrugs that hydrolyze in the aqueous interior. Two PEGylated colchicine-derived prodrugs were synthesized by substituting the acyl-moiety with a hydroxyl containing moiety to allow for esterification with an acid-functionalized PEG. By employing glycolic or lactic acid to functionalize colchicine, and by using different PEG acids, the hydrolysis rate of the prodrug could be controlled. Both designed prodrugs were retained in liposomes, whereas colchicine leaked out instantaneously. Indeed, the release kinetics of colchicinoids from the liposomal prodrug formulations appeared determined by the hydrolysis rate of the prodrug. Consequently, by using different biodegradable linkers, the release of colchicinoids from long-circulating liposomes can be tailored.

5. Acknowledgements

This work was supported by MediTrans, an Integrated Project funded by the European Commission under the "nanotechnologies and nano-sciences, knowledge-based multifunctional materials and new production processes and devices" (NMP), thematic priority of the Sixth Framework Program.

6. References

[1] P. Carmeliet, R.K. Jain, Angiogenesis in cancer and other diseases, Nature 407(6801) (2000) 249-257.

[2] P. Baluk, H. Hashizume, D.M. McDonald, Cellular abnormalities of blood vessels as targets in cancer, Curr. Opin. Genet. Dev. 15(1) (2005) 102-111.

[3] P.E. Thorpe, Vascular targeting agents as cancer therapeutics, Clin. Cancer Res. 10(2) (2004) 415-427.

[4] C. Kanthou, G.M. Tozer, Tumour targeting by microtubule-depolymerizing vascular disrupting agents, Expert Opin. Ther. Targets 11(11) (2007) 1443-1457.

[5] J.W. Lippert, 3rd, Vascular disrupting agents, Biorg. Med. Chem. 15(2) (2007) 605-615.

[6] G.M. Tozer, C. Kanthou, B.C. Baguley, Disrupting tumour blood vessels, Nat. Rev. Cancer 5(6) (2005) 423-435.

[7] B. Bhattacharyya, D. Panda, S. Gupta, M. Banerjee, Anti-mitotic activity of colchicine and the structural basis for its interaction with tubulin, Med. Res. Rev. 28(1) (2008) 155-183.

[8] R.B.G. Ravelli, B. Gigant, P.A. Curmi, I. Jourdain, S. Lachkar, A. Sobel, M. Knossow, Insight into tubulin regulation from a complex with colchicine and a stathmin-like domain, Nature 428(6979) (2004) 198-202.

[9] M.A. Jordan, L. Wilson, Microtubules as a target for anticancer drugs, Nat. Rev. Cancer 4(4) (2004) 253-265.

[10] E. Pasquier, S. Honore, D. Braguer, Microtubule-targeting agents in angiogenesis: where do we stand?, Drug Resist. Update 9(1-2) (2006) 74-86.

[11] E. Pasquier, M. Kavallaris, Microtubules: a dynamic target in cancer therapy, IUBMB Life 60(3) (2008) 165-170.

[12] M.P. Keith, W.R. Gilliland, Updates in the management of gout, Am. J. Med. 120(3) (2007) 221-224.

[13] D. Petersel, N. Schlesinger, Treatment of acute gout in hospitalized patients, J. Rheumatol. 34(7) (2007) 1566-1568.

[14] C. Cerquaglia, M. Diaco, G. Nucera, M. La Regina, M. Montalto, R. Manna, Pharmacological and clinical basis of treatment of Familial Mediterranean Fever (FMF) with colchicine or analogues: an update, Curr. Drug Targets Inflamm. Allergy 4(1) (2005) 117-124.

[15] R. Bibas, N.K. Gaspar, M. Ramos-e-Silva, Colchicine for dermatologic diseases, J. Drugs Dermatol. 4(2) (2005) 196-204.

[16] R.A. Terkeltaub, Colchicine update: 2008, Semin. Arthritis Rheum. 38(6) (2009) 411-419.

[17] B.C. Baguley, K.M. Holdaway, L.L. Thomsen, L. Zhuang, L.J. Zwi, Inhibition of growth of colon 38 adenocarcinoma by vinblastine and colchicine: evidence for a vascular mechanism, Eur. J. Cancer 27(4) (1991) 482-487.

[18] Y. Nihei, M. Suzuki, A. Okano, T. Tsuji, Y. Akiyama, T. Tsuruo, S. Saito, K. Hori, Y. Sato, Evaluation of antivascular and antimitotic effects of tubulin binding agents in solid tumor therapy, Jap. J. Cancer Res. 90(12) (1999) 1387-1395.

[19] T. Lammers, W.E. Hennink, G. Storm, Tumour-targeted nanomedicines: principles and practice, Br. J. Cancer 99(3) (2008) 392-397.

[20] D.B. Fenske, P.R. Cullis, Liposomal nanomedicines, Expert. Opin. Drug. Deliv. 5(1) (2008) 25-44.
[21] V.P. Torchilin, Recent advances with liposomes as pharmaceutical carriers, Nat. Rev. Drug Discov. 4(2) (2005) 145.
[22] M. Coimbra, B. Isacchi, L. van Bloois, J.S. Torano, A. Ket, X. Wu, F. Broere, J.M. Metselaar, C.J.F. Rijcken, G. Storm, R. Bilia, R.M. Schiffelers, Improving solubility and chemical stability of natural compounds for medicinal use by incorporation into liposomes, Int. J. Pharm. 416(2) (2011) 433-442.
[23] S.B. Kulkarni, M. Singh, G.V. Betageri, Encapsulation, stability and in-vitro release characteristics of liposomal formulations of colchicine, J. Pharm. Pharmacol. 49(5) (1997) 491-495.
[24] S. Mons, F. Veretout, M.F. Carlier, I. Erk, J. Lepault, E. Trudel, C. Salesse, P. Ducray, C. Mioskowski, L. Lebeau, The interaction between lipid derivatives of colchicine and tubulin: Consequences of the interaction of the alkaloid with lipid membranes, BBA-Biomembranes 1468(1-2) (2000) 381-395.
[25] J. Rautio, H. Kumpulainen, T. Heimbach, R. Oliyai, D. Oh, T. Jarvinen, J. Savolainen, Prodrugs: design and clinical applications, Nat. Rev. Drug Discov. 7(3) (2008) 255-270.
[26] S.J. Bell, C.M. Fam, E.A. Chlipala, S.J. Carlson, J.I. Lee, M.S. Rosendahl, D.H. Doherty, G.N. Cox, Enhanced circulating half-life and antitumor activity of a site-specific pegylated interferon-a protein therapeutic, Bioconj. Chem. 19(1) (2007) 299-305.
[27] S. Parveen, S.K. Sahoo, Nanomedicine: clinical applications of polyethylene glycol conjugated proteins and drugs, Clin. Pharmacokinet. 45(10) (2006) 965-988.
[28] M.J. Roberts, M.D. Bentley, J.M. Harris, Chemistry for peptide and protein PEGylation, Adv. Drug Deliv. Rev. 54(4) (2002) 459-476.
[29] T.L. Nguyen, C. McGrath, A.R. Hermone, J.C. Burnett, D.W. Zaharevitz, B.W. Day, P. Wipf, E. Hamel, R. Gussio, A common pharmacophore for a diverse set of colchicine site inhibitors using a structure-based approach, J. Med. Chem. 48(19) (2005) 6107-6116.
[30] J.D. Bagnato, A.L. Eilers, R.A. Horton, C.B. Grissom, Synthesis and characterization of a cobalamin-colchicine conjugate as a novel tumor-targeted cytotoxin, J. Org. Chem. 69(26) (2004) 8987-8996.
[31] K. Bombuwala, T. Kinstle, V. Popik, S.O. Uppal, J.B. Olesen, J. Vina, C.A. Heckman, Colchitaxel, a coupled compound made from microtubule inhibitors colchicine and paclitaxel, Beilstein J. Org. Chem. 2 (2006) 13.
[32] D. Lagnoux, T. Darbre, M.L. Schmitz, J.L. Reymond, Inhibition of mitosis by glycopeptide dendrimer conjugates of colchicine, Chem. Eur. J. 11(13) (2005) 3941-3950.
[33] A. Brossi, P.N. Sharma, L. Atwell, A.E. Jacobson, M.A. Iorio, M. Molinari, C.F. Chignell, Biological effects of modified colchicines. 2. Evaluation of catecholic colchicines, colchifolines, colchicide, and novel N-acyl- and N-aroyldeacetylcolchicines, J. Med. Chem. 26(10) (1983) 1365-1369.
[34] M.A. Iorio, M. Molinari, A. Brossi, Synthesis of colchifoline from deacetylcolchiceine, Can. J. Chem. 59(2) (1981) 283-284.
[35] P.N. Sharma, A. Brossi, J.V. Silverton, C.F. Chignell, Synthesis and binding to tubulin of colchicine spin probes, J. Med. Chem. 27(12) (1984) 1729-1733.

[36] F.R. Quinn, Z. Neiman, J.A. Beisler, Toxicity and quantitative structure-activity relationships of colchicines, J. Med. Chem. 24(5) (1981) 636-639.

[37] J.M. Zamora, H.L. Pearce, W.T. Beck, Physical-chemical properties shared by compounds that modulate multidrug resistance in human leukemic cells, Mol. Pharmacol. 33(4) (1988) 454-462.

6

A polymeric colchicinoid prodrug with reduced toxicity and improved efficacy for vascular disruption in cancer therapy

B.J. Crielaard [1], S. van der Wal [1], T. Lammers [2], H.T. Le [1], W.E. Hennink [1], R.M. Schiffelers [1], G. Storm [1] and M.H.A.M. Fens [1]

1. Department of Pharmaceutics, Utrecht Institute for Pharmaceutical Sciences (UIPS), Utrecht University, Utrecht, The Netherlands
2. Department of Experimental Molecular Imaging, RWTH – Aachen University, Aachen, Germany

Int. J. Nanomedicine 2011:6 2697–2703

Abstract

Colchicinoids are very potent tubulin-binding compounds, which interfere with microtubule formation, giving them strong cytotoxic properties, such as cell mitosis inhibition and induction of microcytoskeleton depolymerization. While this makes them promising vascular disrupting agents (VDAs) in cancer therapy, their dose-limiting toxicity has prevented any clinical application for this purpose. Therefore, colchicinoids are considered attractive lead molecules for the development of novel vascular disrupting nanomedicine. In a previous study, a polymeric colchicinoid prodrug which showed favorable hydrolysis characteristics at physiological conditions was developed. In the current study, this polymeric colchicinoid prodrug was evaluated *in vitro* and *in vivo* for its toxicity and vascular disrupting potential. Cell viability studies with Human Umbilical Vein Endothelial Cells (HUVECs), as an *in vitro* measure for colchicine activity, reflected the degradation kinetics of the prodrug accordingly. *In vivo*, upon intravenous treatment of B16F10 melanoma-bearing mice with colchicine or with the polymeric colchicinoid prodrug, apparent vascular disruption and consequent tumor necrosis was observed for the prodrug, but not for free colchicine at an equivalent dose. Moreover, a five-fold higher dose of the prodrug was well tolerated, indicating reduced toxicity. These findings demonstrate that the polymeric colchicinoid prodrug has a substantially improved efficacy/toxicity ratio compared to that of colchicine, making it a promising VDA for cancer therapy.

1. Introduction

The extract of *Colchicum autumnale*, which is more commonly known as autumn crocus, wild saffron, naked lady, and by several other names, has been used in the therapy of gout for more than 15 centuries [1]. At present, it is still in clinical use for the treatment of gout, as well as several other inflammatory diseases including Familial Mediterranean Fever (FMF) and Behcet's Disease [2, 3]. Colchicine and its colchicinoid derivatives possess the ability to bind irreversibly to tubulin, forming tubulin-colchicine complexes, which hinder microtubule formation and inhibit cell mitosis [2-4]. It has been described that colchicine possesses anti-inflammatory properties, mainly mediated by inhibition of leukocyte adhesion and activity [2, 5]. At higher doses, tubulin-colchicine complexes induce depolymerization of microtubules, resulting in destabilization of the tubulin cytoskeleton [4, 6, 7]. Whereas most cells rely on actin for their cell morphology, endothelial cells of angiogenic tumor vasculature are more dependent on tubulin to maintain their typically enlongated shape [6, 8]. Therefore, upon colchicinoid-induced microtubule depolymerization, the tumor endothelial cells loose their shape, thereby exposing the vascular basement membrane, which subsequently leads to coagulation, decreased perfusion and hemostasis [9, 10]. This process, known as vascular disruption, deprives the surrounding (tumor) cells of oxygen and nutrients, leading to massive tissue necrosis. Currently, however, there is no use for colchicine and colchicinoids in cancer therapy due to their high systemic toxicity [11]. Although in preclinical cancer models doses of colchicine higher than 5 mg/kg induce a significant reduction in the perfusion of tumors, the maximum tolerated dose (MTD) of colchicine is limited to around 1 mg/kg [12, 13]. Even doses below 0.5 mg/kg, as used in the clinical management of gout and FMF, are frequently accompanied by gastrointestinal comorbidity (e.g. nausea, vomiting and diarrhea) and hematologic disorders, such as thrombocytopenia [14]. Colchicine doses higher than 0.5 mg/kg are generally considered toxic, although lower doses may still cause significant side effects, illustrating its narrow therapeutic index. Overdosing of colchicine may eventually lead to multi-organ failure, including bone marrow suppression, hemolysis, liver failure, renal failure, convulsions and cardiac arrest, and is often lethal [14, 15].

One strategy to limit the side effects caused by colchicinoid therapy is to design colchicinoid prodrugs, which only upon conversion possess pharmacological activity

[16]. Colchicinoids have a partition coefficient (logP) of around 1 and a relatively high volume of distribution (±2 L/kg), which implies that upon intravenous injection they immediately redistribute into the tissues, explaining the high risk for side effects [17-19]. Therefore, by creating a colchicinoid prodrug with improved aqueous solubility its volume of distribution is expected to be reduced, confining its distribution to the circulation and the extracellular compartment and lowering its off-target toxicity. Additionally, in order to keep the prodrug in the proximity of its target cells, i.e. the angiogenic endothelial cells, the tissue penetration of the prodrug may be reduced by increasing its molecular weight. Previously, colchicinoid prodrugs based on glycopeptide dendrimers and cobalamin (vitamin B12) have been synthesized and characterized *in vitro* [20, 21]. However, in order to be converted to the active colchicinoid, both conjugates required cellular uptake in the tumor tissue. For exploiting the direct cytotoxic activity of colchicinoids, i.e. the inhibition of tumor cell mitosis, this is a rational approach. For colchicinoid-induced vascular disruption, however, a colchicinoid prodrug that is converted extracellularly, preferably in the proximity of the tumor vascular endothelium, is needed. This may be achieved by utilizing polymer-based colchicinoid prodrugs that are more readily transformed into the active colchicinoid, such as by hydrolysis of an ester bond which allows conversion in aqueous conditions. Previous work reported the synthesis of a hydrophilic colchicinoid prodrug, where colchicine was derivatized and conjugated to poly(ethylene glycol) (PEG) using a linker liable to hydrolysis [22]. The synthesis of nanomedicines by conjugating PEG-chains (PEGylation) to low-molecular-weight drugs increases the hydrophilicity and size of the construct, and shields them from interactions with plasma proteins [23-25]. Upon i.v. injection, instantaneous and random diffusion of the colchicinoid prodrug into cells is impeded by the relatively large PEG moiety, thereby preventing the binding to tubulin and limiting its toxicity. However, due to the enhanced permeability of the imperfect angiogenic vasculature, the nanosized colchicinoid prodrug may be passively targeted to the tumor tissue, where it, promoted by the reductive microenvironment in the tumor tissue, hydrolyzes to the active colchicinoid [26]. In the present study, a polymeric colchicinoid prodrug containing a hydrolysable linker was studied *in vitro* and *in vivo* for its therapeutic potential and toxicity as vascular disrupting agent.

2. Materials and Methods

2.1. Synthesis of polymeric colchicinoid prodrug

Colchicine was derived and conjugated to PEG_{5000} using methodology reported elsewhere (Figure 1) (Chapter 5, [22]). In brief, colchicine was hydroxyl-functionalized by substituting the *N*-acetyl moiety with a *N*-2-hydroxyacetyl moiety. Subsequently, the hydroxyl group was reacted with methoxy PEG-acetic acid to obtain the hydrolysable polymeric colchicinoid prodrug. The amount of colchicine derivative per milligram of material (i.e. colchicine equivalents) was determined by means of Ultra Performance Liquid Chromatography (UPLC) (Waters, USA), using an Acquity BEH C18 1.7 μm column (Waters) and UV detection at 350 nm (Acquity PDA, Waters). The mobile phase consisted of a gradient from 5 to 95% methanol in water (v/v) and trifluoroacetic acid as modifier.

2.2. In vitro hydrolysis study

The hydrolysis kinetics of the colchicinoid prodrug was determined at 4 °C and 37 °C in phosphate buffer (20 mM, pH 7.4). During 72 h, samples were taken at regular time intervals, and stored at -20 °C before analysis. For each time point, the concentration of colchicinoid prodrug and hydrolyzed prodrug were determined by UPLC, using the methodology described in the previous section.

2.3. In vitro cytotoxicity

Human umbilical vein endothelial cells (HUVECs) were grown at 37 °C and 5% CO_2 in angiogenic growth factor rich EGM-2 medium (Lonza, Verviers, Belgium). Cells were seeded in 96 well-plates (1×10^4 cells/well) for 24 h before further treatment. Subsequently, the cells were incubated with colchicine and colchicinoid prodrug at concentrations ranging from 25 nM – 2.5 μM colchicine equivalents. The cytotoxicity of each drug after 6, 24 and 48 h incubation was determined by colorimetric XTT cell viability assay [27].

2.4. In vivo vascular disrupting efficacy of colchicinoid prodrug

All animal experiments were conducted in agreement with the local applicable Dutch law, "Wet op de dierproeven" (art. 9) (1977) and the European Convention for the Protection of Vertebrate Animals used for Experimental and Other Scientific Purposes (1986). The

mice were housed in steel cages, and water and food were provided *ad libitum*. Female pathogen-free C57BL/6 inbred mice of 21-24 g (Charles River, the Netherlands) were subcutaneously inoculated with 1×10^6 B16.F10 cells. 10 days after tumor cell inoculation, when tumor size reached >100 mm^3, PBS, colchicine (1 mg/kg) and the colchicinoid prodrug (1 and 5 mg/kg, colchicine equivalents) were administered intravenously in the tail vein. The mice were sacrificed 4 and 24 h after injection. The tumors were excised, snap frozen in liquid nitrogen and stored at -80 °C upon sectioning.

2.5. Histological evaluation

Frozen tumor samples (n=3/group) were sectioned (5 µm), acetone fixed and H&E stained. Images were taken with an inverted microscope (Nikon TE2000-U) using NIS elements software (Nikon, Japan). Small magnification (10×) overlapping images were taken of the complete tumor area and subsequently stitched together with PhotoFit software.

3. Results and Discussion

Although colchicine is widely recognized as a promising VDA for cancer therapy, its dose-limiting toxicity has prevented it to live up to its potential [11]. Only by dosing colchicine well above its MTD, significant vascular disruption and subsequent necrosis of tumor tissue could be observed [12, 13]. In the present study, a PEG-based polymeric nanomedicine of colchicine was synthesized in order to attenuate systemic toxicity and to enhance its therapeutic index by improving it aqueous solubility. To this end, colchicine was derived and conjugated to PEG_{5000} via a hydrolysable linker (Figure 1). The molecular structure of colchicine was modified at the acetamido moiety, which is not part of the pharmacophore, creating a colchicinoid also known as colchifoline, with similar anti-inflammatory and tubulin-binding activity [7, 28, 29]. Hydrolysis studies at physiological conditions (37 °C, pH 7.4) showed that the half-life of prodrug conversion was approximately 5 h, whereas at low temperature this was calculated by zero-order extrapolation as approximately 14 d (Figure 1).

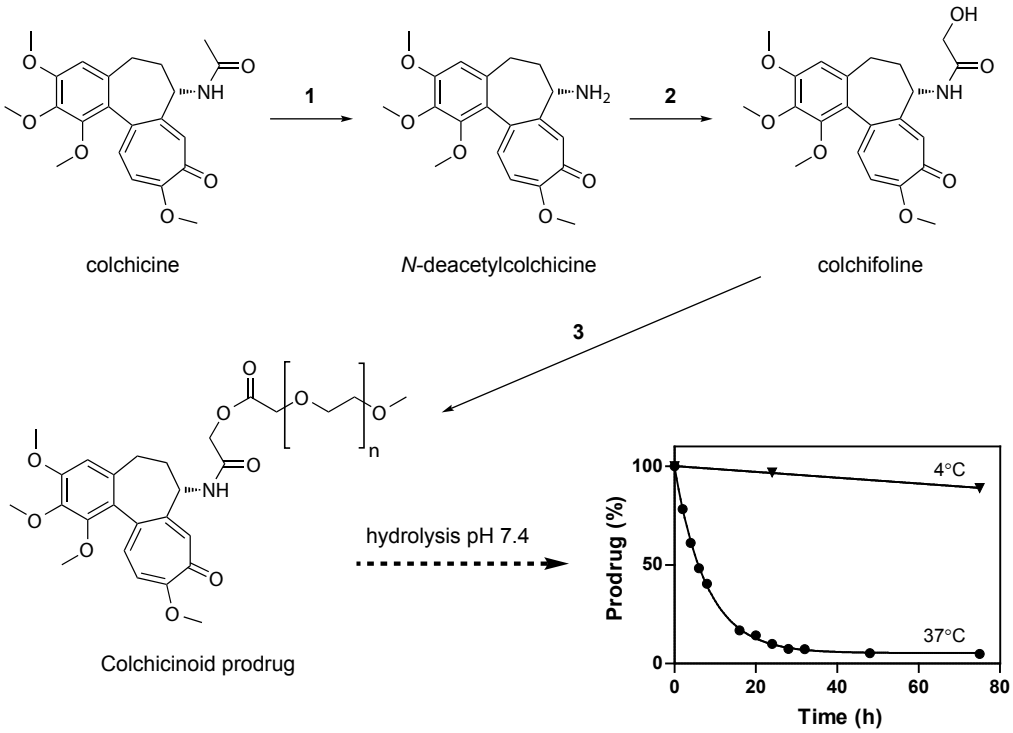

Figure 1. Synthesis and hydrolysis kinetics of colchicinoid prodrug. The synthesis of the colchicinoid prodrug is performed in three steps. (1) Colchicine is deacetylated to obtain *N*-deacetylcolchicine. (2) *N*-deacetylcolchicine is acylated with glycolic acid resulting in a hydroxyl functionalized colchicinoid also known as colchifoline. (3) The colchicinoid is coupled to methoxy PEG_{5000} to form the colchicinoid prodrug. By using esterification to conjugate PEG to the colchicinoid, a prodrug that is hydrolyzable at physiological conditions is created: at 37 °C, the prodrug is cleaved within a day ($t_{1/2}$ 5.4 h), while at 4 °C the hydrolysis rate is limited (calculated $t_{1/2}$ 14 d (zero-order kinetics)).

The conversion rate of the prodrug at physiological conditions correlated with its activity in endothelial cell viability experiments. To investigate the anti-mitotic tubulin-binding capacity as a measure of efficacy, colchicine and the colchicinoid prodrug were incubated at different concentrations (0.025-2.5 μM, colchicine-equivalent) with primary human umbilical vein endothelial cells (HUVECs) (Figure 2). After 6 h of incubation, no or little apparent effects on cell viability were measured for each treatment (two-way ANOVA, $p>0.05$), indicating that several hours of incubation are needed to allow colchicine to interfere with tubulin dynamics. However, after 24 h and 48 h of incubation, HUVEC viability was markedly decreased for both colchicine (dose ≥ 0.025μM, $p<0.001$) and the polymeric colchicinoid prodrug (dose ≥ 0.125μM, $p<0.001$).

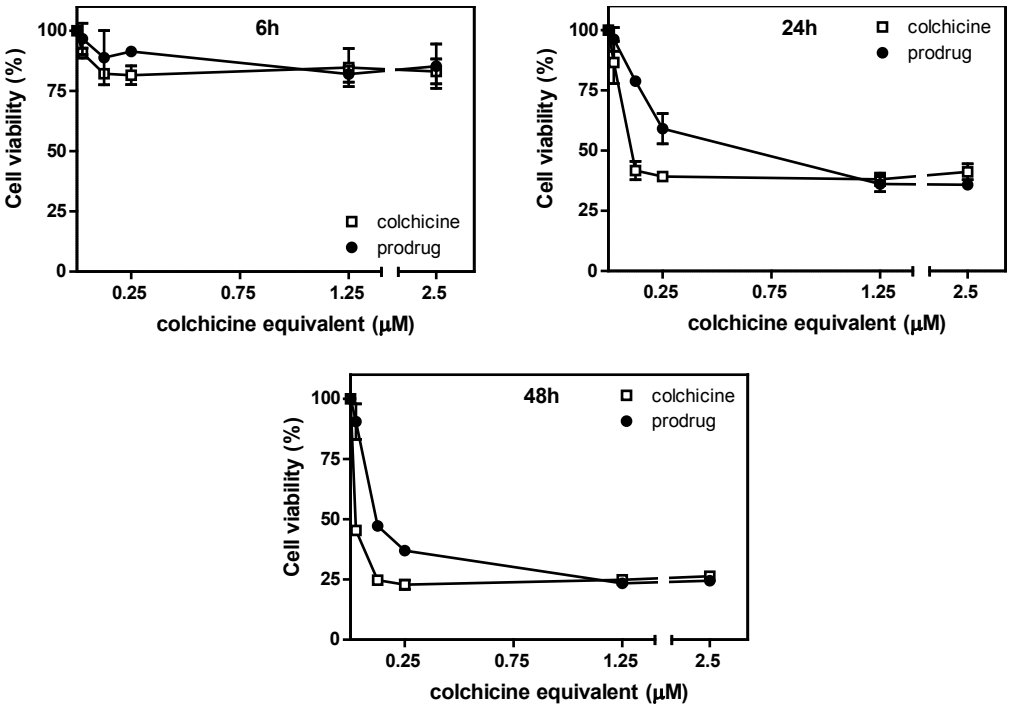

Figure 2. *In vitro* cytotoxicity of colchicine and colchicinoid prodrug. The endothelial cell toxicity of colchicine and the colchicinoid prodrug were determined as measure for their ability to induce damage to angiogenic vasculature. Human umbilical vein endothelial cells (HUVECs) were incubated with colchicine and colchicinoid prodrug at different equivalent concentrations during 6 h, 24 h and 48 h. Subsequently, the cell viability in respect to the untreated cells was determined by XTT assay. Whereas there was only low reduction in cell viability and no difference between the treatments after 6 h of incubation, the colchicinoid prodrug was less cytotoxic than colchicine at 24 h (0.125 and 0.25 μM, $p<0.05$, two-way ANOVA) and 48 h (0.025-0.25 μM, $p<0.05$).

The prodrug, of which >95% is converted after 24 h at 37 °C, showed at the highest doses a similar cytotoxicity when compared with colchicine. However, at lower concentrations the prodrug was less potent than colchicine after 24 h and 48 h incubation ($p<0.05$, 0.125 and 0.25μM at 24 h; 0.025-0.25μM at 48 h), despite the fact that practically all prodrug has been converted at these timepoints. The lower activity of the prodrug can be explained by the delayed availability of the colchicinoid due to the time needed for conversion of the prodrug.

The *in vivo* efficacy and toxicity of colchicine and the colchicinoid prodrug as VDAs in solid tumors was assessed in mice bearing subcutaneous B16F10 melanoma tumors. In order to study the systemic toxicity, the weight of the mice was determined before and 24

h after intravenous treatment with either colchicine or the prodrug. Approximately 8% of total body weight was lost 24 h after administration of 1 mg/kg colchicine ($p<0.05$ one-tailed paired t-test) (Figure 3). The high loss of body weight at 24 h after treatment with 1 mg/kg colchicine, illustrates the high toxicity of colchicine, which limits the maximum dose to a level considered to be insufficient to result in VDA activity [13]. However, at 1 mg/kg colchicine equivalent dose, the polymeric prodrug did not induce significant weight loss, and only upon administration of a five times higher dose (5 mg/kg), it caused a drop in average body weight similar to that of colchicine at its MTD (12%, $p<0.05$). This much higher tolerability of the prodrug compared to free colchicine may therefore allow for colchicinoid doses more likely to result in vascular disrupting activity.

4 h and 24 h after treatment, the mice were sacrificed, and the tumors were excised, sectioned and stained to examine vascular disruption-induced tissue necrosis. No tumor necrosis was observed 4 h (Figure 4A and B) or 24 h (data not shown) after i.v. injection of PBS or colchicine dosed at its MTD (1 mg/kg). The polymeric colchicinoid prodrug, however, induced tissue necrosis in multiple areas in the tumors 4 h after administration, at colchicine equivalent doses of 1 mg/kg and 5 mg/kg (Figure 4C and D, respectively). A similar extent of necrosis (approximately 50% of total tumor mass) was seen after 24 h in the tumors of mice treated with colchicine equivalents of 1 mg/kg or 5 mg/kg of

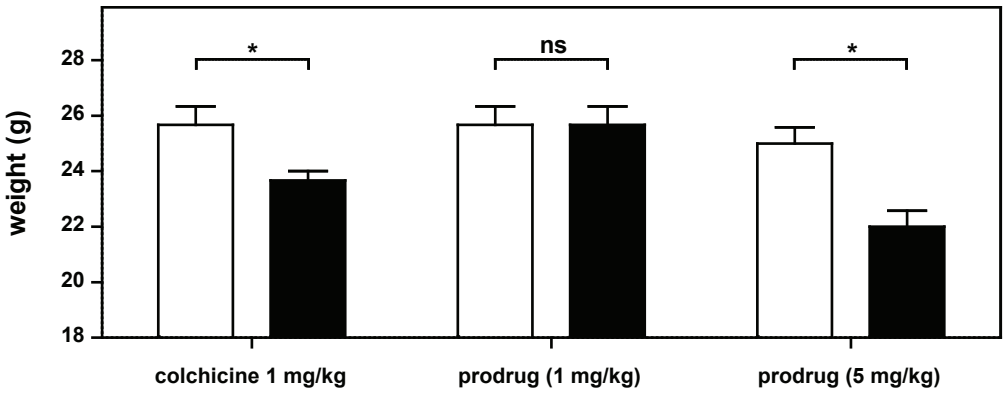

Figure 3. *In vivo* toxicity of colchicine and colchicinoid prodrug: effect on the body weight of mice. To study their *in vivo* toxicity, colchicine (1 mg/kg) and the colchicinoid prodrug (1 mg/kg and 5 mg/kg colchicine equivalents) were intravenously injected into B16F10 melanoma bearing mice. The weight of the mice was measured upon injection (0 h, white bars) and 24 h (black bars) after injection. Significant weight loss was observed for mice treated with 1 mg/kg colchicine (7.7%, $p=0.0371$, one-tailed paired t-test) and 5 mg/kg colchicinoid prodrug (12.0%, $p=0.0175$), but not for mice treated with 1 mg/kg colchicinoid prodrug (0%, $p>0.05$).

colchicinoid prodrug (Figure 4E and F).

Although it has been shown previously for colchicine that i.v. doses of 5 mg/kg or higher are required to induce observable vascular disruption and subsequent necrosis in solid tumors [12, 13], the polymeric colchicinoid prodrug exhibited vascular disrupting efficacy at a much lower dose (1 mg/kg), despite its reduced potency *in vitro*. Polymer-conjugation is a successful strategy in prodrug development that has been employed regularly for improving the aqueous solubility of the parent compound [25]. An improved aqueous solubility changes the tissue distribution, which might explain the potency of the colchicinoid prodrug in relation to colchicine [16]. By employing a PEG-chain larger than

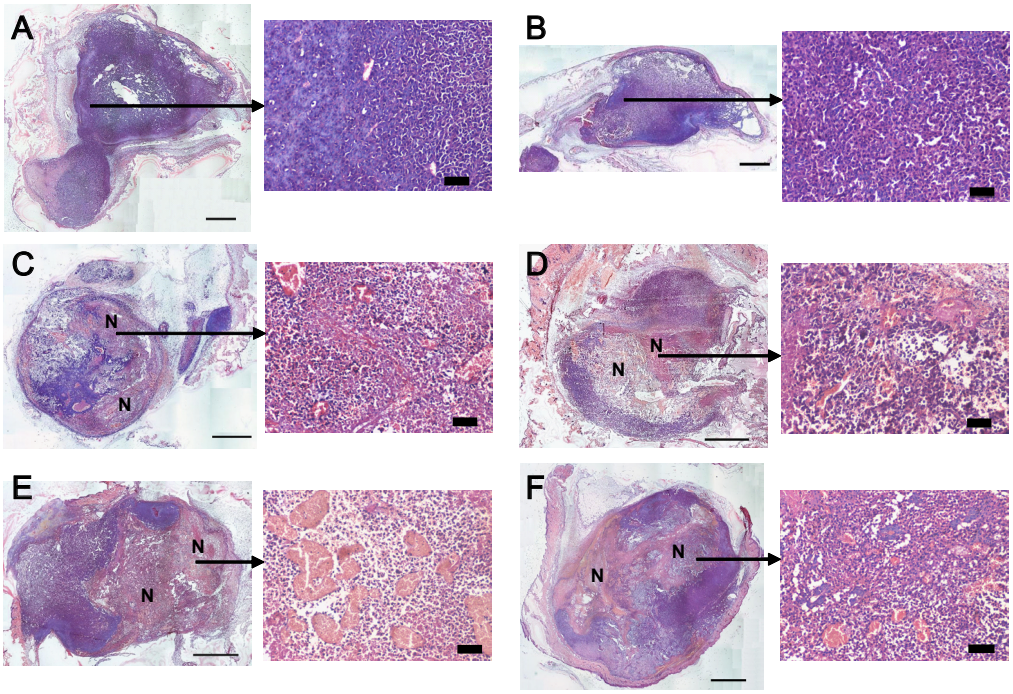

Figure 4. *In vivo* vascular disrupting activity of colchicine and colchicinoid prodrug. To investigate the vascular disrupting activity of colchicine and the colchicinoid prodrug, B16F10 melanoma bearing mice were treated with PBS, colchicine (1 mg/kg) and colchicinoid prodrug (1 mg/kg and 5 mg/kg). The vascular disrupting activity of each treatment was evaluated by histological assessment of tumor tissue necrosis. PBS treated tumors did not show necrosis levels above background (A). 4 hours after injection of 1 mg/kg colchicine tumor sections did not show tumor necrosis levels above control (B). 4 hours after injection of 1 mg/kg (C) or 5 mg/kg (D) of colchicinoid prodrug, areas with congested blood vessels and necrotic cells were observed. 24 h after injection, both 1 mg/kg (E) and 5 mg/kg (F) of the prodrug revealed considerable tumor necrosis. Scale bars of overview images: 1 mm; of magnifications: 50 µm.

35 kDa, or by utilizing colloidal drug delivery systems such as liposomes, a significant decrease in plasma clearance of the colchicinoid prodrug may be achieved, potentially enhancing its *in vivo* efficacy even more [25, 30, 31]. Nevertheless, the vascular disrupting efficacy at a low, non-toxic dose makes the polymeric colchicinoid prodrug presented here a promising VDA for cancer therapy. The observed favorable characteristics of the prodrug *in vivo*, on the one hand, may be related to enhanced accumulation of the prodrug in the tumor tissue mediated by its improved aqueous solubility, limiting its distribution into other tissues and allowing it to penetrate via the 'leaky' immature tumor vasculature [32]. On the other hand, the increased expression and activity of reductive enzymes such as esterases and carboxylesterases in tumor and endothelial cells may augment tumor-specific conversion of the prodrug into the active colchicinoid, and thus improve its efficacy at the target site, while the polymer-conjugation as such limits its toxicity towards other, healthy tissues [26, 33-37].

4. Conclusions

The vascular disrupting efficacy and toxicity of a hydrolysable polymeric colchicinoid prodrug was studied *in vitro* and *in vivo*. The presented data convincingly demonstrate that the rate of hydrolysis of the prodrug at physiological conditions correlates with its reduced *in vitro* efficacy compared to colchicine. *In vivo*, the colchicinoid prodrug was found to be less toxic, while showing higher VDA efficacy than the parent compound, colchicine. Taken together, this study demonstrates the employment of a promising prodrug strategy using a polymeric nanomedicine for improving the vascular disrupting efficacy of colchicinoids while reducing their systemic toxicity, thereby opening the door for the application of these potent VDAs in cancer therapy.

5. Acknowledgements

This work was supported by MediTrans, an Integrated Project funded by the European Commission under the "nanotechnologies and nano-sciences, knowledge-based multifunctional materials and new production processes and devices" (NMP), thematic priority of the Sixth Framework Program.

6. References

[1] E.F. Hartung, History of the use of colchicum and related medicaments in gout, Ann. Rheum. Dis. 13(3) (1954) 190-200.

[2] R.A. Terkeltaub, Colchicine update: 2008, Semin. Arthritis Rheum. 38(6) (2009) 411-419.

[3] E. Ben-Chetrit, M. Levy, Familial Mediterranean fever, The Lancet 351(9103) (1998) 659-664.

[4] R.B.G. Ravelli, B. Gigant, P.A. Curmi, I. Jourdain, S. Lachkar, A. Sobel, M. Knossow, Insight into tubulin regulation from a complex with colchicine and a stathmin-like domain, Nature 428(6979) (2004) 198-202.

[5] E. Niel, J.-M. Scherrmann, Colchicine today, Joint Bone Spine 73(6) (2006) 672-678.

[6] E.L. Schwartz, Antivascular actions of microtubule-binding drugs, Clin. Cancer Res. 15(8) (2009) 2594-2601.

[7] B. Bhattacharyya, D. Panda, S. Gupta, M. Banerjee, Anti-mitotic activity of colchicine and the structural basis for its interaction with tubulin, Med. Res. Rev. 28(1) (2008) 155-183.

[8] E. Pasquier, N. André, D. Braguer, Targeting microtubules to inhibit angiogenesis and disrupt tumour vasculature: implications for cancer treatment, Curr. Cancer Drug Targets 7(6) (2007) 566-581.

[9] G.M. Tozer, C. Kanthou, B.C. Baguley, Disrupting tumour blood vessels, Nat. Rev. Cancer 5(6) (2005) 423-435.

[10] C. Kanthou, G.M. Tozer, Tumour targeting by microtubule-depolymerizing vascular disrupting agents, Expert Opin. Ther. Targets 11(11) (2007) 1443-1457.

[11] M.A. Jordan, L. Wilson, Microtubules as a target for anticancer drugs, Nat. Rev. Cancer 4(4) (2004) 253-265.

[12] B.C. Baguley, K.M. Holdaway, L.L. Thomsen, L. Zhuang, L.J. Zwi, Inhibition of growth of colon 38 adenocarcinoma by vinblastine and colchicine: evidence for a vascular mechanism, Eur. J. Cancer 27(4) (1991) 482-487.

[13] Y. Nihei, M. Suzuki, A. Okano, T. Tsuji, Y. Akiyama, T. Tsuruo, S. Saito, K. Hori, Y. Sato, Evaluation of antivascular and antimitotic effects of tubulin binding agents in solid tumor therapy, Jap. J. Cancer Res. 90(12) (1999) 1387-1395.

[14] Y. Finkelstein, S.E. Aks, J.R. Hutson, D.N. Juurlink, P. Nguyen, G. Dubnov-Raz, U. Pollak, G. Koren, Y. Bentur, Colchicine poisoning: the dark side of an ancient drug, Clin. Toxicol. 48(5) (2010) 407-414.

[15] M. Dickinson, S. Juneja, Haematological toxicity of colchicine, Br. J. Haematol. 146(5) (2009) 465-465.

[16] J. Rautio, H. Kumpulainen, T. Heimbach, R. Oliyai, D. Oh, T. Jarvinen, J. Savolainen, Prodrugs: design and clinical applications, Nat. Rev. Drug Discov. 7(3) (2008) 255-270.

[17] F.R. Quinn, Z. Neiman, J.A. Beisler, Toxicity and quantitative structure-activity relationships of colchicines, J. Med. Chem. 24(5) (1981) 636-639.

[18] J.M. Zamora, H.L. Pearce, W.T. Beck, Physical-chemical properties shared by compounds that modulate multidrug resistance in human leukemic cells, Mol. Pharmacol. 33(4) (1988) 454-462.

[19] S.L. Wallace, B. Omokoku, N.H. Ertel, Colchicine plasma levels: Implications as to pharmacology and mechanism of action, Am. J. Med. 48(4) (1970) 443-448.
[20] J.D. Bagnato, A.L. Eilers, R.A. Horton, C.B. Grissom, Synthesis and characterization of a cobalamin-colchicine conjugate as a novel tumor-targeted cytotoxin, J. Org. Chem. 69(26) (2004) 8987-8996.
[21] D. Lagnoux, T. Darbre, M.L. Schmitz, J.L. Reymond, Inhibition of mitosis by glycopeptide dendrimer conjugates of colchicine, Chem. Eur. J. 11(13) (2005) 3941-3950.
[22] B.J. Crielaard, S. van der Wal, T. Lammers, H.T. Le, W.E. Hennink, R.M. Schiffelers, G. Storm, M.H.A.M. Fens, Liposomes as carriers for colchicine-derived prodrugs: vascular disrupting nanomedicines with tailorable drug release kinetics, Eur. J. Pharm. Sci. 45(4) (2012) 429-435.
[23] S. Parveen, S.K. Sahoo, Nanomedicine: clinical applications of polyethylene glycol conjugated proteins and drugs, Clin. Pharmacokinet. 45(10) (2006) 965-988.
[24] R.B. Greenwald, A. Pendri, D. Bolikal, C.W. Gilbert, Highly water soluble taxol derivatives: 2'-polyethyleneglycol esters as potential prodrugs, Bioorg. Med. Chem. Lett. 4(20) (1994) 2465-2470.
[25] R.B. Greenwald, Y.H. Choe, J. McGuire, C.D. Conover, Effective drug delivery by PEGylated drug conjugates, Adv. Drug Deliv. Rev. 55(2) (2003) 217.
[26] W.A. Denny, Tumor-activated prodrugs - A new approach to cancer therapy, Cancer Invest. 22(4) (2004) 604-619.
[27] D.A. Scudiero, R.H. Shoemaker, K.D. Paull, A. Monks, S. Tierney, T.H. Nofziger, M.J. Currens, D. Seniff, M.R. Boyd, Evaluation of a soluble tetrazolium/formazan assay for cell growth and drug sensitivity in culture using human and other tumor cell lines, Cancer Res. 48(17) (1988) 4827-4833.
[28] A. Brossi, P.N. Sharma, L. Atwell, A.E. Jacobson, M.A. Iorio, M. Molinari, C.F. Chignell, Biological effects of modified colchicines. 2. Evaluation of catecholic colchicines, colchifolines, colchicide, and novel N-acyl- and N-aroyldeacetylcolchicines, J. Med. Chem. 26(10) (1983) 1365-1369.
[29] T.L. Nguyen, C. McGrath, A.R. Hermone, J.C. Burnett, D.W. Zaharevitz, B.W. Day, P. Wipf, E. Hamel, R. Gussio, A common pharmacophore for a diverse set of colchicine site inhibitors using a structure-based approach, J. Med. Chem. 48(19) (2005) 6107-6116.
[30] M.H.A.M. Fens, K.J. Hill, J. Issa, S.E. Ashton, F.R. Westwood, D.C. Blakey, G. Storm, A.J. Ryan, R.M. Schiffelers, Liposomal encapsulation enhances the antitumour efficacy of the vascular disrupting agent ZD6126 in murine B16.F10 melanoma, Br. J. Cancer 99(8) (2008) 1256-1264.
[31] T. Lammers, W.E. Hennink, G. Storm, Tumour-targeted nanomedicines: principles and practice, Br. J. Cancer 99(3) (2008) 392-397.
[32] M.K. Danquah, X.A. Zhang, R.I. Mahato, Extravasation of polymeric nanomedicines across tumor vasculature, Adv. Drug Deliv. Rev. 63(8) (2010) 623-639.
[33] T. Yamada, M. Hosokawa, T. Satoh, I. Moroo, M. Takahashi, H. Akatsu, T. Yamamoto, Immunohistochemistry with an antibody to human liver carboxylesterase in human brain tissues, Brain Res. 658(1-2) (1994) 163-167.

[34] M. Xie, D. Yang, L. Liu, B. Xue, B. Yan, Human and rodent carboxylesterases: Immunorelatedness, overlapping substrate specificity, differential sensitivity to serine enzyme inhibitors, and tumor-related expression, Drug Metab. Disposition 30(5) (2002) 541-547.

[35] M.R. Redinbo, P.M. Potter, Keynote review: Mammalian carboxylesterases: From drug targets to protein therapeutics, Drug Discov. Today 10(5) (2005) 313-325.

[36] T. Satoh, M. Hosokawa, The mammalian carboxylesterases: From molecules to functions, Annu. Rev. Pharmacol. Toxicol. 38(1) (1998) 257-288.

[37] J.A. Crow, K.L. Herring, S. Xie, A. Borazjani, P.M. Potter, M.K. Ross, Inhibition of carboxylesterase activity of THP1 monocytes/macrophages and recombinant human carboxylesterase 1 by oxysterols and fatty acids, Biochimica et Biophysica Acta (BBA) - Molecular and Cell Biology of Lipids 1801(1) (2010) 31-41.

7

Targeted delivery of dexamethasone for rheumatoid arthritis therapy: comparison of different nanocarrier systems

B.J. Crielaard [1], L.D. Quan [2], C.J.F. Rijcken [1,3], W.E. Hennink [1], G. Storm [1], D. Wang [2], T. Lammers [1,4]

1. Department of Pharmaceutics, Utrecht Institute for Pharmaceutical Sciences, Utrecht University, Utrecht, The Netherlands
2. Department of Pharmaceutical Sciences, University of Nebraska Medical Center, Omaha, Nebraska, U.S.A.
3. Cristal Delivery B.V., Utrecht, The Netherlands
4. Department of Experimental Molecular Imaging, RWTH – Aachen University, Aachen, Germany

Manuscript in preparation

Abstract

Previous studies have shown strong therapeutic activity of joint-targeted dexamethasone using arthtrotropic drug delivery systems in several models of rheumatoid arthritis (RA). Dexamethasone encapsulated in long-circulating liposomes, macromolecular polymeric dexamethasone prodrugs, and dexamethasone-loaded core-crosslinked polymeric micelles, are all highly effective in suppressing clinical signs of arthritis compared to the free drug. It is, however, unclear how these systems compare to each other regarding their therapeutic efficacy in RA. The current study deals with the comparison of the anti-arthritic efficacy of three dexamethasone-targeting systems in two preclinical models of arthritis. The selected systems were evaluated at three different single dose levels in the murine collagen antibody-induced arthritis (CAIA) model, and at one single dose level in the adjuvant-induced arthritis (AIA) model in rats. Whereas all systems are highly effective at the highest dose, at lower doses differences in therapeutic efficacy between the systems related to the differences in drug release profile. On the one hand, dexamethasone encapsulated in long-circulating liposomes was the only system that possessed significant therapeutic activity at the lowest dose, but the duration of its effect was not as long-lasting as compared to the other systems. On the other hand, the polymeric dexamethasone-prodrug showed no therapeutic efficacy at doses lower than 10 mg/kg, but its effect prolonged for a longer period of time than that of dexamethasone liposomes. In conclusion, these results demonstrate the value of comparative studies for assessing the differences in therapeutic potential between targeted drug delivery systems for the treatment of arthritis, and likely other disorders.

1. Introduction

Rheumatoid arthritis (RA) is an autoimmune disorder marked by a chronic inflammation of one or several joints, eventually leading to joint destruction and, consequently, disability and chronic pain [1]. Although the pathogenic processes underlying RA are still not elucidated, it is commonly accepted that an endogenous or cross-reactive exogenous antigen is responsible for its initiation [2]. Currently, there is no cure for RA, and present treatments aim to limit disease symptoms and progression. Therefore, the therapeutic strategies used in the clinical management of RA generally aim at limiting joint inflammation and subsequent joint destruction [3]. Ever since the first isolation of cortisone ('compound E') extracted from the adrenal cortex by Edward Kendall in 1936 [4], and its successful application in the therapy of RA and other inflammatory diseases by Philip Hench in the following years [5] (for which they, together with Tadeus Reichstein, received the Nobel prize in Physiology and Medicine in 1950 [6]), glucocorticoids have become an important class of drugs for RA therapy [7, 8]. Since patients using glucocorticoids on a regular basis often experience serious adverse effects, such as cardiovascular complications, Cushing syndrome, osteoporosis and glaucoma [3], active flares of RA may be treated systemically using high doses, a strategy known as pulse therapy [9]. Pulse therapy can result in an effective reduction in disease activity while limiting such chronic side-effects, but, unfortunately, acute adverse effects still occur [10]. In the past, several studies using arthrotropic delivery systems have shown drug targeting to be a valuable strategy for favorably altering glucocorticoid pharmacokinetics and biodistribution, by increasing the drug accumulation in the inflamed joint while reducing its side-effects. For example, dexamethasone, a steroid with strong glucocorticoid activity, encapsulated in (long-circulating) liposomes [11-13], polymeric dexamethasone-prodrugs [14-16], and, more recently, dexamethasone-loaded polymeric micelles [17], were highly effective in reducing active synovial inflammation and preventing joint damage in preclinical models of RA.

Considering the availability of these well-characterized systems for future clinical RA treatment, as well as the continuous development of other (new) systems, there is one apparent clinically relevant question that needs to be answered: which system is the most efficacious? In view of the distinct physiochemical characteristics of each dexamethasone-targeting system, such as particle/molecular size and drug release kinetics, it seems likely

that there are differences in their anti-arthritic potency that only may be revealed when these systems are compared in a single study.

In the current study, the therapeutic effect of targeted dexamethasone associated with long-circulating liposomes, core-crosslinked polymeric micelles, and a polymeric HPMA-dexamethasone conjugate (schematically represented in Figure 1), was evaluated in two distinct preclinical models of arthritis: mice with collagen antibody-induced arthritis (CAIA), a relatively acute, reproducible model of joint inflammation, and rats with adjuvant-induced arthritis (AIA), a chronic model that resembles the immunological

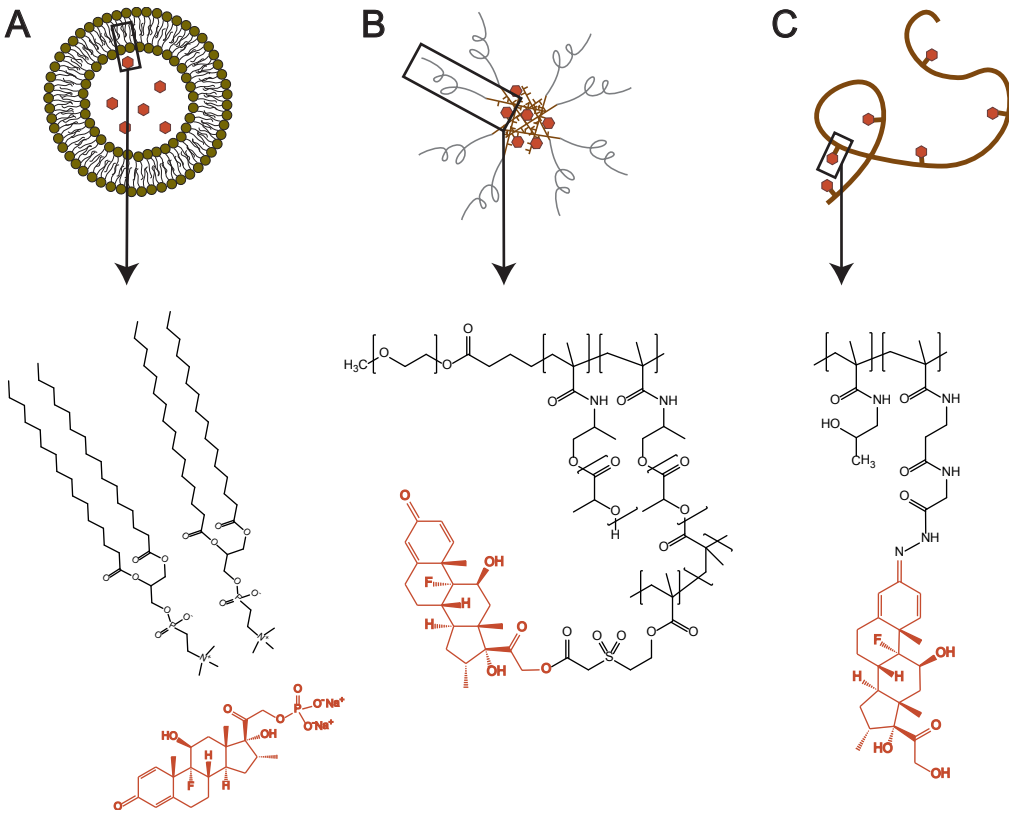

Figure 1. Schematic representation and structure of the evaluated dexamethasone nanocarriers. **A.** Long-circulating liposome (depicted without PEG-coating) encapsulating dexamethasone phosphate (red) in its aqueous core. The dexamethasone prodrug is not conjugated to the liposomal structure, i.e. the phospholipid bilayer. **B.** Dexamethasone-loaded core-crosslinked polymeric micelle. Dexamethasone is covalently entrapped in the hydrophobic core of the polymeric micelle via a sulphone ester-containing linker, allowing hydrolytic release of the drug. **C.** Macromolecular HPMA copolymer-dexamethasone conjugate. Dexamethasone is conjugated to the polymeric HPMA backbone via a hydrazone linkage, enabling hydrolytic release at low pH-conditions.

background of human RA more closely [18-20].

2. Materials and Methods

2.1. Preparation of dexamethasone encapsulating long-circulating liposomes

Liposome-encapsulated dexamethasone (DEX-LCL) was prepared using the lipid film-hydration method. DPPC (Lipoid GmbH, Germany), DSPE-PEG_{2000} (Lipoid) and cholesterol (Sigma Aldrich, Germany) were dissolved in a 1.85:0.15:1 molar ratio in 5-10 mL ethanol. A lipid film was formed in a roundbottom flask by rotary evaporation (Buchi, Switzerland), and dried further under a nitrogen flow. The lipid film was hydrated with a 100 mg/mL solution of dexamethasone phosphate (BUFA, The Netherlands) in reversed osmosis water to form liposomes. The size and polydispersity of the liposomes were reduced by repeated extrusion of the dispersion through two polycarbonate filters with varying pore sizes (Whatman, USA) mounted in an LIPEX extruder (Northern Lipids Inc, Canada). Unencapsulated dexamethasone was removed by dialysis against PBS at 4 °C for 48 h. The dexamethasone concentration in the liposomal dispersion was measured, upon extraction of the aqueous phase [21], by Ultra Performance Liquid Chromatography (UPLC) (Waters) equipped with an Acquity UPLC BEH C18 column, using acetonitrile/water (1:3) with 0.1% TFA as eluent. Particle size and polydispersity of extruded dispersions was determined by dynamic light scattering using a Malvern ALV CGS-3 (Malvern Instruments). DLS results are given as a z-average particle size diameter and a polydispersity index (PDI), which is expressed on a scale of 0 to 1; 0 meaning complete monodispersity and 1 meaning complete polydispersity. The liposomes had a mean diameter of around 100 nm and a PDI smaller than 0.1.

2.2. Preparation of dexamethasone-loaded core-crosslinked polymeric micelles

Dexamethasone-loaded core crosslinked polymeric micelles (DEX-PM) were prepared as described previously [17]. A polymerizable prodrug of dexamethasone (DMSL-3 [17]) was encapsulated in the hydrophobic core of polymeric micelles, using the heat shock method according to Rijcken et al [22, 23]. In short, one volume of DMSL-3 in ethanol was added to 9 volumes of an ice-cold ammonium acetate buffered (pH 5) solution of poly(ethylene glycol)-*b*-poly(*N*-(2-hydroxypropyl)methacrylamide lactate) (PEG-b-pHPMAmLac$_n$) copolymer with 14% methacrylation (dissolved overnight at 4 °C), KPS and TEMED.

The final concentration of polymer, KPS (Merck, USA), TEMED (Sigma Aldrich, Germany) and DMSL-3 (DEX equivalents) was 20, 1.35, 3 and 2 mg/mL, respectively. Subsequently, by rapid heating to 50 °C while stirring vigorously during 1 min, polymeric micelles were formed. The micelles were covalently stabilized by radical polymerization of the methacrylated polymer side chains present in the micellar core in a N_2-atmosphere for 1 h at RT, and as a result of copolymerization of DMSL-3 during crosslinking, DEX-loaded core-crosslinked polymeric micelles were obtained. Finally, the polymeric micelles were filtered with a 0.2 μm filter to remove aggregated encapsulated drug. The amount of dexamethasone entrapped in the micellar formulation was determined by UPLC upon hydrolysis of the ester bonds at pH 9.4, which was considered complete when a plateau in the dexamethasone concentration was reached [17]. The resulting concentration of dexamethasone was 1.6 mg/mL, which corresponded to an encapsulation efficiency of 80%. The diameter of the polymeric micelles, as determined by DLS, was approximately 70 nm, with a PDI of around 0.1.

2.3. Preparation of polymeric HPMA-dexamethasone prodrug

The polymeric HPMA-dexamethasone prodrug (P-DEX) was synthesized and characterized as described previously [14]. *N*-(2-hydroxypropyl)methacrylamide (HPMA) and acid-cleavable *N*-methacryloylglycylgycyl hydrazonyl dexamethasone-prodrug (MA-Gly-Gly-NHN=Dex) were copolymerized by RAFT polymerization at 50 °C for two days. Upon purification and lyophilization of the final product, P-DEX of MW 36,000 Da and PDI 1.4, as determined by fast protein liquid chromatography (FPLC), was obtained. The amount of DEX present in the polymeric prodrug was determined using HPLC, and was found to be 96 mg/g of copolymer.

2.4. Therapeutic efficacy of targeted dexamethasone in mice with collagen antibody-induced arthritis

All animal experiments were conducted in compliance with the local applicable Dutch law, "Wet op de dierproeven" (art. 9) (1977), and were approved by the ethical committee for animal experimentation. 6 month old male DBA/1 mice were obtained from Janvier (France). The mice were housed in groups of 7 animals, exposed to a 12 h light/dark cycle, with *ad libitum* access to standard dietary pellets for rodents (801730 CRM (E) Expanded, Special Diets Services, England) and tap water.

Table 1. Scoring system for clinical symptoms of arthritis in mice with CAIA [19]

Clinical symptoms	Score
Normal	0
Mild redness, slight swelling of ankle or wrist	1
Moderate swelling of ankle or wrist	2
Severe swelling, including some digits, ankle or foot	3
Maximally inflamed	4

Collagen antibody-induced arthritis (CAIA) was induced using a pre-optimized protocol as suggested by the supplier of the antibody cocktail (Chondrex, USA). On day 0, each mouse was injected intravenously (i.v.) with 150 µL of 10 mg/mL antibody cocktail. Subsequently, 100 µL of 0.5 mg/mL of lipopolysaccharide from *E. coli* 0111:B4 was administered on day 3 by intraperitoneal (i.p.) injection. On day 5, the mice were treated i.v. with PBS, free dexamethasone phosphate (DEX), DEX-LCL, DEX-PM or P-DEX at different doses (1, 5 or 10 mg/kg). Treatment groups consisted of 6-7 mice, and 5 untreated mice without CAIA served as healthy controls. All mice were monitored daily for clinical signs of arthritis from day 4, using a scoring system described by Khachigian [19]. Each limb received a score from 0-4 based on the severity of the inflammation using the scoring system depicted in Table 1, which were summed to obtain the arthritis score. Additionally, to assess the inflammatory swelling of the joints, the diameters of both ankles of each mouse were measured daily using a digital caliper.

2.5. Therapeutic efficacy of targeted dexamethasone in rats with adjuvant-induced arthritis

All animal experiments were performed using a protocol approved by the University of Nebraska Medical Center Institutional Care and Use Committee in accordance with Principles of Laboratory Animal Care [24]. Arthritis was induced by subcutaneous injection of 1 mg *Mycobacterium tuberculosis* H37Ra and 5 mg *N*,*N*-dioctadecyl-*N*',*N*'-bis(2-hydroxyethyl)-1,3-propanediamine (LA, prepared as described in [25]) mixed in 100 µL paraffin oil. On day 15, rats with established AIA were treated with PBS or 10 mg/kg DEX, DEX-LCL, DEX-PM or P-DEX (n=7). One group of 6 rats without AIA served as healthy control. Clinical symptoms of joint inflammation were assessed and scored for

Table 2. Scoring system for clinical symptoms of arthritis in rats with AIA [14]

Clinical symptoms	Score
Normal	0
Slight swelling and/or erythema	1
Low-to-moderate edema and signs involving the tarsals	2
Pronounced edema with limited use of the joint and signs extending to the metatarsals	3
Excessive edema with joint rigidity and severe signs involving the entire hind paw	4

both hind paws of each rat, using the scoring system presented in Table 2, which were summed to obtain the arthritis score. From day 8, the arthritis score of all rats was assessed daily, and the medial to lateral ankle diameter was determined using a digital caliper, as a measure of inflammatory swelling.

2.6. Statistical analysis

All statistical analyses were performed using GraphPad Prism software v5.03. Two-way ANOVA analysis (Repeated measures (mixed model) ANOVA) followed by Bonferroni post-testing was used to evaluate the differences between treatments in time. One-way ANOVA in combination with Bonferroni post-testing was used to determine statistical differences in disease loads between treatment groups.

3. Results and Discussion

In the current study, the therapeutic efficacy of three different targeted delivery systems for dexamethasone, i.e. long-circulating liposomes, polymeric micelles and a polymeric prodrug, was assessed in two models of rheumatoid arthritis. The nanocarrier systems were evaluated at low (1 mg/kg), medium (5 mg/kg) and high (10 mg/kg) dose levels for their anti-arthritic efficacy in the murine collagen antibody-induced arthritis (CAIA) model, a fast and reproducible model in which no actual endogenous immunological response is provoked [19]. Additionally, each system was tested at a 10 mg/kg dose for their long-term arthritis reducing activity in the adjuvant-induced arthritis (AIA) model in rats, a model in which there is in fact a cross-reactive endogenous T-lymphocyte mediated immunologic

response against cartilage proteoglycan, resembling human RA more closely [20, 26, 27]. In the CAIA model, at 1 mg/kg dose, long-circulating liposomes containing dexamethasone (DEX-LCL) effectively reduced disease activity in arthritic mice when compared to free DEX ($p<0.01$ on days 7, 8, 9 and 11, two-way ANOVA), while both DEX-loaded polymeric micelles (DEX-PM) and polymeric DEX-prodrug (P-DEX) were ineffective at that dose (Figure 2A). At the medium dose, i.e. 5 mg/kg, the administration of DEX-PM, also, like DEX-LCL, resulted in a strong amelioration of the clinical signs of joint inflammation ($p<0.05$ on days 7-13, and 7-11, respectively), eventually leading to an arthritis score close to zero until the end of the study (Figure 2B). The treatment with

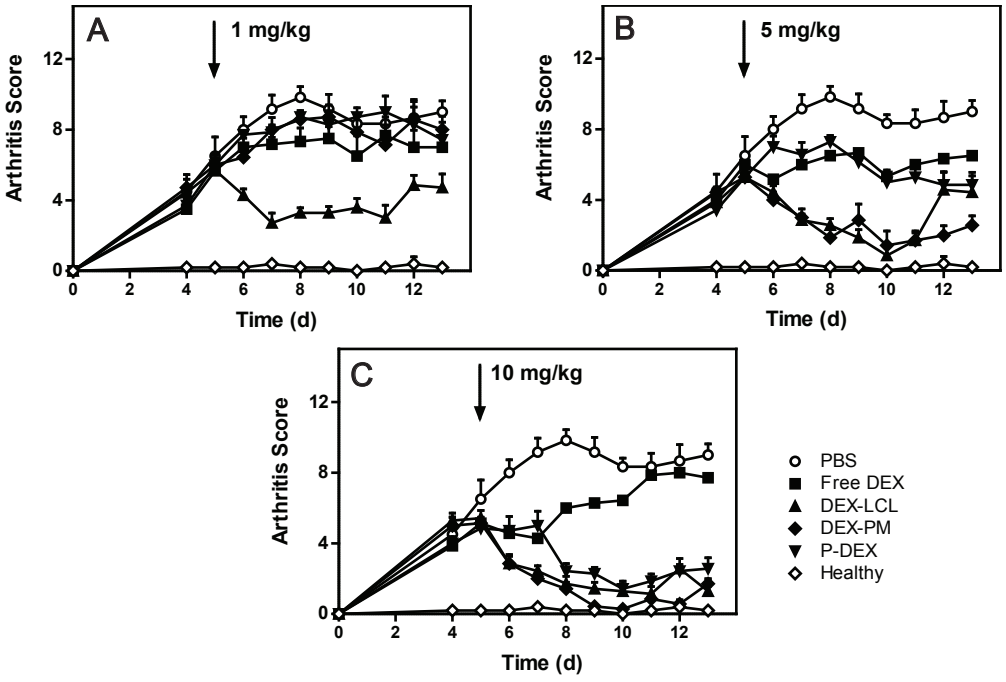

Figure 2. The arthritis score of mice with collagen antibody-induced arthritis (CAIA) upon treatment with free or joint-targeted dexamethasone at three different dose levels, using different targeting systems. Polyarthritis was induced by i.v. injection of a collagen antibody cocktail on day 0, followed by an i.p. administration of LPS on day 3. On day 5 (arrow), when all CAIA-induced animals presented with clear signs of joint inflammation, these mice received a single i.v. administration of free dexamethasone (DEX), dexamethasone phosphate encapsulated in long-circulating liposomes (DEX-LCL), DEX-loaded polymeric micelles (DEX-PM) or polymeric HPMA-dexamethasone prodrug (P-DEX) dosed at 1 mg/kg (A), 5 mg/kg (B), or 10 mg/kg (C) (dexamethasone equivalents). The arthritis score was determined daily using the scoring system presented in Table 1. Control mice received PBS, and one group of mice without CAIA served as healthy controls. The data is presented as the mean score with SEM of each group (n=6-7).

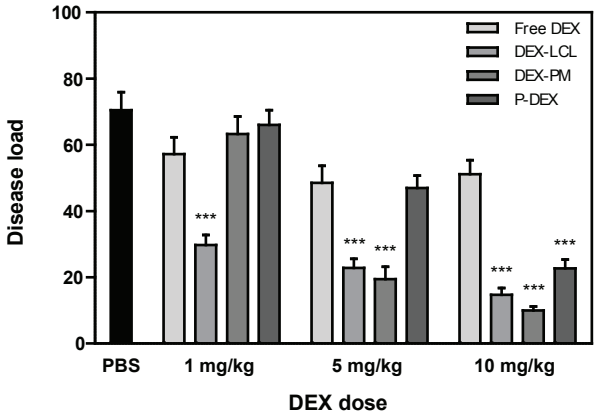

Figure 3. The disease load of mice with CAIA upon treatment with free or joint-targeted dexamethasone at three different dose levels, using different targeting systems. The disease load was defined as the area under the arthritis score curve from treatment (day 5) until the end of the study (day 13). Depicted is the disease load of mice treated with free dexamethasone (DEX), dexamethasone phosphate encapsulated in long-circulating liposome (DEX-LCL), DEX-loaded polymeric micelles (DEX-PM) and polymeric HPMA-dexamethasone prodrug (P-DEX) dosed at 1 mg/kg, 5 mg/kg or 10 mg/kg (dexamethasone equivalents), presented as the mean and SEM of the treatment group (n=6-7). Control animals were injected with PBS. Compared to PBS, the administration of both free and joint-targeted DEX significantly reduced the disease load ($p<0.05$), except for free DEX, DEX-PM and P-DEX dosed at 1 mg/kg. At a 1 mg/kg dose, DEX-LCL was more effective ($p<0.001$) in reducing the disease load than free DEX, DEX-PM and P-DEX. Both DEX-LCL and DEX-PM, dosed at 5 mg/kg, reduced the disease load more ($p<0.001$) than either free DEX or P-DEX at the same dose. At the highest dose, i.e. 10 mg/kg, a significant reduction of mean disease load was reached after treatment with DEX-LCL, DEX-PM or P-DEX, when compared to free DEX. One-way ANOVA followed by Bonferroni's multiple comparison test. ***, $p<0.001$.

P-DEX at this medium dose did not induce an observable reduction in arthritis score when compared to the free drug. Finally, at the highest dose of 10 mg/kg, each system was significantly more effective than the free drug ($p<0.001$ from day 8), illustrated by the drop in arthritis score to values close to that of healthy animals (Figure 2C).

The therapeutic efficacy of the targeted dexamethasone delivery systems on disease activity was supported by the total disease load of the treated arthritic animals (Figure 3). When compared to free DEX at equal doses, the treatment with P-DEX at the highest dose, DEX-PM at a medium or high dose, or DEX-LCL at all tested doses, greatly reduced the disease load of mice with CAIA ($p<0.001$, one-way ANOVA).

Finally, the ankle diameter of all mice was determined upon treatment to evaluate the effect of joint-targeted dexamethasone on inflammatory swelling (Figure 4). Similar to

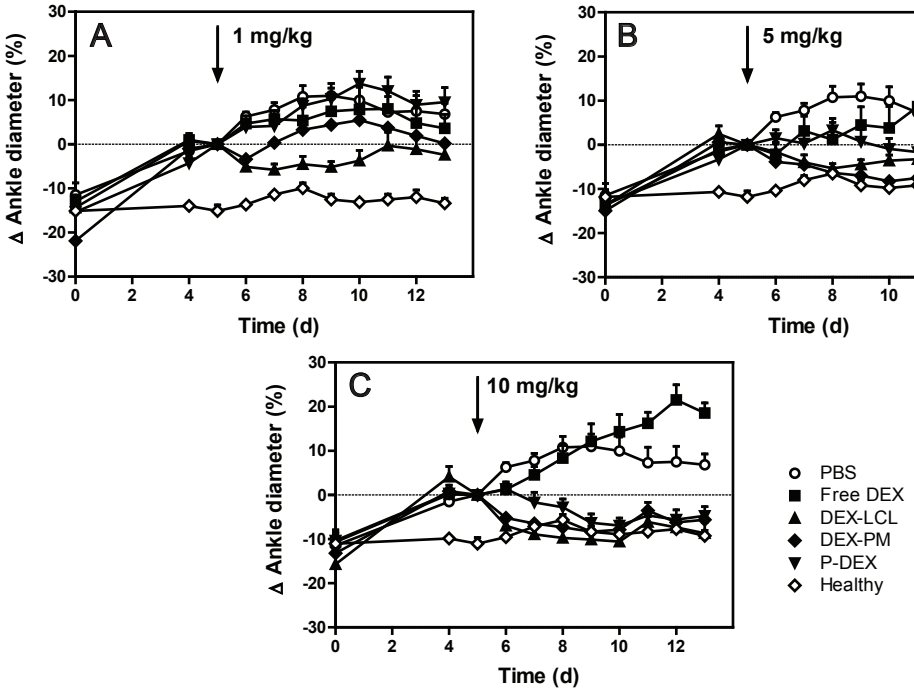

Figure 4. The change in ankle diameter of mice with collagen antibody-induced arthritis (CAIA) upon treatment with free or joint-targeted dexamethasone at three different dose levels, using different targeting systems. Polyarthritis was induced by i.v. injection of a collagen antibody cocktail on day 0, followed by an i.p. administration of LPS on day 3. On day 5 (arrow), when all CAIA-induced animals presented with clear signs of inflammation, these mice received a single i.v. adminstration of free dexamethasone (DEX), dexamethasone phosphate encapsulated in long-circulating liposomes (DEX-LCL), DEX-loaded polymeric micelles (DEX-PM) or polymeric HPMA-dexamethasone prodrug (P-DEX), each dosed at 1 mg/kg (A), 5 mg/kg (B), or 10 mg/kg (C) (dexamethasone equivalents). Control mice received PBS, and one group of mice without CAIA served as healthy controls. The medial to lateral ankle diameter was determined daily using a digital caliper. To evaluate the change in ankle swelling upon treatment, the width on day 5 of mice with CAIA was used as reference measurement (0%). The data is presented as the mean change (%) with SEM of each group (n=6-7).

their therapeutic efficacy towards the clinical arthritis score, the targeted DEX delivery systems influenced the inflammatory joint edema beneficially. Whereas at a 1 mg/kg dose only DEX-LCL was effective in reducing joint swelling ($p<0.05$ on days 9 and 10, compared to free DEX, two-way ANOVA), at the higher doses (5 mg/kg and 10 mg/kg) all three systems showed edema-reducing efficacy superior to that of free dexamethasone at a number of time points after treatment ($p<0.05$).

To demonstrate the therapeutic potential of dexamethasone delivery in a more chronic

preclinical arthritis model with an immunological character more representative for human pathology, the dexamethasone-targeting systems were also evaluated in rats with AIA. When compared with PBS-treated animals, the arthritis score of arthritic rats treated with 10 mg/kg free DEX was reduced during 5 days upon treatment ($p<0.001$ days 17

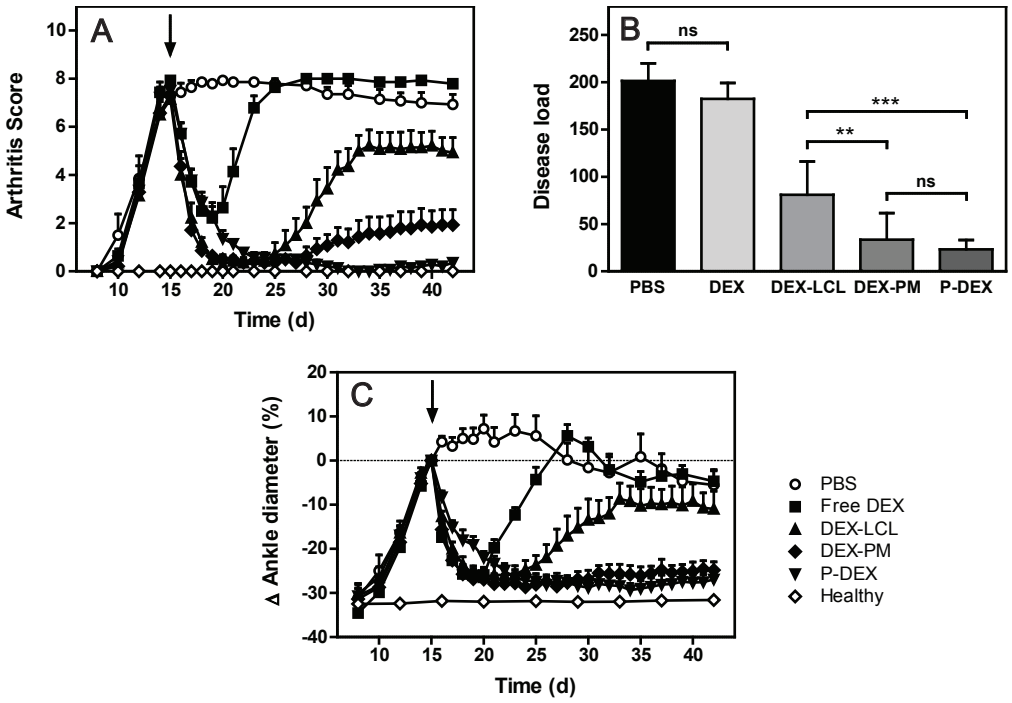

Figure 5. The therapeutic effects of 10 mg/kg targeted dexamethasone in rats with adjuvant-induced arthritis (AIA). Arthritis was induced on day 0 by subcutaneous administration of *Mycobacterium tuberculosis* H37Ra in the base of the tail. On day 15 (arrow), the rats (n=7, all groups) with established arthritis were treated with a single administration of free dexamethasone (DEX), dexamethasone encapsulated in long-circulating liposomes (DEX-LCL), dexamethasone-loaded polymeric micelles (DEX-PM), or polymeric HPMA-dexamethasone prodrugs (P-DEX), all dosed at 10 mg/kg (dexamethasone equivalents). Control rats received PBS, and one group of rats without AIA served as healthy controls. **A.** The arthritis score of all rats (shown as mean with SEM of each group), determined daily using the scoring system presented in Table 2. **B.** The disease load, defined as the area under the arthritis score curve from treatment (day 15) until the end of the study (day 42), of each treatment group (shown as mean with SD). A significant reduction of mean disease load was reached upon treatment with 10 mg/kg DEX-LCL, DEX-PM or P-DEX, when compared to free DEX or PBS ($p<0.001$, one-way ANOVA). The other statistical comparisons between the groups are shown in the graph (***, $p<0.001$; **, $p<0.01$; *, $p<0.05$). **C.** The medial to lateral ankle diameter of all rats (shown as mean with SEM), measured daily using a digital caliper. To evaluate the change in ankle swelling upon treatment, the diameter on day 15 of rats with AIA was used as reference measurement (0%).

to 21, two-way ANOVA), but then returned to a value comparable to that of untreated animals (Figure 5A). In contrast, the administration of either one of the joint-targeted delivery systems resulted in a significant amelioration of clinical signs of arthritis until the end of the study ($p<0.001$, compared to free DEX), leading to arthritis scores similar to that of healthy animals. However, from day 25, i.e. 10 days after treatment, the effect of DEX-LCL started to diminish, while the score of P-DEX-treated rats, as well as that of DEX-PM-treated rats, remained very low during the remainder of the study. From day 29, in case of P-DEX ($p<0.01$ day 29, $p<0.001$ from day 30, two-way ANOVA), and from day 30, in case of DEX-PM ($p<0.01$ day 30, $p<0.001$ from day 31), both polymeric carrier systems were significantly more effective than DEX-LCL. No statistically significant difference between DEX-PM and P-DEX was observed.

The strong therapeutic efficacy of dexamethasone-targeting is also demonstrated when evaluating the disease load of the arthritic rats upon treatment (Figure 5B). A single administration of free DEX did not induce a reduction in long-term disease load (compared to PBS, one-way ANOVA), while the disease load of rats treated with either DEX-LCL, DEX-PM or P-DEX was much lower ($p<0.001$) than that of rats treated with PBS, or DEX. In addition, treatment with DEX-PM or P-DEX was more efficacious in lowering the disease load than DEX-LCL ($p<0.01$ and $p<0.001$, respectively).

Finally, the same trend was observed regarding the therapeutic activity on inflammatory edema of the ankles (Figure 5C). The systemic administration of 10 mg/kg free DEX resulted in a marked, but temporary, decrease in ankle swelling ($p<0.001$ on days 16-23, compared to PBS, two-way ANOVA). In contrast, all dexamethasone delivery systems demonstrated rapid and longer lasting edema-suppressing effects using equivalent doses, which were significantly more effective than the free drug from day 23, i.e. 8 days after treatment ($p<0.01$). While the improved efficacy of DEX-LCL compared to free DEX only lasted until day 30, both DEX-PM and P-DEX where more effective until the end of the study. DEX-PM and P-DEX displayed a similar ankle edema-reducing efficacy, but both systems were more effective than DEX-LCL from day 28 ($p<0.05$).

The observed differences in onset, duration and dose-related therapeutic efficacy of the studied dexamethasone-targeting systems in both models possibly reflect the differences in drug release kinetics, as demonstrated in previous studies, between the carriers [14, 17]. For example, the therapeutic effect of the slow-releasing P-DEX presented itself one (in AIA model) or two days (in CAIA model) later than DEX-LCL and DEX-PM. In

addition, in mice with CAIA, P-DEX was not more efficacious than free DEX at lower doses than 10 mg/kg, while DEX-LCL was already more effective at 1 mg/kg, a 10 times lower dose. However, in the chronic AIA-model in rats, the anti-arthritic effect of P-DEX sustained for a longer period than DEX-LCL. Moreover, the arthritic rats developed diarrhea for 2 days upon treatment with 10 mg/kg free DEX, DEX-LCL, DEX-PM, but not P-DEX, indicating a reduced toxicity profile of P-DEX compared to free DEX, as well as the other targeting systems. While all dexamethasone encapsulated in the aqueous core of liposomes is immediately 'available' once the liposomal bilayer is disrupted (e.g. by degradation in the lysosomes of phagocytic cells), in case of both polymeric systems, the dexamethasone requires to be liberated first, i.e. by hydrolytic cleavage, before it can exert its therapeutic effect. This may also explain why only DEX-LCL is effective at the low 1 mg/kg dose, as in case of the other, slower releasing, systems, there may be an insufficient amount of dexamethasone available to exhibit (observable) anti-arthritic efficacy. When comparing the micellar system with the HPMA-DEX nanocarrier system, the dexamethasone release kinetics of each system is quite different: at pH 7.4 and 37 °C, the polymeric micelles release approximately 40% of their dexamethasone load in a week, whereas the release from the P-DEX at these conditions is negligible [14, 17]. Even when incubated at low-pH conditions (i.e. pH 5.0), to mimic the acidic environment of arthritic joints or that within the cellular lysosomes, the pH sensitive P-DEX demonstrates a relatively slow release profile of around 1% per day. Although the dexamethasone release rate of both DEX-PM and P-DEX is expected to be faster *in vivo* due to the presence of (a)specific enzymatic degradation [28], release rate is most likely a major factor explaining the observed differences between the systems.

To allow detailed evaluation of the therapeutic potential of different drug targeting systems, it is imperative that all these systems are assessed in a single experimental study, since small variations in experimental setup and conditions during *in vivo* efficacy studies make a fair comparison problematic. Remarkably, such a comparative study for targeted delivery systems of glucocorticoids for RA therapy has never been performed before. In fact, to our knowledge, this study is one of the first to evaluate essentially different nanodelivery systems of any therapeutic agent for the treatment of any specific disease.

Possibly because of its large societal impact, as well the good availability of well-characterized preclinical models with clear readout parameters, rheumatoid arthritis is generally the first (and sometimes only) target disease in the development of drug targeting systems

for inflammatory disorders [18, 29]. There are, however, a number of other chronic inflammatory diseases that (could) benefit from a targeted glucocorticoid delivery strategy, including Multiple Sclerosis and Inflammatory Bowel Disease [30]. A comparison of targeted drug delivery systems in preclinical models of these diseases, using a setup similar to the one used in the present study, may provide for valuable information regarding the specific requirements of a successful targeted drug delivery system for treatment of each of these diseases.

Since simple questions often require complicated answers, it is, based on this study, hard to provide an unequivocal answer to the question "which is the delivery system is the most optimal for RA therapy?". For example, on the one hand, during relatively short follow-up in the acute CAIA study, only DEX-LCL was effective at the lowest dose, but all systems were equally effective at the highest. On the other hand, in rats with AIA, the therapeutic activity of P-DEX, but also DEX-PM, sustained for a much longer time than that of DEX-LCL. It is therefore better to stress the heterogeneity between the systems, each having its own merits, rather than claiming superiority of one of them, since, from a patient-perspective, this enables the selection of the optimal dexamethasone-carrier – once regulatory approved – for each specific case of disease. Additional preclinical studies are currently underway to demonstrate long-term effects of each treatment in RA therapy, both on structural and cellular levels. These studies will surely aid in the understanding of the mechanisms determining the efficacy of joint-targeted glucocorticoids, and promote further maturation of targeted delivery systems with clinical potential for the therapy of inflammatory disorders.

4. Conclusions

In the current study, three different targeted drug delivery systems for dexamethasone were evaluated in two preclinical models of rheumatoid arthritis. The previously reported dexamethasone release kinetics of each system appeared to be reflected in the therapeutic profile, illustrating that this comparative study setup may be very useful for assessing the differences in therapeutic activity between several delivery vehicles for the targeting of therapeutic agents to inflammatory diseases.

5. Acknowledgements

This work was supported by MediTrans, an Integrated Project funded by the European Commission under the "nanotechnologies and nano-sciences, knowledge-based multifunctional materials and new production processes and devices" (NMP), thematic priority of the Sixth Framework Program, and NIH grant R01 AR053325.

6. References

[1] L. Carmona, M. Cross, B. Williams, M. Lassere, L. March, Rheumatoid arthritis, Best Pract. Res. Clin. Rheumatol. 24(6) (2010) 733-745.

[2] L. Klareskog, A.I. Catrina, S. Paget, Rheumatoid arthritis, The Lancet 373(9664) (2009) 659-672.

[3] J.N. Hoes, J.W.G. Jacobs, F. Buttgereit, J.W.J. Bijlsma, Current view of glucocorticoid co-therapy with DMARDs in rheumatoid arthritis, Nat. Rev. Rheumatol. 6(12) (2010) 693-702.

[4] E. Kendall, H. Mason, C. Meyers, W. Allers, Physiologic and chemical investigation of the suprarenal cortex, J. Biol. Chem. 114(1) (1936) 57-58.

[5] P. Hench, E. Kendall, C. Slocumb, H. Polley, Effects of cortisone acetate and pituitary ACTH on rheumatoid arthritis, rheumatic fever and certain other conditions: a study in clinical physiology, Arch. Intern. Med. 85(4) (1950) 546-666.

[6] "The Nobel Prize in Physiology or Medicine 1950". Nobelprize.org. 19 Oct 2011 http://www.nobelprize.org/nobel_prizes/medicine/laureates/1950/.

[7] P.C. Gøtzsche, H.K. Johansen, Short-term low-dose corticosteroids vs placebo and nonsteroidal antiinflammatory drugs in rheumatoid arthritis, Cochrane Database Syst. Rev. (1) (2005) Art. No.: CD000189.

[8] J.R. Kirwan, J.W.J. Bijlsma, M. Boers, B. Shea, Effects of glucocorticoids on radiological progression in rheumatoid arthritis, Cochrane Database Syst. Rev.(1) (2007) Art. No.: CD006356.

[9] B. Frediani, P. Falsetti, S. Bisogno, F. Baldi, C. Acciai, G. Filippou, M.R. Bacarelli, P. Filipponi, M. Galeazzi, R. Marcolongo, Effects of high dose methylprednisolone pulse therapy on bone mass and biochemical markers of bone metabolism in patients with active rheumatoid arthritis: a 12-month randomized prospective controlled study, J. Rheumatol. 31(6) (2004) 1083-1087.

[10] B.L.A.M. Weusten, J.W.G. Jacobs, J.W.J. Bijlsma, Corticosteroid pulse therapy in active rheumatoid arthritis, Semin. Arthritis Rheum. 23(3) (1993) 183-192.

[11] R. Anderson, A. Franch, M. Castell, F.J. Perez-Cano, R. Bräuer, D. Pohlers, M. Gajda, A.P. Siskos, T. Katsila, C. Tamvakopoulos, U. Rauchhaus, S. Panzner, R.W. Kinne, Liposomal encapsulation enhances and prolongs the anti-inflammatory effects of water-soluble dexamethasone phosphate in experimental adjuvant arthritis, Arthrit. Res. Ther. 12(4) (2010).

[12] U. Rauchhaus, F. Schwaiger, S. Panzner, Separating therapeutic efficacy from glucocorticoid side-effects in rodent arthritis using novel, liposomal delivery of dexamethasone phosphate: long-term suppression of arthritis facilitates interval treatment, Arthrit. Res. Ther. 11(6) (2009) R190.

[13] J.M. van den Hoven, W. Hofkens, M.H.M. Wauben, J.P.A. Wagenaar-Hilbers, J.H. Beijnen, B. Nuijen, J.M. Metselaar, G. Storm, Optimizing the therapeutic index of liposomal glucocorticoids in experimental arthritis, Int. J. Pharm. 16(2) (2011) 471-477.

[14] X.-M. Liu, L.-D. Quan, J. Tian, Y. Alnouti, K. Fu, G. Thiele, D. Wang, Synthesis and evaluation of a well-defined HPMA copolymer–dexamethasone conjugate for effective treatment of rheumatoid arthritis, Pharm. Res. 25(12) (2008) 2910-2919.

[15] L.-d. Quan, P.E. Purdue, X.-m. Liu, M. Boska, S. Lele, G. Thiele, T. Mikuls, H. Dou, S. Goldring, D. Wang, Development of a macromolecular prodrug for the treatment of inflammatory arthritis: mechanisms involved in arthrotropism and sustained therapeutic efficacy, Arthrit. Res. Ther. 12(5) (2010) R170.

[16] D. Wang, S. Miller, X.-M. Liu, B. Anderson, X.S. Wang, S. Goldring, Novel dexamethasone-HPMA copolymer conjugate and its potential application in treatment of rheumatoid arthritis, Arthrit. Res. Ther. 9(1) (2007) R2.

[17] B.J. Crielaard, L.D. Quan, C.J. Rijcken, M.v.d. Pot, I. Altintas, S.v.d. Wal, R.M. Liskamp, R.M. Schiffelers, W.E. Hennink, C.F. van Nostrum, D. Wang, T. Lammers, G. Storm, Glucocorticoid-loaded core-crosslinked polymeric micelles with tailorable release kinetics for targeted rheumatoid arthritis therapy, Chapter 4 (2012).

[18] M. Hegen, J.C. Keith, M. Collins, C.L. Nickerson-Nutter, Utility of animal models for identification of potential therapeutics for rheumatoid arthritis, Ann. Rheum. Dis. 67(11) (2008) 1505-1515.

[19] L.M. Khachigian, Collagen antibody-induced arthritis, Nat. Protoc. 1(5) (2006) 2512-2516.

[20] W. van Eden, B.H. Waksman, Immune regulation in adjuvant-induced arthritis: possible implications for innovative therapeutic strategies in arthritis, Arthritis Rheum. 48(7) (2003) 1788-1796.

[21] E. Bligh, W. Dyer, A rapid method of total lipid extraction and purification, Can. J. Biochem. Physiol. 37(8) (1959) 911-917.

[22] C.J.F. Rijcken, T.F.J. Veldhuis, A. Ramzi, J.D. Meeldijk, C.F. van Nostrum, W.E. Hennink, Novel fast degradable thermosensitive polymeric micelles based on PEG-block-poly(N-(2-hydroxyethyl)methacrylamide-oligolactates), Biomacromolecules 6(4) (2005) 2343-2351.

[23] C.J.F. Rijcken, C.J. Snel, R.M. Schiffelers, C.F. van Nostrum, W.E. Hennink, Hydrolysable core-crosslinked thermosensitive polymeric micelles: synthesis, characterisation and in vivo studies, Biomaterials 28(36) (2007) 5581-5593.

[24] Guide for the care and use of laboratory animals. NIH Publication No. 85-23. Revised 1985.

[25] T. Cronin, H. Faubl, W. Hoffman, J. Korst, Xylenediamines as antiviral agents. US patent 4,034,040. 1977.

[26] W. van Eden, J.E.R. Tholet, R. van der Zee, A. Noordzij, J.D.A. van Embden, E.J. Hensen, I.R. Cohen, Cloning of the mycobacterial epitope recognized by T lymphocytes in adjuvant arthritis, Nature 331(6152) (1988) 171-173.

[27] J. Holoshitz, Y. Naparstek, A. Ben-Nun, I.R. Cohen, Lines of T Lymphocytes Induce or Vaccinate against Autoimmune Arthritis, Science 219(4580) (1983) 56-58.

[28] A.J.M. D'Souza, E.M. Topp, Release from polymeric prodrugs: Linkages and their degradation, J. Pharm. Sci. 93(8) (2004) 1962-1979.

[29] T.K. Kvien, Epidemiology and burden of illness of rheumatoid arthritis, Pharmacoeconomics 22(2 Suppl.) (2004) 1-12.

[30] B.J. Crielaard, T. Lammers, M.E. Morgan, L. Chaabane, S. Carboni, B. Greco, P. Zaratin, A.D. Kraneveld, G. Storm, Macrophages and liposomes in inflammatory disease: Friends or foes?, Int. J. Pharm. 416(2) (2011) 499-506.

8

An in vitro assay based on surface plasmon resonance to predict the in vivo circulation kinetics of liposomes

B.J. Crielaard [1], A. Yousefi [1], J.P. Schillemans [1], C. Vermehren [2], K. Buyens [3], K. Braeckmans [3], T. Lammers [1,4] and G. Storm [1]

1. Department of Pharmaceutics, Utrecht Institute for Pharmaceutical Sciences (UIPS), Utrecht University, Utrecht, The Netherlands
2. Department of Pharmaceutics, The Danish University of Pharmaceutical Sciences, Copenhagen, Denmark
3. Laboratory of General Biochemistry and Physical Pharmacy, Ghent University, Ghent, Belgium
4. Department of Experimental Molecular Imaging, RWTH – Aachen University, Aachen, Germany

J. Control. Release. 2011 156(3):307-1420;

Abstract

The adsorption of blood proteins onto liposomes and other colloidal particles is an important process influencing the circulation time. Proteins adsorbed to the surface of liposomes can mediate recognition of the liposomes by macrophages of the reticuloendothelial system (RES) facilitating their clearance from the circulation. Coating liposomes with poly(ethylene glycol) (PEG) decreases the blood clearance considerably, most likely due to reduced protein adsorption and/or liposome aggregation. By using the relation between clearance and protein binding, the present study introduces an *in vitro* assay measuring interactions of liposomes with proteins to predict their blood clearance *in vivo*. Such assay is valuable since it limits time and costs, and importantly reduces the number of animals required for pharmacokinetic investigations of new formulations. In the current study, Surface Plasmon Resonance (SPR) and fluorescence Single Particle Tracking (fSPT) were used to study liposome-protein interactions and blood induced liposome aggregation *in vitro*. By means of SPR the interactions between proteins and liposomes coated with PEG of different molecular weights and at different densities (PEG_{2000} in 2.5%, 5% and 7%; PEG_{5000} in 0.5%, 1.5% and 2.5%), were measured for several plasma proteins: human serum albumin (HSA), apolipoprotein E (ApoE), α2-macroglobulin (α2-M), β2-glycoprotein (β2-G) and fibronectin (Fn). Liposomes coated with PEG interacted less with all proteins, an effect which increased with the PEG surface density. In parallel, fSPT analysis showed that the exposure of liposomes to full blood did not change the liposome size, indicating that aggregation is not a strong attributive factor in the clearance of these liposomes. In addition, the SPR measurements of the interactions between liposomes and proteins were correlated with the blood clearance of the liposomes. For each protein, the degree of protein-liposome interaction as determined by SPR showed a moderate to strong positive correlation with the clearance of the liposome type.

1. Introduction

Since the conceptual introduction of Thomas Huxley's 'very cunningly contrived torpedo' in 1881 [1] and Paul Ehrlich's 'magic bullet' in 1907 [2], much research has been focused on developing systems for targeted drug delivery. In the 1970s this led to the development and characterization of colloidal systems, such as liposomes and micelles, for drug encapsulation and delivery. In 1974, Gregoriadis et al showed for the first time the therapeutic potential of liposomes as a drug carrier system in metastatic cancer [3]. Liposomes have thereafter shown therapeutic value as drug carriers in many other diseases, including bacterial and fungal infections [4, 5], arthritis [6, 7] and multiple sclerosis [8]. The improved delivery of drugs to their target site obtained by the encapsulation in nanosized carrier systems can be explained by the increased permeability of the vasculature in tumors and inflamed tissues, which is referred to as the Enhanced Permeability and Retention (EPR) effect [9]. The EPR-enabled targeting capability of colloidal delivery systems and macromolecules is strongly promoted by a long plasma half-life, as this increases the time interval during which extravasation can take place [10-14].

Phagocytic cells from the reticuloendothelial system (RES) are primarily responsible for the elimination of liposomes and other nanoparticulate drug delivery systems from the circulation [15]. Although the precise mechanism has not been completely elucidated yet, there is strong evidence that there is an important role for serum proteins which adsorb onto the outer surface of liposomes, thereby facilitating phagocytosis by macrophages [16-19]. This process of protein adsorption has been directly related to a decreased plasma residence time of liposomes [20, 21].

Several surface modifications of liposomes have been studied to prevent, retard or inhibit plasma protein adsorption, including the incorporation of polyethylene glycol (PEG)-conjugated lipids in the lipid bilayer [22]. The circulation time of these PEGylated 'stealth' liposomes is considerably prolonged; it has been hypothesized that the highly hydrophilic PEG chains form a 'steric barrier' which opposes protein adsorption to the liposomal surface and subsequent elimination by the RES [23-25]. In addition, it has been suggested that the improvement of the colloidal stability of liposomes due to PEGylation is another mechanism that contributes to extend their circulation time [26, 27].

Although PEGylated liposomes show a relatively long circulation half-life, the lack of biodegradability and the possible immunogenicity of PEG remain points of concern

in their clinical application [28, 29]. Further research concerning the optimization in composition and surface coating of liposomes is therefore still in progress [30, 31]. In the development and optimization of particulate drug delivery systems such as liposomes, the determination of their pharmacokinetic profile plays a central role. However, determining the pharmacokinetic characteristics of newly designed formulations often requires large numbers of animals, and is therefore expensive and time consuming. To limit the number of animals needed, and to improve cost- and time-effectiveness of pharmacokinetic research, *in vitro* screening tools predicting the *in vivo* pharmacokinetic fate of the carrier system are highly needed for selecting promising candidates for further *in vivo* testing. Since the circulation longevity of a liposome is proposed to be primarily related to the extent of protein adsorption to its surface [21], measuring the total quantity of adsorbed proteins might provide the basis for such an *in vitro* assay. Unfortunately, the traditional ways of quantifying proteins adsorbed to the surface of liposomes are time-consuming and typically involve washing and separation steps which could easily lead to an underestimation of the amount of protein bound to the surface [32-35]. Especially proteins loosely bound on the outer part of the protein corona are easily removed during these separation steps. Nevertheless, such 'loosely bound' proteins may be of great importance in the clearance mechanism, since they are more 'available' for recognition by and interaction with phagocytic cells of the RES [36].

In the present study, Surface Plasmon Resonance spectrometry (SPR) was used to study the interaction of PEGylated liposomes with proteins known to adsorb onto the surface of liposomes and other nanocarriers [37-41]. SPR is a powerful tool for real-time monitoring of interactions between different molecules, without the need to wash or separate during measurement [42]. Although SPR is mostly used for protein-protein and protein-small molecule interactions, it might also be useful in the measurement of interactions between proteins and liposomes.

When, in addition to the surface adsorption of proteins, blood-induced aggregation of liposomes plays a significant role in the circulation time *in vivo*, a considerable increase in particle size should be observable during *in vitro* incubation with full blood. Fluorescence Single Particle Tracking (fSPT) is a novel technique which measures the Brownian motion of nanoparticles to calculate their size, and is able to do this in physiological media, such as blood [43]. fSPT is therefore a highly suitable tool to examine the effect of blood exposure on the size of (un)PEGylated liposomes.

The first aim of the present work was to evaluate SPR and fSPT for measuring the interactions between liposomes and blood proteins with SPR and fSPT. SPR was used to measure the extent of binding of several blood proteins to liposomes coated with PEG of different molecular weights chain lengths and at different densities. In parallel, fSPT was used to investigate whether exposure of these liposomes to full human blood leads to aggregation of liposomes. The second aim was to identify a correlation between the SPR measured liposome-protein binding and the blood clearance in mice, which could allow estimation of the *in vivo* circulation kinetics of nanoparticulate systems using an *in vitro* assay based on SPR.

2. Materials and Methods

2.1. Materials

1,2-dipalmitoyl-*sn*-glycero-3-phosphoethanolamine-*N*-[methoxy(polyethylene glycol)-2000] (DPPE-PEG_{2000}), 1,2-dipalmitoyl-*sn*-glycero-3-phosphoethanolamine-*N*-[methoxy(polyethylene glycol)-5000] (DPPE-PEG_{5000}) and 1,2-dipalmitoyl-*sn*-glycero-3-phosphoethanolamine-*N*-(lissamine rhodamine B sulfonyl) (Rho-PE) were purchased from Avanti Polar Lipids, USA. L-3-phosphatidyl[*N*-methyl-^{3}H]choline,1,2-dipalmitoyl ([^{3}H]DPPC) was obtained from GE Healthcare (Amersham, UK). Dipalmitoylphosphatidylcholine (DPPC) was a provided by Lipoid, Germany. Human Serum Albumin (HSA) and octyl-β-D-1-thioglucopyranoside (OG) were obtained from Sigma-Aldrich, Germany. Human apolipoprotein E (ApoE), fibronectin, β2-glycoprotein I (β2-G) and α2-macroglubolin (α2-M) were purchased at Calbiochem (USA). 1-Ethyl-3-(3-dimethylaminopropyl)-carbodiimide (EDC), *N*-hydroxysuccinimide (NHS) and ethanolamine were all obtained from GE Healthcare, USA. HEPES buffered saline (HBS) of pH 7.4 was composed of 10 mM HEPES (Acros, Belgium) and 135 mM NaCl (Sigma-Aldrich. Acetate buffer of 10 mM (pH 4.5) was prepared from glacial acetic acid and sodium acetate (Sigma-Aldrich).

2.2. Liposome preparation

DPPC and either DPPE-PEG_{2000} (in molar ratios of 2.5%, 5.0% or 7.0% of total lipid) or DPPE-PEG_{5000} (0.5, 1.5 or 2.5 mol%) were dissolved in 5-10 mL ethanol (absolute) in a 50 mL roundbottom flask. The organic phase was evaporated using rotary evaporation

(Buchi, Switzerland) at 50 °C, resulting in a dry lipid film, which was dried further under nitrogen flow for 30 min. The lipid film was then hydrated with HBS to form liposomes. The size and polydispersity was subsequently decreased by extruding the dispersion at 50 °C through two polycarbonate filters (Whatman, USA) mounted in an LIPEX extruder (Northern Lipids Inc, Canada). Starting with two extrusions through a double filter of 200 nm and two extrusions through filters of 200 and 100 nm, the liposomes were extruded ten times through two filters of 100 nm, to reach an average diameter of 100 nm. Particle size and polydispersity of extruded dispersions were determined by dynamic light scattering (DLS) using a Malvern ALV CGS-3 (Malvern Instruments, UK). DLS results are given as a z-average particle size diameter and a polydispersity index (PDI), which is expressed on a scale of 0 to 1; 0 meaning complete monodispersity and 1 meaning complete polydispersity. The ζ-potential in of the liposomes in HBS was determined using a Zetasizer 3000 (Malvern Instruments, UK).

Total lipid concentration was determined using a method developed by Rouser et al [44], which is based on the colorimetric determination of PO_4^{3-}. After destruction of phospholipids by perchloric acid, anorganic phosphate was formed. This was subsequently transformed into phosphomolybdate acid using hexa-ammoniummolybdate, which was converted to a blue colored compound due to reduction of ascorbic acid during heating. This quantity was determined spectrophotometrically at 797 nm. All liposomal dispersions were diluted in HBS to a concentration of 300 μM lipid.

2.3. Protein immobilization

Surface plasmon resonance (SPR) studies were performed with a BIAcore3000 (GE Healthcare, USA). Human serum albumin, apolipoprotein E, α2-macroglubolin, β2-glycoprotein I and fibronectin were immobilized on carboxymethylated dextran matrix-covered sensor chips (CM5; GE Healthcare, USA), following the general protocol provided by the supplier. Carboxyl groups on the surface of the sensor chip were activated by 0.4 M EDC/0.1 M NHS (1:1). After exploring the optimal pH for amine coupling by performing a series of scouting runs, each protein was dissolved in acetate buffer (10 mM, pH 4.5) at a concentration of 20 μg/mL, of which 500 μL was injected in a flow cell at a rate of 5 μL/min to allow coupling of primary amines to the activated carboxyl groups on the surface of the chip. The immobilization process was monitored continuously and stopped when all protein (10 μg) was injected. Unreacted activated carboxyl groups were

deactivated by 1 M ethanolamine hydrochloride, pH 8.5. The surface was washed with 50 mM NaOH to remove any non-covalently bound material from the surface. One flow cell of each chip was activated with EDC/NHS and then de-activated with ethanolamine hydrochloride, to function as a control flow cell with which binding to the dextran matrix could be assessed. Running buffer was HBS which was filtered through a 200 nm membrane and degassed before use.

2.4. SPR analysis of liposome-protein interactions

Each type of liposome dispersion (300 μM) was injected through all flow cells for 40 min at a flow rate of 5 μL/min. The surface of the chip in each flow cell was washed with 5 μL of 40 mM OG before initiating the next run. Complete removal of bound material was checked by comparing the baseline before injection and after washing. When the recovery of the chip surface was incomplete, the chip was replaced by another chip on which the respective protein was immobilized. In the case of HSA and ApoE, but not for α2-M, β2-G and Fn, the chips needed to be replaced during the experiments, because of incomplete recovery after washing, i.e. the resonance angle did not return to zero. Binding of particles or molecules to the surface of the sensor chip causes a change in refractive index at the surface of the chip, which leads to a shift in resonance angle. There is a linear relationship between the change in mass at the surface of the chip and the shift in resonance angle [42]. This resonance angle shift is expressed in resonance units (RU); 1 RU equals a change of 10^{-4} °, which for proteins represents the binding of approximately 1 pg of globular protein to 1 mm^2 surface [45]. The change in RU in each flow cell after sample injection, minus the change in RU in the blank flow cell, represents the extent of liposomal adsorption to the immobilized proteins (Δ RU). Experiments were done at least in triplicate for each liposomal formulation, and were conducted at 25 °C.

2.5. In vivo circulation time studies

To determine the pharmacokinetic profile of each liposome composition, DPPC liposomes radiolabelled with [^{3}H]DPPC were prepared without PEG or containing DPPE-PEG_{2000} (2.5 mol%, 5.0 mol%, 7.0 mol%) or DPPE-PEG_{5000} (0.5 mol%, 1.5 mol%, 2.5 mol%). The liposomes were injected intravenously in the tail vein of NMRI mice. The injected dose corresponded to 70 μmol DPPC/kg and 3.1 MBq [^{3}H]DPPC/kg. Experimental groups consisted of 4-6 mice. Blood samples were taken at 15, 30, 60, 120, 240, and 360

min after injection, which were bleached before liquid scintillation counting.

2.6. Aggregation of liposomes in blood

To assess whether exposure to full blood induces liposomal aggregation of DPPC liposomes or PEGylated DPPC liposomes, Fluorescence Single Particle Tracking (fSPT) was used to measure the mean size distribution of the different liposome dispersions upon incubation with blood. Uncoated DPPC liposomes and DPPC liposomes coated with PEG_{2000} (2.5 mol%, 5 mol%, 7 mol%) or PEG_{5000} (0.5 mol%, 1.5 mol%, 2.5 mol%) were fluorescently labeled by adding 0.1 mol% Rho-PE to the lipids during preparation. Blood from a male healthy volunteer was collected in tubes containing lithium heparin (Terumo Europe, Belgium). 500 µL of each liposome dispersion (40 mM lipid) was injected in 5 mL of circulating human whole blood, being kept at 37 °C. A peristaltic pump (BL 760 FB, Bellco, Italy) and silicone tubing with an inner diameter of 1.6 mm (Helix medical, USA) were used to construct an artificial circulation system, maintaining a bloodflow of approximately 5 mL/min. At 1, 30, 60, 90 and 120 min after injection, samples were taken from the blood circulation and diluted 1:5000 in HBS before fSPT measurement. fSPT setup, measurements and data analysis were performed as described previously [43]. All formulations were incubated and analyzed in triplicate.

2.7. Data analysis

BIAevaluation software (version 4.1, Biacore) was used to analyze the data acquired by SPR. The *in vivo* pharmacokinetic data were fitted by MultiFit v07.08.2006 software, using one compartment log-linear regression analysis. Correlations and statistical analyses were done using GraphPad Prism software v5.03. Protein-liposome interactions were compared using one-way ANOVA analysis with Tukay post-testing.

3. Results

3.1. Liposome compositions

The liposomes used in this study were composed of DPPC and coated with different densities of DPPE-PEG_{2000} or DPPE-PEG_{5000}. Dynamic light scattering and ζ-potential measurements showed that the different liposomes had a relatively monodisperse size distribution (PDI ± 0.1) with a z-average diameter of around 100 nm, and a neutral

Table 1. Characteristics of liposome compositions

PEG		Z-average diameter (nm)	Mean PDI	Average Zeta potential (mV)
Molecular weight (Da)	*Surface density (%)*			
-		100	0.14	0.1 ± 0.4
2000	2.5	90	0.08	-0.6 ± 0.4
2000	5.0	90	0.09	0.0 ± 0.9
2000	7.0	90	0.09	-1.8 ± 1.0
5000	0.5	100	0.08	-1,1 ± 0.8
5000	1.5	110	0.07	1,1 ± 1.0
5000	2.5	100	0.11	-0,4 ± 2.3

ζ-potential in HBS (Table 1). DLS analysis showed that the DPPE-PEG coated formulations were stable for several weeks when stored at 4 °C. In contrast, the DPPC liposomes without DPPE-PEG showed severe aggregation within several days, marked by an increased mean particle size and polydispersity index, and therefore fresh DPPC liposomes were prepared for each experiment.

3.2. Protein immobilization

Protein-coated dextran surfaces were prepared by injecting 10 μg of human serum albumin (HSA), apolipoprotein E (ApoE), α2-macroglobulin (α2-M), β2-glycoprotein I (β2-G) or fibronectin (Fn) in separate pre-activated flow cells. The immobilization process resulted in a substantial change in resonance angle of each flow cell, indicating successful coupling of the different proteins (Table 2). The change in RU in the blank flow cell, due to EDC/NHS activation and ethanolamine hydrochloride deactivation, was approximately 200 RU.

Table 2. Characteristics of protein coated chips

Protein	Abbreviation	Mass (kDa)	ΔRU after initial immobilization
Human Serum Albumin	HSA	66	9×10^3
Apolipoprotein E	ApoE	36	7×10^3
α2-Macroglobulin	α2-M	163	15×10^3
β2-Glycoprotein I	β2-G	38	4×10^3
Fibronectin	Fn	440	5×10^3

ΔRU – change in resonance angle (1RU = 10^{-4} °)

3.3. SPR measurement of protein-liposome interactions

To study the interaction between proteins and liposomes with SPR, liposomes coated with different PEGs of different molecular weights and at several densities, were injected in flow cells containing immobilized HSA, ApoE, α2-M, β2-G and Fn. Although liposomes with higher PEG coating densities showed less non-specific binding to the surface of protein-free chips, as measured in the blank flow cells, the overall non-specific binding was low for all liposome compositions (Figure 1). The relatively small shift in the control flow cell shows that there is limited non-specific binding of the liposomes onto the sensor surface. The change in RU after injection of (PEGylated) DPPC liposomes was 10- to

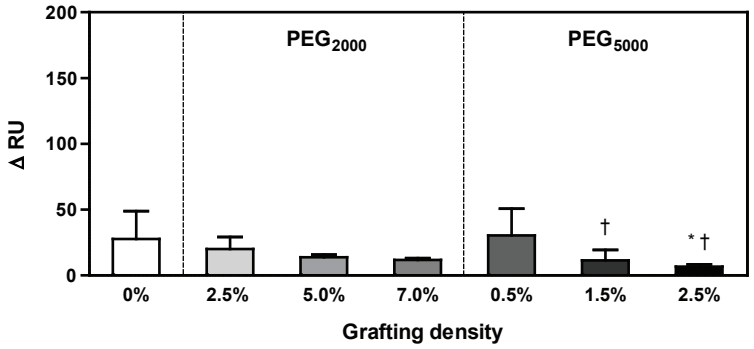

Figure 1. Non-specific binding of PEGylated DPPC liposomes to the blank (uncoated) SPR chip. Change in resonance angle of the chip without protein after exposure to DPPC liposomes and DPPC liposomes coated with either PEG_{2000} or PEG_{5000}. Shown are the average changes in resonance units (ΔRU) with the standard deviation of 7-9 experimental runs. * significantly different to DPPC; † significantly different to 0.5% PEG_{5000}. $p<0.05$, one-way ANOVA with Tukay post-test.

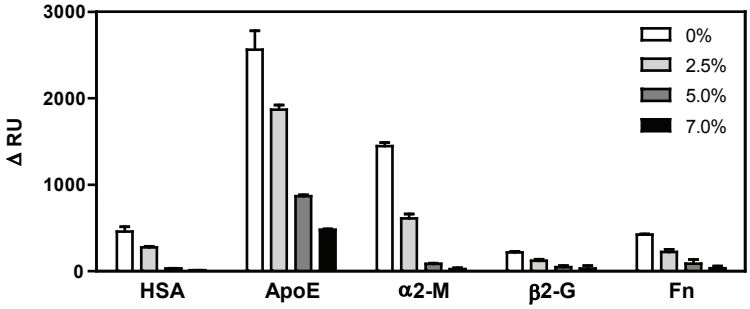

Figure 2. Effect of PEG_{2000} grafting density on protein adsorption of DPPC liposomes. Change in resonance angle of protein coated chips after exposure to liposomes coated with different densities of PEG_{2000}. Shown are the average changes in resonance units (ΔRU) and the standard deviations of 3-5 experimental runs. For each protein*, all different grafting densities showed significant differences in protein adsorption ($p<0.01$, one-way ANOVA with Tukay post-test), except 5.0% vs 7.0% surface density for HSA, α2-M, β2-G and Fn.

* HSA = human serum albumin; ApoE = apolipoprotein E; α2-M = α2-macroglobulin; β2-G = β2-glycoprotein I; Fn = fibronectin

100-fold larger in the protein-coated flow cells than in the control flow cells, which indicates binding to the immobilized proteins (Figure 2 and Figure 3). The injection of DPPC liposomes without PEG coating caused the largest shift in resonance angle while the incorporation of DPPE-PEG_{2000} (Figure 2) or DPPE-PEG_{5000} (Figure 3) in the

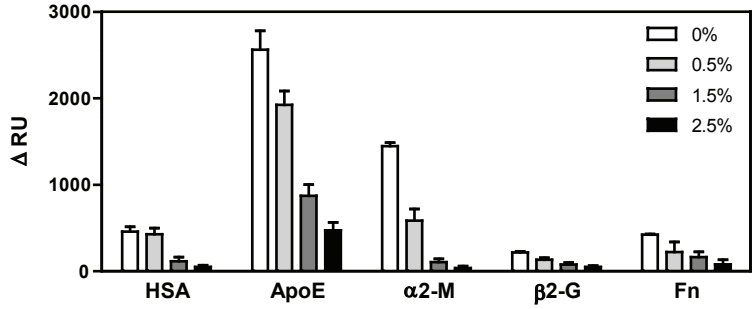

Figure 3. Effect of PEG_{5000} grafting density on protein adsorption of DPPC liposomes. Change in resonance angle of protein coated chips after exposure to liposomes coated with different densities of PEG_{5000}. Shown are the average changes in resonance units (ΔRU) and the standard deviations of 3-5 experimental runs. For each protein*, all different grafting densities showed significant differences in protein adsorption ($p<0.01$, one-way ANOVA with Tukay post-test), except 0% vs 0.5% surface density for HSA; 0.5% vs 1.5% and 0.5% vs 2.5% surface density for fibronectin; and 1.5% vs 2.5% surface density for HSA, α2-M, β2-G and Fn.

* HSA = human serum albumin; ApoE = apolipoprotein E; α2-M = α2-macroglobulin; β2-G = β2-glycoprotein I; Fn = fibronectin

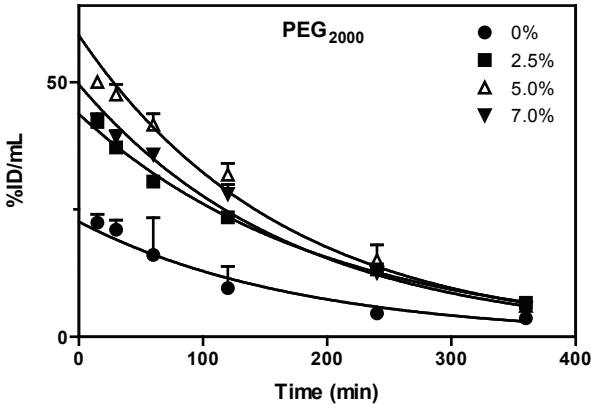

Figure 4. Effect of surface density of PEG_{2000} on the clearance of DPPC liposomes from blood. DPPC liposomes and PEG_{2000}-coated (2.5%, 5.0% and 7.0% surface density) DPPC liposomes labeled with [^{3}H]DPPC were intravenously injected in NMRI mice. The blood levels of [^{3}H]DPPC (mean ± SEM, n=4-6 mice) are depicted as the percentage of injected dose per mL blood (y-axis, %ID/mL) in time (x-axis, min), fitted by one compartment log-linear regression analysis (curves).

liposomal bilayer reduced the binding to each studied protein. The ApoE-coated surface showed the highest degree of adsorption the investigated liposomes. Incorporation of DPPE-PEG_{2000} into the lipid bilayer decreased the binding of each protein, an effect which increased with the PEG_{2000} surface density (Figure 2). The differences were significant for all tested proteins ($p<0.01$) except for the two highest PEG_{2000} densities (i.e. 5.0% and 7.0%) in case of HSA, α2-M, β2-G and Fn. The incorporation of DPPE-PEG_{5000} yielded similar results, and the effect of PEG_{5000} density increase on protein adsorption was comparable to that of PEG_{2000} for most proteins. All differences were significant ($p<0.01$), except for HSA in case of 0% versus 0.5% PEG_{5000} density, for Fn in case of 0.5% versus 1.5% and 2.5% PEG_{5000} densities, and for HSA, α2-M, β2-G and Fn in case of 1.5% versus 2.5% PEG_{5000} density. ApoE showed the highest degree of binding of all proteins tested and was the only protein that showed a significant reduction of protein adsorption for each increase in PEG density.

3.4. In vivo liposome clearance

NMRI mice were injected i.v. with [^{3}H]DPPC liposomes or [^{3}H]DPPC liposomes coated with DPPE-PEG_{2000} or DPPE-PEG_{5000} at different densities to study the pharmacokinetic profile of each liposome type. The incorporation of DPPE-PEG into the liposomal surface improved the circulation profile of DPPC liposomes, both when PEG_{2000} (Figure 4) and

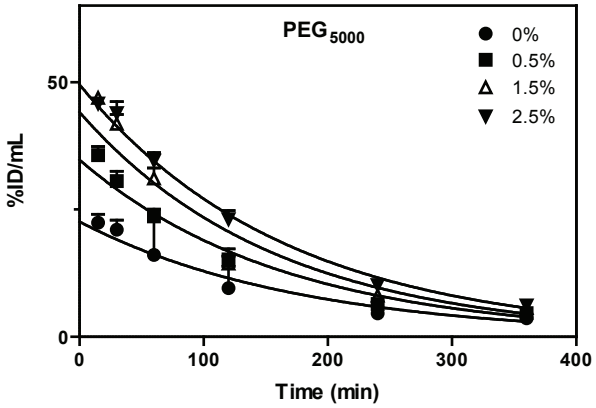

Figure 5. Effect of surface density of PEG_{5000} on the clearance of DPPC liposomes from blood. DPPC liposomes and PEG_{5000}-coated (0.5%, 1.5%, 2.5% surface density) DPPC liposomes labeled with [^{3}H]DPPC were intravenously injected in NMRI mice. The blood levels of [^{3}H]DPPC (mean ± SEM, n=4-6 mice) are depicted as the percentage of injected dose per mL blood (y-axis, %ID/mL) in time (x-axis, min), fitted by one compartment log-linear regression analysis (curves).

PEG_{5000} (Figure 5) were used. The pharmacokinetic profile of each liposome type was calculated from the blood clearance curves by fitting the [^{3}H]DPPC doses present in the circulation at each time point using a one compartment log-linear regression analysis (Table 3). The apparent volume of distribution (V_d), calculated from the extrapolated concentration at t_0, was twice as high for the liposomes without PEG compared to the

Table 3. Pharmacokinetic characteristics of (PEG-coated) DPPC liposomes, calculated from the fitted curves (one compartment kinetics).

Liposome composition	**C_0** *(%·mL^{-1})*	**k_e** *(min^{-1})*	**V_d** *(mL)*	**AUC** *(%·min·L^{-1})*	**Clearance** *(mL·min^{-1})*	**Curve fit** *(r^2)*
DPPC	23	0.0056	4.4	4.0	0.025	0.95
+ 2.5 mol% PEG_{2000}	44	0.0052	2.3	8.5	0.012	1.00
+ 5.0 mol% PEG_{2000}	59	0.0061	1.7	9.8	0.010	0.99
+ 7.0 mol% PEG_{2000}	50	0.0058	2.0	8.5	0.012	0.99
+ 0.5 mol% PEG_{5000}	35	0.0061	2.9	5.7	0.018	0.97
+ 1.5 mol% PEG_{5000}	44	0.0063	2.3	7.0	0.014	0.94
+ 2.5 mol% PEG_{5000}	50	0.0060	2.0	8.2	0.012	0.99

C_0 – extrapolated concentration at t_0; k_e – elimination rate constant; V_d – apparent volume of distribution; AUC – area under the curve

liposomes that did have a PEG coating, indicating a rapid clearance from the circulation upon injection. In addition, the total clearance of DPPC liposomes is greatly improved by PEGylation with PEG_{2000}, though differences in surface density were not reflected strongly. For liposomes coated with PEG_{5000}, the clearance was reduced considerably when a higher surface density was present.

3.5. Correlation of protein binding to the clearance of liposomes

The SPR binding results were correlated with the corresponding blood clearance for each liposome type to investigate whether the *in vitro* SPR measurements of protein interactions correlate with the *in vivo* clearance of liposomes. The extent of interaction of a liposome composition with each protein showed a positive relationship with its clearance (Figure 6). The Pearson's correlation coefficients (r) varied from 0.78 to 0.89, and were all statistically significant ($p<0.05$) (Table 4). This shows that there is a moderate to strong positive correlation between the extent of protein binding measured *in vitro* by SPR and the *in vivo* plasma clearance of liposomes.

3.6. Aggregation of liposomes in blood

Liposomal aggregation upon exposure to human blood was assessed by Fluorescence Single

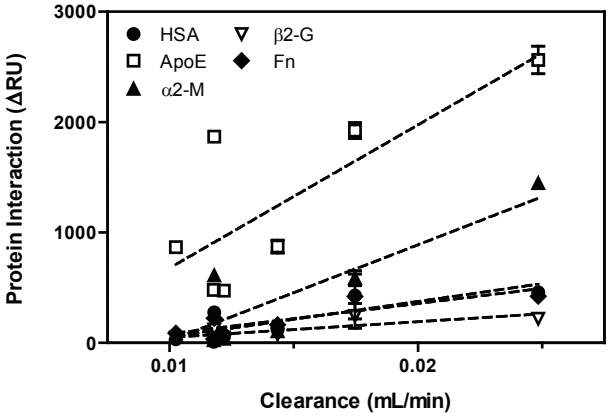

Figure 6. Correlation between protein interaction measured with SPR and the plasma clearance of liposomes. Correlation of the protein-liposome interaction measured with SPR (y-axis, expressed in ΔRU) between (PEG-coated) DPPC liposomes and human serum albumin (●), apolipoprotein E (□), α2-macroglobulin (▲), β2-glycoprotein (▽), and fibronectin (◆); and the liposome clearance from the circulation (x-axis, expressed in mL/min).

Table 4. Correlation protein-liposome interaction and clearance of (PEG-coated) DPPC liposomes. Shown are Pearson's correlation coefficient (r) with coefficient of determination (r^2) and the two-tailed p-value (p) of each correlation.

Protein	r	r^2	p
Human Serum Albumin	0.82	0.67	0.025
Apolipoprotein E	0.78	0.61	0.038
α2-Macroglobulin	0.89	0.78	0.008
β2-Glycoprotein I	0.80	0.65	0.029
Fibronectin	0.84	0.71	0.017

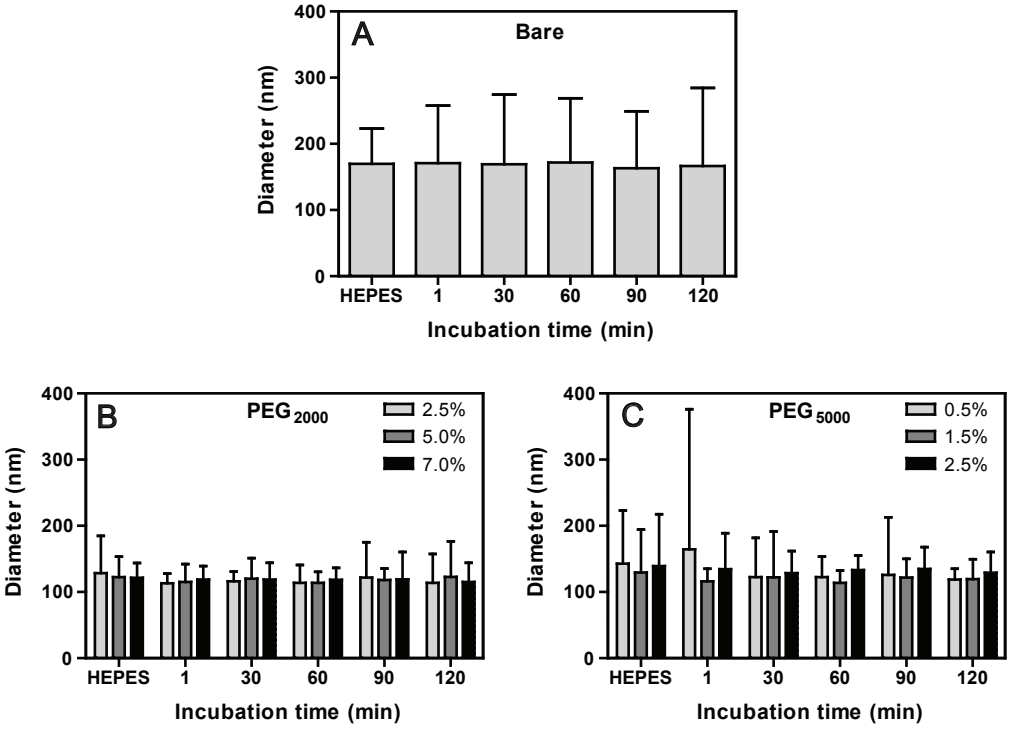

Figure 7. Mean diameter of DPPC liposomes without PEG or coated with either PEG_{2000} or PEG_{5000} at different densities upon incubation with full human blood. DPPC liposomes (A) and DPPC liposomes coated with different densities of PEG_{2000} (B) and PEG_{5000} (C) were incubated at 37 °C in heparinized full human blood. The mean liposome diameter was measured by fSPT before incubation (in HEPES buffer) and after 1 min, 30 min, 60 min, 90 min and 120 min of incubation. Depicted is the mean diameter (±SD) of each liposome composition incubated and analyzed in triplicate.

Particle Tracking (fSPT) particle size measurements. After incubation up to 120 min, no significant changes in liposome size and polydispersity were observed for either bare, PEG_{2000}- or PEG_{5000}-coated liposomes (Figure 7). The initial size of the liposomes without PEG-coating was larger than that of the liposomes that contained PEG, indicating that some aggregation had already occurred in the uncoated formulation before measurement. Subsequent incubation in full blood did not lead to changes in liposome size and size distribution, which implies that there was no significant aggregation induced by exposure to blood.

4. Discussion

In the current study, a novel *in vitro* assay is presented to measure the interactions between liposomes and blood proteins, which can be used to predict the *in vivo* blood clearance of liposomes and – although not tested – likely other nanocarriers. The main advantages of SPR above conventional techniques for protein adsorption measurements are its speed and the absence of separation and washing steps, which could readily remove loosely bound proteins. The extent of protein adsorption measured by means of SPR was shown to correlate strongly with the blood clearance of DPPC liposomes, bare or PEGylated, which implies that the *in vivo* plasma kinetics can be approached *in vitro* using SPR. Liposomes without a PEG-coating showed the highest binding with all proteins tested, and had a much larger apparent volume of distribution (V_d) and a higher clearance compared to PEGylated liposomes, which indicates rapid uptake by the cells of the RES [46]. Although there is general consensus that protein surface adsorption plays an important role in the clearance of nanomedicines from the bloodstream, it has never been completely elucidated whether inhibition of protein surface adsorption is indeed the most important mechanism by which the inclusion of PEG-lipids in the liposomal bilayer improves the circulation time [26, 47, 48]. Other proposed mechanisms include the prevention of liposomal self-aggregation [26], prevention of liposome-cell interactions [49], and increased adsorption of proteins ('dysopsonins') that 'shield' against clearance from the circulation [50, 51]. Especially albumin has been proposed as being a dysopsonin, either by hiding the liposome particles from the reticuloendothelial system (RES) or by preventing the adsorption of other (opsonizing) proteins [50, 52, 53]. The present study shows that more densely PEGylated liposomes bind less to all tested proteins, including albumin. Therefore, since

there is no sign of specific interaction of PEG with albumin, it seems unlikely that albumin functions as a dysopsonin for PEGylated liposomes.

There is a number of reports that used SPR to address the interaction of nanoparticles with (plasma) proteins [54-57]. In most cases, this was done using a reversed method: first the particles were immobilized on the surface of the chip and subsequently the proteins of interest were injected into the flow cell [58]. Such a setup requires that each different type of nanoparticle is covalently bound to the surface of a flow cell, which makes screening experiments time-consuming and likely leads to introduction of measurement artifacts due to differences in nanoparticle immobilization. Conversely, using a single protein-coated chip to measure several unmodified nanoparticles makes comparisons between different nanoparticles much more reliable. To our knowledge, there has been only one study that measured the interaction of surface-modified colloidal particles with protein-coated surfaces using a setup similar to the one presented here [56]. In that study, bovine serum albumin was immobilized onto chips that subsequently were used to evaluate the adsorption kinetics of bare and poly(ethylene glycol-propylene oxide-ethylene glycol) (PEG-PPO-PEG)-coated polystyrene latex particles. The PEG-PPO-PEG-coating reduced the binding to albumin compared to the binding of bare particles, similar to the data presented here. While albumin is the most abundant protein in blood, and therefore a logical choice, it may be that the binding to other proteins is of more predictive value. Therefore, in the present study four other proteins were selected for the SPR binding measurements, based on their suggested role in the clearance of liposomes: apolipoprotein E [40], α2-macroglobulin [38], β2-glycoprotein I [37] and fibronectin [39]. While the correlation between protein binding and blood clearance of each composition was moderate to strong for all measured proteins, the binding to ApoE was the highest and showed the strongest reduction upon PEGylation with PEG_{2000} or PEG_{5000}. This suggests that there may be an important role for ApoE in the opsonization process of liposomes.

Surface charge is a known stimulatory factor in aggregation [59], opsonization [21, 60, 61] and clearance of nanocarriers [21, 62-64]. Previously it has been shown that PEGylated cationic liposomes show strong aggregation upon incubation in full human blood [43]. Therefore, liposome compositions based on DPPC, which have a neutral ζ-potential at physiological pH and ionic strength, were used in the present study. To investigate whether aggregation might be an additional process attributing to the clearance of these liposome compositions, fSPT was used to monitor the size of all formulations during incubation

with heparinized human blood. No significant changes in size or size distribution could be observed during 2 h of exposure, indicating that it is unlikely that there is a strong effect of liposomal self-aggregation on the blood clearance of the liposomal compositions used in this study. It is important to note that opsonization *in vivo* is a complex process with continuous ad- and desorption of different competing proteins [65], and therefore, any *in vitro* setup will have its limitations with respect to the extrapolation to the *in vivo* situation. For example, of the blood proteins not included in the present study, some may be very relevant in the clearance of liposomes and other nanoparticles, and would help to make the correlations between SPR binding and plasma clearance even stronger [66].

5. Conclusions

This study demonstrates that SPR and fSPT are suitable techniques to evaluate the interactions between blood proteins and liposomes. The extent of protein binding measured by SPR is dependent on the density of PEG present on the surface of the liposome, where higher PEG densities lead to reduced binding. The size distribution of the liposome dispersions measured using fSPT did not change upon incubation in full human blood, which indicates that aggregation of these liposome compositions did not occur. Secondly, the extent of protein-liposome interaction measured by SPR showed a moderate to strong positive correlation with the clearance of the liposome composition. Therefore, the application of SPR can be considered as a promising tool for the evaluation of liposome-protein interactions *in vitro*, as well as for predicting the blood clearance of liposomes – and likely other nanocarriers – *in vivo*.

6. Acknowledgements

This work was supported by MediTrans, an Integrated Project funded by the European Commission under the "nanotechnologies and nano-sciences, knowledge-based multifunctional materials and new production processes and devices" (NMP), thematic priority of the Sixth Framework Program.

7. References

[1] T.H. Huxley, The connection of the biological sciences with medicine, Science 2(63) (1881) 426-429.

[2] P. Ehrlich, Experimental researches on specific therapy. On immunity with special relationship between distribution and action of antigens. Harben Lecture, Royal Institute of Public Health, London, 1908, p. 107.

[3] G. Gregoriadis, C.P. Swain, E.J. Wills, A.S. Tavill, Drug-carrier potential of liposomes in cancer chemotherapy, The Lancet 303(7870) (1974) 1313-1316.

[4] R.M. Schiffelers, G. Storm, I.A.J.M. Bakker-Woudenberg, Therapeutic efficacy of liposomal gentamicin in clinically relevant rat models, Int. J. Pharm. 214(1-2) (2001) 103-105.

[5] G. Lopez-Berestein, R.L. Hopfer, R. Mehta, K. Mehta, E.M. Hersh, R.L. Juliano, Liposome-encapsulated amphotericin B for treatment of disseminated candidiasis in neutropenic mice, J. Infect. Dis. 150(2) (1984) 278-283.

[6] J.M. Metselaar, M.H.M. Wauben, J.P.A. Wagenaar-Hilbers, O.C. Boerman, G. Storm, Complete remission of experimental arthritis by joint targeting of glucocorticoids with long-circulating liposomes, Arthritis Rheum. 48(7) (2003) 2059-2066.

[7] W. Hofkens, L.C. Grevers, B. Walgreen, T.J. de Vries, P.J.M. Leenen, V. Everts, G. Storm, W.B. van den Berg, P.L. van Lent, Intravenously delivered glucocorticoid liposomes inhibit osteoclast activity and bone erosion in murine antigen-induced arthritis, J. Control. Release 152(3) (2011) 363-369.

[8] J. Schmidt, J.M. Metselaar, M.H.M. Wauben, K.V. Toyka, G. Storm, R. Gold, Drug targeting by long-circulating liposomal glucocorticosteroids increases therapeutic efficacy in a model of multiple sclerosis, Brain 126(8) (2003) 1895-1904.

[9] H. Maeda, J. Wu, T. Sawa, Y. Matsumura, K. Hori, Tumor vascular permeability and the EPR effect in macromolecular therapeutics: a review, J. Control. Release 65(1-2) (2000) 271-284.

[10] H. Maeda, L.W. Seymour, Y. Miyamoto, Conjugates of anticancer agents and polymers: advantages of macromolecular therapeutics in vivo, Bioconj. Chem. 3(5) (1992) 351-362.

[11] T. Lammers, V. Subr, P. Peschke, R. Kühnlein, W.E. Hennink, K. Ulbrich, F. Kiessling, M. Heilmann, J. Debus, P.E. Huber, G. Storm, Image-guided and passively tumour-targeted polymeric nanomedicines for radiochemotherapy, Br. J. Cancer 99(6) (2008) 900-910.

[12] D. Peer, J.M. Karp, S. Hong, O.C. Farokhzad, R. Margalit, R. Langer, Nanocarriers as an emerging platform for cancer therapy, Nature Nanotech. 2(12) (2007) 751-760.

[13] M.E. Davis, Z. Chen, D.M. Shin, Nanoparticle therapeutics: an emerging treatment modality for cancer, Nat. Rev. Drug Discov. 7(9) (2008) 771-782.

[14] T. Lammers, W.E. Hennink, G. Storm, Tumour-targeted nanomedicines: principles and practice, Br. J. Cancer 99(3) (2008) 392-397.

[15] T.M. Allen, L. Murray, S. MacKeigan, M. Shah, Chronic liposome administration in mice: effects on reticuloendothelial function and tissue distribution, J. Pharmacol. Exp. Ther. 229(1) (1984) 267-275.

[16] G.L. Scherphof, J.A.A.M. Kamps, Receptor versus non-receptor mediated clearance of liposomes, Adv. Drug Deliv. Rev. 32(1-2) (1998) 81-97.

[17] S.C. Semple, A. Chonn, P.R. Cullis, Interactions of liposomes and lipid-based carrier systems with blood proteins: Relation to clearance behaviour in vivo, Adv. Drug Deliv. Rev. 32(1-2) (1998) 3-17.

[18] C.R. Alving, N.M. Wassef, Complement-dependent phagocytosis of liposomes: suppression by "stealth" lipids, J. Liposome Res. 2(3) (2008) 383-395.

[19] A. Vonarbourg, C. Passirani, P. Saulnier, J.-P. Benoit, Parameters influencing the stealthiness of colloidal drug delivery systems, Biomaterials 27(24) (2006) 4356.

[20] S.C. Semple, A. Chonn, P.R. Cullis, Influence of cholesterol on the association of plasma proteins with liposomes, Biochemistry (Mosc). 35(8) (1996) 2521-2525.

[21] A. Chonn, S.C. Semple, P.R. Cullis, Association of blood proteins with large unilamellar liposomes in vivo. Relation to circulation lifetimes, J. Biol. Chem. 267(26) (1992) 18759-18765.

[22] A.L. Klibanov, K. Maruyama, V.P. Torchilin, L. Huang, Amphipathic polyethyleneglycols effectively prolong the circulation time of liposomes, FEBS Lett. 268(1) (1990) 235-237.

[23] D. Marsh, R. Bartucci, L. Sportelli, Lipid membranes with grafted polymers: physicochemical aspects, BBA-Biomembranes 1615(1-2) (2003) 33-59.

[24] J. Senior, C. Delgado, D. Fisher, C. Tilcock, G. Gregoriadis, Influence of surface hydrophilicity of liposomes on their interaction with plasma protein and clearance from the circulation: Studies with poly(ethylene glycol)-coated vesicles, BBA-Biomembranes 1062(1) (1991) 77-82.

[25] P.J. Photos, L. Bacakova, B. Discher, F.S. Bates, D.E. Discher, Polymer vesicles in vivo: correlations with PEG molecular weight, J. Control. Release 90(3) (2003) 323-334.

[26] C. Allen, N. Dos Santos, R. Gallagher, G.N.C. Chiu, Y. Shu, W.M. Li, S.A. Johnstone, A.S. Janoff, L.D. Mayer, M.S. Webb, M.B. Bally, Controlling the physical behavior and biological performance of liposome formulations through use of surface grafted poly(ethylene glycol), Biosci. Rep. 22(2) (2002) 225-250.

[27] D. Needham, T.J. McIntosh, D.D. Lasic, Repulsive interactions and mechanical stability of polymer-grafted lipid membranes, BBA-Biomembranes 1108(1) (1992) 40-48.

[28] T. Ishida, X. Wang, T. Shimizu, K. Nawata, H. Kiwada, PEGylated liposomes elicit an anti-PEG IgM response in a T cell-independent manner, J. Control. Release 122(3) (2007) 349-355.

[29] J. Szebeni, L. Baranyi, S. Savay, J. Milosevits, R. Bunger, P. Laverman, J.M. Metselaar, G. Storm, A. Chanan-Khan, L. Liebes, F.M. Muggia, R. Cohen, Y. Barenholz, C.R. Alving, Role of complement activation in hypersensitivity reactions to doxil and hynic PEG liposomes: experimental and clinical studies, J. Liposome Res. 12(1-2) (2002) 165-172.

[30] B. Romberg, W. Hennink, G. Storm, Sheddable coatings for long-circulating nanoparticles, Pharm. Res. 25(1) (2008) 55-71.

[31] M.C. Woodle, Controlling liposome blood clearance by surface-grafted polymers, Adv. Drug Deliv. Rev. 32(1-2) (1998) 139-152.

[32] S.L. Megan, P. Daniela, B. Rolando, K.M. Bruce, Protein adsorption on derivatives of hyaluronic acid and subsequent cellular response, J. Biomed. Mater. Res. A 91A(3) (2009) 635-646.

[33] N. Dos Santos, C. Allen, A.-M. Doppen, M. Anantha, K.A.K. Cox, R.C. Gallagher, G. Karlsson, K. Edwards, G. Kenner, L. Samuels, M.S. Webb, M.B. Bally, Influence of poly(ethylene glycol) grafting density and polymer length on liposomes: Relating plasma circulation lifetimes to protein binding, BBA-Biomembranes 1768(6) (2007) 1367-1377.

[34] A. Gessner, A. Lieske, B.R. Paulke, R.H. Müller, Influence of surface charge density on protein adsorption on polymeric nanoparticles: analysis by two-dimensional electrophoresis, Eur. J. Pharm. Biopharm. 54(2) (2002) 165-170.

[35] S.M. Moghimi, H.M. Patel, Serum-mediated recognition of liposomes by phagocytic cells of the reticuloendothelial system - The concept of tissue specificity, Adv. Drug Deliv. Rev. 32(1-2) (1998) 45-60.

[36] D. Walczyk, F.B. Bombelli, M.P. Monopoli, I. Lynch, K.A. Dawson, What the cell "sees" in bionanoscience, J. Am. Chem. Soc. 132(16) (2010) 5761-5768.

[37] A. Chonn, S.C. Semple, P.R. Cullis, b2-glycoprotein I is a major protein associated with very rapidly cleared liposomes in vivo, suggesting a significant role in the immune clearance of non-self particles, J. Biol. Chem. 270(43) (1995) 25845-25849.

[38] J. Molnar, S. McLain, C. Allen, H. Laga, A. Gara, F. Gelder, The role of an a2-macroglobulin of rat serum in the phagocytosis of colloidal particles, BBA-Protein Struct. 493(1) (1977) 37-54.

[39] K.M. Yamada, K. Olden, Fibronectins - adhesive glycoproteins of cell surface and blood, Nature 275(5677) (1978) 179-184.

[40] X. Yan, F. Kuipers, L.M. Havekes, R. Havinga, B. Dontje, K. Poelstra, G.L. Scherphof, J.A.A.M. Kamps, The role of apolipoprotein E in the elimination of liposomes from blood by hepatocytes in the mouse, Biochem. Biophys. Res. Commun. 328(1) (2005) 57-62.

[41] M. Lundqvist, J. Stigler, G. Elia, I. Lynch, T. Cedervall, K.A. Dawson, Nanoparticle size and surface properties determine the protein corona with possible implications for biological impacts, Proc. Natl. Acad. Sci. U. S. A. 105(38) (2008) 14265-14270.

[42] E. Stenberg, B. Persson, H. Roos, C. Urbaniczky, Quantitative determination of surface concentration of protein with surface plasmon resonance using radiolabeled proteins, J. Colloid Interface Sci. 143(2) (1991) 513-526.

[43] K. Braeckmans, K. Buyens, W. Bouquet, C. Vervaet, P. Joye, F.D. Vos, L. Plawinski, L.c. Doeuvre, E. Angles-Cano, N.N. Sanders, J. Demeester, S.C.D. Smedt, Sizing nanomatter in biological fluids by fluorescence single particle tracking, Nano Lett. 10(11) (2010) 4435-4442.

[44] G. Rouser, S. Fleischer, A. Yamamoto, Two dimensional thin layer chromatographic separation of polar lipids and determination of phospholipids by phosphorus analysis of spots, Lipids 5(5) (1970) 494-496.

[45] L.G. Fägerstam, Å. Frostell-Karlsson, R. Karlsson, B. Persson, I. Rönnberg, Biospecific interaction analysis using surface plasmon resonance detection applied to kinetic, binding site and concentration analysis, J. Chromatogr. 597(1-2) (1992) 397-410.

[46] T.M. Allen, C.B. Hansen, D.E.L. de Menezes, Pharmacokinetics of long-circulating liposomes, Adv. Drug Deliv. Rev. 16(2-3) (1995) 267.

[47] D.D. Lasic, F.J. Martin, A. Gabizon, S.K. Huang, D. Papahadjopoulos, Sterically stabilized liposomes: a hypothesis on the molecular origin of the extended circulation times, BBA-Biomembranes 1070(1) (1991) 187-192.

[48] P.L. Ahl, S.K. Bhatia, P. Meers, P. Roberts, R. Stevens, R. Dause, W.R. Perkins, A.S. Janoff, Enhancement of the in vivo circulation lifetime of -[alpha]-distearoylphosphatidylcholine liposomes: importance of liposomal aggregation versus complement opsonization, BBA-Biomembranes 1329(2) (1997) 370-382.

[49] S.A. Johnstone, D. Masin, L. Mayer, M.B. Bally, Surface-associated serum proteins inhibit the uptake of phosphatidylserine and poly(ethylene glycol) liposomes by mouse macrophages, BBA-Biomembranes 1513(1) (2001) 25-37.

[50] M. Vert, D. Domurado, Poly(ethylene glycol): Protein-repulsive or albumin-compatible?, J. Biomater. Sci. Polym. Ed. 11(12) (2000) 1307-1317.

[51] S.M. Moghimi, I.S. Muir, L. Illum, S.S. Davis, V. Kolb-Bachofen, Coating particles with a block co-polymer (poloxamine-908) suppresses opsonization but permits the activity of dysopsonins in the serum, BBA-Mol. Cell. Res. 1179(2) (1993) 157-165.

[52] K. Furumoto, J.-I. Yokoe, K.-i. Ogawara, S. Amano, M. Takaguchi, K. Higaki, T. Kai, T. Kimura, Effect of coupling of albumin onto surface of PEG liposome on its in vivo disposition, Int. J. Pharm. 329(1-2) (2007) 110-116.

[53] T. Shehata, K.-i. Ogawara, K. Higaki, T. Kimura, Prolongation of residence time of liposome by surface-modification with mixture of hydrophilic polymers, Int. J. Pharm. 359(1-2) (2008) 272-279.

[54] J.J. Kremer, R.M. Murphy, Kinetics of adsorption of b-amyloid peptide Ab(1-40) to lipid bilayers, J. Biochem. Bioph. Methods 57(2) (2003) 159-169.

[55] R.J. Green, M.C. Davies, C.J. Roberts, S.J.B. Tendler, A surface plasmon resonance study of albumin adsorption to PEO-PPO-PEO triblock copolymers, J. Biomed. Mater. Res. 42(2) (1998) 165-171.

[56] S.L. McGurk, M.C. Davies, C.J. Roberts, S.J.B. Tendler, P.M. Williams, Screening the biointeractions of submicron sized particles intended for site-specific delivery using surface plasmon resonance, J. Colloid Interface Sci. 218(2) (1999) 456-461.

[57] T. Cedervall, I. Lynch, S. Lindman, T. Berggard, E. Thulin, H. Nilsson, K.A. Dawson, S. Linse, Understanding the nanoparticle-protein corona using methods to quantify exchange rates and affinities of proteins for nanoparticles, Proc. Natl. Acad. Sci. U. S. A. 104(7) (2007) 2050-2055.

[58] M. Besenicar, P. Macek, J.H. Lakey, G. Anderluh, Surface plasmon resonance in protein-membrane interactions, Chem. Phys. Lipids 141(1-2) (2006) 169-178.

[59] S. Li, W.-C. Tseng, D.B. Stolz, S.-P. Wu, S.C. Watkins, L. Huang, Dynamic changes in the characteristics of cationic lipidic vectors after exposure to mouse serum: implications for intravenous lipofection, Gene Ther. 6(4) (1999) 585-594.

[60] A. Chonn, P.R. Cullis, D.V. Devine, The role of surface charge in the activation of the classical and alternative pathways of complement by liposomes, J. Immunol. 146(12) (1991) 4234-4241.

[61] F. Roerdink, N.M. Wassef, E.C. Richardson, C.R. Alving, Effects of negatively charged lipids on phagocytosis of liposomes opsonized by complement, BBA-Biomembranes 734(1) (1983) 33-39.

[62] T.M. Allen, C. Hansen, J. Rutledge, Liposomes with prolonged circulation times: factors affecting uptake by reticuloendothelial and other tissues, BBA-Biomembranes 981(1) (1989) 27-35.

[63] G. Sahay, D.Y. Alakhova, A.V. Kabanov, Endocytosis of nanomedicines, J. Control. Release 145(3) (2010) 182-195.

[64] A. Gabizon, D. Papahadjopoulos, The role of surface charge and hydrophilic groups on liposome clearance in vivo, BBA-Biomembranes 1103(1) (1992) 94-100.

[65] L. Vroman, A.L. Adams, Findings with the recording ellipsometer suggesting rapid exchange of specific plasma proteins at liquid/solid interfaces, Surf. Sci. 16 (1969) 438-446.

[66] M.P. Monopoli, D. Walczyk, A. Campbell, G. Elia, I. Lynch, F. Baldelli Bombelli, K.A. Dawson, Physical-chemical aspects of protein corona: relevance to in vitro and in vivo biological impacts of nanoparticles, J. Am. Chem. Soc. 133(8) (2011) 2525-2534.

9

Summarizing discussion

B.J. Crielaard

1. Summarizing discussion

The field of targeted drug delivery has made great progress during the last decades. A large variety of nanomedicines has been developed and evaluated in a number of preclinical models, several of which have reached clinical application, demonstrating the value of drug targeting in the therapy of various diseases. The aim of this thesis is, first of all, to explore the therapeutic potential of several targeted nanomedicines in the treatment of various inflammatory diseases. Also cancer, in which inflammation plays an important role as well, was in focus. Secondly, the thesis focuses on comparing different nanocarrier systems of dexamethasone for the treatment of rheumatoid arthritis (RA), and reports of the development of an *in vitro* assay to predict the *in vivo* circulation kinetics of nanosized drug delivery systems.

The starting point of this thesis is established and described in **Chapter 2**, which provides a concise overview of drug targeting strategies currently employed for the treatment of chronic inflammatory diseases, focusing on targeted nanomedicines for the treatment of rheumatoid arthritis (RA), multiple sclerosis (MS) and, to a lesser extent, inflammatory bowel disease (IBD).

1.1. Drug targeting to inflammatory diseases

Research dealing with widening the scope of an established nanomedicine is presented in **Chapter 3**, where a formulation composed of dexamethasone phosphate encapsulated in long-circulating liposomes (LCL-DXP), which has previously shown therapeutic activity in RA [1, 2], is evaluated in preclinical models of two chronic inflammatory diseases, i.e. MS and IBD. Dexamethasone phosphate is a hydrophilic prodrug of dexamethasone, a corticosteroid with potent glucocorticoid activity (approximately 6-10 times higher than prednisolone [3]), which shows rapid, enzymatically catalyzed, hydrolytic conversion to the parent compound ($t_{1/2}$ ~ 5 min) *in vivo* [4]. It was anticipated that targeting dexamethasone to the sites of inflammation would be therapeutically beneficial in these models. While liposomal-targeted dexamethasone was indeed therapeutically efficacious in mice with experimental autoimmune encephalomyelitis (EAE), an often-employed preclinical model of MS, LCL-DXP therapy surprisingly resulted in a dose-related aggravation of disease activity in mice with dextran sodium sulfate-induced (DSS) colitis. There are several reasons that may explain the counter-effective effects of liposomal targeted

dexamethasone in the DSS-model of IBD.

Firstly, it is possible that dexamethasone-targeting is not an effective strategy for IBD therapy. This is, however, not very likely, since high and preferentially local doses of corticosteroids (e.g. by enema) as such are in fact clinically used to induce remission of active disease [5]. Secondly, it might be that there was no substantial target tissue accumulation of liposomal dexamethasone. Although in this study no tissue concentrations of dexamethasone were determined, no or minimal localization of targeted dexamethasone would result in a similar effect on disease activity as PBS or free DXP treatment, rather than worsening it. Therefore, it seems likely that actual liposomal drug accumulation took place. Moreover, several studies have demonstrated the accumulation of long-circulating liposomes and other nanocarrier systems in inflamed intestinal mucosa of rodents with DSS-induced colitis [6], as well as in the intestine of patients with active IBD [7], indicating that inflammation-targeting in IBD is a viable strategy. A third possible explanation for the unexpected effects of liposomal dexamethasone in the DSS-model, might lie in the nature of the animal model in combination with that of the delivery system. As extensively discussed in Chapter 3, tissue-residing macrophages are of key importance in DSS-induced colitis by protecting the intestine against invading microorganisms. In addition, macrophages are responsible for the elimination of liposomes (and other nanoparticulates) from the circulation, which results in a nearly instantaneous release of the payload encapsulated in their aqueous core upon lysosomal destabilization of the liposomal phospholipid bilayer [8]. Treatment with corticosteroid-loaded liposomes may therefore lead to an intense downregulation of macrophage activity, resulting in a reduced defense against mucosal infection.

To investigate the value of a targeted delivery system with a controlled dexamethasone release profile for the treatment of inflammatory disorders, dexamethasone-loaded core-crosslinked polymeric micelles (DEX-PM) were developed and evaluated *in vivo* in **Chapter 4**. While core-crosslinked polymeric micelles have been studied previously in several preclinical cancer models for the targeted delivery of anti-cancer therapeutics to tumors [9, 10], this study was the first to extend their therapeutic applicability towards a non-malignant disease. Polymerizable dexamethasone prodrugs were synthesized by employing hydrolytically cleavable thioether-based linkers containing a methacrylate moiety, to allow, upon core-crosslinking, transiently stable entrapment of dexamethasone inside the hydrophobic core of the micelles. The *in vitro* drug release rate from the micelle could be controlled by using linkers with various degrees of oxidation of the thioether:

the electron-withdrawing properties of the oxygen atom(s) reduced the electron density at the ester bond, thereby making it more susceptible to hydroxyl ion-driven hydrolysis. Subsequent *in vivo* evaluation of DEX-PM with the highest dexamethasone release rate demonstrated a high therapeutic potential of DEX-PM in two different models of RA. In mice with collagen antibody-induced colitis (CAIA), an acute and reproducible arthritis model, a single injection of DEX-PM dosed at 5 mg/kg or 10 mg/kg induced a strong reduction in clinical signs of arthritis, such as swelling and redness, whereas free dexamethasone (DEX) displayed, even at 10 mg/kg, only moderate anti-arthritic activity. Similar effects were observed in rats with adjuvant-induced arthritis (AIA). At 10 mg/kg, the systemic administration of free DEX resulted in a transient decrease in clinical signs of arthritis, whereas a single administration of DEX-PM led to a (nearly) complete disease remission that lasted until the end of the study, 10 days after treatment.

These findings are encouraging for further evaluation, by exploring the value of DEX-PM in the therapy of other inflammatory disorders. Particularly the tailorable character of the drug release kinetics from this system, i.e. allowing adjustment of the rate of dexamethasone release, e.g. by using different linkers in a single system, makes this system very versatile, since different disorders may require different dexamethasone release kinetics.

1.2. Targeting of angiogenesis – Vascular disruption

By exploiting the abnormal architecture of the endothelial cells of newly formed blood vessels, vascular disrupting agents (VDAs), which interfere with the structural stability of these cells, are able to specifically target and disrupt pathological vasculature. Angiogenesis, i.e. the formation of new vasculature from existing blood vessels, or sprouting, is stimulated in tissues where there is an increased demand, or decreased supply, of oxygen and/or nutrients, and is therefore involved in many disorders [11]. Although angiogenesis is mostly associated with malignant tumor growth, it is also observed in chronically inflamed tissues in RA, MS and IBD [12-14]. **Chapter 5** reports on the synthesis and liposomal encapsulation of two colchicinoid prodrugs. Colchicine and its derivatives (colchicinoids), which are clinically used in low doses as anti-inflammatory agents for gout therapy, bind irreversibly to tubulin, hindering its functioning in microtubule dynamics, making them extremely potent VDAs. However, a colchicine dose close to its MTD is required to achieve considerable vascular disrupting efficacy, limiting the clinical use of these drugs. The encapsulation of colchicine (or a colchicinoid)

in a drug carrier system, such as liposomes, to enable its targeting to the target tissue, may therefore be a suitable strategy for improving the narrow therapeutic index of these colchicinoids. Unfortunately, the moderate hydrophobicity of colchicinoids allows them to readily pass the liposomal bilayer, hampering their stable liposomal encapsulation. To circumvent this, two hydrophilic colchicinoid prodrugs based on poly(ethylene glycol) (PEG) were prepared using hydrolytically cleavable linkages. First, colchicine was derivatized with glycolic acid or lactic acid at its acetamide moiety, which is not part of the pharmacophore and therefore not essential for its vascular disrupting activity [15], creating two different colchicinoids with an hydroxyl moiety suitable for further esterification. Subsequently, PEG_{5000} was conjugated to the colchicinoids to render them hydrophilic, allowing their stable encapsulation in the aqueous core of long-circulating liposomes. As expected, the rate of prodrug conversion was dependent on the type of linker used: the colchicinoid prodrug prepared from glycolic acid, containing an ester of a primary alcohol, hydrolyzed approximately 40 times faster than the prodrug prepared from lactic acid, which contained an ester of a secondary alcohol. The colchicinoid release kinetics from prodrug-loaded long-circulating liposomes reflected the conversion rate of each prodrug. Upon their encapsulation in liposomes, both the prodrugs are confined to the aqueous core due to their hydrophilicity and size, and only after prodrug conversion the therapeutically active colchicinoid may leak through the liposomal bilayer. Previously, it has been shown that, due to the enhanced permeability and retention (EPR) effect, the systemic administration of long-circulating liposomes results in their accumulation in the tumor tissue, and localize in the interstitial space close to the vasculature [16]. Therefore, using these liposome-encapsulated colchicinoid prodrugs, it is possible to achieve high concentrations of colchicinoids in the vicinity of the tumor vascular endothelium.

In **Chapter 6**, the colchicinoid prodrug based on glycolic acid, which possessed the highest conversion rate, was further evaluated *in vitro* and *in vivo* to assess the tubulin-binding and vascular disrupting activity of the prodrug construct. Upon incubation of the colchicinoid prodrug with human umbilical vein endothelial cells (HUVECs), to study its antimitotic tubulin-binding capacity, the prodrug appeared to be less cytotoxic than colchicine at similar doses. This difference can be explained by the delay in availability of the active agent, since only after conversion of the prodrug is the colchicinoid 'free' to exert its tubulin-binding activity. Interestingly, in B16F10 melanoma tumor-grafted mice, a single administration of the prodrug efficaciously disrupted the tumor vasculature,

resulting in extensive necrosis of the tumor tissue, while colchicine at similar dose did not show any vacular disrupting activity. In addition, colchicine induced a considerable decrease in the body weight of mice, illustrating its high toxic profile, whereas the same dose of prodrug did not result in a drop in weight. Only at a 5 times higher dose than colchicine, the prodrug caused a similar weight loss. The improved therapeutic efficacy and better tolerability of the colchicinoid prodrug compared to colchicine, is likely due to the changed molecular properties of the agent, which keep it for a longer time in the circulation, close to the vascular endothelium, thereby enabling tumor-specific accumulation and conversion.

Although these results show that the targeting of colchicine, either by using a liposomal nanocarrier system with tailorable release kinetics or by changing the aqueous solubility and molecular size of the therapeutic agent, may form an interesting and promising strategy for vascular disruption in tumor therapy, it may be applicable as well in other diseases that present with pathological angiogenesis. For example, in RA therapy, anti-angiogenic therapies that prevent the delivery of nutrients to sites of inflammation within the synovium and thereby reduce the inflammation, have been recognized as useful tools [17].

1.3. Drug targeting to inflammatory disease and cancer

Finally, to combine the efforts described in the previous chapters, as well as by others, while focusing on the ultimate goal of drug delivery, i.e. treating patients, the last section of the thesis deals with drug targeting research from a disease perspective. A comparison of three different nanocarrier systems of dexamethasone for the treatment of RA is presented in **Chapter 7**. Dexamethasone loaded in long-circulating liposomes (DEX-LCL) and polymeric dexamethasone prodrugs (P-DEX), both extensively studied nanomedicines for RA therapy, as well as dexamethasone-loaded core-crosslinked polymeric micelles (DEX-PM), a novel targeted dexamethasone delivery system with efficacious anti-arthritic activity, as reported in **Chapter 4**, were evaluated in parallel for their therapeutic efficacy in two models of RA. Whereas all tested nanomedicines were considerably more effective than the free drug, differences in strength, timing and duration of the therapeutic effect between the nanocarrier systems, appeared to be related to their inherent physicochemical characteristics. For example, in case of long-circulating liposomes the therapeutic agent is encapsulated in its aqueous core, which upon disruption of the liposomal bilayer (e.g. due

to lysosomal degradation) may be readily released [8]. It is therefore not surprising that, in this study, DEX-LCL displayed its anti-rheumatic efficacy at a lower dose, more rapidly, and for a shorter period of time, when compared to the relatively slow dexamethasone-releasing P-DEX. Since there are many different types of nanocarrier systems available for the treatment of several diseases, this type of comparative research is especially useful for gaining deeper insights concerning the relative strengths and weaknesses of various nanomedicines with respect to a specific therapeutic application. These insights may facilitate the selection of the most appropriate nanomedicine for the treatment of each individual patient.

In **Chapter 8** an essentially different methodology for finding an optimal nanocarrier is followed, by developing an assay for correlating *in vitro* analysis with the *in vivo* characteristics of nanomedicines. Since most nanomedicines exploit the EPR effect to deliver drugs to tumors and to other sites of inflammation, the circulation time of a nanocarrier system is a critical parameter determining its *in vivo* therapeutic efficacy: an extended circulation time of a nanomedicine formulation increases its statistical chance to localize in the target tissue and thereby improves the therapeutic efficacy of the associated drug. An important factor determining the circulation time of nanocarriers, such as liposomes, is the adsorption of plasma proteins to their surface upon intravenous administration [18]. Therefore, in this study, the adsorption of proteins to the surface of different types of (un)PEGylated liposomes was investigated using Surface Plasmon Resonance (SPR) and subsequently correlated to their clearance from the circulation. By employing SPR for this purpose, it was possible to do such measurements in real-time, under dynamic conditions and, importantly, without washing, thereby mimicking the *in vivo* situation as close as possible. The demonstrated correlation between protein-binding *in vitro*, as measured by SPR, and the circulation time *in vivo* of PEGylated liposomes, would in principle allow rapid screening of many types of nanomedicines, to predict their circulation time, with minimal *in vivo* experimentation. While such assay would surely help the development of nanomedicines with prolonged circulation kinetics, the advantages regarding time, costs and, above all, animal welfare, are obvious.

In conclusion, the targeted delivery of dexamethasone using long-circulating liposomes was therapeutically efficacious in preclinical models of RA and MS, but not in IBD. In addition, dexamethasone loaded in core-crosslinked micelles possessed strong anti-arthritic activity in two distinct models of RA. The comparison of three different nanocarriers of

dexamethasone, i.e. long-circulating liposomes, core-crosslinked polymeric micelles and macromolecular polymeric HMPA-dexamethasone prodrug, for RA therapy, provided deeper insights in the therapeutic efficacy of each of the systems. The targeted delivery of colchicinoids, which are equally active derivatives of the vascular disrupting agent colchicine, may be achieved by the encapsulation of hydrophilic polymeric colchicinoid prodrugs in the aqueous core of liposomes. Even without using a delivery system, this colchicinoid prodrug shows strong vascular disrupting activity in a preclinical tumor model. Finally, a useful *in vitro* tool for predicting the *in vivo* circulation kinetics of liposomes has been developed, by correlating the protein adsorption to the surface of liposomes, as measured by SPR, to the plasma clearance of the liposome type in question.

2. References

[1] R. Anderson, A. Franch, M. Castell, F.J. Perez-Cano, R. Bräuer, D. Pohlers, M. Gajda, A.P. Siskos, T. Katsila, C. Tamvakopoulos, U. Rauchhaus, S. Panzner, R.W. Kinne, Liposomal encapsulation enhances and prolongs the anti-inflammatory effects of water-soluble dexamethasone phosphate in experimental adjuvant arthritis, Arthrit. Res. Ther. 12(4) (2010).

[2] J.M. van den Hoven, W. Hofkens, M.H.M. Wauben, J.P.A. Wagenaar-Hilbers, J.H. Beijnen, B. Nuijen, J.M. Metselaar, G. Storm, Optimizing the therapeutic index of liposomal glucocorticoids in experimental arthritis, Int. J. Pharm. 16(2) (2011) 471-477.

[3] A. Gilman, L. Goodman, Goodman & Gilman's The Pharmacological Basis of Therapeutics, The McGraw-Hill Companies Inc, New York, 2006.

[4] P. Rohdewald, H. Möllmann, J. Barth, J. Rehder, H. Derendorf, Pharmacokinetics of dexamethasone and its phosphate ester, Biopharm. Drug Disposition 8(3) (1987) 205-212.

[5] J.R.F. Cummings, S. Keshav, S.P.L. Travis, Medical management of Crohn's disease, BMJ 336(7652) (2008) 1062-1066.

[6] T. Aychek, K. Vandoorne, O. Brenner, S. Jung, M. Neeman, Quantitative analysis of intravenously administered contrast media reveals changes in vascular barrier functions in a murine colitis model, Magn. Reson. Med. 66(1) (2011) 235-243.

[7] A. Brouwers, D. De Jong, E. Dams, W. Oyen, O. Boerman, P. Laverman, T. Naber, G. Storm, F. Corstens, Tc-99m-PEG-liposomes for the evaluation of colitis in Crohn's Disease, J. Drug Target. 8(4) (2000) 225-233.

[8] M. Naito, H. Nagai, S. Kawano, H. Umezu, H. Zhu, H. Moriyama, T. Yamamoto, H. Takatsuka, Y. Takei, Liposome-encapsulated dichloromethylene diphosphonate induces macrophage apoptosis in vivo and in vitro, Journal of Leukocyte Biology 60(3) (1996) 337-344.

[9] Y. Li, K. Xiao, J. Luo, W. Xiao, J.S. Lee, A.M. Gonik, J. Kato, T.A. Dong, K.S. Lam, Well-defined, reversible disulfide cross-linked micelles for on-demand paclitaxel delivery, Biomaterials 32(27) (2011) 6633-6645.

[10] M. Talelli, M. Iman, A.K. Varkouhi, C.J.F. Rijcken, R.M. Schiffelers, T. Etrych, K. Ulbrich, C.F. van Nostrum, T. Lammers, G. Storm, W.E. Hennink, Core-crosslinked polymeric micelles with controlled release of covalently entrapped doxorubicin, Biomaterials 31(30) (2010) 7797-7804.

[11] P. Carmeliet, R.K. Jain, Angiogenesis in cancer and other diseases, Nature 407(6801) (2000) 249-257.

[12] Z. Szekanecz, T. Besenyei, Á. Szentpétery, A.E. Koch, Angiogenesis and vasculogenesis in rheumatoid arthritis, Curr. Opin. Rheumatol. 22(3) (2010) 299-306.

[13] S. Danese, M. Sans, C. de la Motte, C. Graziani, G. West, M.H. Phillips, R. Pola, S. Rutella, J. Willis, A. Gasbarrini, C. Fiocchi, Angiogenesis as a novel component of inflammatory bowel disease pathogenesis, Gastroenterology 130(7) (2006) 2060-2073.

[14] M.A. Proescholdt, S. Jacobson, N. Tresser, E.H. Oldfield, M.J. Merrill, Vascular endothelial growth factor is expressed in multiple sclerosis plaques and can induce inflammatory lesions in experimental allergic encephalomyelitis rats, J. Neuropathol. Exp. Neurol. 61(10) (2002) 914-925.

[15] T.L. Nguyen, C. McGrath, A.R. Hermone, J.C. Burnett, D.W. Zaharevitz, B.W. Day, P. Wipf, E. Hamel, R. Gussio, A common pharmacophore for a diverse set of colchicine site inhibitors using a structure-based approach, J. Med. Chem. 48(19) (2005) 6107-6116.

[16] F. Yuan, M. Leunig, S.K. Huang, D.A. Berk, D. Papahadjopoulos, R.K. Jain, Mirovascular permeability and interstitial penetration of sterically stabilized (stealth) liposomes in a human tumor xenograft, Cancer Res. 54(13) (1994) 3352-3356.

[17] A.M. Roccaro, F. Russo, T. Cirulli, G.D. Pietro, A. Vacca, F. Dammacco, Antiangiogenesis for rheumatoid arthritis Current Drug Target - Inflammation & Allergy 4(1) (2005) 27-30.

[18] A. Chonn, S.C. Semple, P.R. Cullis, Association of blood proteins with large unilamellar liposomes in vivo. Relation to circulation lifetimes, J. Biol. Chem. 267(26) (1992) 18759-18765.

10

Appendix

1. Nederlandse samenvatting voor niet-ingewijden

1.1. Geneesmiddelrichten

Gerichte geneesmiddel bezorging, zoals de, weinig charmante, letterlijke vertaling van 'targeted drug delivery' naar het Nederlands luidt, heeft zich in de laatste tientallen jaren ontwikkeld tot een gunstige strategie voor de behandeling van verschillende ziekten.

Normaal gesproken, wanneer een geneesmiddel ingenomen of (intraveneus) toegediend wordt, verdeelt het zich via de bloedbaan over het gehele lichaam. Dit heeft als gevolg dat, ten eerste, van de totale dosis slechts een fractie in het aangedane weefsel ('target tissue' ofwel 'doelweefsel') terecht zal komen, en dat, ten tweede, de rest van de dosis in andere, gezonde, weefsels ongewenste bijwerkingen kan veroorzaken. Een goed voorbeeld is haarverlies bij bepaalde vormen van chemotherapie tegen kanker, doordat de behandeling alle sneldelende cellen binnen het lichaam aanvalt, zowel de kanker- als de haarcellen.

Succesvol 'geneesmiddelrichten' ('drug targeting') heeft daarom twee voordelen. Aan de ene kant zal een grotere hoeveelheid van de totale dosis van het gerichte medicijn in het doelweefsel terecht komen, wat in veel gevallen in een groter therapeutisch effect zal resulteren. Aan de andere kant zal er minder van de totale dosis in andere gezonde weefsels terecht komen, waardoor de behandeling met minder bijwerkingen gepaard zal gaan, ofwel hogere doseringen gebruikt kunnen worden.

Inmiddels meer dan een eeuw geleden beschreven de schrijver-bioloog Thomas Huxley en de arts-chemicus Paul Ehrlich een toekomst waar dokters konden beschikken over een 'very cunningly contrived torpedo' (zeer listig gefabriceerde torpedo) of 'Zauberkugeln' (toverkogels), die zelfstandig hun weg zouden kunnen vinden naar het zieke weefsel, en gezonde weefsels daarbij met rust zouden laten. Hoewel we nog ver van een dergelijke toekomst verwijderd zijn, hebben ontwikkelingen sinds het midden van de vorige eeuw er wel voor gezorgd dat deze werkelijkheid een stukje dichterbij gekomen is.

Door geneesmiddelen te 'verpakken' in zeer kleine deeltjes (dragersystemen) met een doorsnede variërend van 50-200 nm (1 nanometer is 1.000× zo klein als 1 micrometer, en 1.000.000× zo klein als 1 millimeter) en deze vervolgens intraveneus toe te dienen, is het namelijk mogelijk een grotere fractie van het medicijn in de doelweefsels te krijgen. Deze strategie maakt gebruik van de beperkte doorlaatbaarheid van de bloedvatwand voor deeltjes van deze grootte, waardoor de geneesmiddel-beladen dragers (nanomedicijnen) in de bloedbaan blijven totdat ze hieruit onttrokken worden door de lever en milt. Echter, in

tegenstelling tot de gezonde weefsels, zijn in ontstoken weefsels en kankerweefsels de bloedvaten juist extra doorlaatbaar om aan de vraag naar ontstekingscellen en voedingsstoffen te kunnen voldoen. Dit heeft in de praktijk tot gevolg dat in deze doelweefsels de nanomedicijnen wel uit de bloedbaan kunnen treden, alwaar het 'meegereisde' medicijn zijn werk kan doen. Figuur 1 geeft een duidelijke illustratie van dit principe.

In dit proefschrift worden een aantal strategieën voor het richten van geneesmiddelen naar doelweefsels in verschillende ontstekingsziekten en kanker onderzocht. Allereerst wordt in **hoofdstuk 1** de achtergrond en doel van het onderzoek, dat is beschreven in dit proefschrift, uiteengezet.

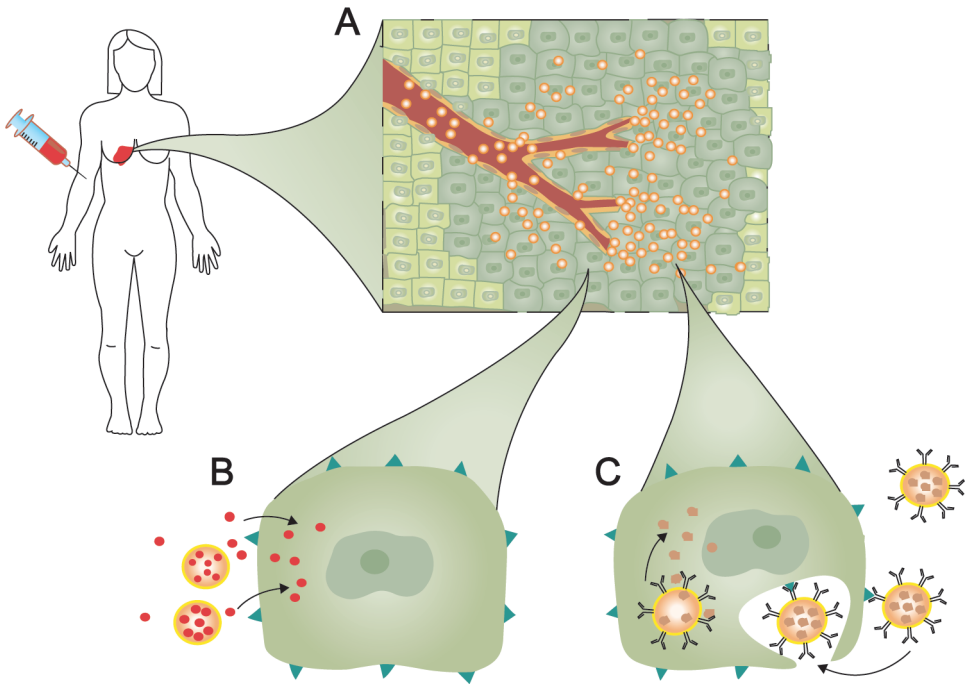

Figuur 1. Schematische weergave van geneesmiddelrichten. Minuscule geneesmiddel-beladen dragersystemen, ofwel nanomedicijnen, worden intraveneus toegediend aan een patiënt, in dit geval een patiënte met borstkanker. Doordat, in tegenstelling tot 'normale' bloedvaten in gezonde weefsels, de bloedvaten in het aangedane weefsel – het kankergezwel – doorlaatbaar zijn voor deeltjes van deze grootte, zullen de nanomedicijnen na verloop van tijd in dit doelweefsel ophopen (A). Na ophoping in het weefsel kan het dragersysteem het beladen geneesmiddel geleidelijk vrijgeven (B), of eerst opgenomen worden in de doelcellen, alvorens het geneesmiddel wordt vrijgegeven (C). Uit T.M. Allen, P.R. Cullis, Drug Delivery Systems: Entering the Mainstream, Science 303(5665) (2004) 1818-1822. Herdrukt met toestemming van AAAS.

Interessant genoeg houden vele onderzoekers binnen het veld van geneesmiddelrichten zich uitsluitend bezig met kanker, terwijl deze aanpak ook bij andere, hetzij minder levensbedreigende ziekten, erg succesvol kan zijn. Dit wordt geïllustreerd in **hoofdstuk 2**, waar een overzicht wordt gegeven van de reeds ontwikkelde geneesmiddeldragersystemen voor de behandeling van chronische ontstekingsziekten zoals reumatoïde artritis (RA, chronische gewrichtsontsteking), multiple sclerose (MS, chronische zenuwontsteking) en Inflammatory Bowel Disease (IBD, chronische darmontsteking).

1.2. Geneesmiddelrichten voor ontstekingsziekten

Liposomen, kunstmatige blaasjes die bestaan uit één of meer dubbele fosfolipidenlagen die een waterig compartiment omgeven, iets wat globaal doet denken aan de structuur van cellen, zijn waarschijnlijk het bekendste dragersysteem voor geneesmiddelen. In **hoofdstuk 3** zijn liposomen beladen met dexamethason, een krachtig kunstmatig glucocorticoïde afgeleid van het lichaamseigen bijnierschorshormoon cortisol. Glucocorticoïden hebben een sterke ontstekingsremmende werking en worden daarom veelvuldig toegepast bij diverse ontstekingsziekten. De keerzijde van het gebruik van glucocorticoïden is het grote aantal bijwerkingen dat er vaak mee gepaard gaat, wat in veel gevallen de dosering en toedieningsfrequentie beperkt. Eerder onderzoek heeft laten zien dat de toepassing van glucocorticoïd-beladen liposomen in diermodellen van RA leidt tot een sterke en langdurige afname van symptomen van gewrichtsontsteking, terwijl vergelijkbare dosering 'niet-ingepakte' glucocorticoïden slechts een matig effect hadden. In navolging van dit onderzoek zijn dexamethason-beladen liposomen onderzocht voor hun therapeutische activiteit in twee andere ziektemodellen, namelijk in een diermodel van MS en in een diermodel van IBD.

In het model van MS was er, zoals verwacht, alleen een duidelijke afname van symptomen van zenuwontsteking na een eenmalige intraveneuze toediening van dexamethason-liposomen, en niet na een vergelijkbare dosis 'vrij' dexamethason. Echter, in muizen met chronische darmontsteking leidde de behandeling met dexamethason-liposomen niet tot een vermindering van symptomen. Sterker nog, in vergelijking met de dieren die het 'vrije' geneesmiddel ontvingen, hadden deze dieren na behandeling juist meer bloed bij de ontlasting, een symptoom dat duidt op een verslechtering van de ziekte. Hoewel het niet helemaal duidelijk is waarom de toepassing van dexamethason-beladen liposomen in het ene model wel een gunstig effect heeft, terwijl in het andere model er juist een verslechtering

optreedt, worden er een aantal mogelijke verklaringen gegeven voor deze bevindingen. Zo spelen bijvoorbeeld de macrofagen, de cellen die o.a. verantwoordelijk zijn voor het opruimen van binnendringende micro-organismen en 'rommel', zoals lichaamsvreemde liposomen en andere dragersystemen, een belangrijke rol in de therapeutische activiteit van de dexamethason-beladen liposomen. Het is aannemelijk dat de macrofagen mogelijk een belangrijke beschermende rol hebben bij IBD, terwijl ze bij MS en RA juist onderdeel zijn van het ziekteproces.

Door de inherente structurele eigenschappen van liposomen is een gereguleerde afgifte van het ingevangen geneesmiddel moeilijk te bewerkstelligen. Zoals een luchtbel niet gedoseerd leeg kan lopen, zal een verstoring of afbraak van de wand van het liposoom leiden tot een snelle vrijgave van zijn waterige inhoud. Om te onderzoeken of een dragersysteem met de capaciteit tot gereguleerde afgifte van waarde kan zijn voor de behandeling van chronische ontstekingsziekten, is in **hoofdstuk 4** een nieuw dexamethason-dragersysteem, gebaseerd op polymeren micellen, ontwikkeld en beproefd in een diermodel van RA. Micellen, welke bijvoorbeeld dagelijks gebruikt worden in de vorm van zeep, zijn zelfvormende structuren bestaande uit moleculen die zowel een hydrofiel (waterlievend) als een hydrofoob (waterafstotend) uiteinde bevatten. In een waterige omgeving, zoals de bloedbaan, kan de structuur van een micel worden omschreven als een hydrofobe kern omgeven door een hydrofiele mantel.

Voor dit onderzoek is het dexamethason-molecuul eerst zodanig gemodificeerd zodat, na chemische stabilisering van de polymeren micellen, het geneesmiddel fysiek gekoppeld is aan de micellaire structuur. Deze koppeling is echter gevoelig voor water, wat inhoudt dat bij blootstelling aan water deze koppeling zal verbreken (hydrolyse). Er zijn drie verschillende afgeleiden van dexamethason bereid, elk met een andere gevoeligheid voor hydrolyse, en vervolgens ingesloten in de hydrofobe kern van de polymeren micellen. Gedurende de blootstelling aan een waterige omgeving was er een gedoseerde afgifte van dexamethasone door de dexamethason-beladen micellen, waarbij de afgiftesnelheid werd bepaald door gevoeligheid van de dexamethasone-afgeleide voor hydrolyse.

Daarna is het snelst vrijgevende type dexamethason-beladen micel onderzocht voor haar therapeutische activiteit in twee verschillende diermodellen van RA. In muizen met gewrichtsontsteking was er een sterk ontstekingsremmend effect van de dexamethason-beladen micellen wanneer intraveneus toegediend in middelhoge (5 mg/kg) of hoge (10 mg/kg) dosering. Vrije dexamethason had in de hoge dosering (10 mg/kg) slechts een

matig effect. Een vergelijkbaar resultaat werd behaald in ratten met gewrichtsontsteking. Terwijl een hoge dosering (10 mg/kg) van vrije dexamethason resulteerde in een tijdelijke vermindering van de verschijnselen van gewrichtsontsteking, leidde de toediening van dexamethason-beladen micellen tot een bijna volledig verdwijnen van ontstekingsverschijnselen tot het eind van de studie, 10 dagen na behandeling.

1.3. Bestrijden van bloedvatnieuwvorming – bloedvatontwrichting

Een andere vorm van een gerichte therapie is het aanvallen van nieuw gevormde bloedvaten. Bij veel ziekten is er in de aangedane weefsels een voortdurend toenemende vraag naar zuurstof en voedingsstoffen. Om aan deze vraag te kunnen voldoen, wordt in deze weefsels een proces in gang gezet die de aangroei van nieuwe bloedvaten, ook wel angiogenese genoemd, stimuleert. Hoewel angiogenese vooral wordt geassocieerd met de groei van kwaadaardige gezwellen bij kanker, is dit proces veelal ook aanwezig in chronische ontstekingsziekten zoals RA en MS. Door haar belangrijke rol in de ontwikkeling van deze ziekten, wordt angiogenese gezien als een geschikt aangrijpingspunt voor (nieuwe) behandelingsstrategieën. Eén van deze strategieën is het ontwrichten van nieuw gevormde bloedvaten.

In de volgende twee hoofdstukken wordt de ontwikkeling en evaluatie van een nieuw nanomedicijn voor bloedvatontwrichting beschreven. Colchicine, een natuurlijke stof gewonnen uit de plant herfsttijloos, wordt tegenwoordig vooral gebruikt in de behandeling van jicht, maar heeft daarnaast nog andere eigenschappen die het geschikt maken voor bloedvatontwrichting. Waar een celskelet dat bestaat uit actine zorgt voor de vorm van 'normale' bloedvatcellen, zijn de bloedvatcellen van nieuw gevormde bloedvaten voornamelijk afhankelijk van een celskelet die bestaat uit tubuline. Colchicine bindt zeer sterk aan tubuline, en kan zo de vorm en structuur van deze nieuw gevormde bloedvatcellen verstoren. Door de verstoring treedt er zeer snel een bloedstollingsproces op, vergelijkbaar met een wondje, en zal de bloedstroom in het bloedvat tot stilstand komen. Aangezien het omliggende weefsel afhankelijk is van dit bloedvat, zal een dergelijke verstopping leiden tot het afsterven van dit weefsel. Omdat dit alleen bij nieuwgevormde, tubuline-afhankelijke, bloedvaten zal gebeuren, kan deze strategie worden gezien als een gerichte therapie.

Helaas zijn in het geval van colchicine erg hoge doseringen nodig om effectieve bloedvatontwrichting te veroorzaken. Door de zeer ernstige, vaak dodelijke, bijwerkingen die colchicine in deze dosering kan veroorzaken, is het in deze vorm niet geschikt voor deze

toepassing. Een dragersysteem, dat gebruik maakt van de toegenomen doorlaatbaarheid van de bloedvaten in bijvoorbeeld kwaadaardige gezwellen, en zo een grotere fractie van de dosis in het doelweefsel terecht kan doen komen, zou hierbij uitkomst kunnen bieden. De eigenschappen van colchicine bemoeilijken echter de stabiele insluiting in een dragersysteem. Daarom wordt in **hoofdstuk 5** de bereiding van twee 'prodrugs' van colchicine beschreven, welke vervolgens worden ingevangen in liposomen. Een prodrug is een inactieve vorm van een geneesmiddel, die pas na biologische of chemische omzetting(en) actief wordt. Dit kan bijvoorbeeld omzetting in de lever zijn (biologisch), of door blootstelling aan bepaalde omstandigheden (chemisch). De prodrugs beschreven in hoofdstuk 5 zijn, in tegenstelling tot de oorspronkelijke stof colchicine, zeer goed in water oplosbaar en kunnen daarom goed in het waterige compartiment van liposomen ingesloten worden. Doordat door blootstelling aan water de prodrugs via hydrolyse geleidelijk worden omgezet naar de actieve stof, welke redelijk ongehinderd door de wand van de liposomen naar buiten kan, wordt na verloop van tijd de belading afgegeven. De twee prodrugs in deze studie hebben een verschillende gevoeligheid voor hydrolyse. Na insluiting in liposomen bleek dat, zoals verwacht, de afgiftesnelheid evenredig was met de hydrolyse snelheid, wat laat zien dat de afgiftesnelheid te beheersen is.

Vervolgens is in **hoofdstuk 6** de prodrug met de snelste omzettingssnelheid onderzocht voor zijn capaciteit tot tubulinebinding in vaatwandcellen en bloedvatontwrichting in een diermodel van kanker. Na het toedienen van de prodrug aan gekweekte vaatwandcellen bleek het minder effectief aan tubuline te binden dan de oorspronkelijke stof colchicine. Dit is toe te schrijven aan de lagere beschikbaarheid van de actieve stof, aangezien de prodrug eerst omgezet moet worden alvorens het actief aan tubuline kan binden. Het is daarom opmerkelijk dat een enkele intraveneuze toediening van de prodrug aan muizen met kanker leidde tot een hoge mate van ontwrichting van de bloedvaten in het gezwel, terwijl een vergelijkbare dosering van colchicine geen effect liet zien. Daarbij werd de behandeling met colchicine slecht verdragen, gekenmerkt door een sterk verlies van lichaamsgewicht. De behandeling met een vergelijkbare dosering van de prodrug werd veel beter verdragen en leidde niet tot gewichtsverlies. Alleen wanneer een 5× hogere dosering werd gegeven, leidde de behandeling met de prodrug tot een sterke daling in het lichaamsgewicht.

De hogere capaciteit tot vaatwandontwrichting en de betere tolereerbaarheid van de prodrug ten opzichte van colchicine, duidt erop dat er inderdaad een hogere fractie van

de dosis de doelweefsels bereikt en er een kleinere fractie in andere weefsels ongewenste bijwerkingen veroorzaakt. Dit heeft waarschijnlijk te maken met de veranderde eigenschappen van de stof, het is hydrofieler, waardoor het langer in de bloedsomloop blijft, nabij de vaatwandcellen waar het zijn activiteit uit moet oefenen.

1.4. Geneesmiddelrichten in ontstekingsziekten en kanker

Het laatste deel van dit proefschrift richt zich ten slotte op de vraag welk dragersysteem het meest geschikt is voor de behandeling van een bepaalde ziekte. Een vergelijking tussen drie verschillende dragersystemen voor de behandeling van RA is gepresenteerd in **hoofdstuk 7**. In deze studie zijn dexamethason-beladen liposomen, polymeren prodrugs van dexamethason, en dexamethason-beladen micellen onderzocht voor hun ontstekingsremmende werking in twee verschillende diermodellen van RA. Waar alle geteste dragersystemen aanzienlijk beter presteerden dan een vergelijkbare dosering van het 'vrije' geneesmiddel, waren er subtiele verschillen tussen de drie systemen die gerelateerd leken te zijn aan de verschillende inherente eigenschappen van elk van de systemen. Zo is in het geval van liposomen het dexamethason ingevangen in het waterige compartiment, en zal het, na verstoring van de omgevende wand, snel aan de omgeving vrijgegeven worden. Het is daarom begrijpelijk dat de intraveneuze behandeling met dexamethason-beladen liposomen een snel, maar minder langdurig gewrichtsontstekingsremmend effect had, en bovendien bij de laagste dosering (1 mg/kg) al effectief was. Aan de andere kant was de polymeren prodrug van dexamethason, die het dexamethason veel langzamer afgeeft, alleen actief bij de hoogste dosering (10 mg/kg). Daarbij trad dit effect pas later op, maar was het wel veel langer werkzaam dan de dexamethason-beladen liposomen. Zoals eerder beschreven in hoofdstuk 4, bieden de dexamethason-beladen micellen ook de mogelijkheid tot een gedoseerde afgifte van het geneesmiddel. Zij doen dit echter sneller dan de polymeren prodrug, wat als gevolg had dat ze al een duidelijk ontstekingsremmend effect lieten zien bij een middelhoge dosis (5 mg/kg). Bovendien hield het effect langer aan dan na behandeling met liposomen.

Aangezien er inmiddels een groot aantal verschillende dragersystemen ontwikkeld zijn, waarbij het onduidelijk is hoe deze zich tot elkaar verhouden, is het van belang dat er dit soort vergelijkend onderzoek gedaan wordt. Dit geeft namelijk een beter inzicht in de sterke en zwakke kanten van een dragersysteem, en maakt zo een gefundeerde keuze voor een systeem voor de behandeling van een bepaalde ziekte mogelijk.

In **hoofdstuk 8** is een compleet andere strategie voor het bepalen van een optimaal dragersysteem gevolgd. Zoals eerder uitgelegd, exploiteren de meeste nanomedicijnen de toegenomen doorlaatbaarheid voor 'grotere' deeltjes van de vaatwand in de bloedvaten van aangedane weefsels om zo een hogere fractie van de toegediende dosis in deze doelweefsels terecht te doen komen. Om dit te bereiken zijn ze in hoge mate afhankelijk van hun circulatietijd – de duur dat de dragersystemen zich in de bloedbaan bevinden. Immers, hoe langer de minuscule deeltjes rondgepompt worden, des te meer er op de plek van bestemming aan zullen komen – vergelijkbaar met een regenton; hoe langer het regent, des te meer water er in de ton zal komen te staan. Een belangrijke factor die de circulatietijd van dragersystemen zoals liposomen bepaalt, is de mate van binding van eiwitten aan het oppervlak van de drager na intraveneuze toediening.
In deze studie is onderzocht of de mate van eiwitbinding aan liposomen gerelateerd kan worden aan de circulatietijd van deze liposomen na intraveneuze toediening. Hierbij is gebruik gemaakt van Surface Plasmon Resonance (SPR), een ingenieuze technologie die het mogelijk maakt de binding van eiwitten in het laboratorium te kunnen bepalen, waarbij de omstandigheden in de bloedbaan zo goed mogelijk worden nagebootst. Omdat er inderdaad een rechtstreeks verband tussen SPR-gemeten eiwitbinding en de circulatietijd in muizen bleek te zijn – meer liposomen met een hogere mate van eiwitbinding hebben een kortere circulatietijd – is het met deze techniek in principe mogelijk om een groot aantal verschillende nanomedicijnen te testen en hun circulatietijd te schatten zonder gebruik te hoeven maken van proefdieren. Met het oog op de tijd en geld dat proefdieronderzoek kost, kan deze techniek het leven van veel onderzoekers een stuk eenvoudiger maken. En dat van proefdieren natuurlijk ook.
Tot slot wordt in **hoofdstuk 9** een overzicht gegeven van de bevindingen die zijn beschreven in dit proefschrift.

1.5. Conclusie

Hoewel de 'toverkogel' nog ontwikkeld moet worden, is het richten van geneesmiddelen een goede strategie gebleken voor de behandeling van verschillende ziekten. In dit proefschrift zijn een aantal gevestigde en nieuwe dragersystemen voor geneesmiddelrichten in verschillende ziekten onderzocht. In modellen van reumatoïde artritis, multiple sclerose en kanker is het voordelige effect van gerichte nanomedicijnen duidelijk aangetoond. In het geval van chronische darmontsteking zal verder onderzoek moeten uitwijzen of een

gerichte strategie hier ook van waarde zou kunnen zijn.

2. Curriculum Vitae

Bart Crielaard was born on June 17th 1980, in Emmen, The Netherlands. Upon graduation in 1998 from secondary school at Augustinus College in Groningen, he started studying Medicine at University of Groningen. During his medical internships he developed a specific interest in Radiology, which led him to do an elective internship at the department of Radiology at University Medical Center Groningen (UMCG) under the supervision of Dr. E.J. van der Jagt. After obtaining his Medical Degree in 2004, Bart started a transitional program at the University of Groningen, which enabled him to enter the Master's program Biomedical Engineering at the same university in 2005. As part of the Master's program, he worked for 6 months on a research project under the supervision of Dr. D. Neut and Prof.dr. D.W. Grijpma at the department of Biomedical Engineering at the University of Groningen, during which he focused on the development of an antibiotic-releasing biodegradable polymer for osteomyelitis therapy. In addition, he did a research internship at DSM Biomedical in Geleen, The Netherlands, under the supervision of Dr. A.A. Dias and Dr. G. Mihov, where he was involved in the development of an imageable coating for biomedical instruments. In 2007, Bart obtained his Master's degree in Biomedical Engineering with a specialization in Biomaterials, and started a PhD project at the department of Pharmaceutics, Utrecht Institute for Pharmaceutical Sciences (UIPS), Utrecht University. This project, which was part of MediTrans, an Integrated Project funded by the European Commission under the thematic priority of the Sixth Framework Program, was supervised by Prof.dr. G. Storm, Prof.dr.ir. W.E. Hennink, Dr. T. Lammers and Dr. R.M. Schiffelers. During his work as a PhD candidate, Bart investigated new targeted nanomedicines for the treatment of inflammatory disorders and cancer, which resulted in this thesis. In addition, he was involved in the teaching of students of the Pharmacy Bachelor program, and was member of the UIPS PhD Education Committee.

3. List of publications

Crielaard BJ, van der Wal S, Le HT, Bode AT, Lammers T, Hennink WE, Schiffelers RM, Fens MH, Storm G. Liposomes as carriers for colchicine-derived prodrugs: vascular disrupting nanomedicines with tailorable drug release kinetics. Eur J Pharm Sci. 2012; 45(4):429-435.

Crielaard BJ, van der Wal S, Lammers T, Le HT, Hennink WE, Schiffelers RM, Storm G, Fens MH. A polymeric colchicinoid prodrug with reduced toxicity and improved efficacy for vascular disruption in cancer therapy. Int J Nanomedicine. 2011; 6:2697-703.

Crielaard BJ, Yousefi A, Schillemans JP, Vermehren C, Buyens K, Braeckmans K, Lammers T, Storm G. An in vitro assay based on surface plasmon resonance to predict the in vivo circulation kinetics of liposomes. J Control Release. 2011; 156(3):307-14.

Crielaard BJ, Lammers T, Morgan ME, Chaabane L, Carboni S, Greco B, Zaratin P, Kraneveld AD, Storm G. Macrophages and liposomes in inflammatory disease: friends or foes? Int J Pharm. 2011; 416(2):499-506.

Crielaard BJ, Lammers T, Schiffelers RM, Storm G. Drug targeting systems for inflammatory disease: One for all, all for one. J Control Release 2011. In press. doi: 10.1016/j.jconrel.2011.12.014.

Coimbra M, Crielaard BJ, Storm G, Schiffelers RM. Critical factors in the development of tumor-targeted anti-inflammatory nanomedicines. J Control Release. 2011; In press. doi: 10.1016/j.jconrel.2011.10.019.

Vader P, Crielaard BJ, van Dommelen SM, van der Meel R, Storm G, Schiffelers RM. Targeted delivery of small interfering RNA to angiogenic endothelial cells with liposome-polycation-DNA particles. J Control Release. 2011; In press. doi: 10.1016/j.jconrel.2011.09.080.

Cittadino E, Ferraretto M, Torres E, Maiocchi A, Crielaard BJ, Lammers T, Storm G, Aime S, Terreno E. MRI evaluation of the antitumor activity of paramagnetic liposomes loaded with prednisolone phosphate. Eur J Pharm Sci. 2012; 45(4):436-441.

Neut D, Kluin OS, Crielaard BJ, van der Mei HC, Busscher HJ, Grijpma DW. A biodegradable antibiotic delivery system based on poly-(trimethylene carbonate) for the treatment of osteomyelitis. Acta Orthop. 2009; 80(5):514-9.

Crielaard BJ, Rijcken, CJF, Quan LD, van der Wal S, Altintas I, van der Pot M, Kruijtzer JA, Liskamp RMJ, Schiffelers RM, van Nostrum CF, Hennink WE, Wang D, Lammers T, Storm G. Glucocorticoid-loaded core-crosslinked polymeric micelles with tailorable release kinetics for targeted rheumatoid arthritis therapy. Submitted for publication.

"There are sadistic scientists who hurry to hunt down errors instead of establishing the truth."
Marie Curie, 1867 - 1934

4. Tot slot

Eerlijk gezegd was ik deze woorden van dank in eerste instantie begonnen met een beschouwend stukje over onderzoek en hoe mijn pad tot een promotie heeft mogen leiden. Hoe soms kleine keuzes, of zelfs omstandigheden, dit gevolg kan hebben.
Het begon nogal een lang verhaal te worden.

Omdat ik me realiseerde dat waarschijnlijk niemand daar echt op zit te wachten, in elk geval niet hier, zal ik proberen het enigszins kort te houden. Dat zal niet meevallen, want er moet nou eenmaal een aantal mensen bedankt worden, en ik wil niemand daarin tekortdoen. Mocht dat toch het geval zijn, sorry. Ik moet daarom iedereen op het hart drukken dat mijn dank voor iedereen echt verder gaat dan een paar woorden op een stuk papier.

Gert, als projectleider en inspirator van MediTrans heb jij het fundament gelegd voor mijn promotie. Tijdens de vele MediTrans meetings heb ik bewondering gekregen voor hoe je met een ontspannen en humoristische stijl mensen aan je weet te binden en van de Europese 'melting pot' toch één geheel hebt weten te maken. Ik heb je begeleiding, in het bijzonder tijdens het laatste jaar toen we wat vaker aan jouw nieuwe tafel hebben gezeten, altijd als plezierig ervaren. Ik ben je erg dankbaar dat je me deze kans geboden hebt.

Twan, jouw gedrevenheid en neus voor publiceren heeft er zonder twijfel voor gezorgd dat dit proefschrift er in deze vorm gekomen is; voor vrijwel alle hoofdstukken was jouw bijdrage een essentieel ingrediënt. Ik heb groot respect voor je creativiteit en je vermogen om kansen te herkennen en te creëren. Gezien je verscheidenheid aan aanstellingen (naast Utrecht ook in Heidelberg en Aken) en je werkgerelateerde reislustigheid ben je fysiek niet veel in Utrecht geweest, maar je was altijd direct beschikbaar via email of telefoon, weekenden en nachten niet uitgezonderd. Ik wil je daarom bedanken voor onze prettige samenwerking. En voor je opmerkelijke vertrouwen in artsen, zeker voor een farmaceut.

Wim, doordat ik vooral bezig was met biologie en slechts in mindere mate met chemie (al moet ik toegeven dat er uiteindelijk toch behoorlijk wat chemie in dit proefschrift is beland), heb je je weinig gemengd in de inhoudelijke invulling van het project. Maar dit

betekent niet dat je niet betrokken was. Integendeel, ik heb je oprechte betrokkenheid erg gewaardeerd, zowel wat betreft de voortgang van het onderzoek, als op persoonlijk vlak. Ik ben daarom blij dat ik de rol 'Wim' in veel promotievideo's heb mogen spelen. Bedankt.

Ray, jij was mijn eerste vraagbaak voor alle (dier)experimentele vragen, en ik denk dat ik door de jaren heen jouw kamer het vaakst ongevraagd binnengelopen ben (en dat zegt wat denk ik toch). Ik wil je bedanken voor je ontwapenende openheid, je ideeën, en je praktische hulp tijdens dierexperimenten.

Er zijn daarnaast een behoorlijk aantal andere mensen van essentiële waarde geweest voor de totstandkoming van dit proefschrift.
Ebel, ik wil je enorm bedanken voor je hulp tijdens de in vivo experimenten. Ik was niet 's werelds beste planner, maar ondanks dat je vaak je handen al behoorlijk vol had, was je altijd bereid een gaatje voor me te vinden. Hans, bedankt voor je meedenken en hulp in de dierstallen. Barbara, Lidija, Louis, Kim en Mies, bedankt voor jullie hulp en oplossend vermogen binnen en buiten het lab. Marcel, Steffen, Cristianne, Afrouz, Maria, Roy, Aloïs, Joris, Isil, this thesis would be a lot thinner if it wasn't for your contributions. Liz en Aletta van de vakgroep Farmacologie, bedankt voor de brainstormsessies en jullie hulp met het DSS colitis model voor hoofdstuk 3. Kevin en Koen van de Universiteit Gent, bedankt voor de samenwerking en jullie bijdrage voor hoofdstuk 8. My colleagues from the University of Nebraska Medical Center, Ling-Dong and Dong, I enjoyed our collaboration and thank you for your work with the AA rat model, making the realization of chapter 4 and 7 possible.

I should also mention my MediTrans buddies, Marina and Amir V., with whom I traveled to so many different conferences (thank you Gert!). Marina, your relaxed and outgoing character made you a great company to travel with. Amir, the MD who cannot get drunk, you are one of a kind. I enjoyed having you as my roommate. I think with no other man I shared more hotel rooms, and I am glad it was with you.

Het grootste, en misschien wel mooiste, deel van mijn tijd als AIO heb ik doorgebracht in laboratorium Z505 van het Wentgebouw. Zo had ik het erg getroffen met mijn beide buurvrouwen. Ethlinn, ik heb veel bewondering voor jouw analytisch inzicht en

gedrevenheid. Ik ben je nog altijd erg dankbaar voor het luisterend oor en de verstandige woorden die je me bood in tijden van tegenslag. Maria, I am still not sure whether I prefer you on my left or right side. I think I like both. Anyway, I am glad that you will be on either during my defense. Maar ook de andere oud-Z505'ers waren belangrijk voor het succes van ons lab. Joris, bedankt voor de flinke dosis relativering en spitsvondigheid (vond ik nou echt een Joris-woord). Ellen, je ontembare enthousiasme is onvergetelijk. Inge, jouw combinatie van rust en humor is uniek. Frits, de gang werd altijd een stuk drukker als jij kwam lunchen, maar als Groninger kan ik je directe karakter erg waarderen. And also Sylvia, Naushad, Afrouz en Grzegorz thank you for your gezelligheid!

Na de verhuizing was ik gelukkig weer omringd door voldoende buurvrouwen. Emmy, Kimberley and Hajar, although it was only a short stay, I want to thank you for the fun and memorable discussions we have had. En natuurlijk Pieter, we hebben elkaar eigenlijk pas echt leren kennen na de herverdeling in het David de Wied-gebouw. Onze verschillende visies op sommige levens- en wetenschapskwesties leverden enkele leuke discussies op. Bedankt voor je betrokkenheid, en veel succes op Hinksey Heights, Southfield en Studley Wood!

Besides working there were plenty of other ways to have fun, most often in combination with a few beers. To the older (Sabrina, Joris, Ellen, Ethlinn, Inge, Enrico, Marcel, Pieter, Marina, Wim, Amir V., Amir G., Rolf, Niels) and to the more recent (Roy, Markus, Maria, Isil, Luis, Yang, Albert, Francisco, Peter, Negar, Kristel) colleagues and friends: thank you for all the laughs we had.
But of course also all the others of Biofarmacie (Robbert Jan, René, Tina, Herre, Huub, Daan, Herman, Maryam, Vera, Anastasia, Eduardo, Abdul, Georgi, Martin, Paul, Erik, Burcin, Merel, Filis, Sima, Shima, Neda, Mernoosh, Farshad, Mazda), thank you!

Ook buiten 'de zaak' stonden er altijd veel mensen die voor me klaar: Hartman, al bijna een kwart eeuw een trouwe en nabije vriend. Hoewel we op diverse plekken veel tijd met elkaar hebben doorgebracht, zoals Duitsland, Spanje, Tsjechië, Slowakije, Hongarije en Portugal (ik had graag geëindigd met Kaapverdië…), maar 's avonds na het werk met een six-pack thuis op de bank foeteren op het slechte spel van Ajax blijft toch wel één van mijn favorieten. Josien, mijn squash-maatje/nichtje, dank voor je hulp bij het

wegmeppen van balletjes. En af en toe enkele irritaties. Het deed en doet me goed. Ook Marcel T. en Marieke bedankt voor jullie voortdurende interesse. And a bit further away: Romy, Marcelino, Ica and Nuno, thank you very much for your support and your impressive hospitality whenever it was time for a break (it was always 'nice'!).

En wat is een promotie zonder paranimfen?
Olav, al sinds het begin van de cursus, bijna 14 jaar geleden, delen wij een vergelijkbare visie op de geneeskunde en de wetenschap. Jouw enthousiasme voor beide is aanstekelijk, met als gevolg dat ik regelmatig heb genoten van onze levendige discussies onder het genot van een biertje. Ik daarom ben vereerd dat je mijn paranimf zal zijn.

Maria, fofinha, we have been working together a lot, and I think in many aspects we form a very good team, both in and outside the lab. Although my gratitude extents much further than these few words, I want to thank you so much for your help, your support in difficult times, and your presence. I consider myself extremely lucky to have you on my side. Krrrrr!

Tot slot mijn familie. Allereerst wil ik me verontschuldigen aan al mijn ooms, tantes, neven en nichten voor alle keren dat ik met veel moeite mijn onderzoek tevergeefs probeerde uit te leggen. Ik hoop dat de Nederlandse samenvatting een paar pagina's terug iets meer succes heeft gehad.
Gert, Willeke, Marloes en Marnix, bedankt voor jullie steun en jullie oprechte interesse in jullie kleine broertje.
Pa, ik weet zeker dat je trots was geweest.
Ma, ik waardeer je vertrouwen, zelfs na de vele educatieve omzwervingen (wellicht ga ik nu écht werken), het is spijtig dat je dit moment niet met Pa kan delen. Bedankt voor je steun, interesse en natuurlijk je hulp met de Nederlandse samenvatting. Zoals je vroeger hielp met mijn eerste werkstukken, heb je me nu kunnen helpen met mijn laatste.

Bart